Synthesis of polymer-polymer hybrids by miniemulsion polymerisation and characterisation of hybrid latex

Ravindra Udagama

N° d'ordre : 157-2009 Année 2009

THESE

présentée

devant l'UNIVERSITE CLAUDE BERNARD - LYON 1

pour l'obtention

du DIPLOME DE DOCTORAT

(arrêté du 7 août 2006)

présentée et soutenue publiquement le 05.10.09

par

Ravindra UDAGAMA

SYNTHESIS OF POLYMER-POLYMER HYBRIDS BY MINIEMULSION POLYMERISATION AND CHARACTERISATION OF HYBRID LATEX

JURY: M. P. CHAUMONT, Président
Mme. M. J. BARANDIARAN
M. C. CRETON
Mme. K. OUZINEB
M. T. F. L. McKENNA
Mme. E. BOURGEAT-LAMI

UMR 5265, Laboratoire de Chimie, Catalyse, Polymères et Procédés (C2P2), Bat F308, B.P. 2077, 43 Bd du 11 Novembre 1918, 69616, Villeurbanne, France.

UNIVERSITE CLAUDE BERNARD - LYON I

Président de l'Université	**M. le Professeur L. COLLET**
Vice-président du Conseil Scientifique	M. le Professeur J.F. MORNEX
Vice-président du Conseil d'Administration	M. le Professeur J. LIETO
Vice-président du Conseil des Etudes et de la Vie Universitaire	M. le Professeur D. SIMON
Secrétaire Général	M. G. GAY

SECTEUR SANTE

Composantes

UFR de Médecine Lyon R.T.H. Laënnec	Directeur : M. le Professeur P. COCHAT
UFR de Médecine Lyon Grange-Blanche	Directeur : M. le Professeur X. MARTIN
UFR de Médecine Lyon-Nord	Directeur : M. le Professeur J. ETIENNE
UFR de Médecine Lyon-Sud	Directeur : M. le Professeur F.N. GILLY
UFR d'Odontologie	Directeur : M. O. ROBIN
Institut des Sciences Pharmaceutiques et Biologiques	Directeur : M. le Professeur F. LOCHER
Institut Techniques de Réadaptation	Directeur : M. le Professeur MATILLON
Département de Formation et Centre de Recherche en Biologie Humaine	Directeur : M. le Professeur P. FARGE

SECTEUR SCIENCES

Composantes

UFR de Physique	Directeur : Mme. le Professeur S. FLECK
UFR de Biologie	Directeur : M. le Professeur H. PINON
UFR de Mécanique	Directeur : M. le Professeur H. BEN HADID
UFR de Génie Electrique et des Procédés	Directeur : M. le Professeur G. CLERC
UFR Sciences de la Terre	Directeur : M. le Professeur P. HANTZPERGUE
UFR de Mathématiques	Directeur : M. le Professeur A. GOLDMAN
UFR d'Informatique	Directeur : M. le Professeur S. AKKOUCHE
UFR de Chimie Biochimie	Directeur : Mme. le Professeur H. PARROT
UFR STAPS	Directeur : M. C. COLLIGNON
Observatoire de Lyon	Directeur : M. le Professeur R. BACON
Institut des Sciences et des Techniques de l'Ingénieur de Lyon	Directeur : M. le Professeur J. LIETO
IUT A	Directeur : M. le Professeur M. C. COULET
IUT B	Directeur : M. le Professeur R. LAMARTINE
Institut de Science Financière et d'Assurances	Directeur : M. le Professeur J.C. AUGROS

To My Parents & Pushpika.....

My heartiest thanks to…

I would like to thank Prof. Philippe Chaumont for acting as the president of my examination jury and I am grateful to Prof. Maria J. Barandiran and Dr. Costantino Creton for agreeing to be present on my jury as external examiners. I would like to thank Dr. Keltoum Ouzineb for her presence in the jury. I am grateful to Prof. Timothy McKenna, a co-director of my PhD thesis for inspiring me to undertake this thesis and for sourcing the funding required to bring my ideas to fruition. I would also like to thank Prof. McKenna and Dr. Elodie Bougret-lami, the other co-director of my thesis, for their guidance and valuable discussions.

I would like to thank Dr. Roger Spitz, former director of Laboratoire de Chimie et Procédés de Polymérisation (LCPP) for allowing me to work at the lab. Of course, I would also like to thank Sylvie and Nathalie as well for helping me get my administrative affairs with LCPP in order.

I always sought out Mr. Christian Graillat's advice and assistance whenever I had difficulties and I am grateful to him for helping me, sharing his vast knowledge and unequalled body of experience in emulsion polymerisation with me. I would like to thank Dr. F. Boisson at Service de RMN de la FRPL, FR2151/CNRS, BP24, 69390, Vernaison for doing NMR analysis of my samples. I am grateful to Pierre-Yves for helping me prepare and analyse my transmission electron microscopy (TEM) samples. I thank Jenny Faucheu at Mateis, Insa de Lyon for doing wet stem analysis of my samples. Elise Degrandi, a PhD student of Dr. Costantino Creton, helped me with many of my characterisation studies and I am grateful for the many fruitful discussions we shared. I am grateful to Dr. Carolina de las Heras Alarcon of University of Surrey for carrying out atomic force microscopy (AFM) analysis of my samples. I also thank Mrs. V. Doukova and Mr. A. Utgenannt (University of Surrey) for assistance with the DSC analysis.

When I came to France without knowing French, I fortunately had some very good friends to help me. I gratefully recall the assistance Norma, Prakash and Lars provided me when I was overwhelmed with yet more complicated French administrative problems. I remind the friendship of Indian friends especially KJR and Shashank who shared my loneliness during my first visit to Lyon. I had a very interesting time at LCPP with the research group who was there from 2005 to 2008. I greatly appreciate the warm friendship of Jean-Pierrs, David, Virginie & Erik, Julien, Alex, Hugo, Luc, Ricardo, Remi, Rafael, Raul, Fernanda, Hamilton, Ali, Salima and others. I remember the joyful trips to the Alps with David and company and to Ardesh with Jean-Pierrs. I am grateful to LCPP and Napoleon project for sponsoring me to travel to St.Sebastian and Stockholm to participate in the Emulsion Polymerisation course and the Napoleon meeting. I am grateful to Dr. Keltoum Ouzineb and CYTEC for sponsoring me for my visit to CYTEC.

I am grateful to Prakash for helping me solve my visa problems, allowing my wife Pushpika and my daughter to join me in France. I am grateful to Pushpika for tolerating the monotonous life; she spent much time at home during my thesis. Our Sri Lankan friends (Karu Ayya, Malini Akka and family) provided us with helpful assistance. I greatly appreciate the free accommodation they provided to me out of the kindness of their hearts during my two to three weeks long visits to Lyon from Canada. We had a happy time in Lyon with Karu & family, Lars & Harriot, Erik & Virginie, Prakash, Shashank & Rashmi, Agustin & Mari, Thuan, Helen, and other friends.

When I came to Canada, Ula, Jordan, Raul, Mary and other friends at the Department of Chemical Engineering at Queen's Univeristy helped me for my relocation. I always sought Jordan's help regarding my academic and non-academic work. I am grateful to Jordan for reading my thesis and correcting grammatical errors. Our relatives, Nande & Kumudu who live in Canada helped us giving free accommodation during our stay in Toronto. I gratefully remind their help.

I couldn't have completed this long journey without the sacrifice and guidance of my parents and teachers. Any proper acknowledgement must begin and end with them!

Summary

The objectives of work presented in this thesis are to understand droplet and particle formulation processes in order to make useful polymer-polymer hybrids in aqueous dispersions and use our fundamental understanding of these processes to:

1. Improve monomer conversion as much as possible.

2. Understand impact of these processes on hybrid film properties.

Specific case studies of interest under commercially feasible conditions (i.e. solids content of 50wt %) were done based on two systems namely alkyd-acrylic and polyurethane-acrylic. Miniemulsification, miniemulsion polymerisation and characterisation of hybrid latex, chemical incorporation of alkyd and polyurethane to acrylic monomers were studied in detail. We have been able to successfully synthesise and characterise hybrid latex of about 100nm in particle diameter and high solids content (50wt %) to be used in coating and adhesive applications.

Résumé

Les objectifs du travail présenté ici sont de comprendre les procédés de formulation des gouttelettes et des particules afin de faire des hybrides polymère-polymère de qualité en dispersions aqueuses et d'utiliser notre compréhension fondamentale de ces procédés pour :

1. Augmenter le taux de conversion de(s) monomère(s) autant que possible.

2. Comprendre l'impact de ces procédés sur les propriétés des films hybrides.

Des cas particuliers ont été étudiés dans des conditions commercialement viables (taux de solide de 50% en masse) basés sur deux systèmes appelés alkyde-acryliques et polyuréthane-acrylique. La préparation des miniémulsions, la polymérisation en miniémulsion et la caractérisation des latex hybrides, l'incorporation chimique d'alkyde et de polyuréthane dans les monomères acryliques ont été étudiés en détails. Nous sommes parvenus à synthétiser et caractériser des latex hybrides avec de haut taux de solides (50% en masse) composés de particules de 100nm de diamètre utilisables dans des applications de revêtement et d'adhésifs.

ABBREVIATIONS & SYMBOLS

A_s	specific surface area (m^2)
AA	acrylic acid
AFM	atomic force microscopy
AIBN	azobisisobutyronitrile
BA	butyl acrylate
BPA	bisphenol a
CMC	critical micellar concentration
CTA	chain transfer agent
D_d	droplet diameter
D_p	particle diameter
DG	degree of grafting
DLS	dynamic light scattering
DSC	differential scanning colorimetry
FTIR	Fourier transmission infra red spectroscopy
GC	gas chromatography
GPC	gel permeation chromatography
HEMA	hydroxy ethyl methacrylate
KPS	potassium persulphate
LPO	dilauryl peroxide
MMA	methyl methacrylate
MBS	sodium bi sulphite
N_d	number of droplets

N_p	number of polymer particles
NCO	iso cyanate
NMR	nuclear magnetic reference spectroscopy
ODA	octadecyl acrylate
PI	polydispersity index
PU	polyurethane
PBA	poly butyl acrylate
PMMA	poly methyl methacrylate
SFS	sodium formaldehyde sulfoxylate
T_g	glass transition temperature
TBHP	tertiary butyl hydroperoxide
THF	tetra hydrofuran
TEM	transmission electron microscopy
TSC	total solid content

TABLE OF CONTENTS

Introduction

A kinetically stable emulsion of very small droplets is, for historical reasons, called a miniemulsion. A miniemulsion is similar to a conventional emulsion polymerisation system in the sense that one can use similar monomers, surfactants and initiators to make a dispersion of particles of the size 50-500nm in diameter. The major difference between the two systems lies in the nucleation process. In a conventional emulsion, droplets are quite large relative to micelles and particles. These droplets are in the range of 1-10µm diameter and are dispersed in an aqueous solution of surfactant, typically at a concentration that exceeds the critical micelle concentration (CMC). Since monomer droplets are relatively large (1-10 µm) compared to the size of monomer-swollen micelles (10-20nm), the surface area of the micelles is orders of magnitude greater than that of the monomer droplets in a conventional emulsion. As a result, the probability of a radical entering into the monomer droplets is very low, and most particles are formed by either homogenous (precipitation of chains formed via polymerisation in the aqueous phase) or heterogeneous nucleation (micellar nucleation). On the other hand, in a miniemulsion the droplets are generated in such a way that they are small enough to effectively capture free radicals and thereby become the principle locus of polymerisation. However, for this to happen, the presence of free surfactant in the aqueous phase of a miniemulsion needs to be below the CMC (if micelles are present, they will be the favoured locus of polymerisation since they would have a much higher surface area).

Conventional emulsion polymerisation is extensively employed as an industrial process to manufacture various products such as paints, adhesives, impact modifiers and numerous other products. The diffusion of monomer from monomer swollen droplets to the polymerisation site through the aqueous phase is an essential feature of emulsion polymerisation and hence this process is limited to monomers which are hydrophilic enough to diffuse through the aqueous phase. While presenting certain advantages such as rapid reaction rates, this particular feature of emulsion polymerisation makes it very challenging to incorporate other materials in the polymer phase in the reactor. Therefore other polymerisation techniques such as solution or bulk polymerisation must be used to

synthesise commercially important, hydrophobic compounds like alkyd resins. The emission of volatile organic compounds (VOCs) has become a major environmental concern, thus making this last route less desirable than water-based processes.

Different methods of incorporating these hydrophobic compounds in environmental friendly acrylic latexes have been studied, for example the formulation of physical blends of alkyds or polyurethanes with acrylic latexes[1]. However the major problem of these physical blends is their poor properties such as hazy or non-uniform films which can in large part be attributed to the incompatibility of the two polymer types. Miniemulsion polymerisation provides an attractive solution to this problem since these highly hydrophobic compounds can be incorporated into monomer droplets during the miniemulsification process[2]. This means that they can be mixed with the final polymer in molecular level and if they possess unsaturated bonds, they can be chemically reacted with the growing polymer chains during polymerisation.

Latex particles containing two or more polymers are called hybrid polymer particles[3]. The idea of hybrid materials is to combine the properties of materials (polymers, fillers, additives etc) with complementary characteristics. Water-borne, environmentally friendly hybrid polymers that synergistically combine the positive properties of materials can be synthesised by miniemulsion polymerisation and this process is called hybrid miniemulsion polymerisation[4]. A comparative overview of emulsion and miniemulsion polymerisation is presented in Chapter 1.

Researchers have been investigating the use of hybrid miniemulsion polymerisation to produce various industrially important chemically active materials such as alkyd resins, polyurethanes (PU), epoxy resins and silicones[5-8]. If one considers alkyd-acrylic hybrid systems, these systems have been studied with respect to different aspects such as limiting monomer conversion and hybrid particle morphology[9]. The chemical incorporation of PU in acrylic polymers and the morphology of these hybrid systems have also been studied[7]. Most of these systems have been studied for academic purposes and the industrial application of these systems is rarely discussed. Developing hybrid systems which can be applied in industrial scale is a main goal of the current study.

Introduction

The objective of the work presented in this thesis is to synthesise and characterise hybrid latexes with high solids (50%) and low particle size (~100nm) by miniemulsion polymerisation for coating and adhesive applications. Since the required particle size is as low as 100nm (diameter) for a hybrid system of 50% solids, the miniemulsification procedure plays an important role in our system. Different miniemulsification techniques were studied to achieve a particle size of 100nm for a system of 50% solids. A comprehensive discussion on the miniemulsification of monomer-resin hybrid system is presented in Chapter 2.

An alkyd resin with unsaturated double bonds (reactive alkyd resin) was used in Chapter 3 for the synthesis of a hybrid latex for coating applications. A polyurethane (PU) with NCO functional groups (reactive PU) has been used in the synthesis of hybrid latexes for adhesive applications. We sought to understand possible reasons for limiting monomer conversion in alkyd-acrylic hybrid systems and tried to increase the final monomer conversion without creating new particles. The evolution of the droplet to particle mapping (N_p/N_d) in the presence of varying amounts of alkyd was therefore an important parameter in our study. We correlated the evolution of this quantity with the droplet stability and the individual monomer conversions (in order to account for their different reactivities). A discussion on the alkyd-acrylic hybrid system is presented in Chapter 3.

Since the objective behind the use of reactive PU was to incorporate it efficiently in the organic phase in order to obtain desirable adhesive products, the NCO functional groups were studied quantitatively and qualitatively. The NCO functional groups were reacted with 2-hydroxyethylmethacrylate (HEMA) and thereby PU segments were incorporated into the acrylic polymer chains chemically. The importance of use of free NCO functions in hydrophobic chain extension reactions with hydrophobic chain extenders such as bisphenol A and thereby the increase of hydrophobicity of hybrid particles was also studied. A detailed study of these chemical reactions and their effect on properties, particularly adhesive properties, are presented in Chapter 4.

The following figures (Figure 1 and Figure 2) illustrate the key differences between conventional emulsion polymerisation and miniemulsion polymerisation.

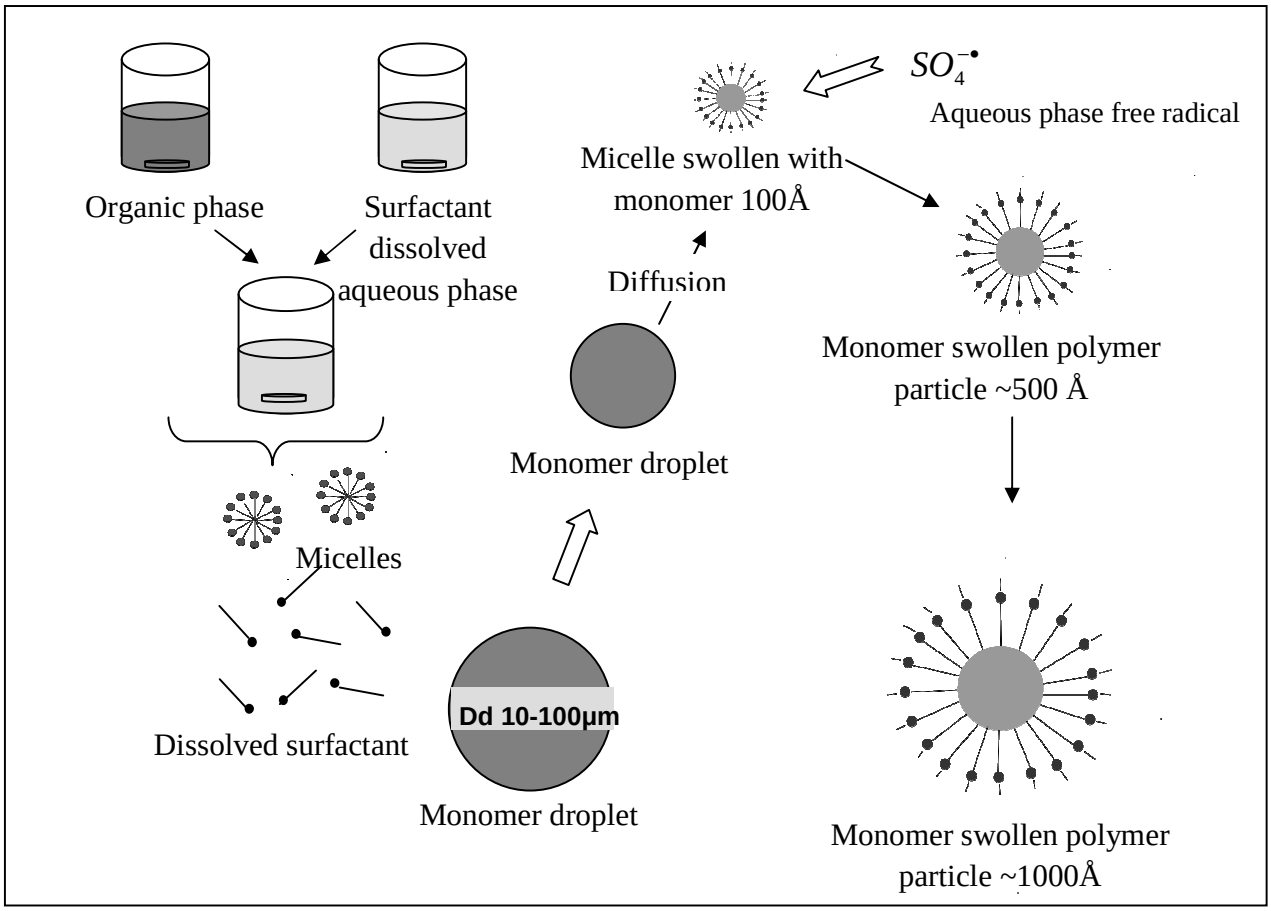

Figure 1. An illustration of emulsion polymerisation

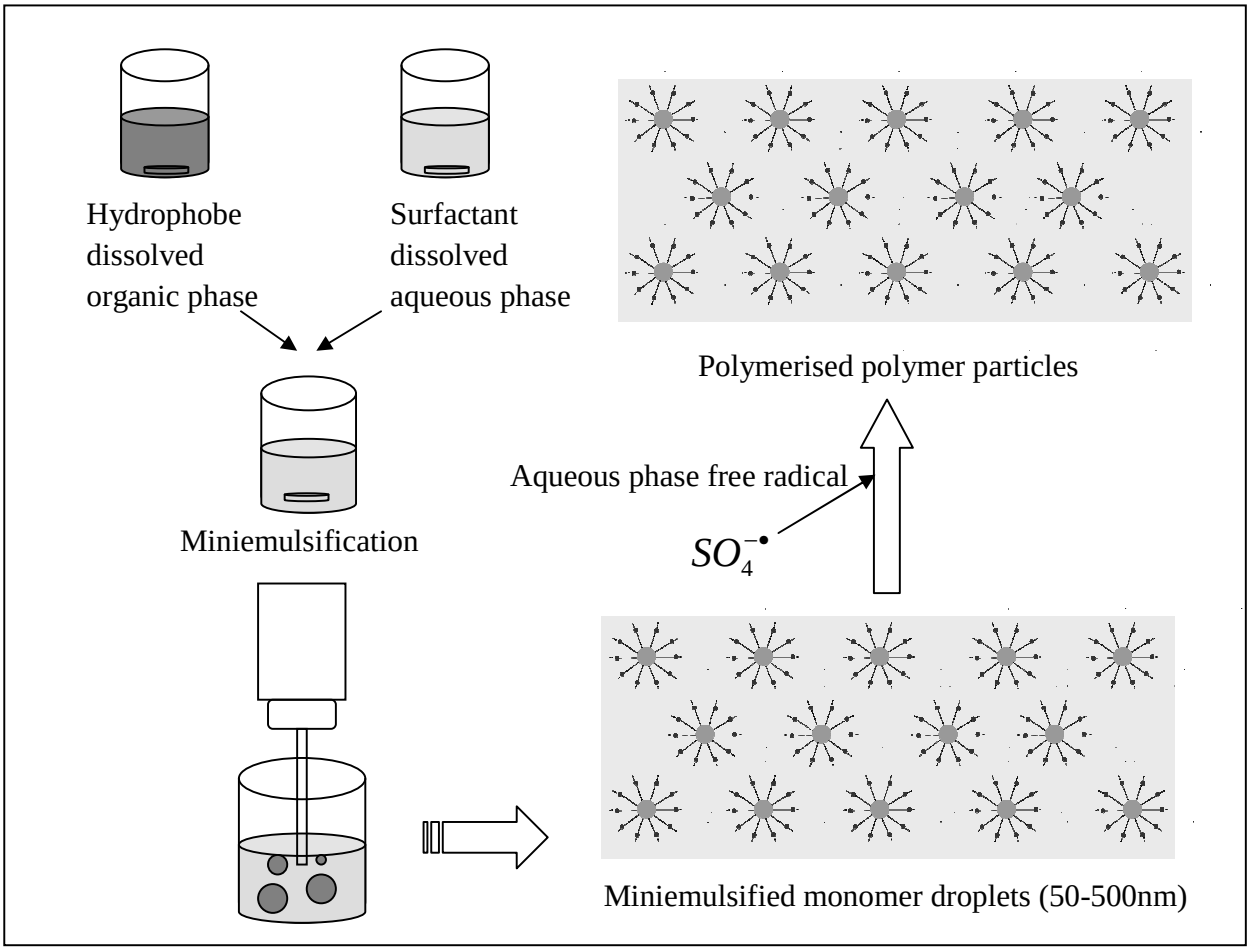

Figure 2. An illustration of mini emulsion polymerisation

CHAPTER 1

Bibliographic Review

1-1 The basic concepts of emulsion and miniemulsion polymerisation.

1-2 Miniemulsification process.

1-3 Alkyd-acrylic hybrid miniemulsion polymerisation.

1-4 Polyurethane-acrylic hybrid miniemulsion polymerisation.

1-5 Summary and conclusions.

1.1 The basic concepts of emulsion and miniemulsion polymerisation.

Before discussing the concepts of hybrid systems and hybrid miniemulsion polymerisation, it is useful to briefly review the fundamental concepts of emulsion and miniemulsion polymerisation techniques. We will briefly discuss the basic concepts of two techniques in this section.

1.1.1 Emulsion Polymerisation

An emulsion is defined as a stable dispersion of water insoluble or partly water soluble monomer(s) (the organic phase) in an aqueous phase which consists of surface active material. The essential components of an emulsion polymerisation recipe are water, monomer(s), surfactants and initiator(s). The surfactants or emulsifier molecules are composed of hydrophilic and hydrophobic moieties which facilitate the homogeneous dispersion of the organic phase in the aqueous phase. The initiator decomposes in the aqueous phase to produce free radicals which initiate the polymerisation reaction. If the concentration of surfactant is above the critical micelle concentration (CMC), micelles are formed, and these typically become the main loci of reaction during the early stage of the polymerisation.

The classical emulsion polymerisation was first described by Harkins[10-12]. It is an extremely simplified description of what is now accepted to be a more complex series of events, but it nevertheless remains useful to illustrate the major features of emulsion polymerisation. For a

more detailed treatment see the studies on emulsion polymerisation[13, 14]. According to the Harkins model, a batch emulsion polymerisation can be divided into three intervals.

Interval 1:

This is the particle formation or nucleation stage. This stage begins with the initiation of the polymerisation by free radicals generated in the aqueous phase. According to this model, particles form when a free radical enters a micelle swollen with monomer, thus beginning the polymerisation. This interval is characterised by an increasing polymerisation rate due to an increase in the number of particles with time. This interval ends with the disappearance of micelles. Harkins considered that micellar nucleation is the only means of particle formation.

Interval 2:

During this stage the number of particles is assumed to remain constant if there is no coagulation, and the reactor contains growing polymer particles, dispersed monomer droplets which act as monomer reservoirs for the growing particles, surfactants dissolved in aqueous phase and adsorbed on the surface of the organic phases. Due to their small size (<<1µm) it is impossible to swell the particles beyond a certain point. Thus the concentration of monomer in the particles is constant at the saturation concentration. The rate of polymerisation can therefore be considered to constant under these conditions. The disappearance of monomer droplets marks the end of this interval.

Interval 3:

The number of particles is once again assumed constant, but the concentration of monomer in particles decreases since there are no longer any monomer droplets to act as a monomer reservoir. However the rate of polymerisation can either decrease due to decreasing monomer concentration or increase due to an accumulation of radicals inside the particles. This increase of rate of polymerisation is referred to as gel or Tromsdorff effect, brought on by an increase in the local viscosity. In addition, if the increase in the local viscosity is strong enough it can provoke a decrease in the mobility of small molecules, thereby causing radical desorption from the particles to diminish. This latter phenomenon is known as the glass effect, can also lead to a decrease in

the rate of polymerisation if the monomer molecules cannot diffuse to the growing ends of the polymer chains.

1.1.2 Nucleation

Particle nucleation is one of the most critical events in emulsion and miniemulsion polymerisation since the formation and stabilisation of particles is the key to continue polymerisation process. Although Harkins[10-12] considered micellar nucleation as the only means of nucleation, Priest[15] showed for the first time that homogeneous nucleation could be predominant under surfactant free conditions especially in the presence of hydrophilic monomers. Ugelstad et al[16] were the first to demonstrate that under conditions in which the droplet size is small enough, droplet nucleation could be a significant factor. Accordingly three major mechanisms for particle formation in latex production have been proposed: micellar, homogeneous and droplet nucleation.

1.1.2.1 Micellar Nucleation

When the surfactant is present above the CMC in the aqueous phase, micelles are formed. When monomer is dispersed in this surfactant solution, monomer droplets stabilised by surfactant are formed and some of the monomer swells the micelles. Since the monomer-swollen micelles (10-20nm in diameter) are significantly smaller in size than the monomer droplets (1-10µm in diameter), the surface area of the micelles is orders of magnitude greater than that of the monomer droplets. When the initiator decomposes to form free radicals, these react with the monomer dissolved in the aqueous phase to form short chain oligoradicals. As these oligoradicals continue to add chain units via reaction with the aqueous phase monomer they become more hydrophobic and after they reach a certain length "z" they are hydrophobic enough that they become "surface active" and the hydrophobic portion of the molecule can enter the organic phase[17, 18]. Since the surface area of monomer swollen micelles is greater than that of monomer droplets, most of the oligoradicals are captured by micelles. After the nucleation of monomer swollen micelles, they become monomer swollen particles and continuously grow by propagation, with the monomer droplets acting as a monomer reservoir. The disappearance of monomer swollen micelles marks the end of micellar nucleation. Micellar nucleation is typically

complete in a batch reactor at low monomer conversion (2-10%). That this point most of the monomer is located in the monomer droplets. These large monomer droplets disappear at around 40-60% overall monomer conversion.

1.1.2.2 Homogeneous Nucleation

The idea of homogeneous nucleation was first put forward by Priest[15] and a quantitative mechanism was proposed by Fitch and Tsai[19] and further developed by Hansen and Ugelstad[20]. At surfactant concentrations below the CMC, monomer dissolved in the aqueous phase will still react in the presence of a free radical initiator. However in the absence of micelles, the oligoradicals continue to grow beyond the value "z" until they reach a length "j_{crit}" at which point the chain becomes coiled in conformation, and subsequently insoluble in the aqueous phase, forming a primary particle[21]. This particle at this stage consists of not only the oligomeric radical but also small molecules such as monomer[21]. These primary particles can be stabilised by dissolved surfactant molecules or by charges come from initiators. If sufficiently stabilised, these particles continue to grow by adsorbing monomer otherwise they coagulate with other particles. The effectiveness of the stabilisation system and the distribution of surface charges in the primary and growing particles determine the size and number of particles nucleated this way[22, 23]. Coagulative nucleation is a derivative of homogeneous nucleation. This mechanism was proposed by Lichti et al[24] and according to this theory the primary particles coagulate either with each other to form more stable particles or they will coagulate with particles that are already present and thereby maintain a sufficient density of charges for their stabilisation.

1.1.2.3 Droplet Nucleation

Ugelstad et al.[16] showed that under conditions in which the droplet size is small enough i.e. the specific surface area is large enough, droplet nucleation could be a viable means of particle nucleation. Due to the large diameter (1-10µm) and small number (~10^{13} versus 10^{21} micelles) of droplets, nucleation of monomer droplets has typically been neglected in emulsion polymerisation[25]. However the existence of droplet nucleation for the emulsion polymerisation of vinyl chloride stabilised with a combination of anionic surfactants and fatty alcohols had been

suggested by Ugelstad et al.[26]. The key requirement for droplet nucleation is the presence and maintained stability of small droplets. In fact this is the basis of miniemulsion polymerisation in which small droplets (50-500nm) are created mechanically and kept stable in the presence of a hydrophobe (This is discussed in more detail in the following section). One of the distinguishing features of droplet nucleation as opposed to micellar or homogeneous nucleation is the nature of the particles at "birth"[25]. Droplets, which are nucleated into particles, begin as nearly 100% monomer. Particles created by conventional emulsion polymerisation can eventually swell to volume fractions of monomer from about 0.3 to 0.6 in the presence of monomer droplets. It is therefore to be expected that one could observe a different polymer quality according to the method of nucleation.

1.1.3 Miniemulsion Polymerisation

Miniemulsion polymerisation involves the use of an effective surfactant/hydrophobe system, typically coupled with a mechanical energy source to produce very small (50-500nm) monomer droplets. In the first successful example of miniemulsion polymerisation by Ugelstad et al[16]., they stirred 1-hexadecanol (cetyl alcohol; CA) with water and sodium dodecyl sulfate (SDS) at 60°C and then styrene was added under stirring. It was found that the miniemulsions they created were stable for 2 weeks. The monomer miniemulsions were polymerised at 60°C and it was found that a large fraction of polymer particles were formed by droplet nucleation when a relatively modest amount of surfactant was used. After this first example of miniemulsion polymerisation, our understanding of the technique has been advanced through numerous experimental studies[27-32]. It was found that with ordinary stirring equipment, addition of hexadecane did not give the rapid emulsification that could be obtained with 1-hexadecanol[28]. The need for a more efficient homogenisation system arose. When hexadecane-containing emulsions were homogenised with a Manton-Gaulin high pressure laboratory homogeniser, extremely stable monomer miniemulsions were obtained[28]. At present different homogenisation devices such as ultrasonication[33], rotor-stators[34] and static mixtures[35] have been evolved for the purpose of miniemulsification.

Chapter 1: Bibliographic Review

Maintaining the stability of very small droplets of a miniemulsion is a key requirement. The droplets must be stabilised both against degradation by molecular diffusion (Ostwald ripening, a monomolecular process; we will discuss this in more detail below) and against coalescence by collisions (a bimolecular process)[36, 37]. Coalescence can be prevented by using an appropriate surfactant in sufficient amount [13, 37].

The role of the hydrophobe is to control the diffusion of monomer from small droplets to large droplets. The idea of diffusion of monomer from small droplets to large droplets (referred to as Ostwald ripening) was first presented by Higuchi and Misra[38]. It was based on the fact that due to the surface energy, the chemical potential of the monomer in small droplets is higher than in large droplets or plane surfaces. As a result, monomer diffuses from small to large droplets, leading to larger and larger droplets. Higuchi and Misra[38] explained that the addition of a small amount of a water insoluble compound would retard the emulsion degradation by molecular zdiffusion because the slow rate of diffusion of the water –insoluble compound would permit the monomer to remain essentially equilibrated among the droplets.

The chemical potential of the monomer (μ) in a monomer droplet of diameter *d*, can be expressed as[39]:

$$\mu = \ln(1-\phi_c) + (1-m_{mc})\phi_c + \chi_{mc}\phi_c^2 + \frac{4\gamma V_m}{dRT} \qquad \text{Equation 1}$$

Where ϕ_c is the volume fraction of the hydrophobe, m_{mc} is the ratio of the molar volume of hydrophobe and monomer, χ is the interaction parameter, V_m is the molar volume of the monomer, γ is the interfacial tension, *R* is the universal gas constant, and *T* is the temperature. This equation is based on the Flory–Huggins lattice theory of polymer solutions[40], with the extension of Morton et al.[39] involving the addition of an interfacial energy term for spherical phases, and the further extension of Ugelstad and Hansen[41] for phases not involving a polymer as one of their components. The first two terms of the equation represent the entropy of mixing and the third term represent the enthalpy of mixing[42]. Accordingly the first three terms represent the partial molar free energy of mixing and the fourth term represents the partial molar free energy of swelling. For smaller values of (ϕ_c), the chemical potential (μ) can be expressed as

follows.

$$\mu = -m_{mc}\phi_c + \chi_{mc}\phi_c^2 + \frac{\alpha}{d} \qquad \text{Equation 2}$$

Where $\alpha = {}^{4\gamma V_m}\!/_{RT}$

Sood and Awasthi[42] have shown that the difference in the chemical potential ($\Delta\mu$) of two droplets of diameters d_1 and d_2 and hydrophobe volume fractions ϕ_1 and ϕ_2 is given by the following equation:

$$\Delta\mu = \alpha(\frac{1}{d_1} - \frac{1}{d_2}) - (\phi_{c1} - \phi_{c2})[m - \chi(\phi_{c1} + \phi_{c2})] \qquad \text{Equation 3}$$

In the absence of the hydrophobe ($\phi_{c1 \text{ and }} \phi_{c2}$), only the first term in this equation, arising from the contribution to the free energy from swelling, accounts for $\Delta\mu$ of the two droplets. $\Delta\mu$, in this case, can never be diminished, as the mass transfer through the molecular diffusion of the monomer from small droplets (having higher μ values) to large droplets (having lower μ values) will further increase this difference[42]. As can be seen from the equation, this irreversible change in the droplet sizes can be retarded when a hydrophobe is present. In its presence, the mass transfer of the monomer from the smaller droplets to the larger droplets changes their composition. As can be seen from the equation, this can result in the equalisation of their chemical potentials, as the second term arising from the mixing of the two components compensates for the first term due to the swelling[42]. The minimum stable diameter of a droplet depends on the efficiency of the hydrophobe, which is a function of interaction parameter (χ). This is discussed in more detail in section 1.3 (Alkyd-acrylic hybrid systems).

1.1.3.1 Choice of Hydrophobe

A compound should have certain properties to be used as a hydrophobe. The requisite properties for a hydrophobe: high monomer solubility, low water solubility and low molecular weight[2, 25]. The need for these properties can be seen from Equation 3. An ideal hydrophobe should have high monomer solubility, and thus lead to strong interactions between itself and the monomer.

For example if 1-hexadecanol and hexadecane are compared, hexadecane is more soluble in monomer than 1-hexadecanol. The low solubility of 1-hexadecanol in monomer is due to its higher polarity due to the presence of OH functional group[42]. Therefore 1-hexadecanol is more non ideal than hexadecane and has a higher positive value for χ[42]. As a result the value of the negative term associated with χ of the Equation 3 is higher for 1-hexadecanol and hence it is less efficient in this role. Low molecular weight will give a high ratio of hydrophobe molecules to monomer molecules (*m* in Equation 3) in the droplet[25] and thereby the efficiency of hydrophobe is increased. Low water solubility enhances the distribution of the hydrophobe in the organic phase that favors the monomer drops, giving a higher volume fraction of hydrophobe in the droplet[25]. Accordingly all of these three factors will retard monomer loss via Ostwald ripening.

1.1.4 Kinetics of Emulsion and Miniemulsion Polymerisation

Smith and Ewart[43] extended Harkins' theory to describe micellar nucleation quantitatively. They quantified the rate of homopolymerisation according to following equation.

$$R_p = K_p \times [M]_p \bar{n} \times \frac{N_p}{N_A} \qquad \text{Equation 4}$$

Where R_p is polymerisation rate (mol.min^{-1}.L^{-1}), k_p is propagation rate constant (L.mol^{-1}.min^{-1}), $[M]_p$ is concentration of monomer in particles (mol.L^{-1}), $\bar{n}$ is average number of radicals per particle, N_p is number of particles per litre of emulsion and N_A is Avagadro's constant. The extension of this equation to the case of multiple monomers is possible and has been discussed in several papers[44, 45]. However, we do not discuss the kinetics of both emulsion and miniemulsion polymerization in detail during this study. For a more detailed study of the kinetics of miniemulsion polymerisation see the kinetic studies of Bechthold et al[46]. Suffice to say that Equation 4 can be used to describe the kinetics of both systems, with the major difference lying in the fact that the monomer concentrations at low to moderate conversion will be higher in miniemulsion than emulsion polymerisation.

1.2 Miniemulsification Process

Miniemulsions are produced by applying mechanical energy to an emulsion. Due to differences in attractive interactions between the molecules of the two liquid phases of an emulsion, an interfacial tension, γ exists between the two liquids everywhere they are in contact[47]. When larger droplets are mechanically broken in to smaller droplets, an additional interfacial area, ΔA is created[47]. If thermodynamics of this system are considered, surfactants reduce the interfacial tension and hence reduce the surface free energy ($\Delta G = \gamma \Delta A$) required to increase any interfacial area[48]. However a much higher amount of energy, significantly higher than the difference in surface energy, $\gamma \Delta A$ is required to rupture bigger droplets. A large portion of the energy input into the system can be lost to viscous resistance during agitation, resulting in the creation of heat[49, 50]. In addition, in a realistic system, a significant amount of coalescence can occur in the emulsification vessel, away from the energy source.

In earliest miniemulsification studies, mechanical energy was often provided using only simple stirring[16]. Some of the early work describes the use of agitators such as the Omni-mixer and Ultraturrax[36]. Currently there are a number of dispersion devices available that are capable of meeting this requirement, including ultrasonication, rotor-stator systems, static mixers[51] and high-pressure homogenisers[52].

1.2.1 Ultrasonication

Emulsification using ultrasound was first reported in 1927[33] and the first patent was granted for this type of system in 1944 in Switzerland[53]. A schematic diagram of an ultrasonic system is illustrated in Figure 1. The sonifier produces ultrasonic waves that cause the molecules to oscillate about their mean position as the waves propagate. During the compression cycle, the average distance between the molecules decreases, whilst during rarefaction the distance increases. The rarefaction results in a negative pressure that may cause the formation of voids or cavities[54, 55] (cavitation bubbles) that may grow in size. High-frequency vibrations applied to a diphasic liquid system provides a different means of breaking and dispersing a bulk phase: large drops (ca. 80 mm), produced by the instability of interfacial waves, are broken into smaller ones by acoustic cavitation[56, 57]. The rupture of liquids and the effects connected with the motion of

these cavities are collectively referred as cavitation phenomenon[58-61]. In the succeeding compression cycle of the wave, the bubbles are forced to contract and may even disappear totally. The shock waves produced on the total collapse of the bubbles result in the break-up of the surrounding monomer droplets[62].

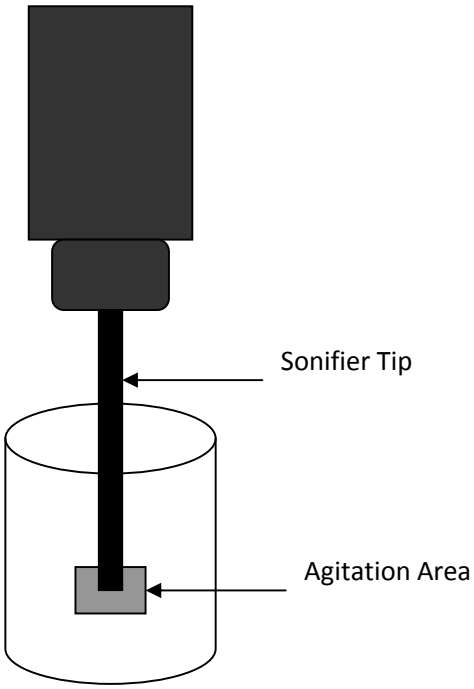

Figure 1. Schematic representation of a Sonifier

Increasing the amplitude (intensity) of the sonifier and/or increasing the time of sonication will result in a decrease in average droplet size of the emulsion[63]. This results from the fact that droplet break up only occurs in a relatively small region near the sonication tip, and a certain time is needed to ensure that all of the fluid in the vessel has passed through the sonication region a sufficient number of times. The time required to ensure complete emulsification is strongly dependent on the flow patterns in the vessel containing the miniemulsion[64]. For every specific emulsion formulation, a limiting value for ideal application of energy exists. This means that there is a limit at which the interfacial surface area has been maximised and thus droplet size has been minimised. Additional input of energy can eventually lead to a reduction of

polydispersity of the droplets[56]. In this process, the droplets are broken up into smaller droplets, which re-aggregate into droplets immediately afterwards. Thus homogenisation by sonication is limited to small amounts of emulsion and low viscosities, as the majority of energy input into the system during the sonication of very viscous mixtures gets wasted in the form of excessive heat production (due to viscous resistance).

1.2.2 Rotor-stator systems

Figure 2 presents a picture of the mixer head (5.5 cm) of a typical rotor-stator system. The mechanisms behind the operation of a typical rotor-stator system can be described as follows[51, 65, 66]. As the blades rotate a vacuum is created that draws the fluid into the assembly. The fluid is then driven towards the periphery of the head by centrifugal forces where it is subjected to milling action in the space between the ends of the blades and the slots of the stator. Finally, the fluid is subjected to high hydraulic shear when it is ejected at high velocities through the narrow slots of the stator and circulated in the vessel. The high fluid acceleration at the outlet of the rotor-stator provokes the circulation of fluid throughout the vessel. The circulatory pattern ensures that fluid is continually drawn into the assembly, thus maintaining the mixing cycle.

Figure 2. Picture of the mixed head of a typical rotor-stator system

1.2.3 Static Mixer

The static mixer is a motionless mixing device composed of mixing elements of an appropriate shape, arranged in a repetitive fashion and equipped in a hollow housing pipe[35]. A fluid is made to flow over a series of mixing elements which have the effect of dividing, accelerating and

recombining the liquid in a geometric sequence to achieve either a high degree of mixing with little energy, or to effectively disperse one fluid in another[34, 67, 68]. A fluid flow introduced to the mixer is divided at the front of the mixing element (flow division).When the flow passed the element, the fluid is mixed by a radial rotation of the flow within the mixing element (radial mixing with the acceleration).The flow direction is reversed at the connection point between the elements (flow recombining).

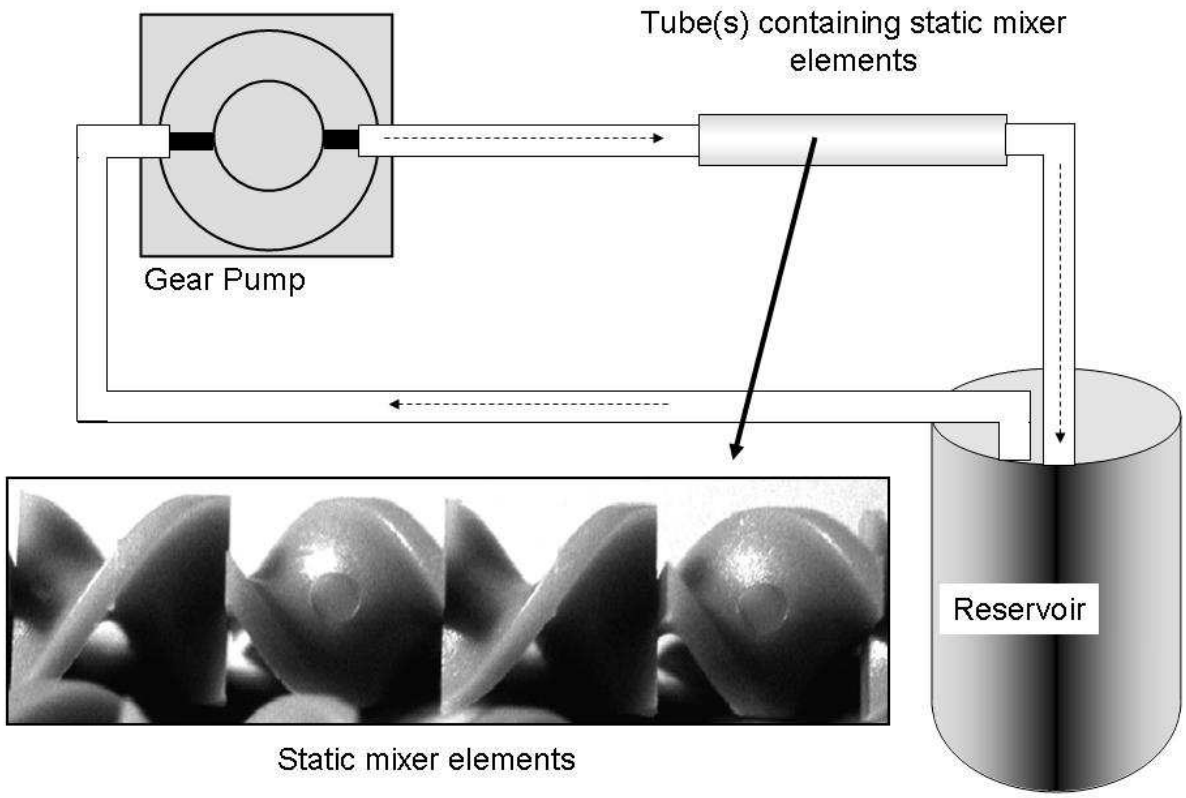

Figure 3. Schematic representation of a static mixer[68]

1.3 Alkyd-Acrylic Hybrid Miniemulsion Polymerisation

In the context of the investigations presented in this thesis, hybrid miniemulsion polymerisation refers to a process by which water-based coatings and traditionally solvent-based resins can be grafted in a single step, with the resulting product having the properties of both the water-based coating and the resin[3-5, 9, 69, 70]. Apart from the alkyd-acrylic or polyurethane-acrylic hybrid systems, other hybrid systems based on different pre polymers such as epoxy resins and silicones have also been studied[6, 8, 71-73].

The need for such hybrid systems has arisen due to increasing environmental concern over the emission of VOC from the conventional one-phase, solvent based processes[69, 74]. Recently, water-based polyacrylate latex coatings have become more widely used because of environmental and health concerns, and ease of water cleanup. However acrylic latexes still lack some of the more desirable properties of alkyds such as gloss, durability, hardness, and water and chemical resistance[4]. Conventional acrylic latex coatings lack any crosslinking mechanism but in the solvent-based alkyd resin systems, the double bonds in the alkyd react with atmospheric oxygen during drying, forming a crosslinked film[69]. Therefore waterborne environmental-friendly hybrid polymers that synergistically combine the positive properties of alkyd resins with the fast drying and color retention of acrylic latexes are of great industrial interest.

The simplest way of preparing acrylic/alkyd hybrids is Physical blends and it has been discussed that these blends often suffer from incompatibility of the two polymer types resulting in hazy or non-uniform films[69]. Several approaches have been used to solve the problem of incompatibility between the acrylic polymers and the oil or alkyd. Nabuurs et al.[5] studied emulsion polymerisation of acrylate monomers in the presence of alkyd. They observed phase separation between the immiscible polyacrylate and alkyd along with low overall conversion. Wang et al.[74] studied the same system and found that the alkyd was copolymerised with the acrylate but phase separation of the resinous compound occurred. All attempts to use macroemulsion polymerisation to graft resins such as polyesters, polyurethanes, and alkyds into acrylics have resulted in complete phase separation of the hydrophobic component from the emulsion[75]. Miniemulsion polymerisation has therefore been considered a more promising approach towards chemically incorporating alkyd into acrylic latex. In the following paragraphs, we will briefly

discuss the different research areas of alkyd-acrylic hybrid systems that are well-documented in the literature.

1.3.1 Grafting Mechanisms in Alkyd-Acrylic Hybrid Systems

The *in situ* grafting of growing polymeric free radicals with an alkyd containing unsaturated double bonds has been studied previously[3, 4, 76]. The predominant polymeric structure of such hybrid systems, as shown by different techniques such as gel permeation chromatography (GPC), NMR, and differential scanning calorimeter[4] (DSC), is poly(acrylate-*graft*-alkyd). The grafting mechanisms of alkyd with different monomers such as methyl methacrylate (MMA) and butyl acrylate (BA) has also been studied[75, 77]. The predominant reactive sites for grafting on the alkyd are the carbon-carbon double bonds (addition) in the natural oils making up the alkyd or the hydrogens allylic to those double bonds(abstraction)[75]. Figure 4 and Figure 5 show the main steps of the reaction routes of grafting by addition.

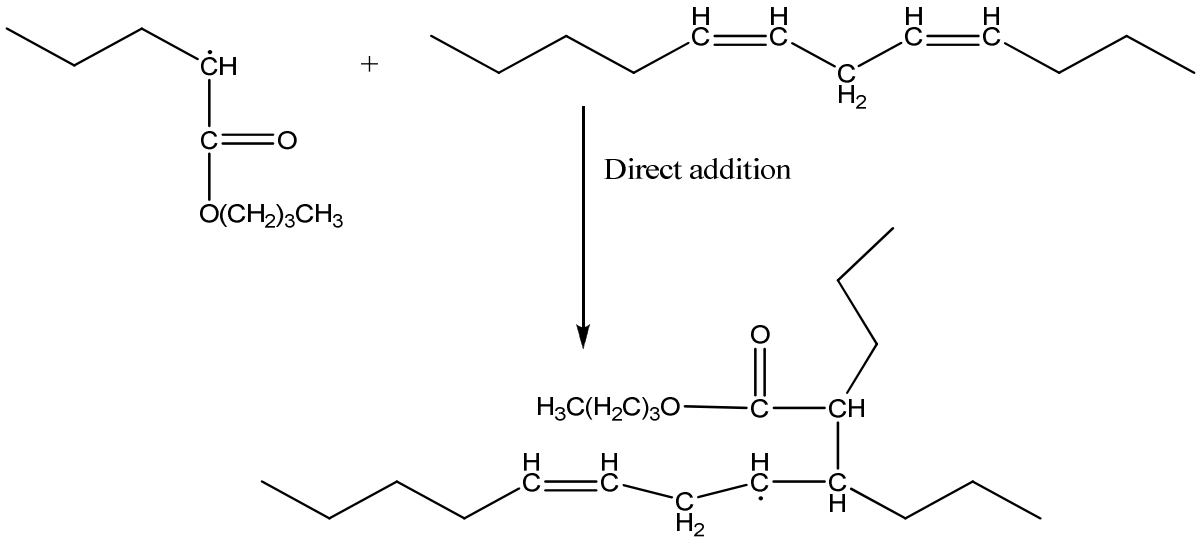

Figure 4. The first step of the reaction route of direct addition

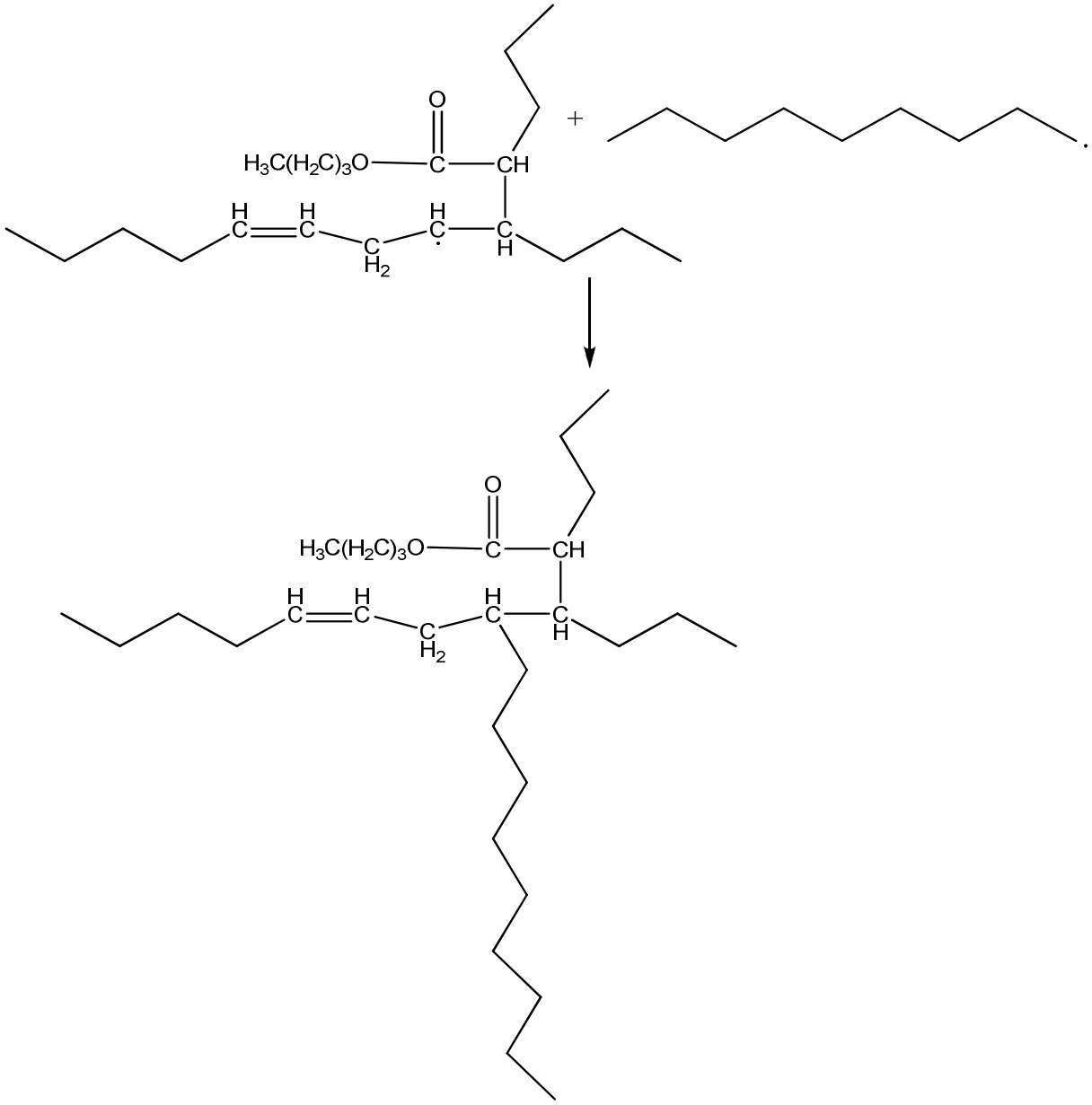

Figure 5. The second step of the reaction route of direct addition

Addition to a double bond is energetically favored over abstraction if only the energy required to interact with a π-bond versus a σ- bond[78] is considered. However, the structure of the groups that surround the reactive polymer site and the steric features of the attacking monomer or chain often influence the overall interaction enough to make abstraction the preferable route of attack[79, 80].

Accordingly, it has been shown that the predominant grafting mechanism of alkyd with MMA is abstraction because of the sterically-hindered reactive center of a PMMA radical while the predominant grafting mechanism of alkyd with BA is addition due to the sterically-relaxed reactive center of a PBA radical[75, 77]. Figure 6 and Figure 7 show the main steps of the reaction route of grafting by hydrogen abstraction.

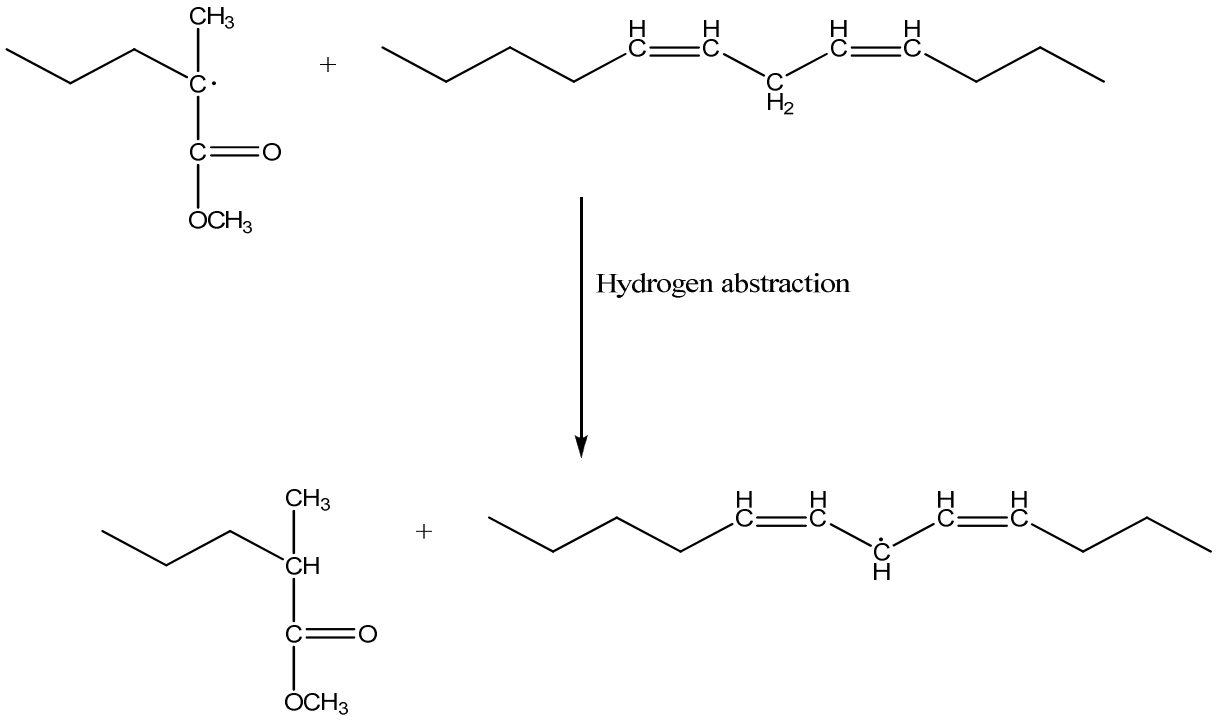

Figure 6. The first step of the reaction route of H abstraction

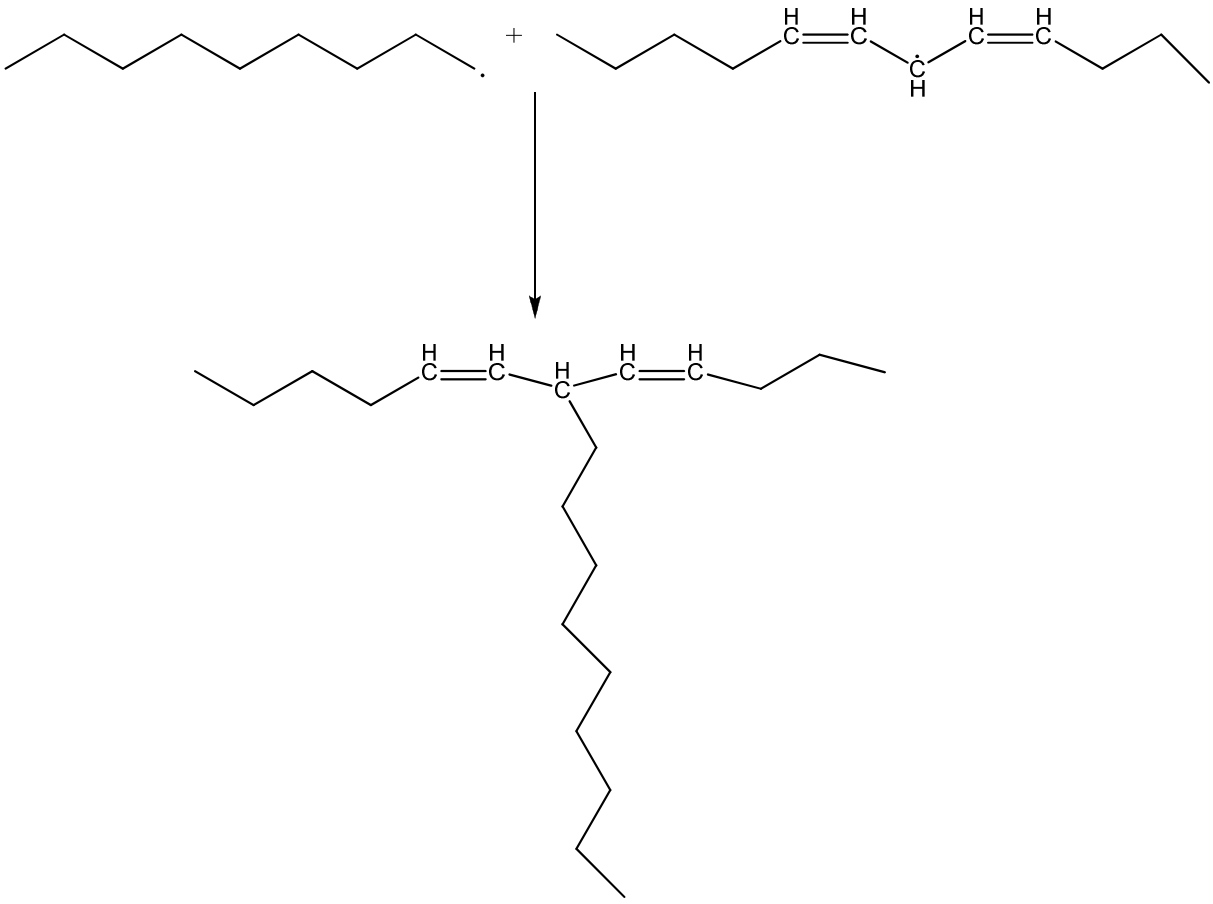

Figure 7. The second step of the reaction route of H abstraction

1.3.2 Morphology of Alkyd-Acrylic Hybrid Particles

Different techniques such as Transmission Electron Microscopy (TEM), Scanning Electron Microscopy (SEM) and Atomic Force Microscopy (AFM) have been used to study the morphology of different acrylic-alkyd hybrid system [9, 81-85]. A core shell morphology, consisting of an alkyd rich core and acrylic rich shell has been established for MMA/Alkyd systems[9, 82]. This is mainly due to the incompatibility between PMMA and alkyd coupled with the highly hydrophobic nature of alkyd[82]. It has been shown that higher esters are non-solvents for PMMA[86]. Since alkyds are essentially higher esters, the incompatibility between the two components leads to a core shell morphology. Since BA is essentially water insoluble[86], the

compatibility between alkyd and PBA is comparatively high. BA reacts quite easily with alkyd through direct addition as discussed in the previous section. Accordingly, BA/Alkyd tends towards a distribution of small alkyd island domains within a continuous PBA particle matrix[82]. The monomer composition (BA/MMA/Acrylic acid) of our alkyd-acrylic system is 49.5/49.5/1 (wt %). A raspberry like core shell morphology has been established for this system based on the fact that the complete phase separation of PMMA shell is avoided by the grafting between PMMA and alkyd[82]. It has been further shown that the choice of initiator (water soluble or oil soluble) does not appear to affect particle morphology[82].

1.3.3 Limiting Monomer Conversion of Alkyd-Acrylic Hybrid System

Limiting monomer conversion of alkyd-acrylic hybrid systems has been a major obstacle for their commercialisation of this hybrid system. Many authors[3-5, 76, 87] have reported this problem Hudda et al[9, 81] have put forward two theories on the cause of limiting monomer conversion. One theory is based on retardative chain transfer from the growing hybrid polymer to the double bonds of alkyd (kinetic mechanism) while the other theory is based on the inaccessibility of certain amounts of monomer due to the trapping of monomer in the hybrid polymer particles[9, 81] (physical mechanism).

When a hydrogen atom allylic to resinous double bond is abstracted by a macroradical, the result is a relatively inactive radical on the resin[75]. This inactive radical leads to a reduction in the overall polymerisation rate and, when approached by another live radical, it terminates with the formation of a grafted alkyd[9]. Theoretically, a limited monomer conversion should not be observed in the saturated alkyd-acrylic system where there are no reactive double bonds on the alkyd, hence no opportunity for allylic hydrogen abstraction to occur. However saturated alkyd-acrylic hybrid systems also show a limiting monomer conversion and a physical mechanism has been put forward based on simulation studies to explain this behaviour[9]. According to this theory, the limiting conversion of hybrid mini-emulsion polymerisation is physical in nature and results from a combination of three factors.

1. The degree of compatibility between the monomer and resinous component.
2. The resultant particle morphology above approximately 50% monomer conversion.
3. The degree of grafting or interactions between the growing polymer and resin.

Although alkyd resins are well soluble in monomers such as MMA and BA, there appears to be some sort of incompatibility between PMMA and alkyd[86]. Since the reactivity of MMA towards a free radical is greater[88] than that of BA, MMA reacts earlier in a batch miniemulsion of MMA and BA. As a result, the PMMA fraction is rich in alkyd grafted hybrid copolymer during the initial stage of polymerisation. Due to the incompatibility of PMMA and alkyd, the morphology of hybrid particles changes to an acrylic rich shell and alkyd rich core[9, 82]. Since the alkyd is predominantly grafted to poly BA[75, 77], a certain amount of monomer most of which is BA is trapped in the alkyd rich core. The trapped monomer becomes inaccessible due to higher viscosity of the shell, resulting in a limiting monomer conversion.[9] We also observed a limiting monomer conversion in our system and attempted to increase the monomer conversion by applying different methods which are described in alkyd-acrylic hybrid system section.

Despite the extensive work done on alkyd-acrylic hybrid systems, it appears that there have not yet been any detailed studies based on the factors such as the variation of the ratio of particle number (N_p) and droplet number (N_d), N_p/N_d with monomer conversion, the change of individual monomer conversion with increasing alkyd quantity and the hydrophobic effect of different hydrophobes. We will investigate these points in the current work since they can provide information on limiting conversion and eventually particle morphology. In addition the hydrophobic effect of alkyd on the organic phase and droplet and particle size distribution under different hydrophobic conditions were also studied.

1.4 Polyurethane-Acrylic Hybrid Miniemulsion Polymerisation

Polyurethanes (PU) are widely used in coating and adhesive applications due to their inherent properties such as solvent resistance, toughness, film formation and abrasion resistance[7, 89-93]. Most urethane formulations are solvent-based, as mentioned above, and solvent-based coatings are less desirable due to the environmental concern regarding high VOC levels[7]. Therefore the possibility of incorporating the positive properties of PU in an environmental friendly water-based system is of great commercial interest[7, 94]. Several approaches to preparing waterborne polyurethane - acrylic hybrid emulsions have been proposed where the aim is to combine the positive properties of acrylic components such as outdoor resistance, pigmentability, fast drying

and colour retention with the aforementioned positive properties of a PU component[1, 95-106]. The most widespread combination is the PU/acrylic emulsion blends. In general a blend or mixture of two different polymers will be immiscible in the absence of specific interactions such as ionomeric interactions[107]. This is a result of thermodynamic inhibition as the free energy of mixing (ΔG_m) of any two polymers is positive for most polymer combinations[108]. Due to the inherent incompatibility between the polyurethane and polyacrylate dispersions, physical blending of the polymers results in phase separation, gel formation and discolouration during storage[109, 110].

1.4.1 Chemical Incorporation of PU in an Acrylic Polymer

Alternative strategies for dispersing reactive PU in the aqueous phase (other than the direct blending) are described in the literature. Aqueous PU dispersions are commonly prepared by the incorporation of ionic groups into the polymer structure to enhance the hydrophilicity of the polymer chains and promote dispersion[111-116]. PUs that contain ionic groups are called PU ionomers[112]. As the traditional way of preparing aqueous PU dispersions requires the presence of hydrophilic segments in the PU backbone, the properties of these PU polymers cannot be as good as those of the hydrophobic ones prepared by solvent-based polymerisation[112].

Reactive PU is a class of PU which contain iso-cyanate (NCO) functional groups; these NCO functional groups can chemically react with other chemically active materials such as hydroxyethyl methacrylate (HEMA). During the polycondensation reaction between NCO functional group and OH functional group, PU segments are chemically grafted to HEMA. When HEMA is polymerised during polymerisation, PU segments are chemically incorporated to the growing polymer chain. The free NCO functions which remain after the reaction with HEMA can be used in hydrophobic chain extension by reacting them with hydrophobic chain extenders such as bisphenol A[109]. The hydrophobicity as well as molecular weight of PU segments can be increased by this way. Figure 8 and Figure 9 show the reaction routes of HEMA grafting to urethane prepolymer and the chain extension of HEMA grafted urethane prepolymer by bisphenol A.

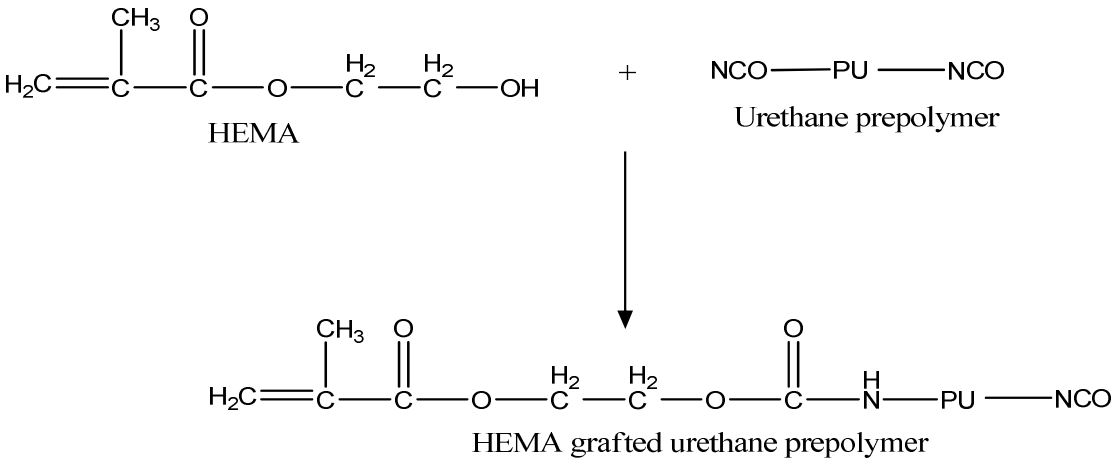

Figure 8. The reaction route of HEMA grafting to urethane prepolymer

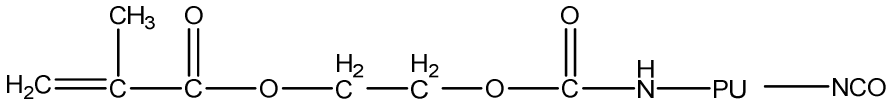

HEMA grafted urethane prepolymer

+

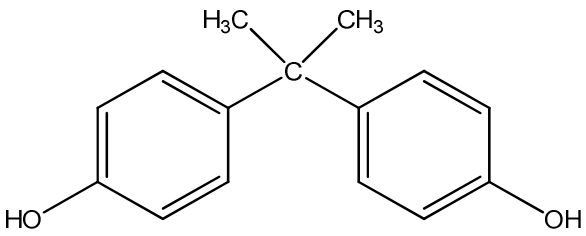

Bisphenol A

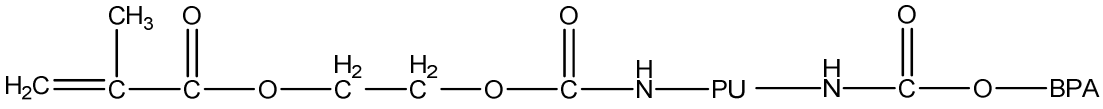

Chain extended HEMA grafted urethane pre polymer

Figure 9. The reaction route of chain extension of HEMA grafted urethane prepolymer

Water-borne environmentally friendly hybrid polymers that synergistically combine the positive properties of hydrophobic PU with positive properties of acrylic latexes, can be synthesised by miniemulsion polymerisation[7, 109, 110, 117, 118]. Most of the work done in this area focused on morphology studies[119], a comparison of the properties of physical blends and hybrids[110], the influence of ingredients on latex properties[94, 109] and the structure and properties of hybrids[120]. We will briefly discuss the morphology and mechanical properties of PU-acrylic hybrid systems in the following section.

1.4.2 Morphology of PU-Acrylic Hybrid Particles

The same techniques (TEM, SEM and AFM) discussed in the alkyd-acrylic system have also been used to study the morphology of PU-acrylic hybrid particles. Different factors which control the morphology of final particles have been studied. These factors fall into two broad categories: thermodynamics and kinetics[119]. Thermodynamic factors determine the equilibrium morphology of final particles, whereas kinetic ones determine the ease of such thermodynamically favoured morphology. Sundberg et al[121] demonstrated the importance of free energy changes (ΔG) to predict the morphology. Since the ΔG is a direct function of the interfacial behaviour of the system, it is an important factor in determining the morphology. Torza and Mason[122] first showed the interfacial behaviour of systems including three immiscible liquids. Since the interfacial tension changes with the composition (different monomer system, monomer to PU ratio, different NCO/OH ratio) the morphology of the hybrid particles also changes with the composition[119].

1.4.3 Mechanical properties of PU- Acrylic Hybrid Particles

Mechanical properties of PU-acrylic hybrid particles have been studied and compared with physical blends. Most of the studies show that hybrid particles show mechanical properties that are superior to those found with physical blends[107, 110, 123]. The improved mechanical strengths of hybrids are due to the inter-diffusion of polymer chains across the original boundaries whereas the separate regions of acrylic and polyurethane components of physical blends are assumed to be the reason for the coarse mechanical properties of the blend[110]. Different factors such as the amount of PU, the NCO/OH molar ratio and the composition of organic phase have been shown to affect the mechanical properties[107, 116, 123]. Although mechanical properties of PU-acrylic hybrid systems have been studied, a detailed study on adhesive properties of this hybrid system is rarely found. Therefore we have studied the factors such as the chemical incorporation of reactive PU through HEMA, the increase in hydrophobicity of the resulting hybrid particles via the chain extension reaction between free NCO functions and bisphenol A, degree of grafting of NCO by HEMA, NCO/OH molar ratio, and the amount of PU in detail to improve the adhesive

properties of hybrid latex. A comprehensive discussion of this system will be presented in the Chapter 4.

1.5 Summary and Conclusions

By contrasting macro and mini emulsions, this discussion showed that it is preferable to use a miniemulsion based approach to make hybrid products. The predominant means of nucleation in miniemulsion systems is droplet nucleation and this avoids the diffusion limitation of very hydrophobic monomers and compounds in conventional emulsion polymerisation. This means that with miniemulsions, hydrophobic compounds such as alkyd resins and polyurethane can be synergistically combined with waterborne acrylic latexes.

Although hybrid miniemulsion polymerisation has been extensively studied, most of these systems are based on low solid content (20%). However, high solids content of at least 50% polymer per unit volume is required for industrial applications. The droplet size of most of previous studies was also in the super micron range and when the submicron range was explored, rarely the size of the dispersed phase was below 250nm. Nanostructured polymer films with high solids content show superior properties in industrial applications such as coatings, adhesives, cosmetics and additives for paper and textiles. We have therefore studied hybrid systems with high solids (50%) and nano sized (100nm) hybrid particles which are industrially important for better filmification.

In this thesis we will study two different hybrid systems. The first system is alkyd-acrylic hybrid system which is based on coating applications and the other one is polyurethane-acrylic hybrid system which is based on adhesive applications. Different techniques of miniemulsification were discussed and we have employed these techniques to produce miniemulsions of high solids (50%) and with average droplet size of 100nm.

The grafting mechanisms, particle morphology and limiting monomer conversion of alkyd-acrylic hybrid system were reviewed. We have attempted to understand the possible reasons and mechanisms related to the discussed features of alkyd-acrylic system and implemented necessary remedial action to over come the problems such as limiting monomer conversion and secondary nucleation of this system without violating the basic principles of miniemulsion polymerisation.

Chapter 1: Bibliographic Review

Different methods of preparation of polyurethane-acrylic system and the properties of these systems were discussed. The chemical incorporation of reactive polyurethane into acrylic latex during hybrid miniemulsion polymerisation has been proven to be a promising method. The features such as the grafting mechanisms, particle morphology, and mechanical properties of PU-acrylic hybrid system were also reviewed. The detailed procedure of developing the hybrid system is described in Chapter 4.

1.6 References

1. Bontinck, D.; Tielemans, M.; Lottz, J. M., Self cross linking acrylic-polyurethane dispersions. *in: Proceedings of the PRA 14th International Conference on Coatings, Community and Care, Copenhagen, Paper 21* **1994**.

2. Asua, J. M., Miniemulsion polymerization. *Prog. Polym. Sci.* **2002,** 27, 1283-1346.

3. Hamersveld, E. M. S. v.; ES, J. J. G. S. v.; Cuperus, F. P., Oil-acrylate hybrid emulsions, mini-emulsion polymerization and characterization *Colloids and Surfaces A: Physiochemical and Engineering Aspects* **1999,** 153, 285-296.

4. Wu, X. Q.; Schork, F. J.; Gooch, J. W., Hybrid Miniemulsion Polymerisation of Acrylic/Alkyd Systems and Characterization of the Resulting Polymers. *J.Polym. Sci. : Polym. Chem* **1999,** 37, 4159-4168.

5. Nabuurs, T.; Baijards, R. A.; German, A. L., Alkyd-Acrylic Hybrid systems for Use as Binders in Waterborne Paints. *Prog.Org.Coat.* **1996,** 27, 163.

6. Kim, J. W.; Kim, J. Y.; Suh, K. D., Preparation of epoxy acrylate emulsion using mixed surfactants and its polymerization. *Polymer Bulletin* **1996,** 36, 141-148.

7. Gooch, J. W.; Dong, H.; Schork, F. J., Waterborne Oil-Modified Polyurethane Coatings via Hybrid Miniemulsion Polymerisation. *J. App. Polym. Sci.* **2000,** 76, 105-114.

8. Yu, Z. Q.; Ni, P. H.; Li, J. A.; Zhu, X. L., Miniemulsion copolymerization of methyl methacrylate and butyl acrylate in the presence of vinyl siloxane rubber. *Colloids Surf. A Physicochem Eng Aspects* **2004,** 242, 9 -15.

9. Hudda, L.; Tsavalas, J. G.; Schork, F. J., Simulation studies on the origin of the limiting conversion phenomenon in hybrid miniemulsion polymerisation. *Polymer* **2005,** 46, 993-1001.

10. Harkins, W. D., A general theory of the reaction loci in emulsion polymerisation. *J.Chem. Phys.* **1945,** 13, 381.

11. Harkins, W. D., A general theory of the reaction loci in emulsion polymerisation II. *J.Chem. Phys.* **1946,** 14, 47.

12. Harkins, W. D., A general theory of the reaction loci in emulsion polymerisation. *J.Am. Chem. Soc*. **1947,** 69, 1428.

13. Fitch, R. M., Polymer Colloids. *A comprehensive Introduction. Academic Press, New York* **1997**.

14. Gilbert, R. G., Emulsion polymerisation: a mechanistic approach. *San Diego: Academic Press* **1995**.

15. Priest, W. J., Particle growth in the aqueous polymerisation of vinyl acetate. *J. Phys.Chem.* **1952,** 56, 1077.

16. Ugelstad, J.; El-Aasser, M. S.; Vanderhoff, J. W., Emulsion Polymerisation: initiation of polymerization in monomer droplets. *J Polym Sci Lett Ed* **1973,** 11, 503-13.

17. El-Aasser, M. S.; Sudol, E. D., in Lovell P. A., Emulsion Polymerisation and Emulsion Polymers. *John Wiley & Sons, New York* **1997,** ch2.

18. Thicket, S. C.; Gilbert, R. G., Emulsion Polymerisation: State of the art in kinetics and mechanisms. *Polymer* **2007,** 48.

19. Fitch, R. M.; Tsai, C. H., Particle formation in polymer colloids. III. Prediction of the number of particles by a homogeneous nucleation theory. *Polym. Colloids, Proc. Symp. Fitch* **1971,** 1970, (73), 73.

20. Hansen, K. F.; Ugelstad, J., Particle Nucleation in Emulsion Polymerization. I. A Theory for Homogeneous Nucleation. *J. Polym. Sci. Polym. Chem. Ed.* **1978,** 16 (8), 1953.

21. Dong, Y., A molecular theory for particle nucleation: Primary particle formation in emulsion polymerization. *Journal of Colloid and Interface Science* **2008,** 326 354–359.

22. Fitch, R. M.; Shih, L. B., Emulsion polymerization. Kinetics of radical capture by particles. *Progress in Colloid & Polymer Science* **1975,** 56, 1-11.

23. Hansen, F. K.; Ugelstad, J., *In Emulsion Polymerization, I. Piirma, Ed., Academic: New York* **1982**.

24. Lichti, G.; Gilbert, R. G.; Napper, D. H., The mechanism of latex particle formation and growth in the emulsion polymerisation of styrene using the surfactant sodium dodecyl sulphate. *J.Polym. Sci. : Polym. Chem* **1983,** 21, 269.

25. Schork, F. J.; Luo, Y.; Smulders, W.; Russum, J. P.; Butte, A.; Fontenot, K., Miniemulsion Polymerisation. *Adv Polym Sci* **2005,** 175, 129-255.

26. Ugelstad, J.; Flogstad, H.; Hansen, F. K.; Ellingsen, T., Studies on the emulsion polymerization of vinyl chloride by seeded polymerization. *IUPAC International Symposium on Macromolecules, Helsinki, July2-7* **1972**.

27. Ugelstad, J.; Hansen, F. K.; Lange, S., Emulsion polymerization of styrene with sodium hexadecyl sulphate/hexadecanol mixtures as emulsifiers. Initiation in monomer droplets. *Macromol Chem* **1974,** 175, 507-21.

28. Azad, A. R. M.; Ugelstad, J.; Fitch, R. M.; Hansen, F. K., Emulsification and emulsion polymerization of styrene using mixtures of cationic surfactant and long chain fatty alcohols or alkanes as emulsifiers. *In: Piirma I., Gordon J.L., editors. Emulsion polymerization, ACS symposium series, Washington, DC:ACS* **1976,** 24, 1-23.

29. Carless, J. E.; Hallworth, G. W., Viscosity of emulsifying agents at oil-water interfaces. *J Colloid Interface Sci* **1968,** 26, 75-88.

30. Hallworth, G. W.; Carless, J. E., Stabilization of oil-in water emulsions by alkyl sulfates. Influence of the nature of the oil on stability. *J Pharm Pharmacol* **1972,** 24, 71-83.

31. Hallworth, G. W.; Carless, J. E., Stabilization of oil-in water emulsions by alkyl sulfates. Influence of the nature of the oil on stability. *J Pharm Pharmacol* **1973,** 25, 87-95.

32. Davis, S. S.; Smith, A., The influence of the disperse phase on the stability of oil-in-water emulsions. *Theory Pract. Emulsion Technol., Proc. Symp.* **1976,** 1974, (325), 325.

33. Wood, R. W.; Loomis, A. L., Physical and biological effects of high-frequency sound waves. *Phil Mag* **1927,** 4, 417.

34. Ouzineb, K.; Lord, C.; Lesauze, N.; Graillat, C.; Tanguy, A. P.; McKenna, T., Homogenization devices for the production of miniemulsions. *Chemical Engineering Science* **2006,** 61, (9), 2994-3000.

35. Hideo, T.; Akihiro, Y.; Fumio, K., Effects of Mixing Functions of Static Mixers on the Formation of CO2 Hydrate from the Two-Phase Flow of Liquid CO2 and Water. *Energy & Fuels* **2005,** 19, 2364-2370.

36. Antonietti, M.; Landfester, K., Polyreactions in miniemulsions. *Prog. Polym. Sci.* **2002,** 27, 689-757.

37. Gennes, P. G. d., Some remarks on coalescence in emulsions or foams. *Chem.Eng.Sci.* **2001,** 56, 5449-5450.

38. Higuchi, W. I.; Misra, J., Physical degradation of emulsion via the molecular diffusion route and its possible prevention. *J Pharm Sci* **1962,** 51, 459-66.

39. Morton, M.; Kaizerman, S.; Altier, M. W., SWELLING OF LATEX PARTICLES. *J Colloid Sci* **1954,** 9, 300-12.

40. Flory, P. J., Principles of Polymer Chemistry. *Cornell University Press: New York* **1953**.

41. Ugelstad, J.; Hansen, F. K., Kinetics and mechanism of emulsion polymerization. *Rubber Chem Technol* **1976,** 49, (3), 536-609.

42. Sood, A.; Awasthi, S. K., Initial Droplet Size Distribution in Miniemulsion Polymerisation. *Journal of Applied Polymer Science* **2003,** 88, 3058–3065

43. Smith, W. V.; Ewart, R. H., Kinetics of emulsion polymerisation. *J. Chem. Phys.* **1948,** 16, (6), 592.

44. Penlidis, A.; Macgregor, J. F.; Hamielec, A. E., Dynamic Modeling of Emulsion Polymerization Reactors. *AlChE Journal* **1985,** 31, (6), 881-889.

45. Rawlings, J. B.; Ray, W. H., The modeling of batch and continuous emulsion polymerization reactors. Part I. Model formulation and sensitivity to parameters. *Polym. Eng. Sci.* **1998,** 28, (5), 237-56.

46. Bechthold, N.; Landfester, K., Kinetics of miniemulsion Polymerisation as revealed by calorimetry. *Macromolecules* **2000,** 33, 4682-4689.

47. Mason, T. G.; Wilking, J. N.; Meleson, K.; Chang, C. B.; Graves, S. M., Nanoemulsions: formation, structure, and physical properties. *J.Phys.:Condens. Matter* **2006,** 18, R635-R666.

48. Abismail, B.; Canselier, J. P.; Wilhelm, A. M.; Delmas, H.; Gourdon, C., Emulsification by ultrasound: drop size distribution and stability. *Ultrason Sonochem* **1999,** 6, 75-83.

49. Walstra, P., Principles of emulsion formation. *Chem.Eng.Sci.* **1993,** 48, (2), 333-49.

50. Friberg, S. E.; Jones, S., *In:Kroschwith JI, editor. Kirk-Othmer encyclopedia of chemical technology, New York: Wiley* **1994,** 9, (4), 393-413.

51. Ouzineb, K., Emulsion and Miniemulsion Polymerisation. *PhD thesis, University of Claude Bernard Lyon-1* **2003**.

52. Schultz, S.; Wagner, G.; Urban, K.; Ulrich, J., High-Pressure Homogenization as a Process for Emulsion Formation. *Chem.Eng. Technol.* **2004,** 27, (4), 361-368.

53. Swiss Patent 394.390. **1944**.

54. Bondy, C.; Sollner, K., Mechanism of emulsification by ultrasonic waves. *Trans Faraday Soc* **1935,** 31, 835-43.

55. Mason, T. J., Industrial sonochemistry: potential and practicality. *Ultrason Sonochem* **1992,** 30, (3), 192-6.

56. Li, M. K.; Fogler, H. S.; , Acoustic emulsification. Part 1. The Instability of the oil-water Interface to form the initial droplets. *J.Fluid. Mech.* **1978,** 88, (3), 499.

57. Li, M. K.; Fogler, H. S., Acoustic emulsification. Part II. The Instability of the oil-water Interface to form the initial droplets. *J.Fluid. Mech.* **1978,** 88, (3), 513-528.

58. Brennen, C. E., Cavitation and Bubble Dynamics. *Cavitation and Bubble Dynamics, Oxford University Press, Oxford.* **1995**.

59. Berthelot, M., *Ann. Physique et Chim.* **1850,** 30, (3), 232.

60. Brown, B.; Goodman, J. E., High-Intensity Ultrasonics. *High-Intensity Ultrasonics, Iliffe Books, London* **1965**.

61. Leighton, T. G., The Acoustic Bubble. *The Acoustic Bubble, Academic Press, London* **1994.**

.

62. Lauterborn, W.; Ohl, C. D., Cavitation bubble dynamics. *Ultrason Sonochem* **1997,** 4, (2), 65-75.

63. Behrend, O.; Ax, K.; Schubert, H., Influence of Continuous Phase Viscosity on Emulsification by Ultrasound. *Ultrason Sonochem* **2000,** 7, 77-85.

64. Amaral, M. d.; Arevalillo, A.; Santos, J. L.; Asua, J. M., Novel Insight into the Miniemulsification Process: CFD Applied to Ultrasonication. *Prog. Colloid and Polym. Sci.* **2004,** 124, 103-106.

65. El-Jaby, U.; McKenna, T. F. L.; Cunningham, M. F., Miniemulsification: An Analysis of the Use of Rotor Stators as Emulsification Devices. *Macromol. Symp.* **2007,** 259, 1-9.

66. Lo´pez, A.; Chemtob, A.; Milton, J. L.; Manea, M.; Paulis, M.; Barandiaran, M. J.; Theisinger, S.; Landfester, K.; Hergeth, W. D.; Udagama, R.; McKenna, T.; Simal, F.; Asua, J. M., Miniemulsification of Monomer-Resin Hybrid Systems. *Ind. Eng. Chem. Res.* **2008,** 47, 6289–6297.

67. Harnby, N.; Edwards, M. F.; Nienow, A. W., Mixing in the Process Industries, 2nd ed.; Butterworth-Heinemann: Oxford. *Mixing in the Process Industries, 2nd ed.; Butterworth-Heinemann: Oxford*
1992, 225-249.

68. Farzi, G.; Bourgeat-Lami, E.; McKenna, T. F. L., Miniemulsions Using Static Mixers: A Feasibility Study Using Simple In-Line Static Mixers. *Journal of Applied Polymer Science* **2009,** 114, 3875-3881.

69. Shoaf, G. L.; Stockl, R. R., Alkyd/Acrylic Hybrid Latexes with Enhanced Oxidative Curing. *Polymer Reaction Engineering* **2003,** 11, (3), 319-334.

70. El-Aasser, M. S.; Sudol, E. D., Miniemulsions: overview of research and applications. *JCT Res.* **2004,** 1, 21-31.

71. Roos, D. D. W.; Knoetze, J. H.; Cooray, B.; Sanderson, R. D., Emulsion Polymerization of an Epoxy-Acrylate Emulsion Stabilized with Polyacrylate. I. Influence of Salt, Initiator, Neutralizing Amine, and Stirring Speed. *Journal of Applied Polymer Science* **1999,** 71, 1347–1360.

72. Pan, G.; Wu, L.; Zhang, Z.; LI, D., Synthesis and Characterization of Epoxy-Acrylate Composite Latex. *Journal of Applied Polymer Science* **2002,** 83, 1736–1743.

73. Marcu, I.; Daniels, E. S.; Dimonie, V. L.; Hagiopol, C.; Roberts, J. E.; MS, E.-A., Incorporation of Alkoxysilanes into Model Latex Systems: Vinyl Copolymerization of Vinyltriethoxysilane and n-Butyl Acrylate. *Macromolecules* **2003,** 36, 328 - 32.

74. Wang, S. T.; Schork, F. J.; Poehlein, G. W.; Gooch, J. W., Emulsion and Miniemulsion Copolymerization of Acrylic Monomers in the Presence of Alkyd Resin. *Journal of Applied Polymer Science* **1996,** 60, 2069-2076.

75. Tsavalas, J. G.; Luo, Y.; Schork, F. J., Grafting Mechanisms in Hybrid Miniemulsion Polymerisation. *J. App. Polym. Sci.* **2003,** 87, 1825-1836.

76. Tsavalas, J. G.; Gooch, J. W.; Schork, F. J., Water-Based Crosslinkable Coatings via Miniemulsion Polymerization of Acrylic Monomers in the presence of Unsaturated Polyester Resin. *J. App. Polym. Sci.* **2000,** 75, 916-927.

77. Tsavalas, J.; Schork, F. J., The morphology of alkyd/acrylate latexes produced via hybrid miniemulsion polymerization: grafting mechanisms. *Prog. Colloid Polym. Sci.* **2004,** 124, 126-130.

78. March, J., Advanced Organic Chemistry: Reactions, Mechanisms and Structures. *Advanced Organic Chemistry: Reactions, Mechanisms and Structures, Fourth Edition.;John Wiley and Sons: New York* **1992**, 1495.

79. Hendry, D. G.; Mill, T.; Pisvkiewicz, L.; Howard, J. A.; Eigenmann, H. K., A Critical Review of H-Atom Transfer in the Liquid Phase: Chlorine Atom, Alkyl, Trichloromethyl, Alkoxy, and Alkylperoxy Radicals. *J Phys Chem Ref Data* **1974,** 3, (4), 937.

80. Odian, G., Principles of Polymerisation. *Principles of Polymerisation; McGraw-Hill: New York* **1970**, 652.

81. Tsavalas, J. G.; Luo, Y.; Hudda, L.; Schork, F. J., Limiting Conversion Phenomenon in Hybrid Miniemulsion Polymerisation. *Polymer Reaction Engineering* **2003,** 11, 277-304.

82. Tsavalas, J. G.; Schork, F. J.; Landfester, K., Particle Morphology Develpoment in Hybrid Miniemulsion Polymerisation. *JCT Res.* **2004,** 1, 53-63.

83. Deriss, M. J.; Karlsson, O. J., Suspension structures and film morphologies of high-solids acrylic-alkyd hybrid binders. *Surface Coatings International Part B: Coatings Transactions* **2005,** 88, 231-316.

84. Colombini, D.; Deriss, M. J.; Karlsson, O. J.; Maurer, F. H. J., Direct and Reverse Mechanical Modelling of an Alkyd Acrylic Hybrid System: A Morphological Study. *Macromolecules* **2004,** 37, 2596-2602.

85. Deriss, M. J.; Karlsson, O. J., High solids waterborne hybrid systems. Effect of surfactant concentration and pH on droplet size and morphology. *Progr Colloid Polym Sci* **2004,** 124, 149-153.

86. Brandrup, J.; Immergut, E. H., *Polymer Handbook, Second Edition, John Wiley & Sons, New York* **1975**.

87. Dong, H.; Gooch, J. W.; Schork, F. J., Water-borne oil modified polyurethane coatings via hybrid miniemulsion polymerisation. *J. App. Polym. Sci.* **2000,** 76, 105.

88. Herk, A. M. v., Pulsed initiation polymerisation as a means of obtaining propagation rate coefficients in free-radical polymerisation *J.M.S.-Rec. Macromol. Chem. Phys* **1997,** C37, (4), 633-648.

89. Kwon, J. Y.; Kim, E. Y.; Kim, H. D., Preparation and properties of waterborne-polyurethane coating materials containing conductive polyaniline. *Macromol. Res.* **2004,** 12, (3), 303-310.

90. Kwak, Y. S.; Park, S. W.; Kim, H. D., Preparation and properties of waterborne polyurethane–urea anionomers—influences of the type of neutralizing agent and chain extender. *Colloid Polym. Sci.* **2003,** 281, (10), 957-963.

91. Dong, A. J.; Hou, G. L.; Sun, D. X., *J Colloid Interface Sci* **2003,** 266, (2), 276-281.

92. Chen, H.; Jiang, X. W.; He, L.; Zhang, T.; Xu, M.; Yu, X. H., Novel Biocompatible Waterborne Polyurethane Using LLysine as an Extender. *J. App. Polym. Sci.* **2002,** 84, 2474-2480.

93. Wen, T. C.; Wang, Y. J.; Cheng, T. T.; Yang, C. H., The effect of DMPA units on ionic conductivity of PEG–DMPA–IPDI waterborne polyurethane as single-ion electrolytes. *Polymer* **1999,** 40, (14), 3979-3988.

94. Zhu, X.; Jiang, X.; Zhang, Z.; Kong, X. Z., Influence of ingredients in water-based polyurethane-acrylic hybrid latexes on latex proerties. *Progress in Organic Coatings* **2008,** 62, 251-257.

95. Klein, H. P.; Schwab, M., Aqueous polyurethane dispersions. *Polym. Paint Col. J.* **1994,** 184, (4357), 444.

96. Jan, Y. H.; Hwang, Y. T.; Shih, C. Y.; Li, H. S., Microphase structure and mechanical properties of the acrylic-polyurethane aqueous dispersions: effects of acrylate polymerization processes. *In: Proceedings of the 22nd Symposium on waterborne, High-Solids, Powder Coatings.* **1995**, 211-223.

97. Derby, R.; Gruber, B.; Klein, R., Acrylic/urethane hybrid polymers: A New Technology for Graphic Arts Applications. *J. Am. Paint J.* **1995,** 79, (21), 57.

98. Chen, G.; Chen, K., Hybridization of Aqueous-Based Polyurethane with Glycidyl Methacrylate Copolymer. *J. App. Polym. Sci.* **1999,** 71, (6), 903-913.

99. Hegedus, C. R.; Kloiber, K. A., Acrylic-polyurethane aqueous dispersions: Structure and properties in industrial coatings. *In: Proceedings of the 21st Symposium on waterborne, High-Solids, Powder Coatings.* **1994,** 2, (1), 144.

100. Gilicinski, A. G.; Andrew, G.; Hegedus, C. R., Mechanical studies of film formation in waterborne coatings by force modulation atomic force microscopy. *Polym. Mater. Sci. Eng.* **1995,** 73, 142.

101. Hegedus, C. R.; Kloiber, K. A., Aqueous acrylic-polyurethane hybrid dispersions and their use in industrial coatings. *J. Coat. Technol.* **1996,** 68, (860), 39.

102. Gilicinski, A. G.; Hegedus, C. R., Film formation in waterborne coatings
ACS Symp. Ser. **1996,** 648, 286.

103. Okamoto, Y.; Hasegawa, Y.; Yoshino, F., Urethane/acrylic composite polymer emulsions. *Prog Org Coat* **1996,** 29, 175-182.

104. Nakayama, Y., Polymer blend systems for water-borne paints. *Prog Org Coat* **1998,** 33, (2), 108.

105. Geurts, J. M.; Tennebroek, R.; Overbeek, A.; Smak, Y. W., Self-crosslinkable urethanes and urethane/acrylics. *In: Proceedings of the XXIV Fatipec Congress, Interlaken.* **1998,** D, pp. D259-D273.

106. Rynders, R. M.; Hegedus, C. R.; Gilicinski, A. G., Characterization of particle coalescence in waterborne coatings using atomic force microscopy. *J. Coat. Technol.* **1995,** 67, (845), 59-69.

107. Brown, R. A.; Coogan, R. G.; Fortier, D. G.; Reeve, M. S.; Rega, J. D., Comparing and contrasting the properties of urethane/acrylic hybrids with those of corresponding blends of urethane dispersions and acrylic emulsions. *Progress in Organic Coatings* **2005,** 52, 73-84.

108. Walsh, D. J., *In: C. Booth, C. Price (Eds.), Comprehensive Polymer Science, Pergamon, Oxford* **1989,** 2, 135.

109. Li, M.; Daniels, E. S.; Dimonie, V.; Sudol, E. D.; El-Aasser, M. S., Preparation of Polyurethane/Acrylic Hybrid Nanoparticles via a Miniemulsion Polymerisation Process. *Macromolecules* **2005,** 38, 4183-4192.

110. Kukanja, D.; Golob, J.; Valant, A. Z.-.; Krajnc, M., The Structure and properties of Acrylic-Polyurethane Hybrid Emulsions and Comparison with Physical Blends. *J. App. Polym. Sci.* **2000,** 78, 67-80.

111. Cheong, I. W.; Nomura, M.; Kim, J. H., Synthesis and aqueous solution behaviour of water-soluble polyurethane (IPDI-PPG-DMPA) resin. . *Macromol Chem Phys* **2000,** 201, 2221-2227.

112. Li, C. Y.; Chiu, W. Y.; Don, T. M., Preparation of Polyurethane Dispersions by Miniemulsion Polymerization. *Journal of Polymer Science: Part A: Polymer Chemistry* **2005,** 43, 4870-4881.

113. Kim, B. K.; Lee, Y. M., Polyurethane ionomers from cycloaliphatic diisocyanate and polytetramethylene glycol. *J Macromol Sci Pure Appl Chem* **1992,** 29, 1207-1221.

114. Lee, J. S.; Kim, B. K., Polyurethane cationomers from polypropylene glycol and isophorone diisocyanate: emulsion characteristics and tensile properties of cast films. *Prog Org Coat* **1995,** 25, 311-318.

115. Lan, P. N.; Corneille, S.; Schacht, E.; Davies, M.; Shard, A., Biocompatibility of biodegradable and nonbiodegradable polymer-coated stents implanted in porcine peripheral arteries. *Biomaterials* **1996,** 17, 2273-2280.

116. Wang, C.; Chu, F.; Guyot, A., Mechanical Properties of Films from Hybrid Acrylic-Polyurethane Polymer Colloids. *Journal of Dispersion Science and Technology* **2006,** 27, 325-330.

117. Zhang, G.; Zhang, Z.; Hu, Z.; Xi, H., Seeded-emulsion polymerization of styrene with waterborne polyurethane stabilizer via 60Co gamma ray. *Colloids and Surfaces A: Physicochem. Eng. Aspects* **2005,** 264, 37-42.

118. Barrère, M.; Landfester, K., High Molecular Weight Polyurethane and Polymer Hybrid Particles in Aqueous Miniemulsion. *Macromolecules* **2003,** 36, 5119-5125.

119. Li, C. Y.; Chiu, W. Y.; Don, T. M., Morphology of PU/PMMA Hybrid Particles from Miniemulsion Polymerization: Thermodynamic Considerations. *Journal of Polymer Science: Part A: Polymer Chemistry* **2007,** 45, 3359-3369.

120. Hirose, M.; Zhou, J.; Nagai, K., The structure and properties of acrylic-polyurethane hybrid emulsions. *Prog Org Coat* **2000,** 38, 27-34.

121. Sundberg, D. D.; Casassa, A. P.; Pantazopoulos, A. P.; Muscato, M. R., Morphology Development of Polymeric Microparticles in Aqueous Dispersions.I. Thermodynamic Considerations. *Journal of Applied Polymer Science* **1990,** 41, 1425-1442.

122. Torza, S.; Mason, S., *J Colloid Interface Sci* **1970,** 33, 67-76.

123. Chen, S.; Chen, L., Structure and properties of polyurethane/polyacrylate latex interpenetrating networks hybrid emulsions. *Colloid Polym. Sci.* **2003,** 282, 14-20.

2. MINIEMULSIFICATION OF MONOMER-RESIN HYBRID SYSTEM

2.1 Introduction

In the previous chapter we briefly discussed some of the techniques currently used to produce miniemulsion droplets. In the current chapter, we will compare these methods in terms of creating droplets of different size under different conditions. The objective of work presented in this thesis is to synthesise high quality hybrid nanoparticles for coating and adhesive applications. In order to achieve better application properties for coatings, adhesives, cosmetics and additives for paper and textiles, nanostructured polymer films are required[1]. Therefore we need to synthesise hybrid nanoparticles with high solids content and controlled particle size. This implies that one would like to obtain particles (and therefore droplets) on the order of 100nm for hybrid systems of at least 50% solids (wt %). The challenge of achieving target droplet size for the desired hybrid systems is the high viscosity of the dispersed phase.

Taylor[2, 3] put forward a relationship for the droplet size of a droplet dispersed in a continuous phase correlating the viscosity of dispersed and aqueous phases. He introduced the term capillary number (*Ca*) which is given by the following equation.

$$Ca = \frac{\eta_m R \dot{\gamma}}{\alpha} \qquad \text{Equation 1}$$

Where η_m is the continuous phase viscosity, R is the droplet radius, $\dot{\gamma}$ is the shear rate, α is the interfacial tension. The dispersed phase viscosity η_d is related to η_m by the viscosity ratio *p* where $p = \frac{\eta_d}{\eta_m}$.

The droplet bursts when *Ca* exceeds a critical value, $Ca_{cr,}$ which depends on *p*. Therefore, for a given set of hydrodynamic conditions, the droplet size is a direct function of dispersed phase viscosity. Several studies[4-6] led to a complete description giving $Ca_{cr,}$ as a function of *p* for flows spanning from simple shear to extensional flow. According to these studies, Ca_{cr} reaches a minimum for *p* between 0.1 and 1[7]. For *p* above 1, an increase in Ca_{cr} is reported until, for *p* around 4, breakup is prevented due to the presence of rotational components in the shear flow

field[7, 8]. For *p* greater than 4, droplets will tumble during start up of flow until an ellipsoidal droplet is obtained, aligned in the flow direction[7, 8].

In this section we will present the formation of waterborne composite monomer-polymer miniemulsions by three different means. We studied three types of homogenisation equipment, namely the rotor-stator, static mixers and the sonifier. The efficiency of these three homogenisation equipments was compared to achieve the required droplet size and the most efficient one retained for the rest of the study.

2.2 Experimental Section

2.2.1 Miniemulsification

The miniemulsification was carried out as follows. First, the coarse emulsion was prepared by dispersing an organic phase in an aqueous phase under mechanical agitation. The organic phase was prepared by dissolving a given amount (0-50 wt% based on the total organic phase) of alkyd resin (SETAL 293 XX – 99; 98% solid and 2% xylene as the solvent; graciously supplied by Nuplex; Synthesebaan, Netherlands) in a mixture of monomers methyl methacrylate (MMA 99+%; from Acros; Illkirch Cedex, France), butyl acrylate (BA 99+%; from Acros; Illkirch Cedex, France) and acrylic acid(AA 99+%; from Acros; Illkirch Cedex, France) (MMA/BA/AA: 49.5/49.5/1wt %). Octadecyl acrylate (ODA 97%; from Sigma Aldrich; Lyon, France) (5 wt% by monomer) was added to the organic phase as a hydrophobe in the absence of alkyd resin. The theoretical total solid content of each formulation was kept at 50(wt %). The aqueous phase was prepared by dissolving the emulsifier, Dowfax-2AI (45%; graciously supplied by DOW Chemicals; La Plaine St Denis Cedex, France) in deionised water. The origin of this formulation will be discussed in Chapter 3. The coarse emulsion was then homogenised using the devices described below.

2.2.2 Homogenisation Devices

A turbo test rotor-stator homogeniser (*RAYNERI*) consisting of a digital display microprocessor, an overhead drive and a homogenising shaft was used to homogenise the initial mixture. The diameter of the mixer-head was 5.5 cm and it was immersed in a coarse emulsion of about 500 mL in volume. The homogenisation was carried out at a rotational speed of 3000 rpm until a constant value of droplet size was achieved.

The static mixer is a motionless mixing device composed of mixing elements of an appropriate shape, arranged in a repetitive fashion and placed in a hollow housing pipe. The mixture was homogenised by causing it to circulate over one or more tubes with an interior diameter (ID) of 1 cm and a length of 100 cm, each containing 4 static mixing elements 15 cm in length and 6.4 mm in diameter[9]. The coarse emulsion was placed in a reservoir with a magnetic stirrer, and then circulated through a tube (or tubes) containing the static mixer elements at a flow rate of 60.6 ml/s until a constant value of droplet size was achieved.

A sonifier (Branson, model CV 26) was operated at 480W for sonication of the miniemulsions. The sonifier tip was immersed in a coarse emulsion of about 200 mL in volume. The sonication was carried out under stirring for 6 minutes by changing the position of the tip at 2 minute intervals.

Dynamic Light Scattering (DLS) was used to measure the droplet size. Average droplet sizes (Dp) were measured by particle size analyzer (ZETASIZER 1000HS_A). Average particle sizes reported here are the averages of 5 measurements per sample. The viscosity was measured by Rheometric Scientific Viscometer (RFSIII) at 25° C and at a shear rate of $100s^{-1}$.

2.3 Results and Discussion

Figure 1 illustrates the evolution of droplet size during homogenisation by rotor-stator for the hybrid systems of 0 to 25% alkyd. Figure 2 illustrates the evolution of droplet size during homogenisation by static mixer for the base miniemulsion (0% alkyd).

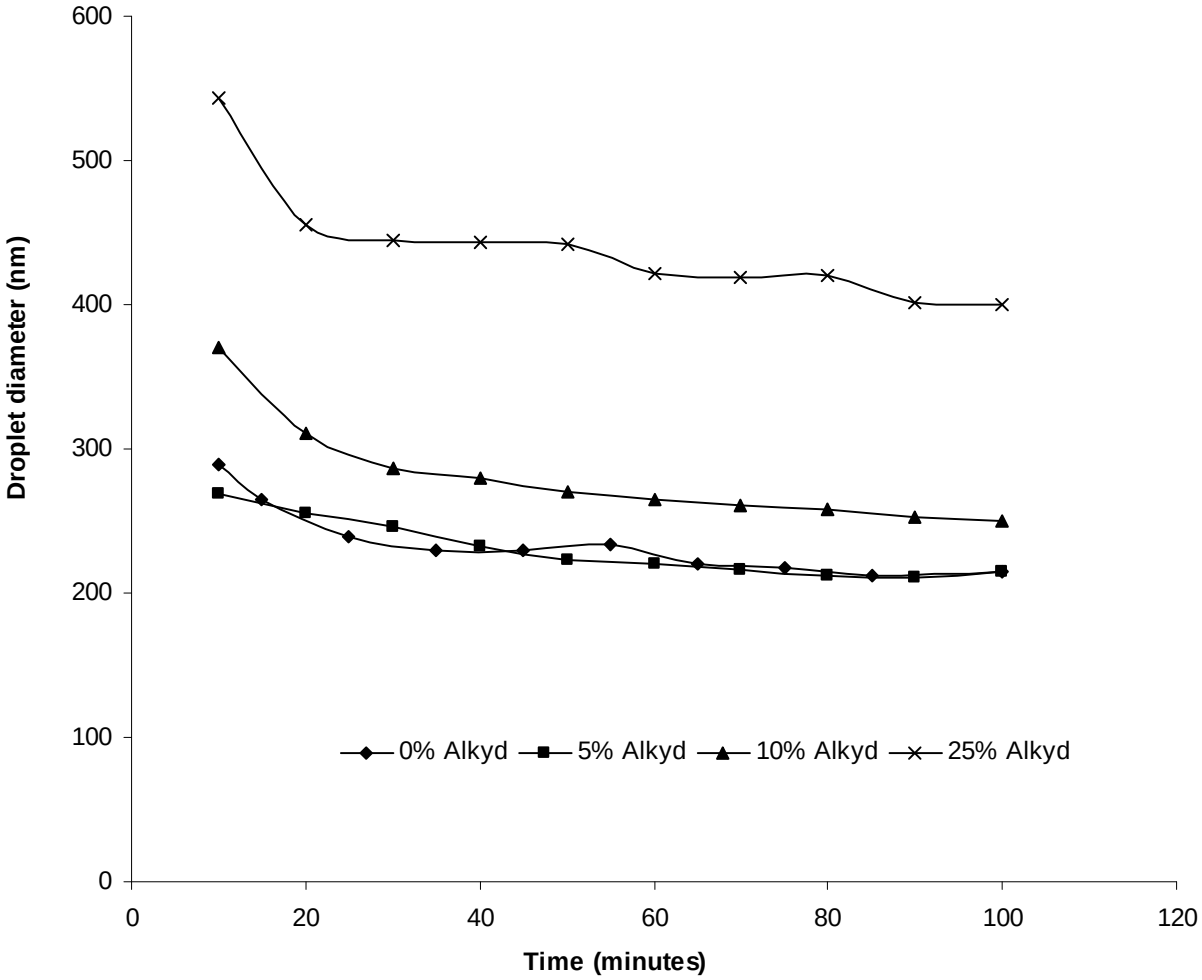

Figure 1. Evolution of droplet size by rotor stator in the presence of varying alkyd quantity

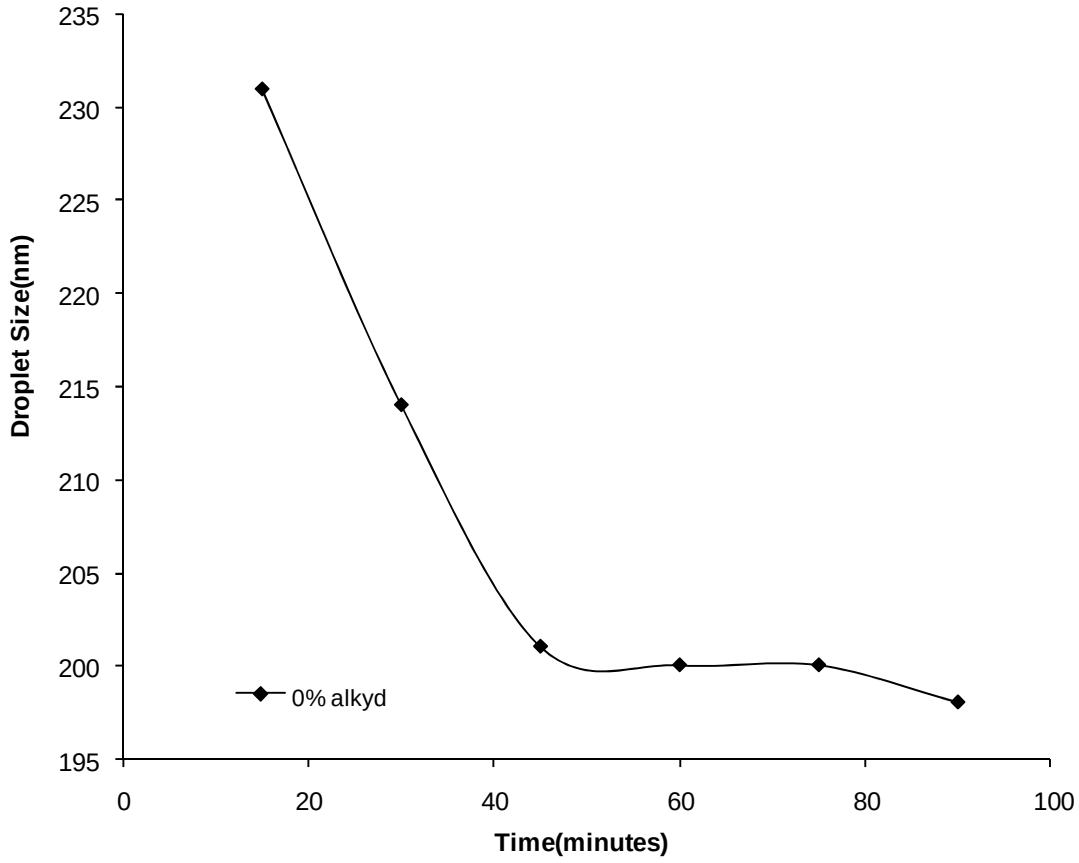

Figure 2. Evolution of droplet size by static mixer in the absence of alkyd

As can be clearly observed, the rotor-stator system and static mixer are not effective enough to reduce the droplet size of the dispersed phase to the required size even in the absence of alkyd resin. Therefore further miniemulsifications were not carried out in the presence of alkyd by static mixer and Figure 3 illustrates the evolution of droplet size for the hybrid system of 0-50% alkyd during sonication.

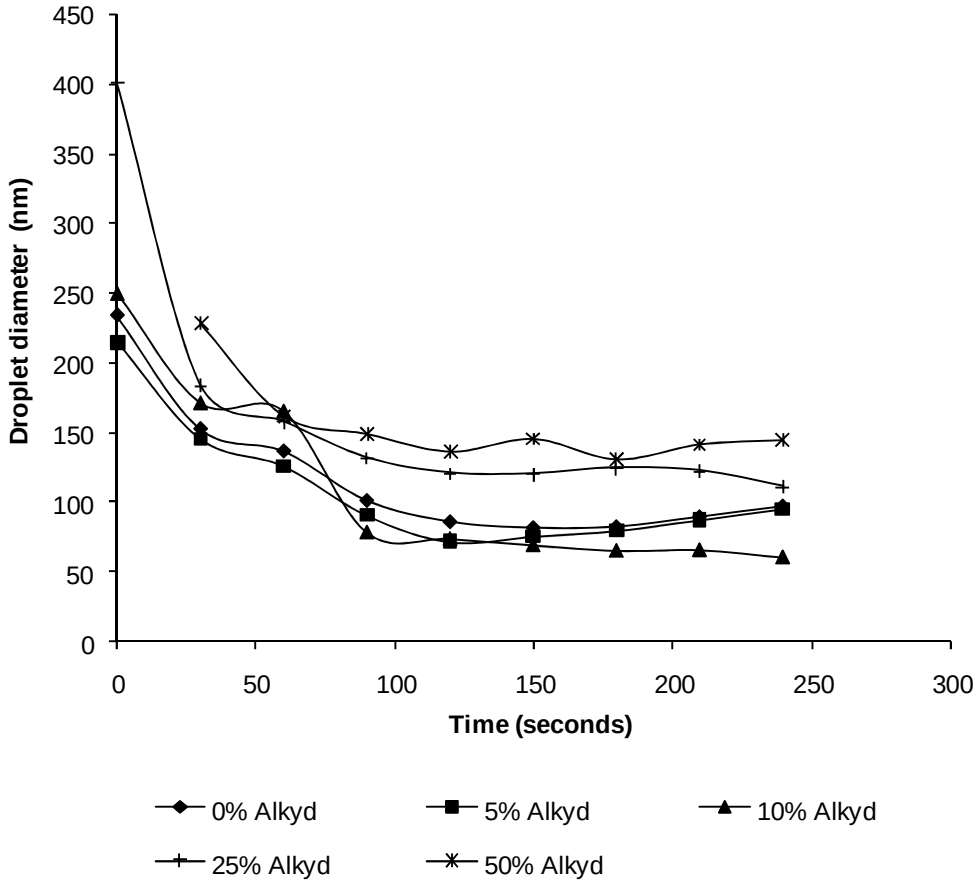

Figure 3 Evolution of droplet size in the presence of varying alkyd quantity during sonication

From Figure 3 it can be seen that sonication is powerful enough to achieve a droplet size closer to 100nm with at least 25% alkyd resin. Figure 4 illustrates the dispersed phase viscosity for increasing alkyd quantity and it is clear that with increasing alkyd quantity, viscosity of the dispersed phase increases. Figure 5 compares the dependence of droplet diameter on the dispersed phase viscosity during homogenisation by rotor stator and sonifier. It is clear that the droplet size increases according to Equation 1 with increasing viscosity. However Mabille et al[10] have shown that under non-quasi-static conditions, the droplet diameter is mainly determined by the applied stress and weakly depends on the dispersed phase viscosity. They have further shown that under their experimental conditions, the dependence of droplet diameter on the dispersed

phase viscosity is as low as 0.2 and droplets could be broken up by applying sudden shear to over come the high dispersed phase viscosities such as 100 Pa.S.

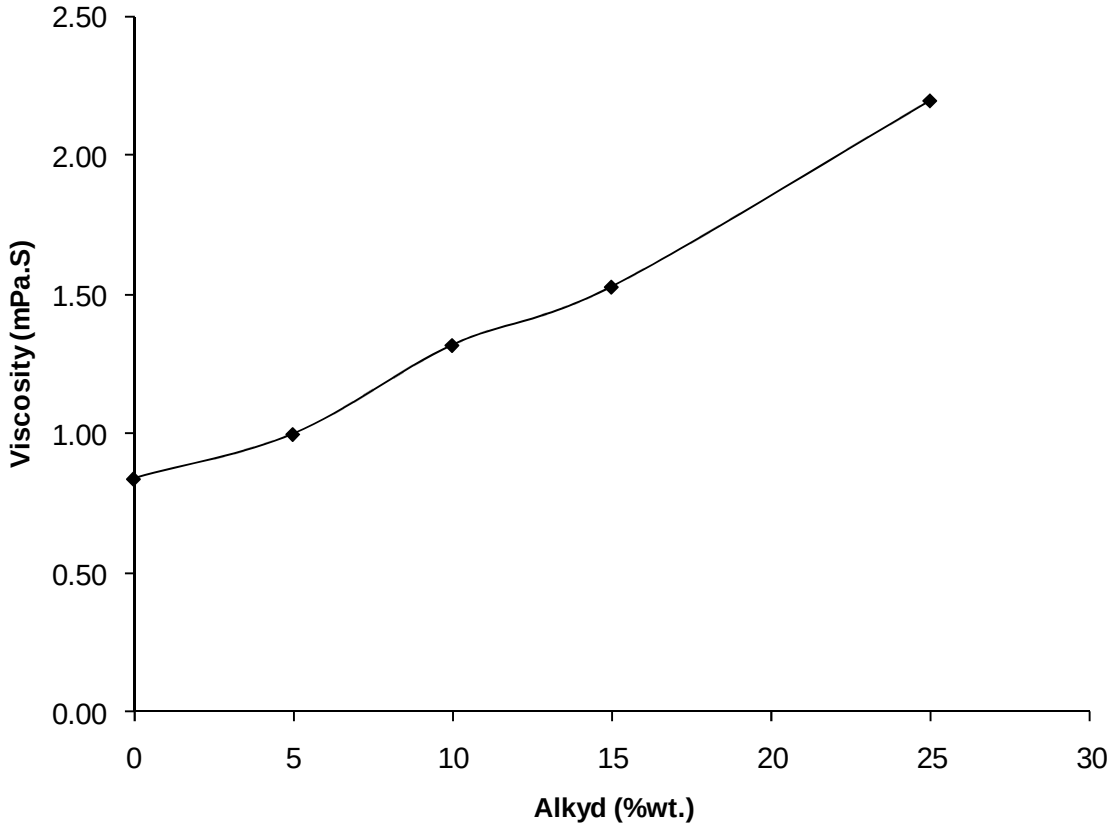

Figure 4. Dispersed phase viscosity in the presence of increasing alkyd quantity

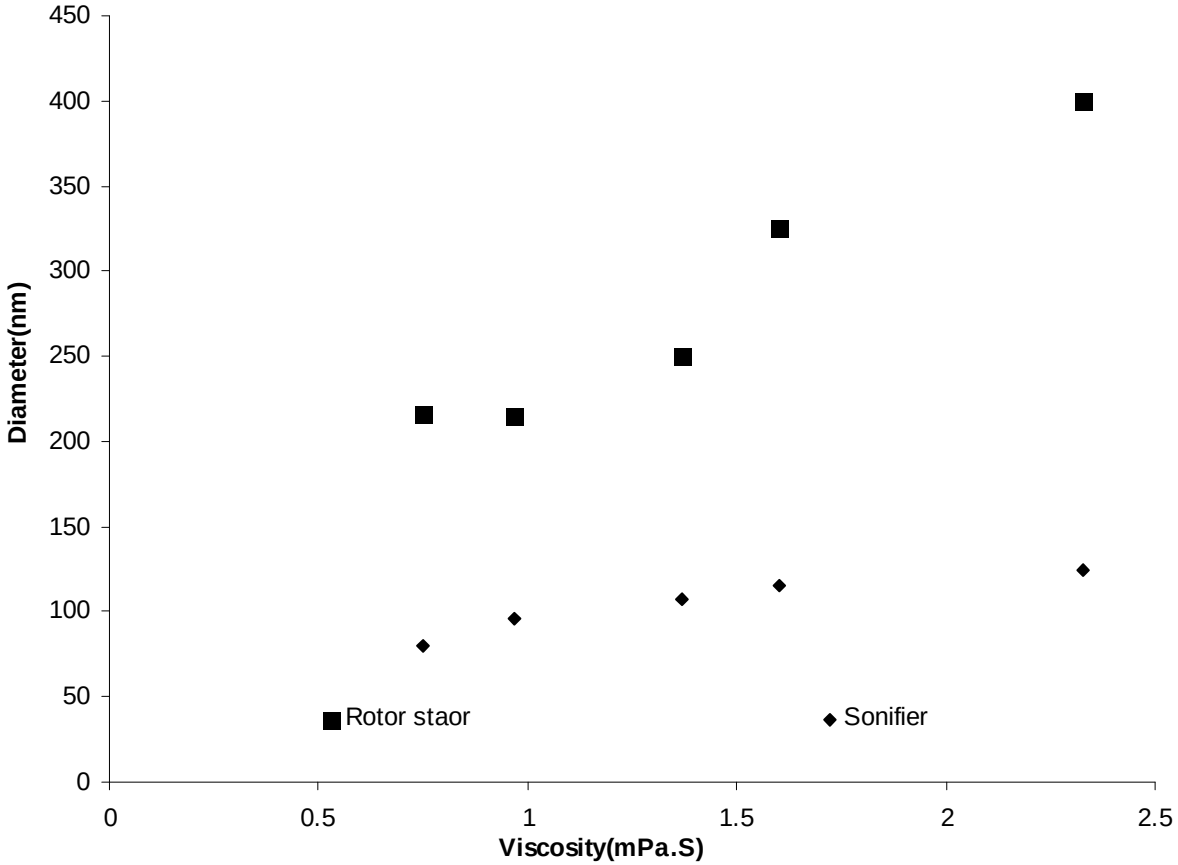

Figure 5. The dependence of droplet diameter on dispersed phase viscosity during miniemulsification by sonifier and rotor stator

The dependence of droplet diameter on viscosity is high when rotor-stator was used for homogenisation according to Figure 5.This means the output of rotor stator is not sufficient enough to overcome the viscous effect of the dispersed phase. Therefore we can conclude that the efficiency of sonifier is greater than rotor stator or static mixer to overcome the dispersed phase viscosity.

2.4 Conclusions

The formation of waterborne monomer-resin miniemulsions was investigated. The goal was to prepare nano-scaled (about 100 nm in diameter), highly concentrated organic phase (50 wt %) miniemulsions containing a high concentration of resin (25 wt% based on the organic phase). The efficiency of three homogenisation devices (rotor-stator, static mixer and sonifier) was compared in terms of the minimum droplet size that could be obtained. It was found that the rotor-stator and static mixer were not effective enough to reduce the droplet size of the dispersed phase to the required size. On the other hand, sonication was an effective avenue to preparing miniemulsions with required droplet size.

The droplet size resulting from droplet breakup increased with increasing resin concentration due to the increasing viscosity of the organic phase. As the viscosity of the organic phase increases, its impact on the droplet size becomes more important. This was evident by comparing the dependence of droplet size on the dispersed phase viscosity during homogenisation by rotor-stator and sonifier. Accordingly, the choice of equipment was the main factor determining the droplet size in systems with a high-viscosity organic phase. Since our objective of the work presented in this thesis is to synthesise and characterise hybrid latex of 50% solid and 100 nm particles, sonication was employed for all subsequent miniemulsification.

2.5 References

1. Lo´pez, A.; Chemtob, A.; Milton, J. L.; Manea, M.; Paulis, M.; Barandiaran, M. J.; Theisinger, S.; Landfester, K.; Hergeth, W. D.; Udagama, R.; McKenna, T.; Simal, F.; Asua, J. M., Miniemulsification of Monomer-Resin Hybrid Systems. *Ind. Eng. Chem. Res.* **2008,** 47, 6289–6297.

2. Taylor, G. I., The viscosity of a fluid containing small drops of another fluid. *Proc. R. Soc.* **1932,** 138, 41-48.

3. Taylor, G. I., The Formation of Emulsions in Definable Fields of Flow. *Proc. R. Soc.* **1934,** A146, 501.

4. Grace, H. P., Dispersion Phenomena in High Viscosity Immiscible Fluid Systems and Application of Static Mixers as Dispersion Devices in Such Systems. *Chem. Eng. Commun* **1982,** 14, 225.

5. Bruijn, R. A. D., Deformation and Breakup of Drops in Simple Shear Flows. *PhD Thesis Eindhoven University of Technology* **1989**.

6. Bentley, B. J.; Leal, L. G., An Experimental Investigation of Drop Deformation and Breakup in Steady Two-Dimensional Linear Flows. *J. Fluid. Mech.* **1986,** 167, 241.

7. Vananroye, A.; Puyvelde, P. V.; Moldenaers, P., Effect of Confinement on Droplet Breakup in Sheared Emulsions. *Langmuir* **2006,** 22, 3972-3974.

8. Desse, M.; Wolf, B.; Mitchell, J.; Budtova, T., Experimental study of the break-up of starch suspension droplets in step-up shear flow. *J. Rheol.* **2009,** 53, (4), 943-955.

9. Farzi, G.; Bourgeat-Lami, E.; McKenna, T. F. L., Miniemulsions Using Static Mixers: A Feasibility Study Using Simple In-Line Static Mixers. *Journal of Applied Polymer Science* **2009,** 114, 3875-3881.

10. Mabille, C.; Calderon, F. L.; Bibette, J.; Schmitt, V., Monodisperse fragmentation in emulsions: Mechanisms and kinetics. *Europhys. Lett.* **2003,** 61, (5), 708-714.

3. ALKYD-ACRYLIC HYBRID MINIEMULSION POLYMERISATION

3.1 Introduction

Alkyd resins are widely employed in paint applications due to their useful properties such as auto-oxidative curing, high gloss and good penetration into wood[1]. As discussed earlier, the synthesis of traditional solvent-borne alkyd resin-based paints has come into disfavour due to the presence of volatile organic species[2], making it important to find alternative processes, preferably water-based ones. The key difficulty in doing so lies in the fact that alkyd resins cannot be incorporated into environmentally friendly acrylic latexes by emulsion polymerisation because they are highly hydrophobic, making it extremely difficult to disperse them in an aqueous environment. One alternative approach, physically blending together alkyds and acrylic based latexes, often suffers from incompatibility between the two polymer types resulting in hazy or non-uniform films[2]. It appears that the best way to make water-borne environmentally friendly hybrid polymers that synergistically combine the positive properties of alkyd resins with the fast drying and colour retention of acrylic latexes is via the polymerisation of a miniemulsion dispersion[1-5].

As discussed earlier, alkyd-acrylic hybrid systems have been studied with respect to different aspects such as limiting monomer conversion and hybrid particle morphology[6-11]. The main challenge for the industrial application of this system is limiting monomer conversion. Two mechanisms, namely kinetic and physical, have been put forward to explain limiting monomer conversion[7, 12]. The retardative chain transfer to alkyd double bonds is the basis of kinetic mechanism. However the kinetic mechanism fails to explain the observed limiting monomer conversion in the presence of saturated alkyd resins[7]. The inaccessibility of trapped monomer to the growing polymer chain is the basis of physical mechanism. We have also observed a limiting monomer conversion in our hybrid system and attempted to understand possible reasons for this based on a study of evolution of N_p/N_d with monomer conversion and change of individual monomer conversion with increasing alkyd.

Although the evolution of N_p/N_d with monomer conversion can be used to track the system's observed features like limiting monomer conversion and changing particle morphology, it has not been thoroughly studied. Therefore in this study we focused our attention on the evolution of N_p/N_d in the presence of varying amounts of alkyd. We correlated this evolution with droplet stability and the individual monomer conversions in order to account for the change in individual monomer conversion with increasing alkyd quantity. We have shown that important information on the change of particle morphology could be found if one looks at the change of individual monomer conversion and the evolution of N_p/N_d simultaneously. Although a number of experimental details can be found in the literature relevant to different hydrophobes[13-17], their efficiency based on the strength of interactions with monomers under different experimental conditions has not been compared in the previous studies. In particular, it would be of interest to compare the efficiency of common hydrophobes like hexadecane to other reactive compounds such as octadecyl acrylate and alkyd resins.

Herein, we present the details of our experimental study performed on a model acrylic-alkyd system. The acrylic part consisted of a mixture of methyl methacrylate (MMA) and butyl acrylate (BA) in equal parts by weight, with 1wt% of acrylic acid (AA). Unless stated otherwise, the alkyd consisted of a long chain unsaturated fatty acid. In the most desirable scenario, all the monomer droplets should contain alkyd resin, and should be polymerised to yield particles on the basis of obtaining a one-to-one copy of droplets to particles. Therefore, as was mentioned above, the ratio of the number of particles to the number of droplets, N_p/N_d, should be as close to one as possible. If there is a deviation from unity in this ratio, then it is preferable that it be slightly less than one rather than slightly greater than one. In the second scenario, if N_p/N_d is greater than one, this implies that new particles have been created during the reaction and these new particles would not contain alkyds. The limit on what constitutes an "acceptable" deviation from the ideal value of one for this parameter will be a function of the application of the final product.

3.2 Experimental Section

Materials

Butyl acrylate (BA 99+ %; from Acros; Illkirch Cedex, France), acrylic Acid (AA 99+ %; from Acros; Illkirch Cedex, France) and methyl methacrylate (MMA 99+ %; from Acros; Illkirch Cedex, France) were used as received. Dowfax-2AI (45%; graciously supplied by DOW Chemicals; La Plaine St Denis Cedex, France) was used as the anionic surfactant and the amount of surfactant mentioned in the recipes always refers to total surfactant weight (active matter + additional water). A long chain unsaturated oil alkyd resin (SETAL 293 XX – 99; 98% solid and 2% xylene as the solvent; graciously supplied by Nuplex; Synthesebaan, Netherlands) was used in the most of experiments. A saturated alkyd resin (98% solid and 2% xylene) supplied by Nuplex was also used in few experiments. Hexadecane (99+%; from Acros; Illkirch Cedex, France) and octadecyl acrylate (ODA 97%; from Sigma Aldrich; Lyon, France) were used as hydrophobes. Potassium persulphate (KPS; from Acros; Illkirch Cedex, France) was used as the water soluble initiator. A solution of 37.5 (%wt) of $NaHSO_3$ (MBS; from Sigma Aldrich; Lyon, France) was used with KPS during the semi-continuous addition of KPS and the amount of $NaHSO_3$ mentioned in the recipes always refers to total weight (active matter + additional water). The oil soluble initiators were dilauryl peroxide (Analytical grade; from Acros; Illkirch Cedex, France) and azobisisobutyronitrile (AIBN Analytical grade; from Acros; Illkirch Cedex, France). Tertiary butyl hydroperoxide (TBHP diluted at 70% in water; from Acros; Illkirch Cedex, France) and sodium formaldehyde sulfoxylate (SFS Analytical grade; from Sigma Aldrich; Lyon, France) were used as the redox initiator pair. Figure 1(a) to (e) show the chemical structures of MMA, BA, AA, alkyd resin and Dowfax 2AI respectively.

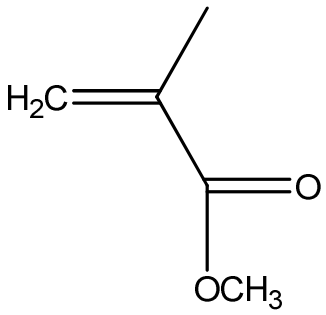

a

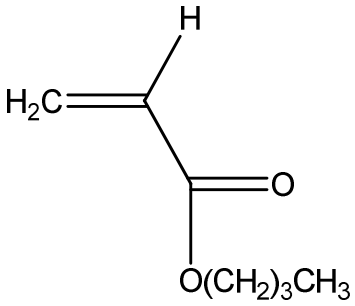

b

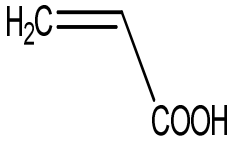

c

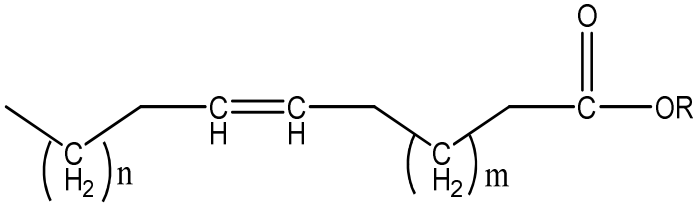

d

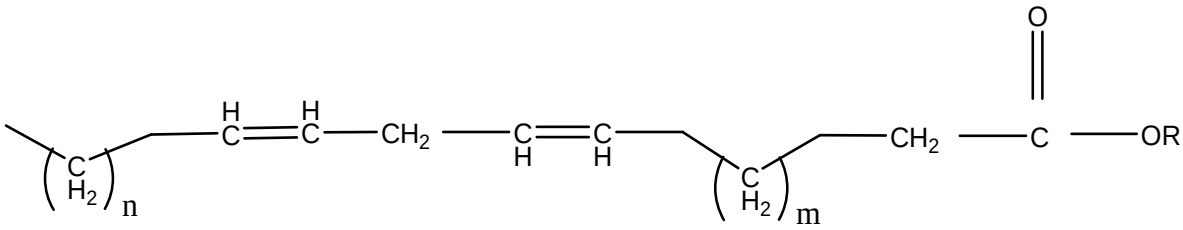

e

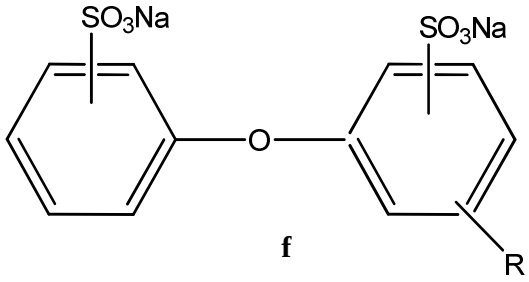

f

Figure 1(a).Chemical structure of MMA. (b).Chemical structure of BA. (c). Chemical structure of AA. (d) & (e). Possible structures deduced by ^{1}H and ^{13}C NMR analysis for alkyd resin (See Annex I for the NMR spectra). (f). Chemical structure of Dowfax 2AI.

Miniemulsion Preparation and Polymerisation

All reactions were carried out in a 200mL jacketed glass reactor connected to a heated water bath for temperature control. The reactor was equipped with a stirrer, a reflux condenser, nitrogen inlet and outlet and a valve on the bottom to remove the latex. The initial runs performed in order to identify and formulate that yielded a stable hybrid mini emulsion are provided in Table 1. Other different recipes were used throughout the course of this work, and in order to facilitate the discussion they will be presented at the pertinent spot during the discussion of results but they are similar to those shown in this table.

Table 1.Experimental runs performed to achieve a stable hybrid miniemulsion

Run	H_2O (g)[b]	Dowfax (g)	BA (g)	MMA (g)	AA (g)	Alkyd (g)	Alkyd (wt%) [a]	ODA (g)	KPS (g)
1	82.50	0.25	9.90	9.90	0.20	0.12	0.6	-	0.04
2	82.50	0.25	9.90	9.90	0.20	0.52	2.6	-	0.08
3	82.50	0.25	9.90	9.90	0.20	0.52	2.5	1.03	0.08

[a] In weight percent based on monomers

[b] Total weight(45% active matter + additional water)

As discussed in Chapter 2, sonication was the homogenisation method employed to produce hybrid mini emulsions. The general procedure followed in these experiments was as follows:

1. The alkyd resin was dissolved in the organic phase by heating at 60°C and magnetic stirring for 30 minutes.
2. The required amount of surfactant was dissolved in the aqueous phase.
3. The organic phase was added slowly to the aqueous phase under gentle stirring. The mixture was then left to mix for 30 minutes.
4. The final mixture was then sonicated for 6 minutes (2*3 times) at 80% of 600W out put power.

Characterisation

The droplet size was measured soon after sonication and then several hours afterward to ensure that the miniemulsion is stable for at least the time necessary to transfer it from the sonication stage to the reactor. Samples were occasionally withdrawn through a valve in the bottom of the reactor for analysis. Conversions were measured by gravimetry. Individual conversion of monomers was detected by gas chromatography (HP5890 SERIES II) and the column was a capillary column. Molecular weight was measured by Gel Permeation Chromatography (GPC) consisting of a WATERS 515 pump, automatic sample injection (WATERS 717 Plus), UV detector (WATERS 410), Differential Refractometric Detector (WATERS 410) and Light Diffusion Detector (Mini dawn Wyatt)} using THF as the eluent. The first column (PLgel 5µm) were followed by three columns (2 x PLgel 5µm Mixed C (300x7.5mm) and 1 PLgel 5µm 500 A (300x7.5mm)). A polymethylmethacrylate standard was used for calculations. Average droplet (D_d) and particle sizes (Dp) were measured with a particle size analyzer (ZETASIZER 1000 HS_A). Average sizes reported here are the averages of at least 5 measurements per sample. Full particle size distributions were measured with a Beckman Coulter LS 230 apparatus (static light scattering). The Critical Micellar Concentration (CMC) of the surfactant in the presence and absence of alkyd was measured by tensiometry (Kruess Processor Tensiometer K12) and the area covered by one surfactant molecule (A_s) was calculated using standard methods (The experimental procedure is described in the Appendix XI). A_s of Dowfax in the both cases was calculated to be 100 $Å^2$/molecule. Atomic force microscopy (AFM)* was used to study the nanostructure of acrylic/alkyd nanocomposite films. The degree of grafting, DG, was measured

by the method described by Tsavalas et al[4]. Selective extraction was performed in a Soxhlet extractor with diethyl ether as solvent. Vacuum-dried samples were weighed in filter paper of known weight and inserted into the extractor. Samples were extracted for durations of at least 24h at the solvent boiling point (40°C). Wet samples were then removed; dried and the residual weight was measured. The Residual weight after extraction was assumed to be homoacrylic polymer. DG was calculated as:

$$\mathrm{DG}\,(\%) = \frac{\text{Acrylic polymer in hybrid}}{\text{Total polyacrylic}} \times 100$$

$$= \frac{\text{Total amount of solid} \times \text{Acrylic weight fraction - Residual weight}}{\text{Total amount of solid} \times \text{Acrylic weight fraction}} \times 100$$

Where the extracted weight is pure homoacrylic polymer and acrylic % is defined as

$$\text{Acrylic weight fraction} = \frac{\text{Total monomer} \times \text{Fractional conversion}}{\text{Total monomer} \times \text{Fractional conversion} + \text{Alkyd} + \text{Initiator} + \text{Surfactant}}$$

However we do not do a detailed analysis on DG during this study. Recently a more accurate method has been developed by Minari et al to determine the DG[18].

3.3 Results and discussion

3.3.1 Influence of the alkyd on polymerisation rate and monomer conversion

The initial runs shown in Table 1 were used to identify formulations that provided a reasonable N_p/N_d ratio. The experimental results of these runs are summarised in Table 2. An increase of particle size by about 30nm compared to the initial droplet size (70nm) was observed in the first two runs. This could be possibly due to the low amount of alkyd resin which was not sufficient enough to control the Ostwald ripening. Adding 5wt% of ODA in the next run and controlling the sonication time to maintain the droplet size around 100nm, enabled to achieve an acceptable N_p/N_d ratio of 0.9 (Run 3). The stability of the miniemulsion of Run 3 was verified during the reaction time and with time. (cf. Figure 2(a) and Figure 2 (b)).

Table 2. Evolution of droplet and particle sizes in Runs 1 to 3.

Run	Alkyd (wt%)	ODA (wt %)	D_d (nm)	D_p (nm)	N_p/N_d	Total Solid Content (%)	Final Monomer Conversion (%)
1	0.6	0	70	100	0.28	20	100
2	2.6	0	65	98	0.23	20	100
3	2.5	5	104	102	0.90	21	100

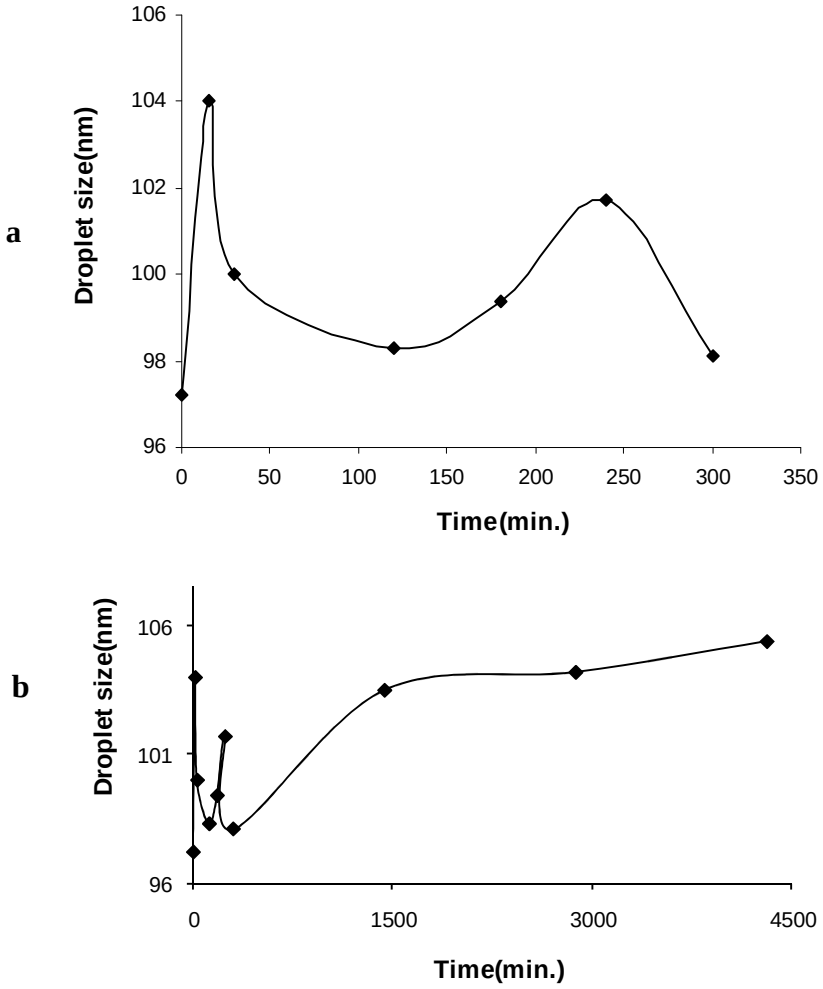

Figure 2(a). Variation of droplet size of run 3 during reaction time. (b). Variation of droplet size of run 3 with time.

Using this initial formulation as a starting point, a second series of runs was done to explore the effect of increasing the alkyd content from 2.5 to 25% (c.f. Table 3). The Run 3 was not repeated and a control run with 0% alkyd was done instead. The recipes of this series of experiments are shown in Table 3.

Table 3. Experimental runs performed to increase the alkyd quantity.

Run	H_2O (g)	Dowfax (g)	BA (g)	MMA (g)	AA (g)	Alkyd (g)	Alkyd (wt%) [a]	ODA (g)	KPS (g)
4	64.0	1.50	19.8	19.8	0.4	0	0	2.0	0.16
5	64.0	1.50	19.8	19.8	0.4	2	5	2.0	0.16
6	64.0	1.50	19.8	19.8	0.4	4	10	2.0	0.16
7	64.0	1.50	19.8	19.8	0.4	6	15	2.0	0.16
8	64.0	1.50	19.8	19.8	0.4	10	25	2.0	0.16

[a] In weight percent based on monomers

Although N_p/N_d remained close to 1 and complete monomer conversion was achieved with 2.5wt% of alkyd resin (cf. Run 3 of Table 2), the runs performed with higher amount of alkyd exhibited a limiting monomer conversion as shown in Figure 3 and Figure 4.

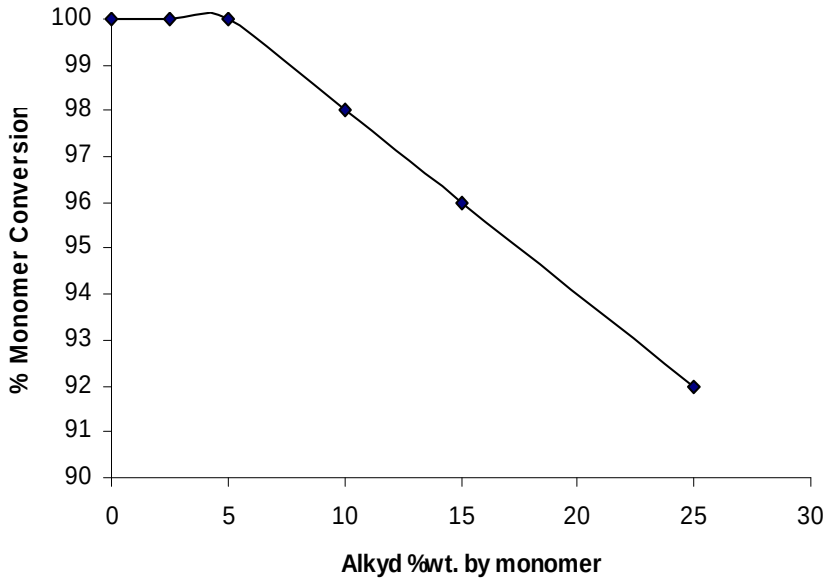

Figure 3. Effect of alkyd quantity on monomer conversion

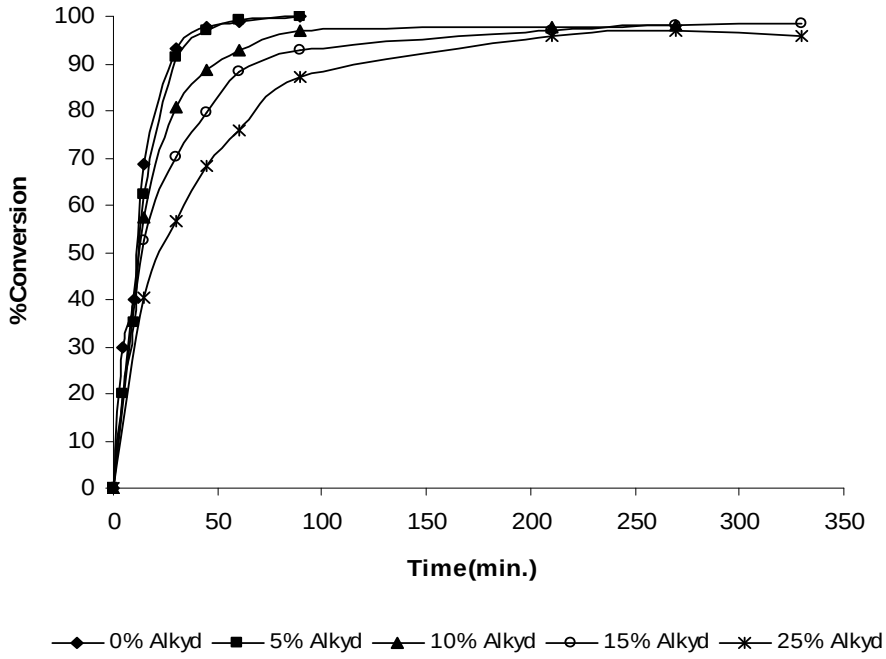

Figure 4. Monomer conversion versus time curves for varying alkyd contents

Not only does the presence of alkyd create a limiting conversion but Figure 4 also shows that the rate of reaction decreases as the alkyd concentration increases (the relationship between alkyd content and N_p/N_d will be discussed below). In an attempt to overcome this limiting conversion, the initiator system was modified in different ways as seen in Table 4.

Table 4. Recipes of the miniemulsion polymerisation reactions performed to increase monomer conversion

Run	H_2O (g)	Dowfax (g)	BA (g)	MMA (g)	AA (g)	Alkyd (g)	ODA (g)	KPS (1) (g)	KPS (2) (g)	$NaHSO_3$ (g)	TBHP (g)	SFS (g)
9	127	4.00	45.00	45.00	0.91	24.10	9.00	0.21	0.40	0.85	-	-
10	125.50	4.00	45.00	45.00	0.91	24.20	9.05	0.21	0.12	0.25	0.24	0.16
11[a]	125.50	4.01	45.00	45.00	0.91	24.10	9.01	0.21	0.12	0.25	0.22	0.16
12[b]	125.50	4.01	45.00	45.10	0.91	24.10	9.00	0.20	0.12	0.25	0.23	0.16

[a] Another dose of TBHP/SFS redox system was added after 5h

[b] The resin was vacuum distilled prior to use.

As illustrated in Table 4, in addition to the initial dose of initiator (KPS-1), a second dose (KPS-2) and $NaHSO_3$ was added semi-continuously for one hour after the first two hours of reaction (Run 9). Despite the increased radical flux in this run, Table 5 shows that no considerable increase of monomer conversion was observed at alkyd levels of 25 wt%. Therefore a third dose of redox initiator was added in runs 10 to 12. The 3rd dose was added as a single shot after 3h of reaction, and the temperature was increased to 80°C for an additional hour. Once again, despite these changes to the rate of generation of free radicals, the final monomer conversion was still only 92% in the presence of 25 %wt of alkyd resin (in other words, unchanged to within the limits of experimental variability). Similarly, another dose of TBHP/SFS redox initiator added after 5h in the next run (Run 11) did not appreciably change the final conversion. In a last run (Run 12), the alkyd resin was vacuum distilled before use in order to remove xylene and any other light components that might be present in the alkyd, but difficult to detect by GC or NMR analyses[19-21]. Indeed, solvents are known to influence the rate of free radical polymerisation and can account for the limiting conversion. As can be seen from Table 5, vacuum distilling the alkyd prior to the miniemulsification process allowed us to increase the final conversion to only 96%.

Table 5. Droplet size, particle size, Np/Nd ratios and monomer conversions for Runs 9-12

Run	Alkyd (wt%)[a]	D_d (nm)	D_p (nm)	N_p/N_d	Solid content (%)	Monomer Conversion (%)
9		147	130	1.26	46	92
10	25	147	125	1.42	46	92
11		145	123	1.42	46	92
12		130	117	1.8	48.4	96

[a] In weight percent based on monomers

In summary, none of the modifications discussed here nor additional trials outlined in Table A1 of Appendix II such as lowering the total solid content, lowering the alkyd quantity to 10wt%, using oil soluble initiators or adding MMA in a semi-continuous way in the presence of KPS or lauryl peroxide (an organosoluble initiator), allowed us to increase the overall conversion. However by a combination of oil soluble initiator (AIBN) and KPS and under enhanced renucleation (adding a secondary dose of surfactant), complete monomer conversion could be achieved for certain ratios of alkyd to monomer. We will discuss this along with examples of the film structure, in the section on modifications and process improvements. A short description of

each experiment carried out to increase monomer conversion is shown in Tables A2 to A5 of appendix III and the variation of N_p/N_d relevant to these experiments are shown in appendix IV.

3.3.2 Individual monomer conversion and degree of grafting

Figure 5 (a) to (c) illustrate the individual monomer conversions for MMA and BA in the absence of alkyd, and in the presence of 5% and 25% alkyd respectively. As expected, for a batch polymerization of MMA and BA, MMA reacts earlier than BA due to its higher reactivity ratio and we arrive at 100% conversion. If one looks at Figure 5(b) and (c), it is apparent that like in the Figure 5(a), MMA reacts completely in all cases. It therefore appears that limiting conversion seen in these last 2 graphs is related to the incomplete conversion of BA. It is thus possible that alkyd preferentially associates with BA. When the structure of BA is compared to that of MMA, it can be seen that butyl acrylate presents far fewer steric hindrances than MMA. Therefore their ability to undergo addition through double bonds is high.

a

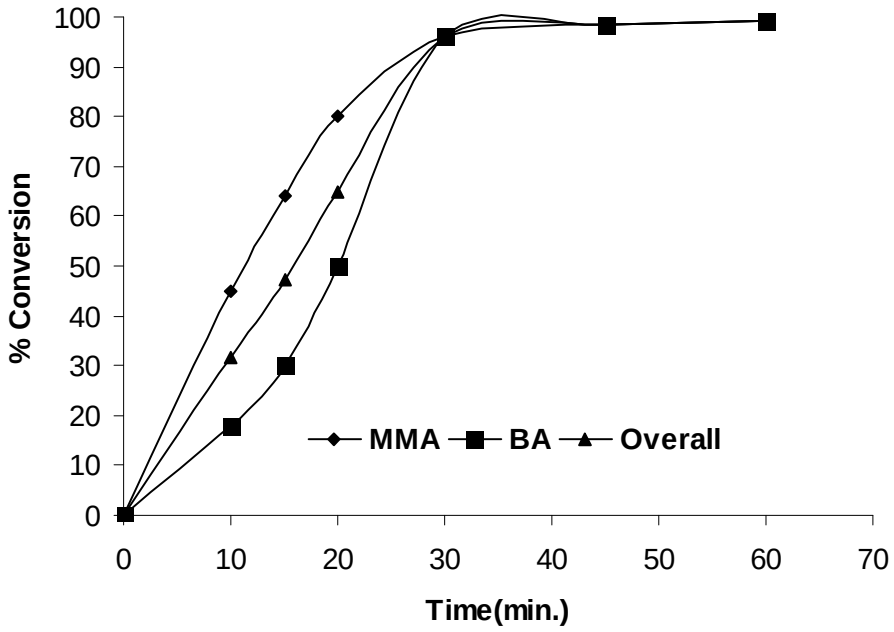

b

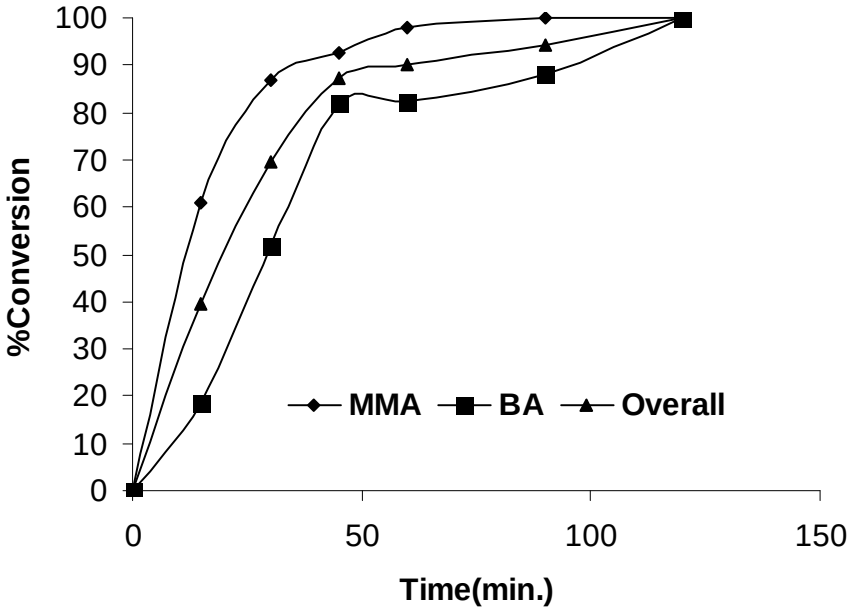

c

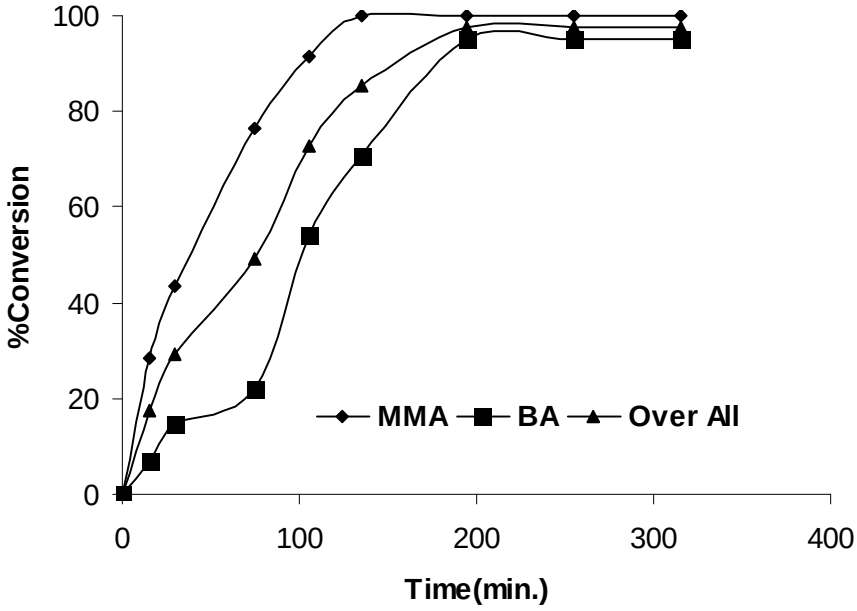

Figure 5(a). Individual monomer conversions versus time for miniemulsion polymerisation reactions conducted in the absence of alkyd. (b). Individual and overall monomer conversions in the presence of 5% alkyd. (c). Individual monomer conversions in the presence of 25% unsaturated alkyd resin

Schork et al[3] have shown that a fairly low K_{tr}/K_P (the ratio of transfer rate to propagation rate constants) value could be observed for BA/alkyd system, and this implies that the mode of attack of a BA radical to the alkyd is through direct addition to a double bond of the resin rather than through chain transfer. The hypothesis that essentially only BA is grafted to the alkyd resin was confirmed by measuring the degree of grafting of the alkyd for different monomer compositions.

To do so, different miniemulsions of various monomer compositions were run with the same basic formulation and solid content as in Table 3 (Run 8). The final products were then fractionated using Soxhlet extraction to determine the degree of grafting and the results of this procedure are shown in Table 6. Although the degree of grafting determined by the solvent extraction method is not very accurate, especially in the case of PBA and 25% alkyd in which high gel content (gel content data are not shown here) affects the numerical value of grafting, there appears to be non-negligible levels of grafting between PBA and alkyd whereas the grafting between PMMA and alkyd was 0%. This trend of grafting is in agreement with Schork et al[3] although the numerical values are different. For example they observed 100% grafting for BA and about 40-50% grafting for MMA. The difference of numerical values could be due to the type of alkyd (i.e. the amount of double bonds and hydrophobicity differences).

Table 6.Selective extraction data of hybrid latex

Monomer composition	Total amount of solid (g)	Acrylic weight fraction (%)	Residual weight (g) after solvent extraction	Degree of Grafting (%)
MMA/BA/AA (49.5/49.5/1)	6.1	77.6	1.7	64
BA	6.9	77.6	3.6	33
MMA	6.2	78.5	5.1	0

Nevertheless, the results presented in this chapter suggest that there is grafting of the unsaturated alkyd on the copolymer, and this takes place essentially with BA. The grafting was further characterised by GPC and also proven by ^{1}H and ^{13}C NMR analyses (see Appendix I for NMR analysis); both of which showed that the double bonds of the alkyd were consumed during polymerisation and hence chemical incorporation of alkyd to the growing copolymer. The GPC

chromatograms of pure alkyd resin and hybrid latex of 25% alkyd are shown in Figure 6 (a) and (b) respectively.

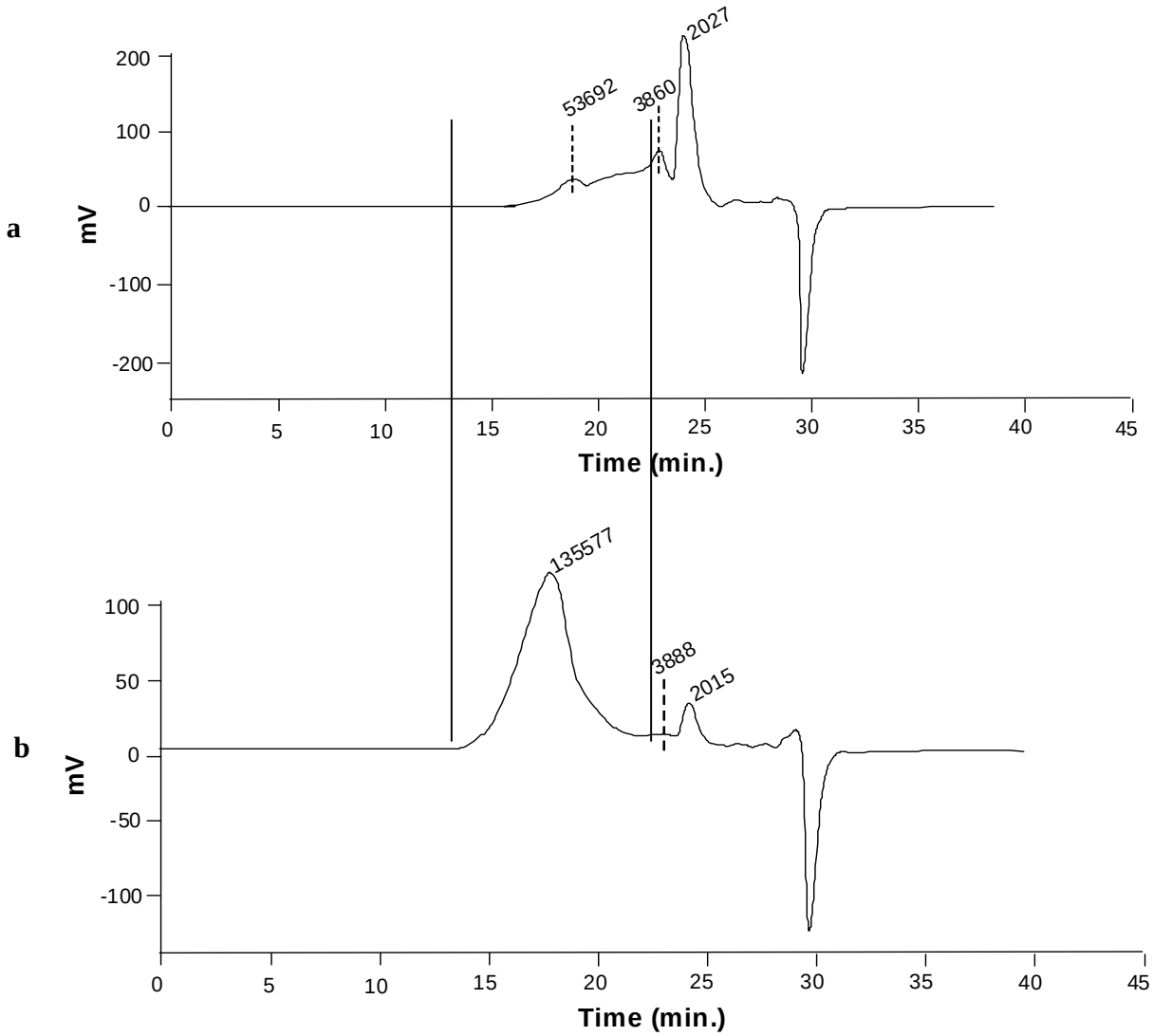

Figure 6(a). GPC analysis of the Setal 293 unsaturated alkyd resin. (b). GPC of copolymer with 25% alkyd resin

The results obtained by DR detector are summarised in Table 7 and Table 8.It is clear that the alkyd resin is not well-defined and does not have a single molecular weight. Although the high molecular weight region is masked by the copolymer peak, two low molecular weight peaks of alkyd resin could be clearly observed. We considered only the alkyd resin peak of molecular weight of 2027 $g.mol^{-1}$ [MP in (a)] and compared the peak area and height of the same peak in (b) (2015 $g.mol^{-1}$) to

verify the chemical incorporation of alkyd to copolymer. According to this analysis, we found that approximately 33% of the alkyd in this peak is grafted to copolymer.

Table 7. GPC analysis of the Setal 293 unsaturated alkyd resin

MP	Mn	Mw	Mz	Mz+1	Mw/Mn	Area (µV*sec)	% Area
53692	68569	108708	257164	613147	1.59	3410183	13.6
3860	6473	10362	16247	21479	1.60	10691733	42.6
2027	1758	1843	1917	1983	1.05	10972102	43.8

Table 8. GPC analysis of copolymer with 25% alkyd resin

MP	Mn	Mw	Mz	Mz+1	Mw/Mn	Area	% Area
135577	67724	445881	4972679	18434897	6.58	22832294	88.8
3888	3969	4207	4455	4697	1.06	968402	3.8
2015	1733	1828	1914	1989	1.06	1899939	7.4

In summary, an analysis of the individual monomer conversion data and grafting experimental results have led to a better understanding of the polymerisation process. It can be concluded that the grafting between the alkyd and copolymer mainly takes place via reaction with the BA, and the overall limiting monomer conversion is due to the low BA conversion. We will correlate this data with the variation of N_p/N_d in the following section in order to better understand the hybrid system with increasing alkyd quantity.

3.3.3 Variation of N_p/N_d with monomer conversion

Next the extent to which there is a one-to-one copying from an emulsion droplet to particle is investigated through analysis of the N_p/N_d ratio throughout the polymerisation process. Figure 7 illustrates the variation of N_p/N_d with monomer conversion for Run 12 containing 25wt% of the vacuum-distilled alkyd resin. It is obvious that N_p/N_d increases after about 40-50% monomer conversion during the polymerisation of this hybrid system, strongly suggesting the occurrence of some type of secondary nucleation of emulsion particles. It should be recalled that we have added different doses of initiator during polymerisation; thus secondary nucleation could be promoted by the intermittent addition of initiator. In order to clarify this fact and shed more light on the effect of the amount of alkyd on N_p/N_d, another series of experiments was performed still using vacuum-distilled alkyd resin and only one dose of initiator based on the recipe of Table 3.

The only parameter that changes in this series of experiments was the quantity of alkyd resin. The changes of properties of initial droplets and the variation of final monomer conversion with increasing alkyd quantity are summarised in Table 9.

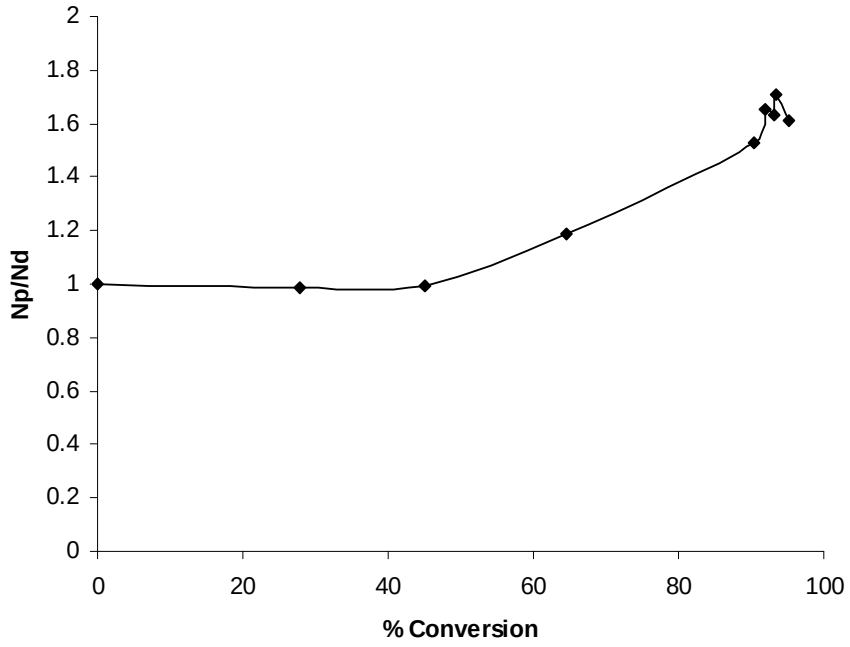

Figure 7. Variation of N_p/N_d with monomer conversion for Run 12

Table 9. Influence of alkyd content on various reaction related parameters (Reactions performed according Table 3 using a vacuum distilled resin).

Alkyd (wt% to) Monomers	Droplet Size(nm)	Final Particle Size(nm)	Particle Coverage by Surfactant (%)	Viscosity (mpa.s) at $100s^{-1}$	Monomer Conversion (%)	Reaction time (minutes)
0	79.4	104.4	20.45	0.75	100	90
5	96.4	98.4	23.22	0.97	100	90
10	107.9	97.8	24.85	1.37	98	270
15	119.0	105.3	26.34	1.60	98	330
25	134.9	116.4	27.61	2.33	96	330

The variation of polydispersity index (PI) with monomer conversion relevant to the above experiments is illustrated in Figure 8.

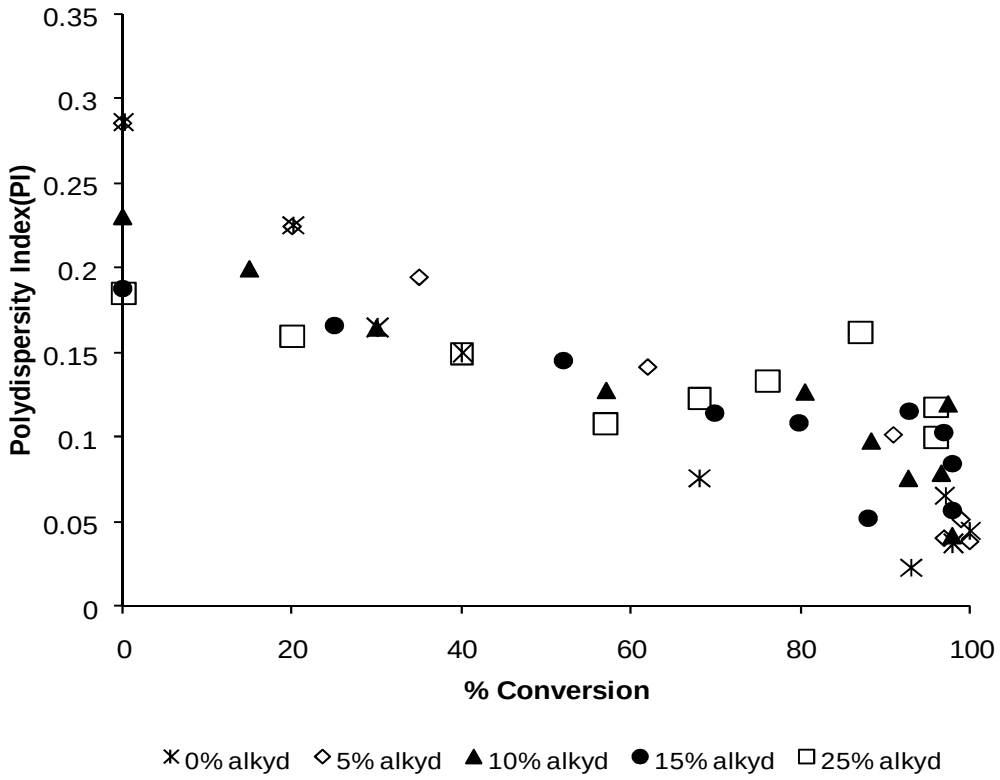

Figure 8. Variation of polydispersity index with monomer conversion for a series of miniemulsion polymerization reactions performed according to the recipes of Table 3 using a vacuum-distilled resin

It can be seen that the initially broad droplet size distributions become narrower after approximately 50% conversion. In fact, as the quantity of alkyd increases, the initial droplet size distribution appears to be narrower. This is possibly due to an increase in viscosity of the organic phase seen in Table 9. As we discussed in Chapter 2, the viscosity of organic phase increases linearly with increasing alkyd quantity. Therefore it is possible that at the higher viscosities associated with the higher levels of alkyd, the cavitation of the ultrasonication does not create the very small (<40 or 50nm) droplets that are created at lower viscosities. The increase of particle size compared to the initial droplet size coupled with rapid narrowing of initial droplet size

distribution in the absence of alkyd suggests the disappearance of a considerable fraction of very small droplets. We will return to this point below.

The variation of N_p/N_d with increasing alkyd quantity as a function of conversion during the polymerisation (with all other quantities remaining unchanged) is shown in Figure 9.

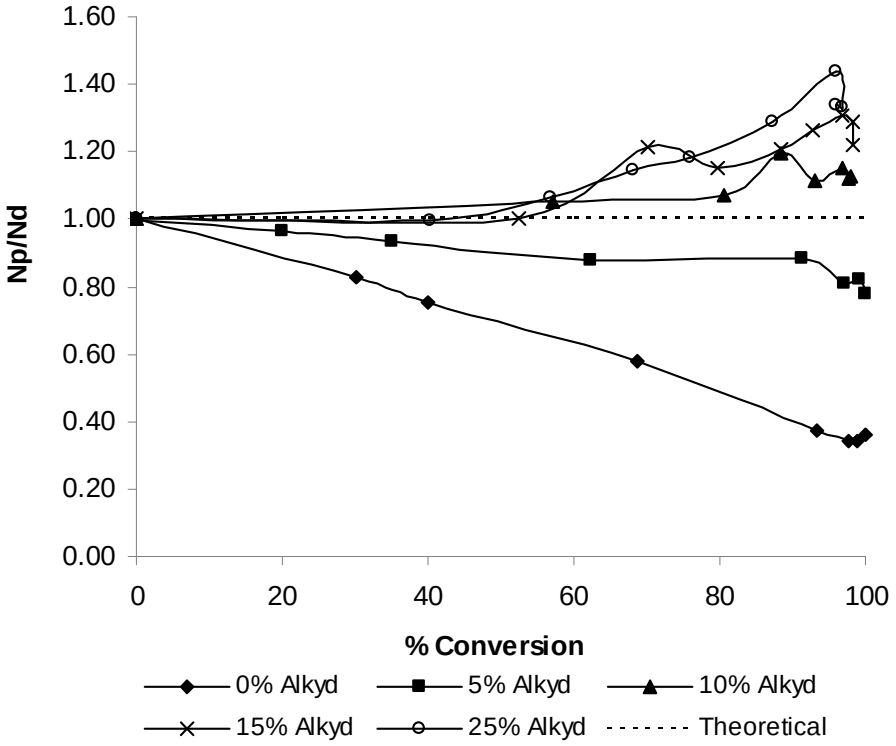

Figure 9. Variation of N_p/N_d with increasing alkyd quantity according to the recipes of Table 3 using a vacuum-distilled resin

We observe two distinct behaviours: one for 0 and 5% alkyd where N_p/N_d is monotonically decreasing and always less than one; and a second behaviour for higher alkyd contents where N_p/N_d increases for conversions higher than 50 %. We will first consider the case of the polymerisations performed without alkyd or with 5% alkyd.

In the presence of 5% alkyd, the N_p/N_d ratio was closer to one compared to the polymerisation performed without alkyd and this implies that the hydrophobic character of the organic phase is significantly increased. As a result the stability of very small droplets is increased. In order to investigate this, the hydrophobic effect of alkyd resin, hexadecane and ODA was compared. As illustrated in Figure 10, similar initial droplet sizes of about 80nm are obtained whatever the

nature of the hydrophobe. However, as the polymerisation proceeds, the average particle size increased by approximately 20nm when hexadecane and ODA were used as the hydrophobe during the first hour of polymerisation, but remained relatively constant when the alkyd was used alone.

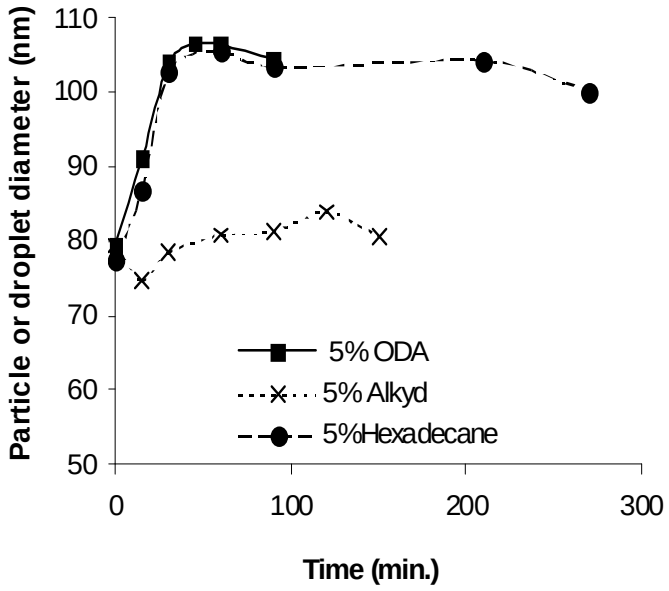

Figure 10. Variation of droplet and particle size with time for three different hydrophobes.

This comparison clearly indicates that the interactions between alkyd and monomer are stronger than that of hexadecane and ODA and hence low levels of alkyd provides a better stabilisation than both hexadecane and ODA. Sood and Awasthi[13] have shown that in a given system with a particular amount of hydrophobe, and depending on the degree of non-ideality of mixing between the monomer and the hydrophobe, there exists a minimum stable diameter in the reactor. They also showed that for the same amount of different hydrophobes (hexadecane and hexadecanol) the minimum stable diameter of styrene is 117 and 187 nm respectively because hexadecanol is more non-ideal than hexadecane. According to these authors, the interaction parameter (χ) for hexadecane and styrene is equal to 0 and for hexadecanol and styrene it is1.69. Based on this difference of interaction parameters, they showed that droplets with a diameter greater than the minimum stable diameter are stable because they fulfil the chemical potential requirement for stability.

Considering the structure (cf. Figure 1(d) & (e)) and the molar mass (cf. Table 7) of the unsaturated alkyd resin determined by NMR and GPC analyses respectively, it is clear that the chain length of the hydrocarbon part of the alkyd is greater than that of hexadecane or ODA. Davis and Smith[22] have shown that the solubility of hydrocarbons in water and in surfactant solutions decreases with an increasing hydrocarbon chain length. They further showed that the solubility of a given hydrocarbon (for example n- hexane) is considerably different in water and in a given surfactant solution. According to them, the solubility of n-hexane in water is $9.5\ 10^{-6}$ $kg.dm^{-3}$ and increases significantly to $2.07\ 10^{-3}$ $kg.dm^{-3}$ in a 10^{-1} $mol.dm^{-3}$ sodium dodecyl sulphate solution. On the other hand, they have shown that single droplet coalescence data, area per molecule data and mobility data are not sensitive predictors of emulsion stability and that significant emulsion instability may arise from a route other than droplet coalescence; namely Ostwald ripening.

In this context, we can conclude that in the presence of equivalent concentration of alkyd resin, the hydrophobic character of the organic phase is greater than that of ODA or hexadecane. As a result, the strong interfacial effect created by Dowfax 2AI which has a low CMC (0.2g/L in deionised water) is counteracted by the alkyd resin. Therefore, the very small droplets are stabilised against Ostwald ripening and hence the original droplet size is retained.

We showed here that the hydrophobic character of the organic phase is significantly increased in the presence of even low amounts of alkyd (typically 5%). We will now discuss the effect of increasing the alkyd content up to 25%, keeping in mind that the hydrophobic character of the organic phase is significantly increased in the presence of alkyd. It should be noted that the trend of variation of N_p/N_d in Figure 9 is similar to that of Figure 7 for a similar quantity of alkyd (e.g. 25%). Hence, it is obvious that homogeneous nucleation is independent of the intermittent addition of initiator. Recall that these are batch experiments, so the re-nucleation of particles observed for this second set of runs is not due to additional monomer or surfactant being added to the system, but rather to a change in the particle morphology.

The individual conversions of MMA and BA in the presence of 25% alkyd are shown in Figure 5(c). As noted above (cf. Figure 4), the overall rate of polymerisation is lower at higher alkyd concentrations. Thus, as expected, the rate of polymerisation is lower with 25% alkyd than 5% alkyd. Nevertheless, in Figure 5(c), it can be seen that the rate of consumption of BA is very low compared to the reaction performed with 5% alkyd, especially during the first 30 minutes of polymerisation. When the overall monomer conversion is 45%, the conversion of MMA is about 70% and the conversion of BA is about 20%. In other words, the polymer formed in the first part of the experiment (i.e. before new particles are created by secondary nucleation) is rich in MMA. It has been shown in the literature that although MMA and an alkyd are totally miscible, there appears to be some sort of incompatibility between PMMA and alkyd[8]. In addition, a change in the particle morphology of alkyd-acrylic hybrids with monomer conversion leading to an acrylic rich shell and alkyd rich core has been observed[6-8].

Figure 11 shows an image of hybrid latex obtained by wet stem technique and it suggests a possible core shell structure for alkyd-acrylic hybrid particles.

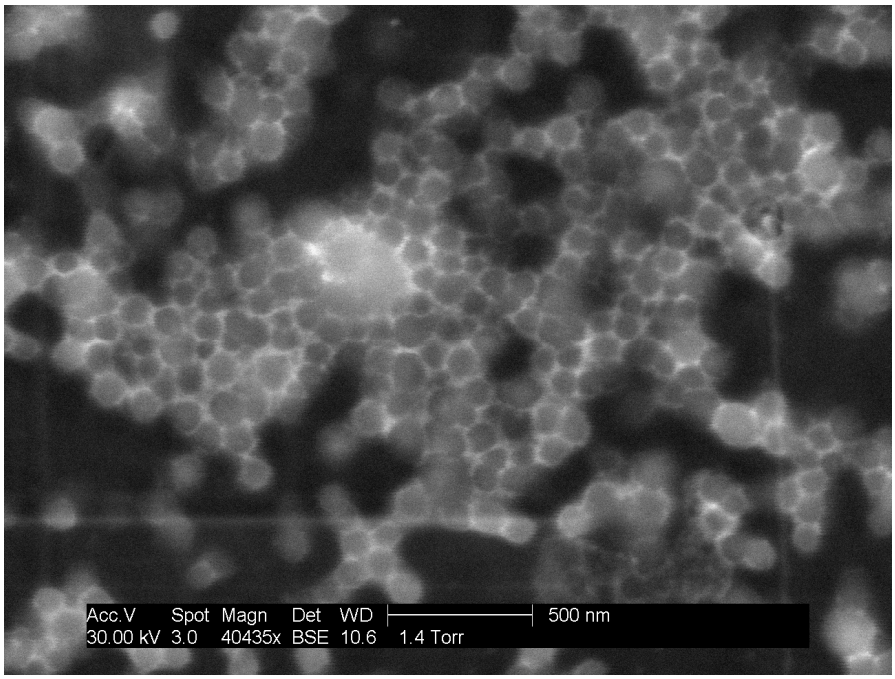

Figure 11. Wet stem image of hybrid latex with 25% alkyd

It is therefore reasonable to assume that the morphology of hybrid particles changed to a PMMA rich shell and alkyd/PBA rich core somewhere near 40-50% overall monomer conversion at higher alkyd contents, and that this change will be all the more significant when the quantity of alkyd in the particle increases. The range of 40-50% conversion corresponds to the point where one begins to see spontaneous renucleation of particles at higher alkyd contents in Figure 9. Apparently, for high alkyd contents, some monomer leaves the particles and is used to create a second, stable population of particles.

Interestingly enough, the re-nucleation for the high alkyd content runs is nevertheless accompanied by a narrowing of the PI (cf. Figure 8). Since the number of particles is increasing in these two runs (15 and 25% alkyd), this means that the average particle size is decreasing. This implies that the size of larger particles is decreasing – in other words that monomer is being ejected from these particles – but the size of the smaller particles increases to an extent obviously less than the size of the larger particles. It is worthwhile to mention that the particles formed by the secondary nucleation can not be hybrid particles. An unintended outcome is greater heterogeneity across the particle population, which will translate into more heterogeneity in the final films.

As per the calculations shown in Appendix XI, the area covered by one surfactant molecule, A_s, in the presence or absence of the alkyd is 100 $Å^2$/molecule for our system, and therefore the surface coverage of droplets by the surfactant was always incomplete (cf. Table 9). We can therefore conclude that there is not a significant release of surfactant in the system. It is therefore possible that the incompatibility between PMMA and alkyd could be a major reason for the increase of N_p/N_d. This incompatibility might limit the ability of the particles to swell, and therefore the residual monomer (mostly BA at this point) could be partially ejected from the particles during the second half of the reaction when the morphology of the particles changes. Note that since A_s does not change when we add the alkyd resin, this further suggests that the droplets themselves are not entirely homogeneous. If the alkyd were located (even partially) at the interface of the droplets, one would expect to see A_s decreases due to a drop in the polarity The fact that this does not occur is evidence that the alkyd is essentially found near the centre of the droplets, surrounded by a “shell” of monomer.

3.3.4 Modifications and process improvements

These results led us to believe that it should therefore be possible to avoid secondary nucleation by controlling the nature of the organic phase. Accordingly, we removed ODA from our system in the presence of 25wt% alkyd. As a result, the broad asymmetric droplet size distribution could be rearranged to narrow symmetric distribution (Figure 12). See Appendix V to VIII for droplet and particle size distribution in the presence of ODA (T-78) and in the absence of ODA (T-100).

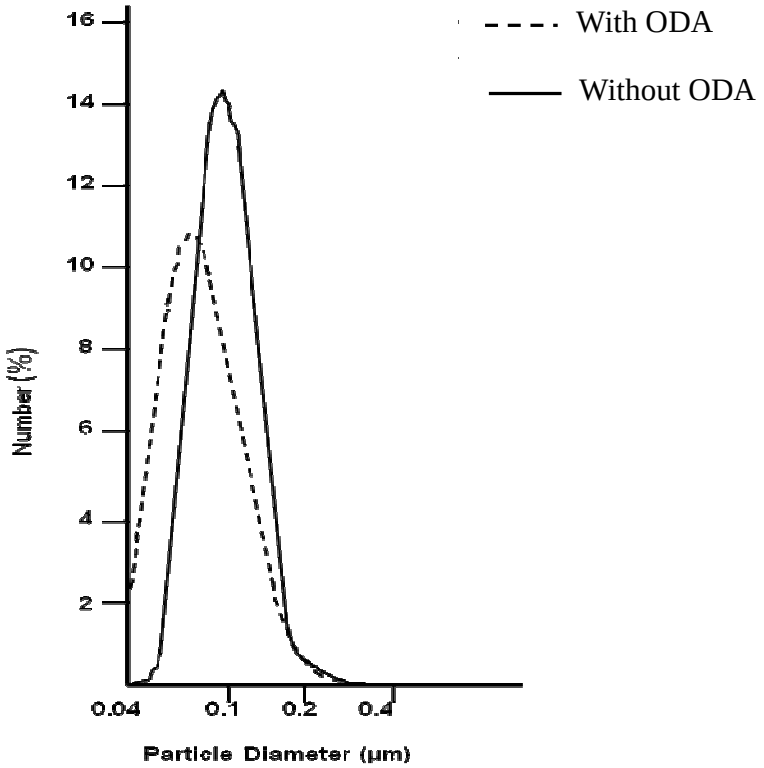

Figure 12. Droplet size distribution in the presence (- - -) and absence(____) of ODA for 50% monomer content MMA/BuA/AA miniemulsions containing 25% alkyd

It is clear that a significant rearrangement of droplet and particle size distribution takes place in the presence of ODA while in the absence of ODA both the initial droplet size distribution and final particle size distribution are similar. This rearrangement of droplet size distribution in the presence of ODA is totally in agreement with the discussion of Sood and Awasthi[13].

The evolution of N_p/N_d for a new series of experiments (without ODA), with a total theoretical solid content of 50 % by weight containing 25 % alkyd in the organic phase and having various monomer compositions (See Table 10) is shown in Figure 13.

Table 10. Formulations for high solid content miniemulsion polymerizations with various monomer compositions*

Run	H_2O (g)	MMA (g)	BA (g)	AA (g)	Alkyd (g)	Conversion (%)	Type of Alkyd
13	118.5	45	45	0.9	25	97	Unsaturated
14	55	45	0	0.45	12.5	99	Unsaturated
15	55	0	45	0.45	12.5	95	Unsaturated
16	118.5	45	45	0.9	25	96	Saturated

*In all cases initiation was carried out as explained previously for Run 12.

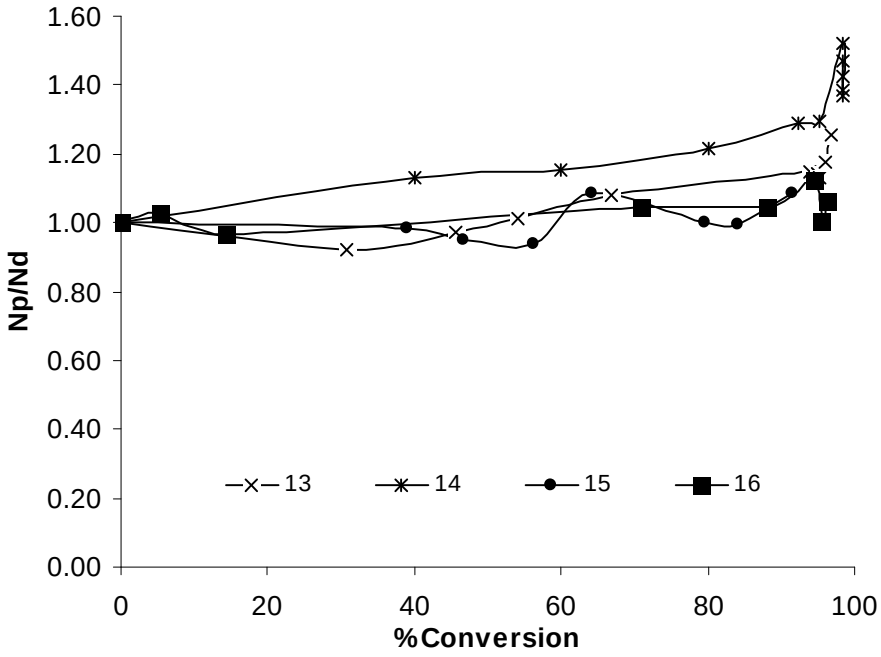

Figure 13. Variation of N_p/N_d with % monomer conversion for miniemulsion polymerisation reactions performed according to the recipes of Table 12 in which ODA was removed and the composition of the monomer mixture was varied.

These experiments were compared to an experiment containing 25wt% of the saturated alkyd resin (Run 16). The degree of secondary nucleation late in the experiment is high when MMA is polymerised alone even in the absence of ODA (Run 14). This could be due to the very low grafting between PMMA and alkyd resulting in poor compatibility between both phases. However, the other experiments show relatively small changes in the N_p/N_d ratio and a limiting conversion of approximately 96% as in the previous cases discussed above. Since we have

controlled the hydrophobicity by removing ODA in the presence of alkyd, the fraction of very small droplets created during miniemulsification is low in the absence of ODA as evident by the droplet size distribution (cf. Figure 12). As a result we could better control the homogenous nucleation and hence the N_p/N_d ratio could be maintained closer to one.

Another interesting result is that the copolymerisation run with the non-reactive saturated alkyd resin shows similar N_p/N_d values and also still exhibits some limiting conversion. A possible reason for the limiting monomer conversion in the presence of both saturated and unsaturated alkyd is the stronger interactions between monomer and alkyd as we have shown here. In other words it appears more likely to a physical effect as proposed by Hudda et al[7] and Guo et al [23] rather than a chemical effect.

The complex nature of limiting monomer conversion is further evident with the last series of experiments carried out by changing the ratio of the monomer to reactive alkyd and the initiator system. The objective of this series of experiments was to relate monomer conversion to film formation and morphology. The experimental recipes for this series of experiments and the characteristics of the miniemulsions and latexes of these experiments are illustrated in Table 11 and Table 12 respectively.

Table 11. Recipes for the experiments carried out by changing the monomer to reactive alkyd

Run	H_2O (g)	Dowfax (g)	BA (g)	MMA (g)	AA (g)	Alkyd (g)	ODA (g)	KPS (1) (g)	KPS (2) (g)	$NaHSO_3$ (g)	TBHP (g)	SFS (g)	AIBN (g)
17	125.0	4.00	45.00	45.00	0.91	-	4.6	0.3	-	-	-	-	-
18[a]	116.0	5.00	45.00	45.00	0.91	25.0	-	0.15	0.15	-	-	-	-
19[b]	118.5	4.00	45.00	45.00	0.91	25.0	-	0.15	0.15	0.32	0.22	0.16	-
20[a]	111.0	5.00	45.00	45.00	0.91	25.0	-	-	0.15	-	-	-	0.3
21	110.0	4.00	22.50	22.50	0.45	45.0	-	-	-	-	-	-	0.3
22[a]	116.0	5.00	22.50	22.50	0.45	45.0	-	-	0.15	-	-	-	0.3
23[a]	116.0	5.00	22.50	22.50	0.45	45.0	-	0.3	0.15	-	-	-	-

[a] The second dose of KPS (KPS (2) in 3mL of water) was added with 1g of Dowfax 2AI in3mL of water after 1.5h from the beginning of reaction for 1h. [b] The initiator system was similar to the system described in Run 12.

Table 12. Characteristics of the miniemulsions and latexes of the experiments 17 to 23

Run	Alkyd (wt% by organic phase)	Droplet Size(nm)	Final Particle Size(nm)	Total Solid Content (Theoretical)(%)	Total Solid Content (Actual) (%)	Monomer Conversion (%)	Reaction time (minutes)
17	0	113	120	45.00	45.00	100	300
18	22	125	111	49.80	48.60	96.8	360
19	22	120	110	49.40	48.00	96.3	360
20	22	117	112	50.00	46.50	93	420
21	50	145	138	45.00	40.40	78.4	360
22	50	144	139	44.00	44.00	100	420
23	50	144	140	44.00	42.00	91.3	420

Before discussing the film structures of these latexes it is worthwhile to discuss the effect of the choice of the initiator system, the ratio of alkyd to monomer and the total solid content on the monomer conversion. When 22% alkyd is present in a 50% solid system (Run 18 and Run 19) a similar monomer conversion could be achieved by the addition of KPS regardless of the method used (a & b). However when AIBN was used instead of KPS (1), the final monomer conversion for a 50% solid system with 22% alkyd was 93% (the loss of radicals by termination is high with AIBN) irrespective of the secondary addition of KPS with Dowfax (Run 20).

When only AIBN was used for a 45% solid system with 50:50 monomer: alkyd ratio, the final monomer conversion was 78.4% (Run 21). Adding a second dose of KPS and Dowfax allowed us to obtain complete conversion, but at the price of creating particles in a secondary nucleation step (N_p/N_d increases; Run 22). It should be noted that a significant difference of particle size could not be observed after re-nucleation. This is possibly due to the very small droplets created during re-nucleation which do not affect the particle size. However when AIBN was replaced by KPS (KPS1) the final monomer conversion was 91.3% for a similar system irrespective of the enhanced renucleation (Run 23). This observation suggests that the polymer chain length which varies with the type of initiator could also affect the limiting monomer conversion. Experiments were carried out to determine the influence of the type of initiator on the final film morphology. For comparison, the structure of a plain acrylic film (Run 17) was examined first. The AFM images in Figure 14 reveal that the particle identity has been retained.

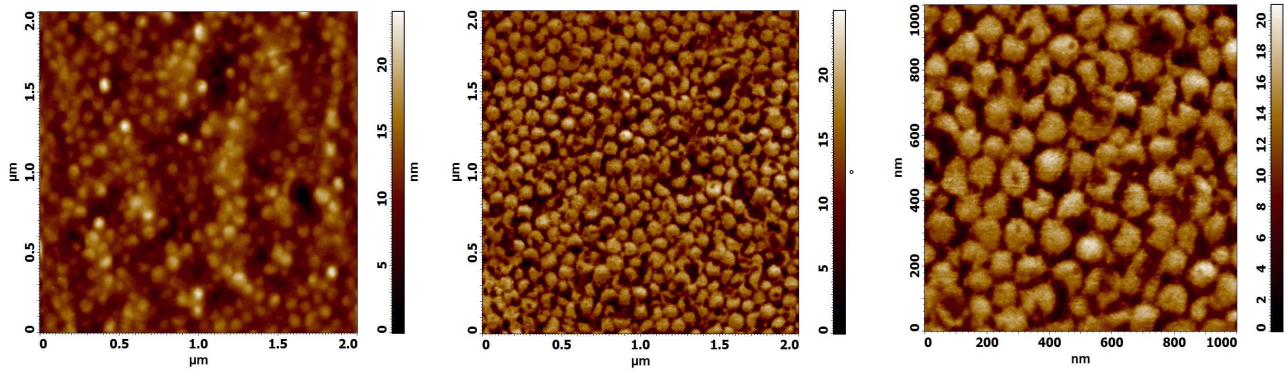

Figure 14. AFM images of the surface of an acrylic latex (Run 17) film: (a) height image and (b) phase contrast image. The scan area is 2 µm x 2 µm. (c) A phase contrast image of the same surface at a higher magnification. The scan area is 1 µm x 1 µm.

The particles have not coalesced at the film surface. DSC analysis has found the glass transition temperature of the latex to be 22 °C. The temperature of film formation was 23 °C. The polymer viscosity will be exceedingly high during film formation, and a model of the process predicts slow particle deformation by a dry sintering mechanism[24].

A phase-contrast image can be considered to be a map of the energy dissipation between the AFM tip and the sample surface[25]. Greater energy dissipation is associated with a stronger viscous component of the viscoelasticity[26]. In the images presented here, more dissipative regions appear darker[27]. The presence of some dark regions in the phase-contrast images of the acrylic in Figure 14 could be coupled with topographic effects or could reflect heterogeneity in particle surfaces.

The structure of the acrylic film can be compared with the structure obtained when the alkyd resin was introduced into the polymer matrix using KPS as an initiator (Run 23). The nanostructure of the hybrid film, as shown in Figure 15, differs markedly. Particle identity is not distinct, which indicates that particle coalescence has occurred. An explanation is obtained from thermal analysis. Two glass transition temperatures (T_gs) were found in DSC analysis of the hybrid: an upper one at 19°C and a lower one at -20°C. The existence of two transitions indicates the existence of two phases.

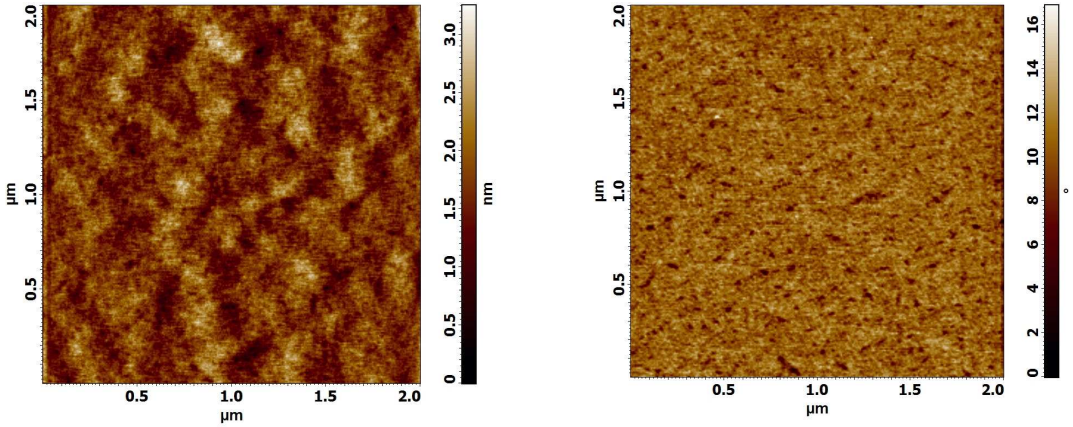

a **b**

Figure 15**.** AFM images of the surface of a film cast from the hybrid latex with KPS as the initiator (Run 23): (a) height image and (b) phase-contrast image. Scan area is 2 µm x 2 µm

The upper transition is ascribed to the acrylic after plasticization, to reduce its T_g by 3 degrees. The plasticized acrylic particles will deform at a greater rate than the neat acrylic. The lower transition is ascribed to an alkyd-rich phase; analysis of the neat alkyd found a T_g of -43°C. Upon close examination of Figure 15, some contrast can be seen in both the height and phase images, in regions that are only tens of nm in size. This size scale is smaller than the particle size. Hence, a likely explanation is that there is heterogeneity within the particles. The alkyd is a viscous liquid that is expected to lead to greater energy dissipation during AFM imaging in comparison to the acrylic copolymer. The dark spots in the phase image are therefore attributed to alkyd-rich regions within the particles. AFM can be sensitive to subsurface structures, so the alkyd phase could be encapsulated within the particles but still be apparent in the images. In the topographic images, the alkyd regions could appear darker because of greater indentation of the AFM tip in the softer phase[28].

The choice of initiator was found to have a pronounced effect on the film structure. When AIBN was used instead of KPS (Run 22), the film morphology is much different than what was found when KPS was used (Run 23). Figure 16 (a) and (b) shows that in the AFM images of Run 22 two phases can be clearly seen.

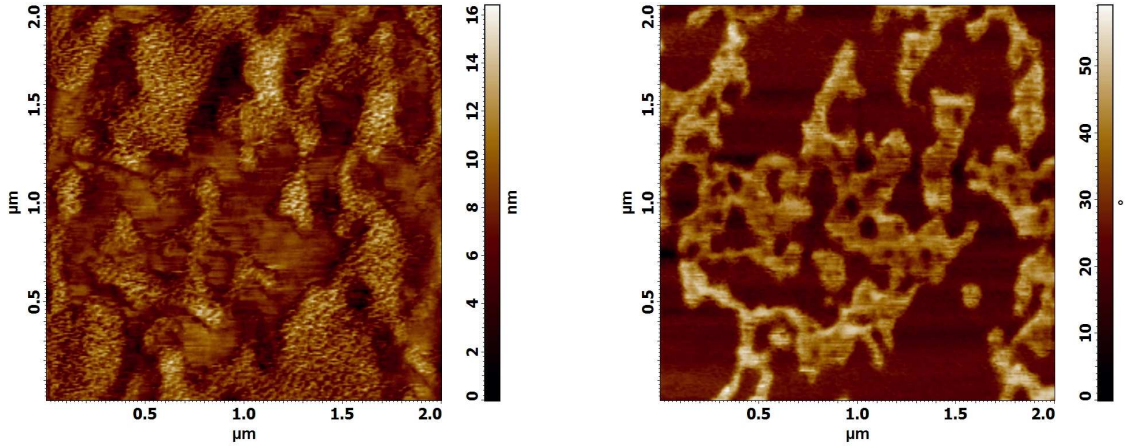

Figure 16. AFM images of the surface of a films cast from a hybrid latex with AIBN as the initiator (Run 22): (a) height image and (b) phase-contrast image. Scan area is 2 µm x 2 µm

The dark regions in the phase image are attributed to an alkyd-rich composition. The regions are up to 1 µm across in some areas, which is much greater than the particle size. Hence, it appears that phase separation between the alkyd and acrylic phases has occurred. Thermal analysis is in agreement, as it reveals two glass transitions.

The question now arises as to why there is such a pronounced effect of the initiator on the final film morphology. There are three possible explanations. First, it is noted that when KPS is the initiator (Run 23), the conversion is low (91%) irrespective of enhanced re-nucleation in comparison to the 100% conversion achieved with AIBN (Run 22) under the similar re-nucleation as in Run 23. The free monomer could be acting as a compatibilizer between the immiscible copolymer and alkyd phases. Secondly, a greater amount of grafting between the alkyd and acrylate might be achieved when KPS is the initiator, preventing phase separation over larger length scales. Finally, the particle structure could be different between the two materials. If the alkyd is not encapsulated within the particles, it will not be restricted from phase separation. We suspect that the first two factors both contribute to the observed differences.

The structure of a film made from a latex initiated with KPS and containing 22 wt% alkyd (Run 18) is presented in Figure 17.

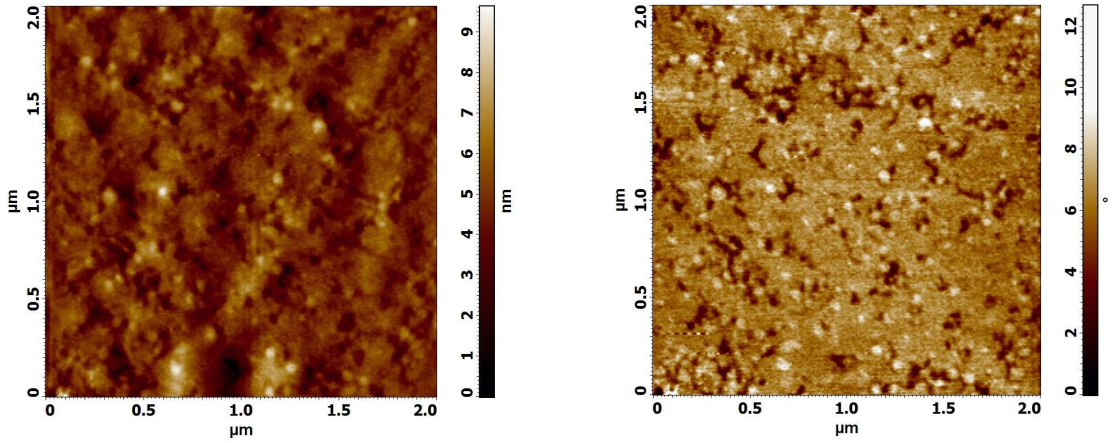

a **b**

Figure 17. AFM images of the surface of a film cast from a hybrid latex with KPS as the initiator and containing 22 wt.% alkyd (Run 18): (a) height and (b) phase. Scan area is 2 µm x 2 µm.

The film structure can be considered to be intermediate between what was found for the plain acrylate (Figure 14) and the hybrid with 50 wt% alkyd (Figure 15). There are brighter regions with a diameter on the order of 100 nm, which are likely to be acrylate-rich particles. There is some particle identity retained in the film, because there is less plasticization with 22 wt% alkyd in comparison to what was found for 50wt% alkyd hybrids. With KPS as the initiator, the amount of phase separation at the film surface is less than what is found when AIBN was used (Figure 17).

3.4 Conclusions

Stable miniemulsions and complete monomer conversion could be achieved while maintaining the ratio of initial number of droplets to final number of particles between 0.8 and 1 when the alkyd quantity was 5% or less. However with the gradual increase of alkyd quantity, the final monomer conversion gradually decreased. We have attempted to increase monomer conversion by different means. However this could not be brought higher than 96% (for a hybrid system of 25% alkyd and 50% solids), and even then it is necessary to purify the alkyd and allow small amounts of re-nucleation to occur. Similar behaviour for unsaturated alkyds suggests that it is not the degree of grafting, but rather interactions between copolymer and alkyd that changes with the ratio of monomer to alkyd which influences the final monomer conversion. It was shown that, as expected, the polymer architecture changes with the initiator system. The variation of monomer conversion for the similar systems but with different initiator systems (AIBN and KPS) suggests that the polymer architecture affects the limiting monomer conversion. This is a strong evidence for our argument that the limiting monomer conversion could be due to the interactions between polymer and alkyd.

We also studied the evolution of N_p/N_d with monomer conversion for different experimental conditions and correlated this evolution with the droplet stability and the individual monomer conversion in order to get a better understanding of the effect of the alkyd content on the miniemulsion polymerisation reaction. It was shown that the observed increase of N_p/N_d after about 40% monomer conversion in the presence of high alkyd quantity (15-25%) is independent of the initiator system but dependent on the hydrophobicity, and that the ratio N_p/N_d could be lowered to 1.2 controlling the hydrophobicity of the organic phase. The interactions between alkyd and monomer were shown to be stronger than that of monomer with hexadecane and monomer with ODA. As a result, the use of alkyd alone as the hydrophobe seems to give better results in terms of stability during the polymerisations than equivalent (or even higher) amounts of ODA and HD.

The most homogeneous film morphology was resulted from the sample of 44% solids with 50 wt% of alkyd and KPS as the initiator. When AIBN was used in the recipe instead of KPS, the

film shows a clear phase separation for a similar monomer+surfactant formulation. However complete monomer conversion could not be achieved with KPS even under enhanced renucleation whereas full monomer conversion could be achieved with AIBN under the similar conditions. When the alkyd quantity was 27.5% a higher monomer (96-97%) conversion could be achieved with KPS for a hybrid system of 50% solids with good film properties. Therefore the best compromises have to be determined before the application of this system.

Acknowledgment

Dr. F. Boisson at Service de RMN de la FRPL, FR2151/CNRS, BP24, 69390, Vernaison carried out NMR analysis of Alkyd resin and Alkyd grafted co-polymer. **Ms. Genny Faucheu** at Mateis, Insa de Lyon did Wet Stem analysis of my samples. **Dr. Carolina de las Heras Alarcón**, Research Fellow in Physics at the Department of Physics, Soft Condensed Matter physics, Faculty of Electronics and Physical Sciences, University of Surrey, Guildford, Surrey GU27XH, carried out the latex film experiments by AFM. I thank **Dr. F. Boisson, Ms. Genny** and **Dr. Carolina** for doing NMR analysis, Wet Stem analysis and AFM analysis of my samples. I also thank **Mrs. V. Doukova** and **Mr. A. Utgenannt** (University of Surrey) for assistance with the DSC analysis.

3.5 References

1. Hamersveld, E. M. S. V.; Es, J. J. G. S. V.; Cuperus, F. P., Oil-acrylate hybrid emulsions, mini-emulsion polymerisation and characterisation. *Colloids and Surfaces A: Physiochemical and Engineering Aspects* **1999,** 153, 285-296.

2. Shoaf, G. L.; Stockl, R. R., Alkyd/Acrylic Hybrid Latexes with Enhanced Oxidative Curing. *Polymer Reaction Engineering* **2003,** 11, 319-334.

3. Schork, F. J.; Tsavalas, J. G., The morphology of alkyd/acrylate latexes produced via hybrid miniemulsion polymerisation: grafting mechanisms. *Progr Colloid Polym Sci* **2004,** 124, 126-130.

4. Tsavalas, J. G.; Luo, Y.; Schork, F. J., Grafting Mechanisms in Hybrid Miniemulsion Polymerisation. *Journal of Applied Polymer Science* **2003,** 87, 1825-1836.

5. Wu, X. Q.; Schork, F. J.; Gooch, J. W., Hybrid miniemulsion polymerisation of acrylic/alkyd systems and characterization of the resulting polymers. *Journal of Polymer Science: Part A: Polymer Chemistry* **1999,** 37, 4159.

6. Tsavalas, J. G.; Luo, Y.; Hudda, L.; Schork, F. J., Limiting Conversion Phenomenon in Hybrid Miniemulsion Polymerisation. *Polymer Reaction Engineering* **2003, ,** 11 277-304.

7. Hudda, L.; Tsavalas, J. G.; Schork, F. J., Simulation studies on the origin of the limiting conversion phenomenon in hybrid miniemulsion polymerisation. *Polymer* **2005,** 46, 993-1001.

8. Tsavalas, J. G.; Schork, F. J.; Landfester, K., Particle Morphology Development in Hybrid Miniemulsion Polymerisation. *JCT Research* **2004,** 1, 53-63.

9. Deriss, M. J.; Karlsson, O. J., Suspension structures and film morphologies of high-solids acrylic-alkyd hybrid binders. *Surface Coatings International Part B: Coatings Transactions* **2005,** 88, 231-316.

10. Colombini, D.; Derris, M. J.; Karlsson, O. J.; Maurer, F. H. J., Direct and Reverse Mechanical Modelling of an Alkyd Acrylic Hybrid System: A Morphological Study. *Macromolecules* **2004,** 37, 2596-2602.

11. Derris, M. J.; Karlsson, O. J., High solids waterborne hybrid systems. Effect of surfactant concentration and pH on droplet size and morphology. *Progr Colloid Polym Sci* **2004** 124, 149-153.

12. Tsavalas, J. G.; Luo, Y.; Hudda, L.; Schork, F. J., Limiting Conversion Phenomenon in Hybrid Miniemulsion Polymerisation. *Polymer Reaction Engineering* **2003,** 11, 277-304.

13. Sood, A.; Awasthi, S. K., Initial Droplet Size Distribution in Miniemulsion Polymerisation. *Journal of Applied Polymer Science* **2003,** 88, 3058–3065

14. Bechthold, N.; Landfester, K., Kinetics of miniemulsion Polymerisation as revealed by calorimetry. *Macromolecules* **2000,** 33, 4682-4689.

15. Li, D.; Sudol, E. D.; El-Aasser, M. S., Miniemulsion and Conventional Emulsion Copolymerisation of Styrene and Butadiene: A comparative Kinetic Study. *Journal of Applied Polymer Science* **2006,** 101, 2304-2312.

16. Asua, J. M., Miniemulsion polymerization. *Prog. Polym. Sci.* **2002,** 27, 1283-1346.

17. Schork, F. J.; Luo, Y.; Smulders, W.; Russum, J. P.; Butte, A.; Fontenot, K., Miniemulsion Polymerisation. *Adv Polym Sci* **2005,** 175, 129-255.

18. Minari, R. J.; Goikoetxea, M.; Beristain, I.; Paulis, M.; Barandiaran, M. J.; Asua, J. M., Molecular Characterization of Alkyd/Acrylic Latexes Prepared by Miniemulsion Polymerization. *Journal of Applied Polymer Science* **2009,** 114, 3143-3151.

19. McKenna, T. F.; Villanueva, A., Effect of Solvent on the Rate constants in Solution Polymerisation. Part II: Vinyl Acetate. *J. Polym. Sci., Part A: Polym. Chem.* **1999,** 37, (5), 589-601.

20. McKenna, T. F.; Villanueva, A.; Santos, A. M., Effect of Solvent on the Rate constants in Solution Polymerisation. Part I: Butyl Acrylate. *J. Polym. Sci., Part A: Polym. Chem* **1999,** 37, (5), 571-588.

21. Nikitin, A. N.; Hutchinson, R. A., Stationary Free Radical Polymerization in the Presence of Intramolecular Transfer to Polymer. *Macromolecules* **2005,** 38, 1581-1590.

22. Davis, S. S.; Smith, A., The influence of the disperse phase on the stability of oil-in-water emulsions. *Theory Pract. Emulsion Technol., Proc. Symp.* **1976,** 1974, (325), 325.

23. Guo, J.; Schork, F. J., Hybrid Miniemulsion Polymerization of Acrylate/ Oil and Acrylate/ Fatty Acid Systems *Macromol. React. Eng* **2008,** 2, 265-276.

24. Routh, A. F.; Russel, W. B., *Ind. Eng. Chem. Res.* **2001,** 40, 4302-4308.

25. Scott, W. W.; Bhushan, B., *Ultramicroscopy* **2003,** 97, 151.

26. Anczykowski, B.; Gotsmann, B.; Fuchs, H.; Cleveland, J. P.; Elings, V. B., *Appl. Surf. Sci* **1999,** 140, 376.

27. Lei, C.; Ouzineb, K.; Dupont, O.; Keddie, J. L., *Coll.Interf.Sci* **2007,** 307, 56-63.

4. POLYURETHANE-ACRYLIC HYBRID MINIEMULSION POLYMERISATION

4.1 Introduction

Polyurethane (PU) dispersions are widely used in different applications such as coatings and adhesives due to their superior properties like gloss, chemical resistance, toughness, flexibility and film formation[1-3]. As discussed before the synthesis of traditional solvent-borne PU dispersions has come into disfavour due to the presence of volatile organic species[1-3]. The similar incompatibility problems inherent to physical blends of alkyd-acrylic system could be observed for the direct blending of a polyurethane dispersion and an aqueous acrylic emulsion because of limited compatibility between PU and polyacrylate[1, 4, 5]. The compatibility between PU and polyacrylate can be increased if a reactive functional group is present in PU. When a PU carries an iso cyanate (NCO) function which can chemically react with other chemically active materials such as hydroxyethyl methacrylate (HEMA), it is referred to as a reactive PU. Different strategies of dispersing reactive PU in the water phase other than the direct blending are described in the literature. For instance aqueous PU dispersions are commonly prepared by the incorporation of ionic groups into the polymer structure to enhance the hydrophilicity of the polymer chains and promote dispersion[6-11]. Those PUs that contain ionic groups are called PU ionomers[6]. As the traditional way of preparing aqueous PU dispersions always needs hydrophilic segments in the PU backbone, the properties of these PU polymers are generally not as good as those of the hydrophobic ones prepared by solvent-based polymerisation[6]. In overcoming this limitation is one of the keys to producing high quality aqueous dispersions containing PU.

We discussed the fact that miniemulsion polymerisation is an ideal method to synthesise water-borne, environmentally friendly hybrid polymers which synergistically combine the positive properties of high molecular weight, hydrophobic PU with the fast drying and colour retention of acrylic latexes. In this new type of dispersion, if the PU has a reactive functional group, a chemical coupling between the urethane and the acrylic components is established and these dispersions are known as acrylic-PU hybrids[12-15].

The mechanical properties of acrylic-PU hybrids have been discussed. However most of the previous studies have been focused on film properties[13], a comparison of mechanical properties of physical blends and hybrids[4], and the structure and properties of acrylic-PU hybrids[16].

Although adhesive properties have also been studied[16], a detailed study on adhesive properties based on tack properties of hybrid latex is rarely found. The main objective of this study was to develop an efficient acrylic – PU hybrid system to be used in adhesive applications. This requires the efficient incorporation of PU segments in acrylic latex. To this end, two different types of PU were used: a high molecular weight, non-reactive PU; and a low molecular weight reactive PU. Because the objective of use of reactive PU was the efficient chemical incorporation of it into the organic phase, the NCO functions were studied quantitatively and qualitatively. The quantitative analysis of NCO functions was done by conductimetry. We studied the hybrid system by changing different parameters such as the ratio of NCO to hydrophobic chain extender (bisphenol A), the amount of chain transfer agent and amount of PU in order to achieve better adhesive properties. In addition, in order to make commercially useful samples, all of the experiments were run with high solid content (40-50%) and average particle sizes on the order of 100 nm. In the most desirable scenario, all the monomer droplets should contain PU. Thus an ideal miniemulsion polymerisation will lead to a one to one copy of droplets to particles.

4.2 Experimental

Materials

Butyl acrylate (BA 99+%; from Acros; Illkirch Cedex, France), acrylic acid (AA 99+%; from Acros; Illkirch Cedex, France) and methyl methacrylate (MMA 99+%; from Acros; Illkirch Cedex, France) were used as received. Dowfax-2A1 (45%; graciously supplied by Dow Chemicals; La Plaine St Denis Cedex, France) was used as the anionic surfactant. A non-reactive PU of molecular weight of 10,837 $g.mol^{-1}$ and a reactive PU (Incorez 701) of molecular weight of 3285$g.mol^{-1}$ were graciously supplied by Euroresin and Industrial Copolymers Limited respectively, and used as received. Bisphenol A (BPA analytical grade; from Sigma Aldrich; Lyon, France), dibutyltin dilaurate (95%; from Sigma Aldrich; Lyon, France) and hydroxyethyl methacrylate (HEMA 97%; from Sigma Aldrich; Lyon, France) were used in the reactions which involved reactive PU. Di-ethyl amine (98+%; from Avocado; La Tour Du Pin, France), isopropanol (99+%; from Carlo Erba; Val de Reuil Cedex, France) and 0.1N standard HCl solution (from Acros; Illkirch Cedex, France) were used as received in the reactions of characterisation of reactive PU. 1-Dodecylmercaptan (98.5%; from Acros; Illkirch Cedex,

France) was used as a chain transfer agent (CTA). Octadecyl acrylate (ODA 97%; from Sigma Aldrich; Lyon, France) was used as the hydrophobe. Potassium persulphate (KPS Analytical grade; from Acros; Illkirch Cedex, France) was used as the water soluble initiator. Tertiary butyl hydroperoxide (TBHP diluted at 70% in water; from Acros; Illkirch Cedex, France) and sodium formaldehyde sulfoxylate (SFS Analytical grade; from Sigma Aldrich; Lyon, France) were used as the redox initiator pair. Tetrahydrofuran (THF Analytical grade; from Fischer Scientific; Illkirch Cedex, France) was used as a solvent for the selective extraction experiments. Deionised water was used throughout the work.

Emulsion Preparation and Polymerisation

The experiments with the non-reactive PU were based on the recipe shown in Table 1 and the experiments with the reactive PU were based on the recipe shown in Table 2 unless otherwise specified.

Table 1. Miniemulsion polymerisation recipe used in the synthesis of acrylic/non-reactive PU hybrid latexes

Raw Material	Weight (g)	Active (weight %) by monomers	Total Solid (%)
Water	55		
Dowfax (45%)	1.7	1.8	
BA	35.8	89.5	
MMA	3.8	9.5	42
AA	0.4	1.0	
ODA	2.06	5.15	
KPS	0.16	0.4	
PU	Variable		

The procedure for the non-reactive PU and the reactive PU was as follows. The non-reactive PU was dissolved in butyl acrylate and this mixture was then dissolved in the rest of the organic phase to attain the desired composition. When using PU levels of 20% (w/w) or above it was necessary to heat the organic phase to 60°C and stir for 30 minutes. The incorporation of reactive PU in to the organic phase will be discussed in the section 4.4.2.3(The reaction between NCO and HEMA and the role of chain extender). In both cases, the surfactant was separately dissolved in the aqueous phase. The organic phase was added slowly to the aqueous phase while stirring. The mixture was further stirred for 30 minutes for the non-reactive PU and 5 minutes for the

reactive PU (in order to minimise the reaction of NCO with water) and sonicated in an ice bath for 6 minutes(2*3times) at 480W power.

Table 2. Miniemulsion polymerisation recipe used in the synthesis of acrylic/reactive PU hybrid latexes

Raw Material	Weight(g)	Active (weight %) by monomers	Total Solid (%)
Water	120		
Dowfax (45%)	4.00	2.00	
BA	80.50	89.50	
MMA	8.50	9.50	
AA	1.00	1.00	
ODA	4.50	5.15	49.80
PU (Incorez 701)	23.60	25.00	
HEMA	Variable	(0-1.6)	
Bisphenol A[a]	Variable		
Dibutyltin dilaurate[b]	0.01		
1-Dodecylmercaptan	Variable	(0-0.4)	
TBHP	0.10		
SFS	0.26		

a: based on free NCO functions remained after the reaction with HEMA(50% of stoichiometric quantity of bisphenol A was used in the reactions from T107 to T 153 and the stoichiometric amount was used in the reactions from T 159 to T 164)

b: 0.005g was used with HEMA and 0.005g was used with bisphenol A.

High Intensity Ultrasonic Processor (Branson, model CV 26) was operated at 600W and 80% power for sonication of miniemulsions. The droplet size was measured soon after sonication and then several hours afterward to ensure that the droplets are stable for a duration of 4-5h (thus if any change in droplet size is observed it will not be attributed to an intrinsic lack of stability of the original dispersion). All reactions were carried out in a 200 mL jacketed glass reactor connected to a heated water bath for temperature control. The reactor was equipped with a stirrer, a reflux condenser, nitrogen inlet and outlet and a valve on the bottom to remove the latex. Samples were occasionally withdrawn through a valve in the bottom of the reactor for analysis. Conversions were measured by gravimetry. Average droplet and particle sizes (Dp) were measured by photon correlation spectroscopy at 90° (Zetasizer 1000 HS_A). Average sizes reported here are the averages of at least 5 measurements per sample. Gel content was determined by selective extraction of a known amount of a vacuum dried latex sample for 24h in

a soxhlet extractor using THF as the solvent. Thermal analysis was done by differential scanning calorimetry at a heating rate of 5°C/Minute (Setaram DSC 131). Three cycles were performed for each sample and the average of last two cycles was recorded as the T_g. CDM 83 conductivity meter was used for conductivity measurements. Molecular weight was measured by Gel Permeation Chromatography Pump (Waters 515), Automatic sample injection (Waters 717 Plus), UV detector (Waters 410), Differential Refractometric Detector (Waters 410) and Light Diffusion Detector (Mini dawn Wyatt) using THF as the eluent. The first column (PLgel 5µm) were followed by three columns 2 x PLgel 5µm Mixed C (300x7.5mm) and 1 PLgel 5µm 500 A (300x7.5mm). A polystyrene standard was used for calculations. Infra red analysis was done by Nicolet Protégé 460 spectrometer. Transmission Electronic Microscopy (TEM - Philips – CM 120) was operated at 80KV to obtain the TEM images of latex. Two series of latex samples were prepared for TEM. A few drops of Phosphotungstic acid was added to one series. Both series were treated under UV light for 1h.

4.3 Characterisation of reactive PU (Incorez 701)

Pure PU was qualitatively characterised by differential scanning calorimetry (DSC) and Infra Red (IR) spectroscopy. A sample for DSC analysis was prepared by dissolving pure PU in the monomer mixture of BA and MMA (90:10 wt %), reacting with excess bisphenol A and finally evaporating the monomers. The measured Tg was -47°C. The standard procedure was followed for IR analysis.

The quantitative characterisation of NCO functions of PU was done by a conductimetric titration method as described by Li et al[1]. Figure 1 represents a typical conductimteric titration curve. A known volume of PU was dissolved in a known volume of monomer mixture (BA/MMA 90/10 wt %). A known amount of di-ethyl amine was added to the solution of PU and dibutyltin dilaurate was added as a catalyst for the reaction between amine and NCO. The reaction was allowed to take place for various periods of time ranging between a few hours and several days. A known volume of each solution was titrated against a known concentrated HCl acid dissolved in isopropanol. The amount of excess or free di-ethyl amine in the solution is determined by the conductimetric titration and the amount of di-ethyl amine that reacted with NCO functions can thus be calculated. Accordingly, the amount of NCO functions per gram of PU was calculated.

According to the conductimetric titration, the number of moles of NCO functions per gram of PU is $61*10^{-5}$. Therefore the molar mass of PU is calculated to be $3285 gmol^{-1}$.

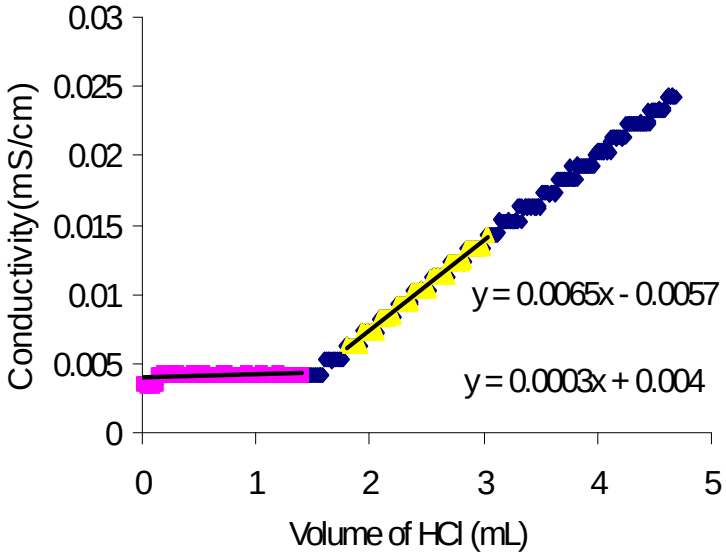

Figure 1. Conductimetric titration curve of amine against HCl

4.4 Results and Discussion

4.4.1 Non-reactive PU

The main characteristics of the latexes obtained in the first series of experiments with non-reactive PU are summarised in Table 3. As can be seen, in the absence of PU the droplet size is comparatively low (103.7 nm). With the incorporation of PU, the droplet size increased to 219.8 nm. This might be due to the increased viscosity of the organic phase in the presence of PU, and has been observed for other systems such as silica[17]. Mabille et al[18] found that droplet size varies as the viscosity to the power of 0.2 under their experimental conditions.

Table 3 Main characteristics of the hybrid miniemulsions and hybrid latexes elaborated in the presence of various amounts of non-reactive PU.

Sample	PU (%)	Droplet Size(nm)	Final Particle Size(nm)	Conversion %	Solid Content (%)	Glass transition temperature(°C)
T-28	0	103.7	131.4	100	42	-36
T-53	20	219.8	169.6	100	46	~ -36 / ~ 75.1

These latexes exhibited poor film properties due to the clear phase separation which could be observed during film formation. (The film properties are not shown here). Therefore the incorporation of reactive PU through HEMA was studied further.

4.4.2 Reactive PU

4.4.2.1 Qualitative characterisation of reactive PU

Figure 2 and Figure 3 show the qualitative analysis of the reactive PU by DSC and FTIR respectively. By knowing the T_g of pure PU, the chemical incorporation of PU and the presence of different micro phases in the hybrid latex can be verified. The presence of different functional groups of pure PU could be verified by FTIR analysis. According to FTIR analysis, the presence of poly propylene glycol (PPG), amide and urethane linkage could be verified in addition to the main functional group of NCO.

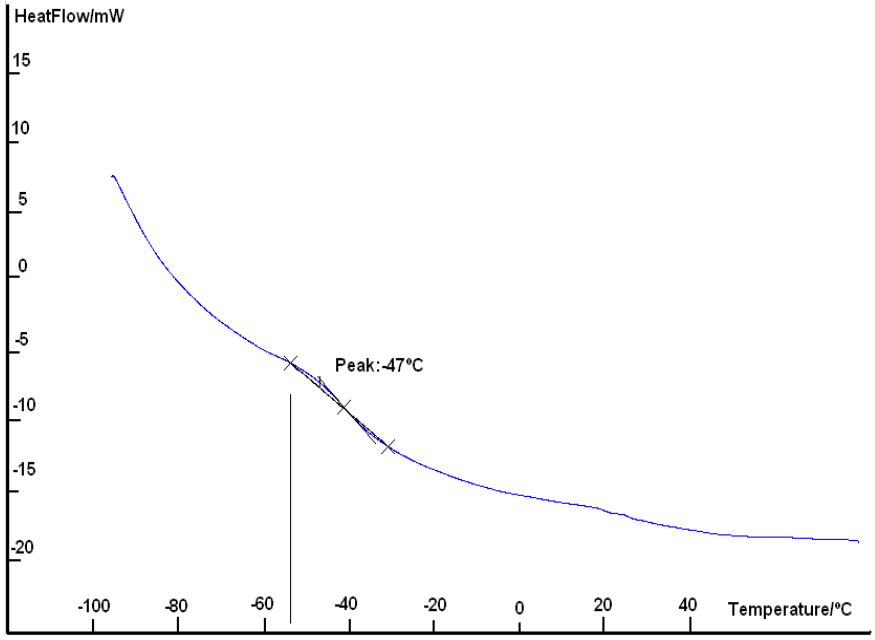

Figure 2. Thermal analysis graph of pure PU

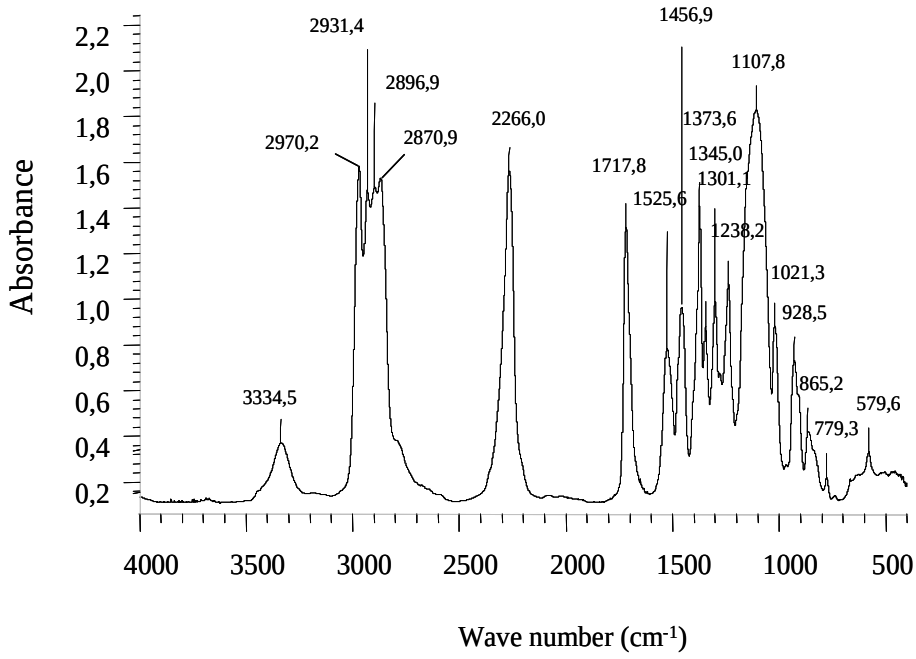

Figure 3. FTIR analysis of PU

4.4.2.2 Quantitative characterisation of reactive PU

Figure 4 illustrates the time dependence of the reaction between NCO functions and di-ethyl amine under our experimental conditions. When comparing the values of NCO functions per gram of PU, it was found that the value relevant to shorter reaction time is less by about $20*10^{-5}$ moles than the value relevant to overnight (12h) reaction time. After analysing more conductimetric titration results of the solution which was allowed to react several days, it was found that the value obtained for NCO functions per gram of PU is constant and as same as the value obtained for overnight reaction. The amount of NCO functions per gram of PU was therefore established as $61*10^{-5}$ moles. Figure 5 illustrates the molar mass analysis of PU by GPC. According to the GPC analysis, the molar mass (Mn) of PU is 4338 while the mass relevant to main peak is 3720 with a polydispersity index of 1.42. As the molar mass calculated by conductimetric titration was purely based only on NCO functions, this value (3285g) was used for further calculations which involved the NCO functions.

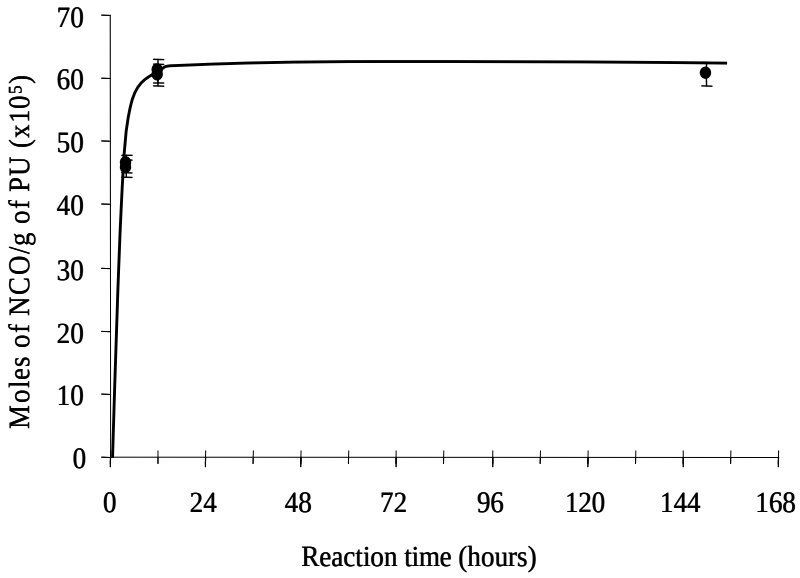

Figure 4. Time dependence of reaction between NCO functions and di-ethyl amine

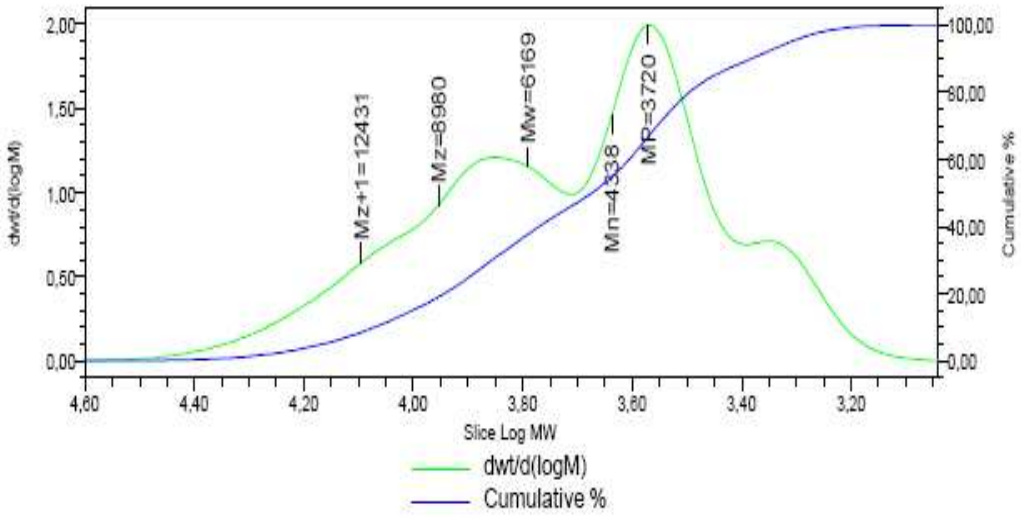

Figure 5. Molar mass analysis of PU by GPC

4.4.2.3 The reaction between NCO and HEMA and the role of chain extender

Figure 6 shows the reaction route between HEMA and urethane prepolymer.

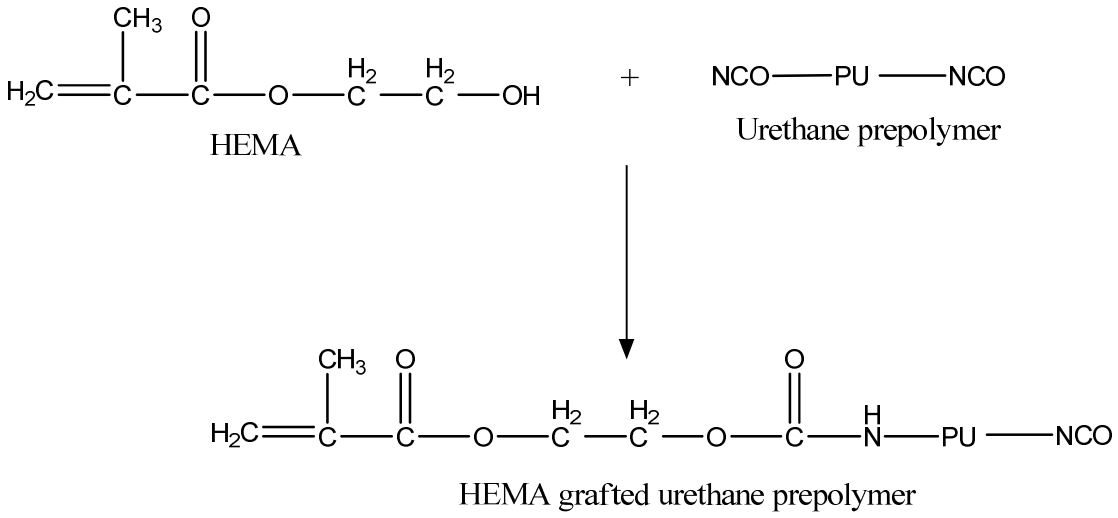

Figure 6. The reaction between HEMA and urethane prepolymer

HEMA is covalently bonded to PU, and therefore plays a very important role in the chemical incorporation of reactive PU into the hybrid system. Since the efficiency of hybridisation strongly depends on this reaction, it was thoroughly studied by conductimetry. The same conductimetric titration method described above was used to determine the yield of the reaction between HEMA and NCO. The reactions between different molar ratios of HEMA and NCO were studied during a fixed reaction period of twelve hours. The yield of reaction of a constant amount of NCO ($61*10^{-5}$ Moles) with increasing HEMA quantity was calculated based on the conductimetric titration data. Figure 7 illustrates the decrease of yield of reaction with increasing HEMA quantity and the relevant degree of grafting of NCO by HEMA. When the molar ratio of HEMA to NCO is 20%, the yield of the reaction is 100%. The weight fraction of HEMA with respect to PU is 1.6% when the yield of the reaction is 100%. Therefore the maximum amount of HEMA that we can add to the hybrid system which gives 100% yield is 1.6% with respect total PU quantity. The corresponding degree of grafting of NCO by HEMA for the maximum amount of HEMA(1.6wt%) and 100% yield is 20% (Since we know the total number of moles of NCO in a given quantity of PU, the degree of grafting can be calculated by knowing the number of moles of HEMA added). Accordingly the degree of grafting of NCO by HEMA can be varied from 0 to 20% and the remaining NCO functions should be neutralised with a chain extender to minimise the reaction between water and hence maintain the stability of hybrid latex.

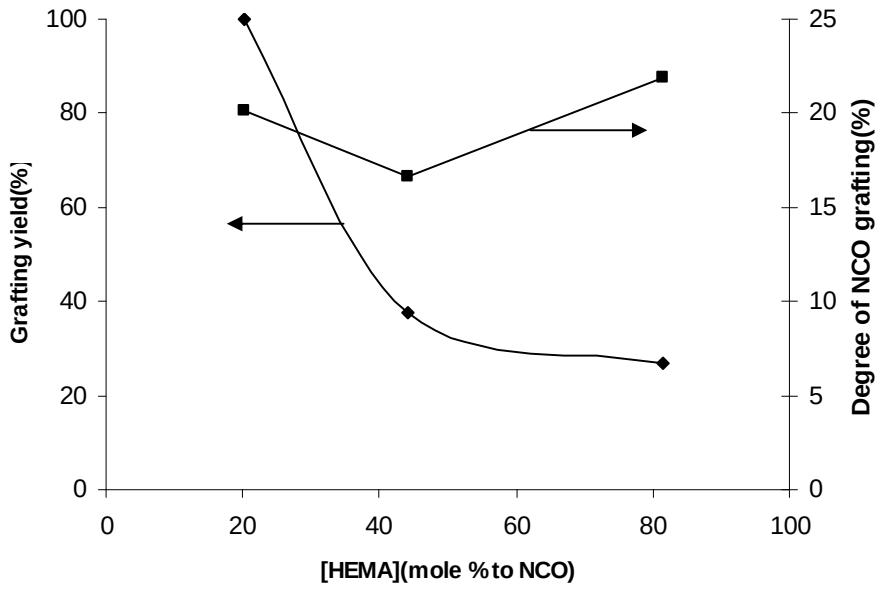

Figure 7. Dependence of grafting yield on increasing HEMA quantity

In fact the chain extender plays a dual role. While the reaction between water and NCO functions are minimised by the chain extender, the molecular weight of PU is also increased due to chain extension. As a result the hydrophobicity of PU is increased. Different types of chain extenders such as hydrophilic and hydrophobic have been described in the literature[1] for the purpose of chain extension of the urethane prepolymer by reacting with free NCO groups. It has been shown that the chain extension reaction primarily occurs at the interface between the latex particles and aqueous phase when the hydrophilic chain extenders are used[1]. As a result the urethane moiety would tend to be pulled towards the interface and this would increase the likelihood that the hybrid latex particles aggregate by bridging flocculation, resulting in extensive flocculation. On the other hand the chain extension reaction takes place inside the latex particles when a hydrophobic chain extender is used. Therefore bisphenol A was used as a hydrophobic chain extender in this study. Figure 8 shows the reaction route between HEMA grafted urethane prepolymer and bisphenol A.

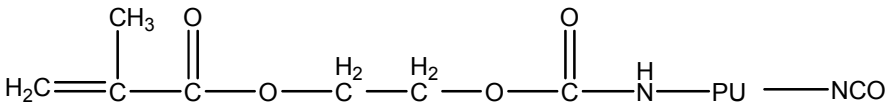

HEMA grafted urethane prepolymer

+

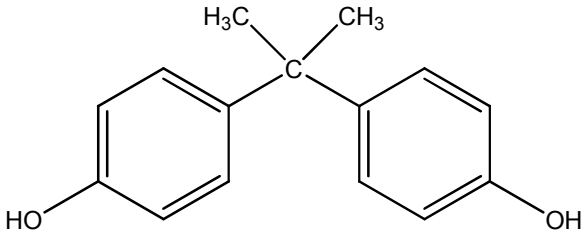

Bisphenol A

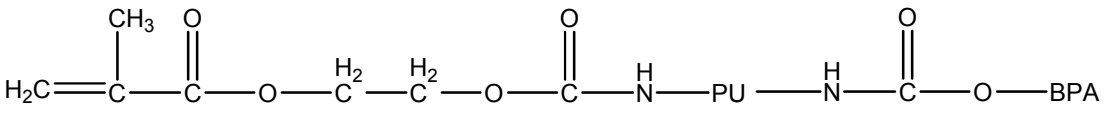

Chain extended HEMA grafted urethane prepolymer

Figure 8. The reaction between HEMA grafted urethane pre polymer and bisphenol A

It has been shown that the reaction between NCO and bisphenol A is time dependent even though it is catalysed by dibutyltin dilaurate[1]. According to Li et al[1], in the absence of the catalyst only 84% yield is resulted during a time period of 74 hours while in the presence of a reasonable amount of catalyst (0.125mM), the reaction takes about 24hours to reach completion. Therefore, the addition of a calculated amount of bisphenol A does not necessarily mean that all free NCO functions are protected from the reaction with water. This was evident by a decrease of the initial droplet size by about 20nm of the mini emulsion of our acrylic-PU system with bisphenol A during a time period of 20 minutes (cf. Table 4). This means during all our experiments, a decrease of droplet size by about 20 nm could be observed during the time period between the sonication and the initiation of polymerisation. Table 4 shows the droplet size measured just after sonication and just before polymerisation. In each experiment the droplet size

measured just before initiation was considered for the calculation of N_d. The decrease of droplet size is due to the loss of NCO functions. Li et al[1] has also shown that about 20% of NCO functions are lost during a time period of 2h. Even though bisphenol A is a hydrophobic chain extender, the use of stoichiometric amount of it considering the amount of free NCO functions, again flocculation occurred in our system. The flocculation could be promoted by the already increased hydrophobicity of droplets by the hydrophobe (ODA) and close proximity between the interior of droplets and the interface of a system of 50% solid and 130nm particle diameter. However under controlled hydrophobic conditions [i.e. in the absence of an additional hydrophobe (ODA)], the stoichiometric amount of bisphenol A could be used and flocculation did not occur. We will discuss this point in detail in the section 4.4.2.5 (modifications and process improvement).

Table 4.The variation of droplet size during the time period between sonication and initiation of polymerisation

Sample	T-143	T-144	T-145	T-146
Droplet size (nm)(just after sonication)	136	138	140	139
Droplet size (nm)(just before initiation)	119.1	120	122.8	126.1

4.4.2.4 Miniemulsion polymerisation and characterisation

During a first series of experiments, 25wt% (respect to monomers) of PU was incorporated into the organic phase. A redox initiator system (TBHP/SFS) was used in the experiments with reactive PU to avoid the side reactions of free NCO groups with water. When KPS was used in the presence of reactive PU, the system was not stable. This could be mainly due to side reactions which can be important in this case as we introduced the totality of PU in the reactor since the beginning of polymerisation (batch process). In a related work, Li et al. [1] have also demonstrated that redox initiators could help minimising side reactions in hybrid system based on reactive PU. Table 5 shows the solid content and gel content of two control samples synthesised by two initiator systems (T-107-redox and T-28-KPS). Figure 9 shows the tack experimental results of the two control samples. The strain of the control sample (T107) is lower than that of the control sample (T28), and this can likely be attributed to high gel content. This in turn might suggest that the redox initiator system could be mainly responsible for the high gel

content. (The reactive oxygen radical in tertiary butyl hydro peroxide may attack the H atom of BA. This results a branched polymer structure which gives a high gel quantity).

Table 5. Solid content and gel content of the control samples synthesised by two initiator systems (T 107-redox and T 28- KPS)

Samples	T-107	T-28
PU	0	0
Solid Content (%)	42	42
Monomer Conversion (%)	100	100
Gel Content (%)	84	72

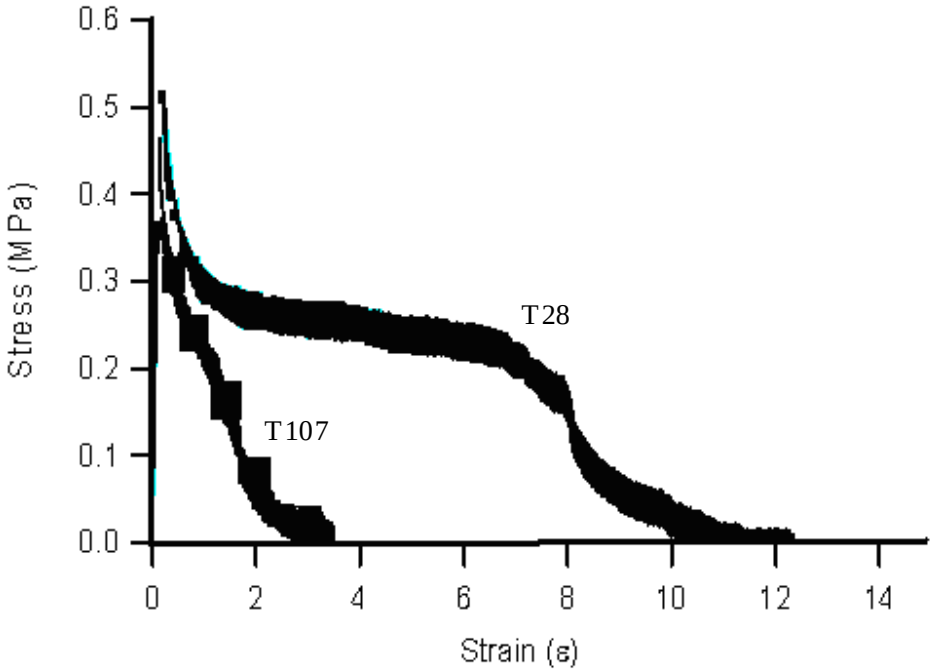

Figure 9. Variation of Stress with increasing strain of latexes in the absence of PU

In order to lower the gel content while using a redox system, a chain transfer agent (CTA) was used in further experiments. The amount of CTA was varied from 0 to 0.3 wt% with respect to monomers. The characteristics of the resulting latexes are summarised in Table 6. Figure 10 (a) and (b) show the evolutions of monomer conversion and N_p/N_d with time of these latexes respectively. As shown by Figure 10 (a) and (b), complete monomer conversion could be achieved while maintaining a good control of N_p/N_d for these latexes. The increase of number of polymer particles and hence a higher N_p/N_d at the beginning of polymerisation [cf. Figure 10 (b)] could be due to homogeneous nucleation and the destruction of some NCO functions due to the

reaction with water. Both these processes lead to smaller particle size and hence an increase of particle number.

Table 6. Main characteristics of the hybrid miniemulsions and hybrid latexes elaborated in the presence of different amount of CTA

Sample	T-144	T-143	T-145	T-146
PU (Incorez-701, %)	25	25	25	25
CTA (%)	0	0.1	0.2	0.3
NCO grafting by HEMA (%)	10-11	10-11	10-11	10-11
Droplet size (nm)	120	119.1	122.8	126.1
Final particle size (nm)	119.9	118	121.4	115.8
N_p/N_d of final latex	8.8E-1	9.0E-1	9.1E-1	1.1E+1
Conversion (%)	100	99.9	100	99.4
Solid content (%)	49.8	49.8	49.8	49.8
Gel content (%)	84	65	44.5	23.6
Molecular weight(Mw) of sol fraction	N/D	508295	3917350	1362970
Molecular weight(Mn) of sol fraction	N/D	36310	63400	17660
Mw/Mn	N/D	14	62	77

The recipe is based on Table 2 except the variables; HEMA 0.2g (0.8 wt% by PU); BPA 0.7g (2.8 wt% by PU)

a

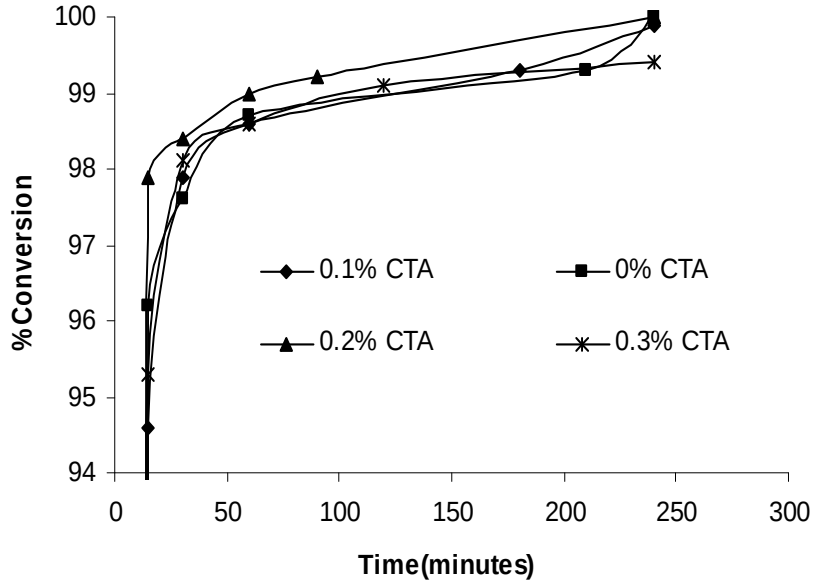

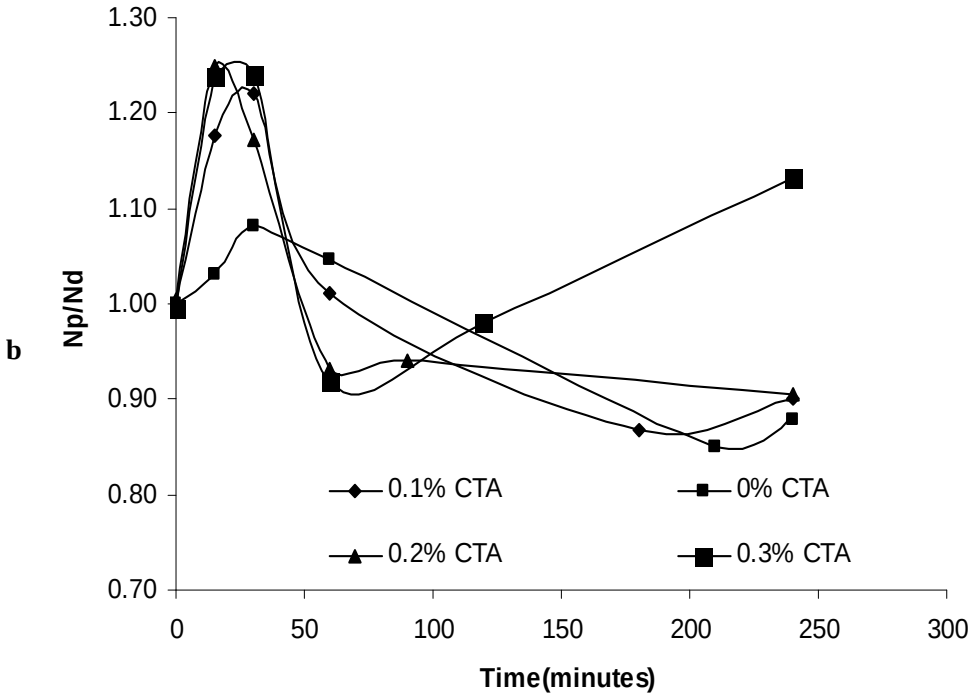

Figure 10(a). Evolution of monomer conversion for a series of miniemulsion polymerisation performed with varying amount of CTA. (b). Evolution of N_p/N_d for the same series of miniemulsion polymerisation performed with varying amount of CTA.

The possible reasons for homogenous nucleation are the ejection of monomer due to high degree of grafting and a composition drift of monomer. As expected, for a batch polymerisation of MMA and BA, MMA reacts faster than BA due to its higher reactivity ratio, and the composition drift occurs because of this. Figure 11 shows the variation of poly dispersity index (PI) during the first hour of polymerisation of the runs shown in Figure 10 (a) and (b). As can be seen in Figure 11, the polydispersity of these runs narrowed during the first hour of polymerisation. This implies that the particles created from homogeneous nucleation became stable by growing their size to the size of original particles. However after about 1 hour, N_p/N_d decreases and this is due to the increase of particle size. It should be noted that almost 99% monomer conversion is completed by this time. Therefore PU has been grafted to copolymer by a fraction (10% in this case) of NCO functions by this time and free NCO functions react with water (in the interface) and with bisphenol A. The increase of particle size is due to the swelling of latex particles due to

the reaction of NCO with water (This is different from the decrease of droplet size when free NCO of droplets react with water). We will discuss this point in detail in the section 4.4.2.5 (modifications and process improvement).

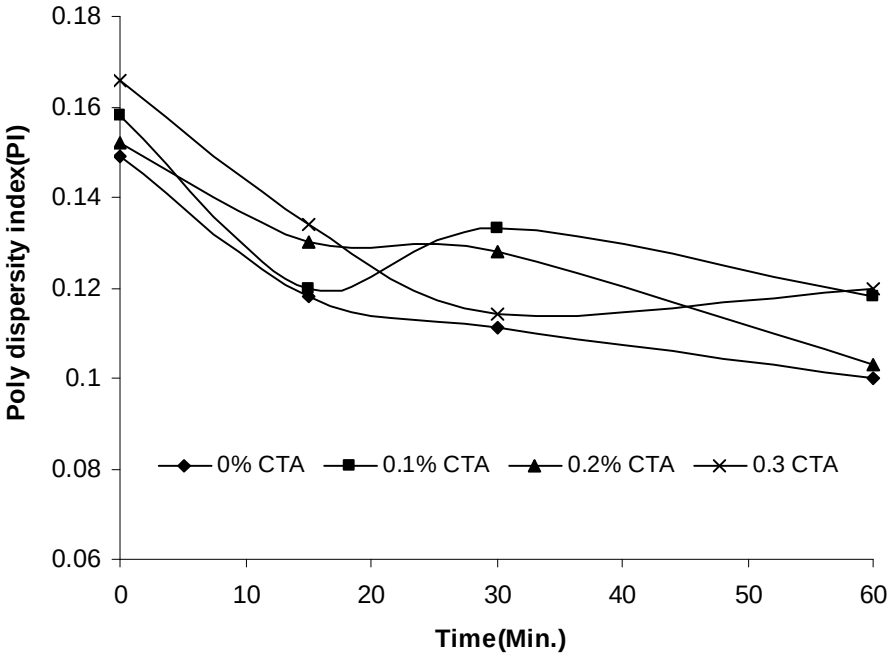

Figure 11. Variation of poly dispersity index for the runs shown in Figure 10 (a) and (b)

It is obvious that the variation of gel content and molecular weight of the sol fraction are due to the effect of CTA (cf. Table 6). In the presence of 0.1% CTA (T143), the gel content is high as well as the chain length of hybrid latex is high. Therefore the solubility of overall hybrid latex in THF is low and hence the measureable Mw and Mn of T143 are comparatively low. With the increase of CTA, the gel content decreases and the solubility of hybrid latex in THF increases. Therefore Mw and Mn of T145 (0.2% CTA) are comparatively high. However Mw and Mn of T146 are lower than that of T145 and this could be due to the short chain length hybrid latex of T146 compared to T145 which could be due to the high amount of CTA. Figure 12 illustrates the stress-strain behaviour of hybrid latexes in the presence of increasing quantities of CTA. According to these experimental results, it was shown that 0.2% of CTA gives better adhesive properties. Therefore, 0.2% of CTA was used in further experiments.

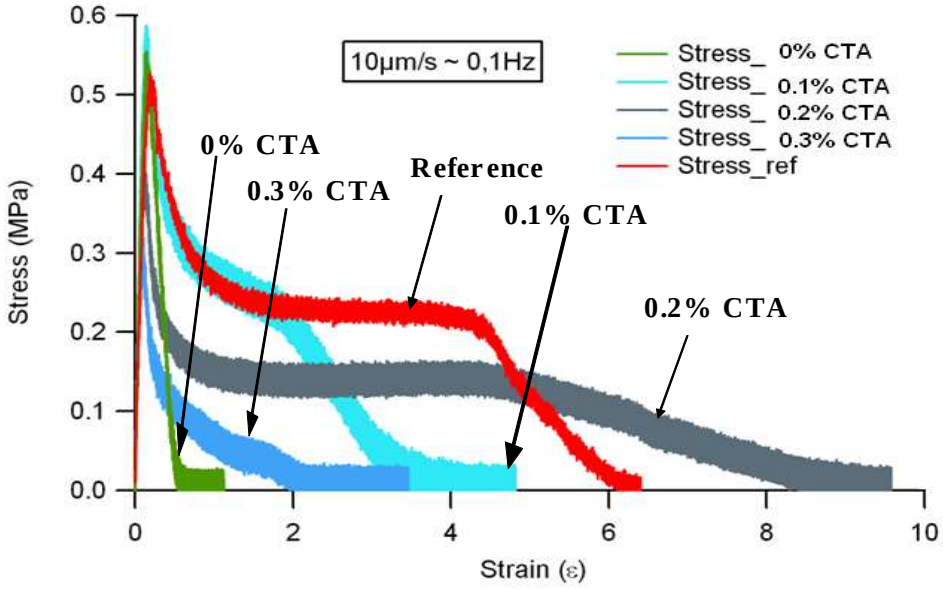

Figure 12. Stress-Strain behaviour of hybrid latexes in the presence of increasing CTA amount

Figure 13 (a) and (b) illustrate the DSC graph of copolymer of BA/MMA/AA (89.5/9.5%1%) and that of hybrid latex with 0.2% CTA and 25% PU (10% of NCO grafted). When comparing the DSC graph of hybrid latex with that of the pure PU (cf. Figure 2) and with pure copolymer [cf. Figure 13(a)], it can be clearly seen a broad heat transition region which is relevant to pure copolymer and PU. In addition several micro phases could be observed in the hybrid latex. A heat transition observed at 60 to 80°C of the hybrid latex could be due to a copolymer rich in PMMA. This heat transition is comparable with the increase of number of polymer particles and hence a higher N_p/N_d at the beginning of polymerisation which could be due to the homogeneous nucleation of MMA.

The degree of grafting of NCO by HEMA in this series of experiments is about 10-11%. In order to find out the best degree of grafting of NCO by HEMA with respect to adhesive properties, the degree of grafting of NCO by HEMA was varied from 5 to 20% in the next series of experiments by varying the amount of HEMA. The quantity of bisphenol A was varied accordingly. The experiments were based on a recipe similar to the recipe described in Table 2 except the mentioned changes. The characteristics of the resulting latexes are summarized in Table 7. Figure 14 (a) and (b) show the evolutions of monomer conversion and N_p/N_d with time of these latexes respectively.

a

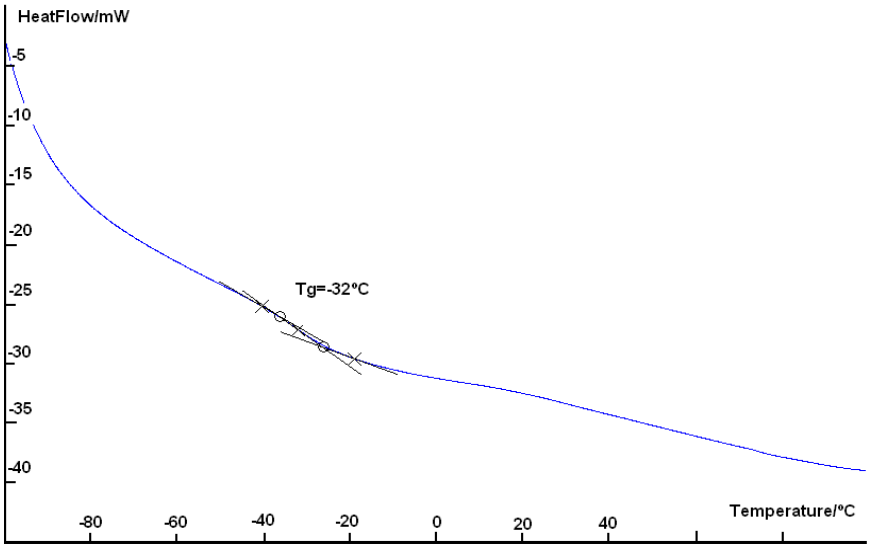

b

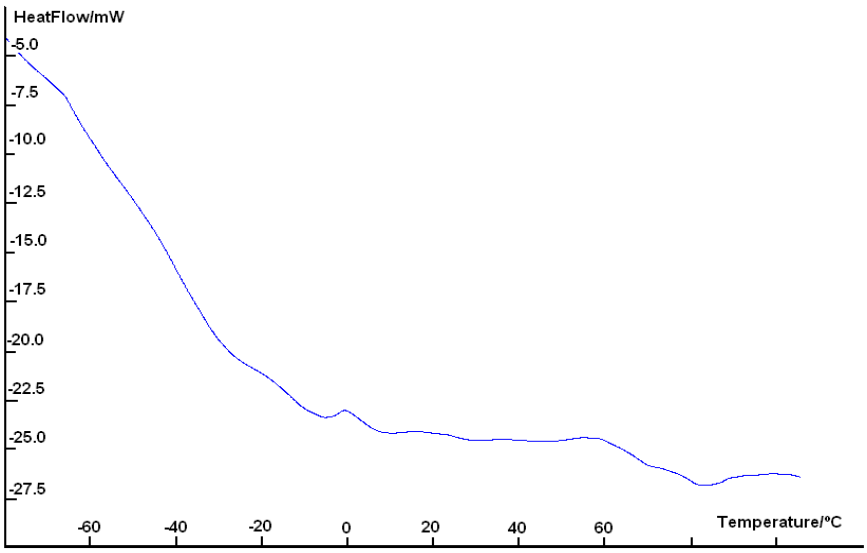

Figure 13(a).DSC graph of copolymer of BA/MMA/AA (89.5/9.5%1%). (b).DSC graph of hybrid latex with 0.2% CTA and 25% PU (10% of NCO grafted)

As can be seen from Figure 14 (a) and (b), complete monomer conversion could be achieved while maintaining a good control of N_p/N_d for this series of experiments also. The trend of variation of N_p/N_d during the reaction period is similar to the earlier series of experiments and hence the same reasons are valid in this case also. The gel content increases gradually with increasing NCO grafting and Mw and Mn of T149 are considerably higher than that of T147. Since the quantity of CTA is constant, the increase of gel content and molecular weight with

increasing NCO grafting could be due to the increase of the incorporation of rigid segments (urethane) to polymer chain. Figure 15 (a) and (b) show the DSC graphs of hybrid latex of 5% NCO grafted and 20% NCO grafted respectively. When comparing the two DSC graphs, with the DSC graphs of pure copolymer [cf. Figure 13(a)], and pure PU (cf. Figure 2) the heat transition relevant to copolymer and PU can be clearly seen in the both graphs [Figure 15 (a) and (b)]. However only two principal heat transitions could be observed in the DSC graph of 20% NCO grafted system while there are several small heat transition regions could be observed both in the 10% NCO grafted system [c.f. Figure 13 (b)] and 5% NCO grafted system [c.f. Figure 15 (a)]. This indicates that PU can be efficiently hybridised with the maximum grafting of NCO (20%) by HEMA. Figure 16 illustrates the stress-strain behaviour of hybrid latexes in the presence of different HEMA/bisphenol A ratios. According to these experimental results, it was shown that 5% and 10% NCO grafting by HEMA give better adhesive properties and therefore 5% and 10% NCO grafting by HEMA were employed under the optimum conditions.

Table 7. Main characteristics of the hybrid miniemulsions and hybrid latexes elaborated in the presence of different amount of HEMA and bisphenol A

Sample Identity	T-147	T-148	T-149
PU (Incorez-701, %)	25	25	25
CTA (%)	0.2	0.2	0.2
NCO grafting (%)	5	15	20
Droplet size (nm)	121.8	123.6	123.6
Final particle size (nm)	129.4	131.1	128.2
N_p/N_d of final latex	7.30E-1	7.34E-1	7.85E-1
Conversion (%)	100	100	100
Solid Content (%)	49.8	49.8	49.8
Gel Content (%)	31	47.2	58.4
Molecular weight(Mw) of sol fraction	288820	N/D	2417400
Molecular weight(Mn) of sol fraction	8970	N/D	52910
Mw/Mn	32	N/D	46

The recipe is based on Table 2 except the variables; HEMA 0.1g, 0.3g & 0.4g respectively; BPA 0.76g, 0.66g & 0.60g respectively.

a

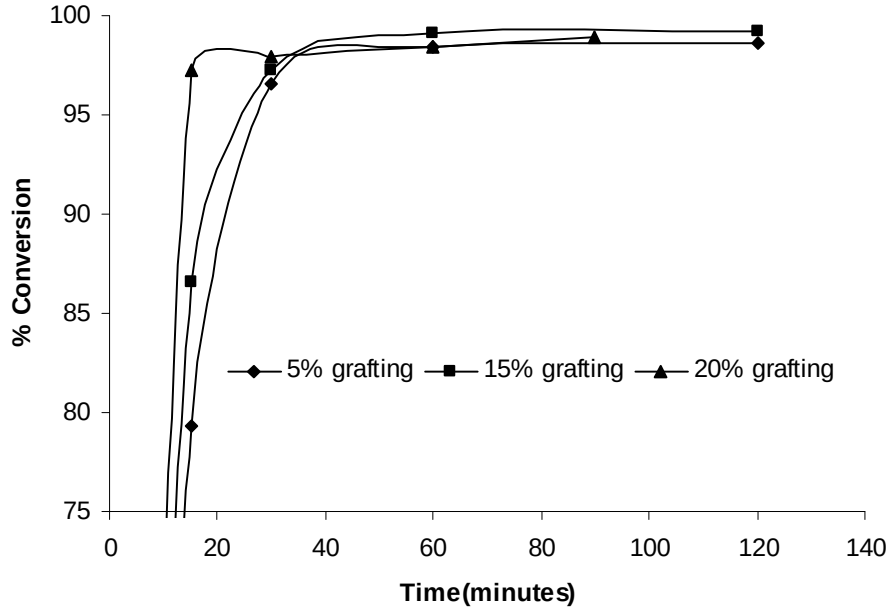

b

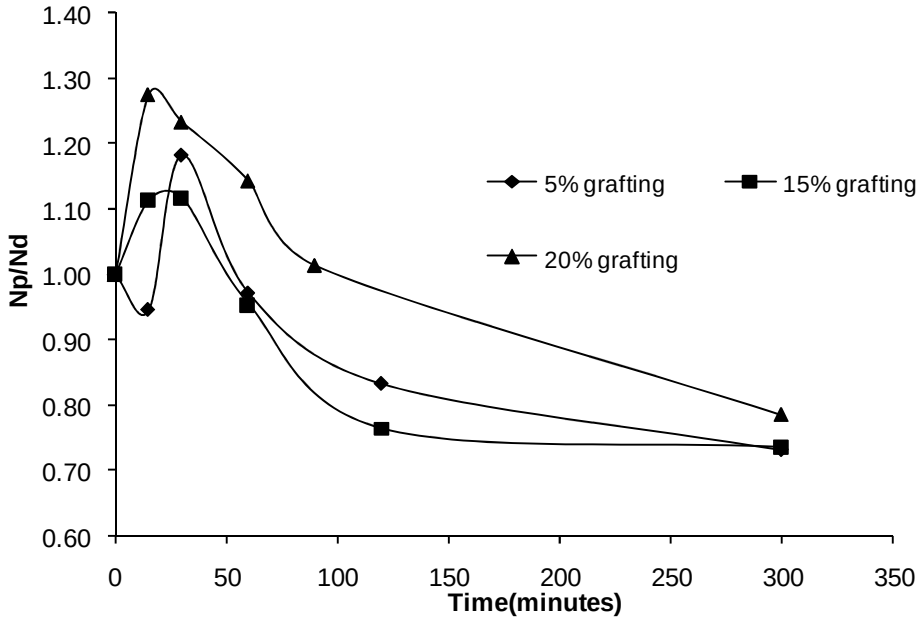

Figure 14 (a). Evolution of monomer conversion for a series of miniemulsion polymerisation performed with different grafting of NCO by HEMA. (b). Evolution of N_p/N_d for the same series of miniemulsion polymerisation performed with different grafting of NCO by HEMA

a

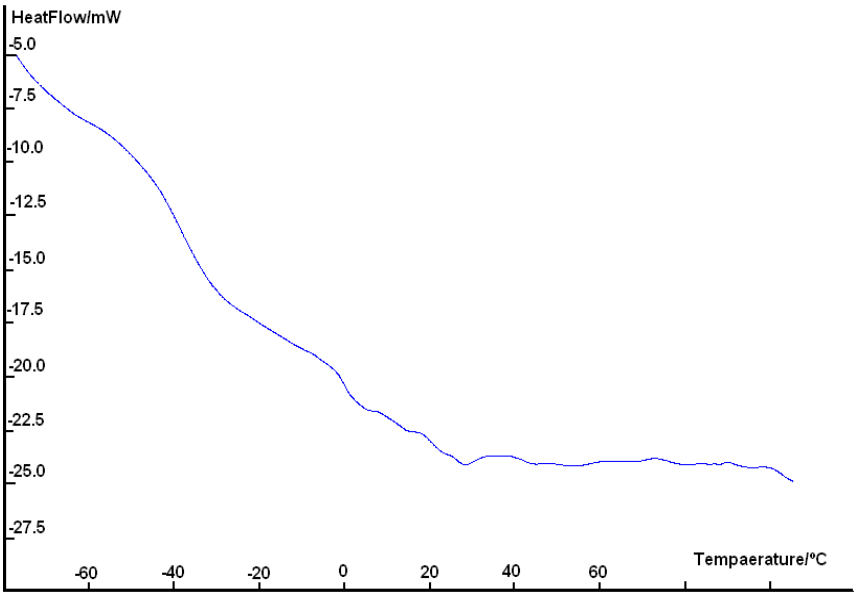

b

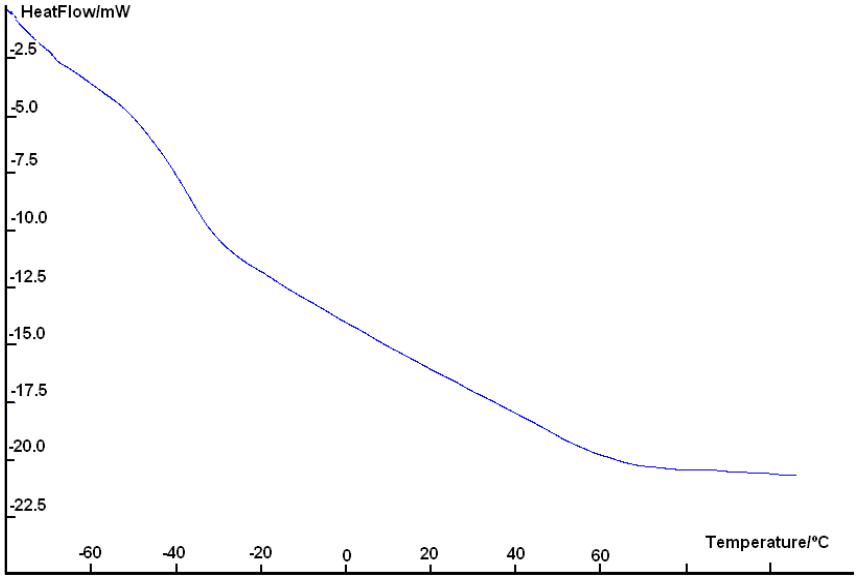

Figure 15 (a). DSC graph of hybrid latex with 0.2% CTA and 25% PU (5% of NCO grafted). (b). DSC graph of hybrid latex with 0.2% CTA and25% PU (20% of NCO grafted).

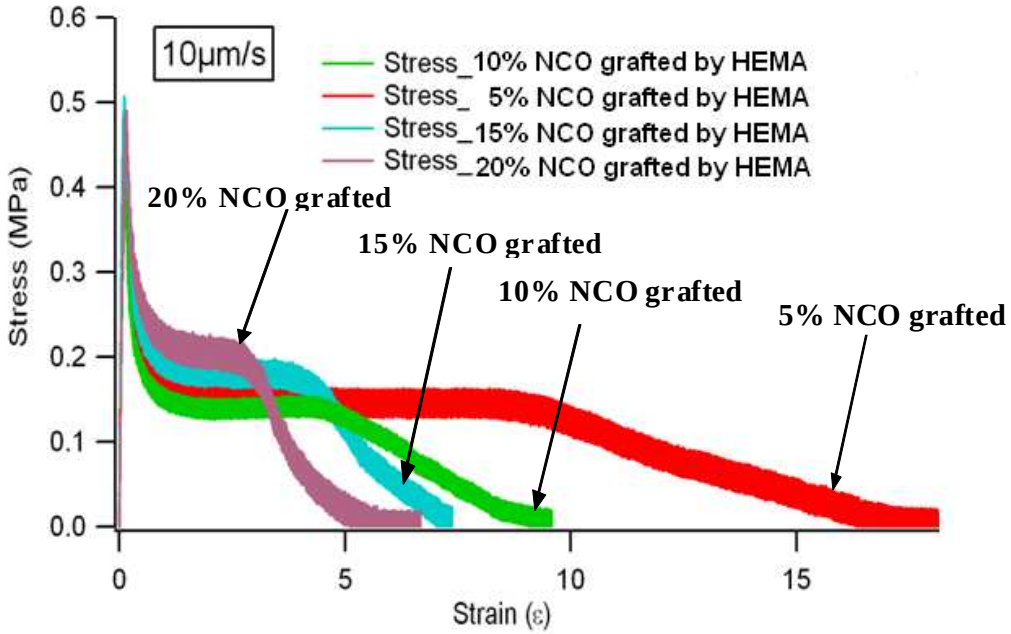

Figure 16. Stress-Strain behavior of hybrid latexes in the presence of different HEMA quantity

During this study, most of the experiments were based on 25% (wt% by monomer) of PU. In order to find out the best amount of PU which gives better adhesive properties, a series of experiments was performed by varying the PU content and keeping the other parameters constant. The basic recipe is similar to the recipe illustrated in Table 2 while the amount of PU was varied from 0 to 50% (wt% by monomer) and the degree of grafting of NCO by HEMA was 10% in each case. The amount of CTA was also kept constant at 0.2% (wt% by monomer). The characteristics of the resulting latexes are summarised in Table 8. Figure 17 (a) and (b) show the evolutions of monomer conversion and N_p/N_d with time for these latexes respectively. Complete monomer conversion could be achieved for this series of experiments also. It should be noted that the increase of particle size compared to the initial droplet size is low with the increasing PU content and hence the stability of hybrid latex is high with increasing PU quantity. It seems that with increasing PU content, the rigidity of hybrid latex increases and hence the gel content increases. This could be due to the hard segments (NCO) of PU and it is known that the hardness and toughness of latex increase in the presence of PU. Since the solubility of hybrid latex in THF decreases with increasing PU, Mw and Mn of T 153 are considerably lower than that of T150.

Table 8. Main characteristics of the hybrid miniemulsions and hybrid latexes elaborated in the presence of different amount of PU

Sample Identity	T 150	T 151	T 152	T 153
PU (Incorez-701, %)	5	15	35	50
CTA (%)	0.2	0.2	0.2	0.2
NCO grafting (%)	10-11	10-11	10-11	10-11
Droplet size (nm)	80.1	104	135.5	148.7
Final particle size (nm)	93.6	105.9	130.5	131.9
N_p/N_d of final latex	5.4E-1	8.2E-1	9.9E-1	1.3E+1
Conversion (%)	100	100	100	100
Solid content (%)	45.5	47.7	49.9	49.9
Gel content (%)	9	29.1	58.2	73.8
Molecular weight(Mw) of sol fraction	3639630	N/D	2808230	558410
Molecular weight(Mn) of sol fraction	83680	N/D	58740	33900
Mw/Mn	43	N/D	48	16

The recipe is based on Table 2 except the variables; HEMA 0.04g, 0.13g, 0.27g & 0.34g respectively; BPA 0.14g, 0.42g, 0.90g & 1.17g respectively.

a

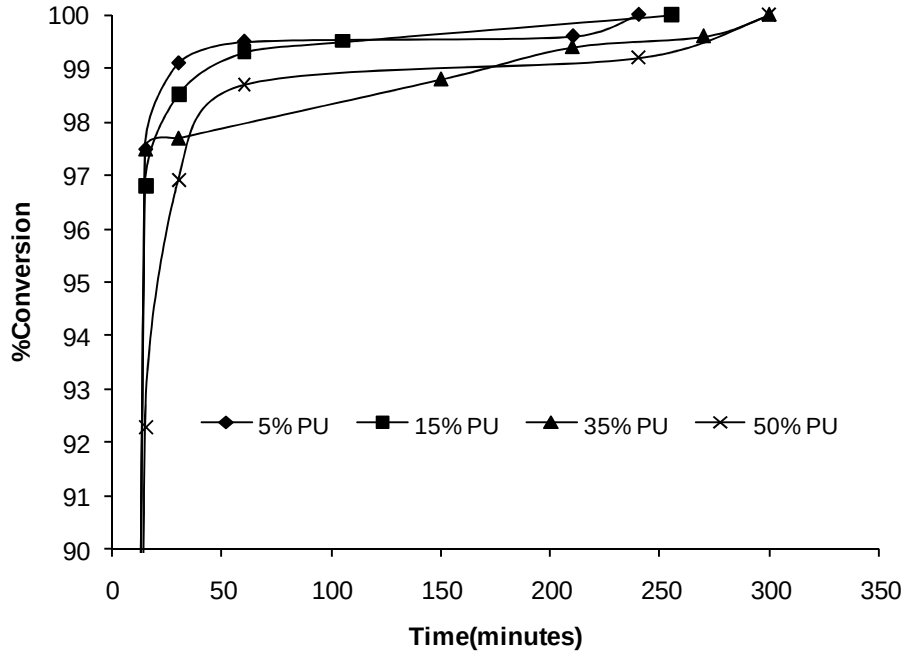

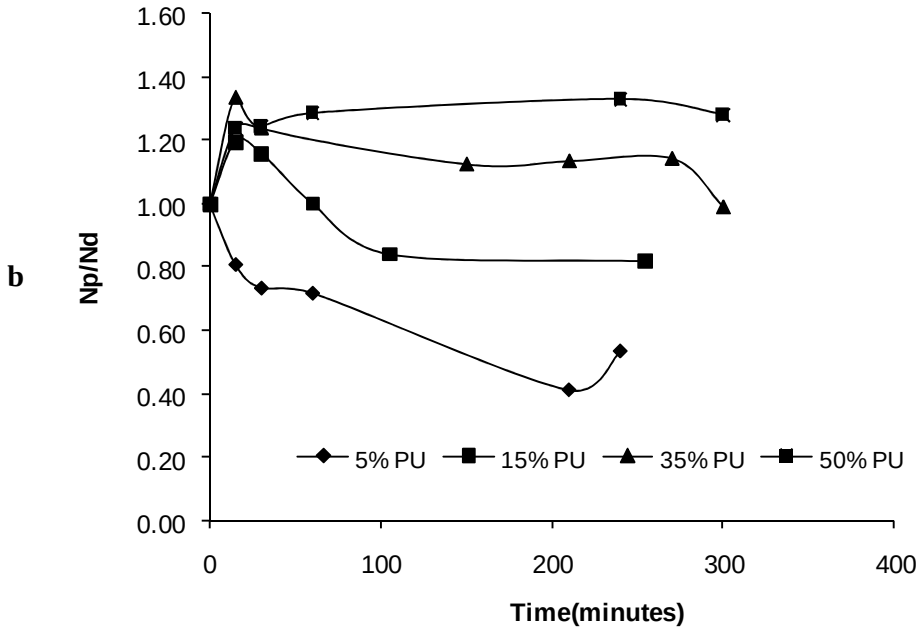

Figure 17(a). Evolution of monomer conversion for a series of miniemulsion polymerisation performed with varying amount of PU. (b). Evolution of Np/Nd for the same series of miniemulsion polymerisation performed with varying amount of PU

Figure 18 illustrates the stress-strain behaviour of hybrid latexes in the presence of increasing PU quantity. According to these experimental results, it was shown that 25% PU is ideal for better adhesive properties with 0.2% CTA and 10% of NCO grafted by HEMA. Finally the similar amount of 25% PU was incorporated in the presence of 0.15% CTA and 5% of NCO grafted by HEMA. The latex characteristics of this sample were similar to that of the samples with 25% PU and adhesive properties were also similar to the case of 25% PU, 0.2% CTA and 10% NCO grafting by HEMA. However it should be noted that a full factorial design might have led to slightly different “optimal” levels, but we expect that this rapid screening allowed us to identify reasonable starting conditions.

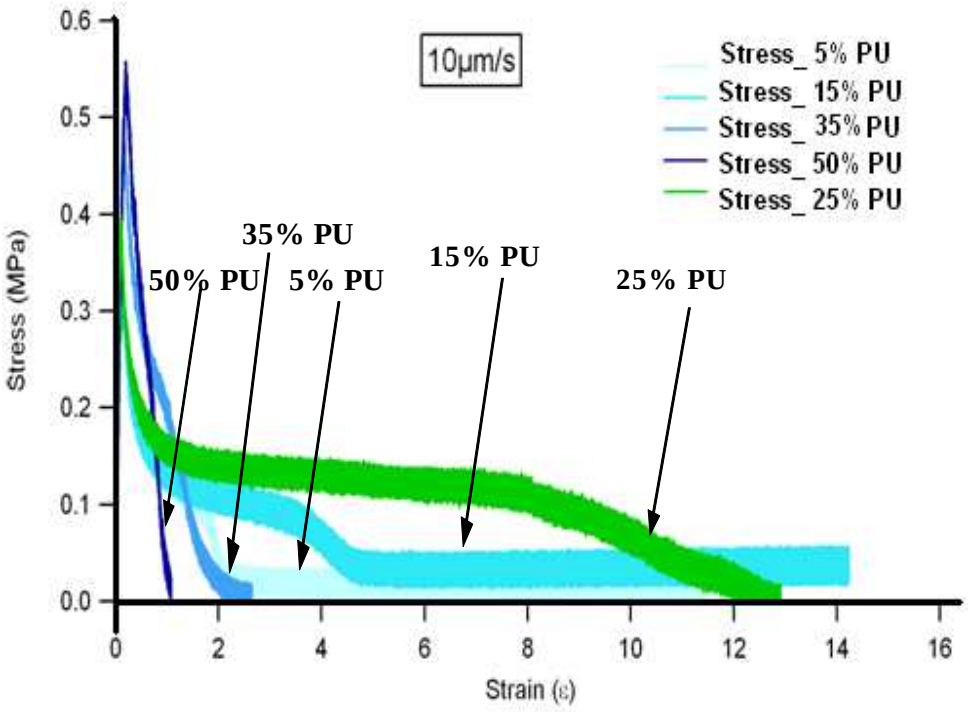

Figure 18. Stress-Strain behavior of hybrid latexes in the presence of different PU quantity

4.4.2.5 Modifications and process improvements

As described above, the role of bisphenol A is hydrophobic chain extension which results due to the reaction between free NCO functions and bisphenol A. However the use of a stoichiometric amount of bisphenol A led to the flocculation of the system during the last stages of polymerisation. A possible reason for this instability is the bridging flocculation which takes place in the interface of hybrid particles. Since we use an additional hydrophobe (ODA) and a chain transfer agent (1-dodecylmercaptan), the interior of droplets is already hydrophobic when bisphenol A is added to the organic phase about 60 minutes before the initiation of polymerisation. It has been shown that the reaction between bisphenol A and NCO is time dependent even under catalytic conditions[1]. Since the interior of droplets is already hydrophobic, it is reasonable to assume that hydrophobic chain extension takes place in the interface of hybrid particles of about 100nm in size, in addition to the interior of particles. As bisphenol A has OH functions, it will most likely be (at least partially) situated at the particle-water interface and flocculation could occur during the chain extension. It is expected that by controlling the

hydrophobic nature of interior of droplets, flocculation could be avoided in the presence of a stoichiometric amount of bisphenol A. In order to verify this fact, following experiment was carried out. A recipe of a previous successful run was used (T145-50% of stoichiometric amount of bisphenol A) but without ODA and with the stoichiometric amount of bisphenol A. All the experimental conditions were similar except the mentioned changes. The characteristics of the hybrid miniemulsions and latexes are illustrated in Table 9.

Table 9. Main characteristics of the hybrid miniemulsions and hybrid latexes elaborated in the presence of 50% Bisphenol A (T-145) and full amount of bis phenol A (T-159)

Sample	T-145	T-159
PU (Incorez-701, %)	25	25
CTA (%)	0.2	0.2
NCO grafting by HEMA (%)	10-11	10-11
Droplet size (nm)	122.8	115.3
Final particle size (nm)	121.4	120.7
N_p/N_d of final latex	9.1E-1	7.63E-1
Conversion (%)	100	100
Solid Content (%)	49.8	49
Gel Content (%)	44.5	48.5
Molecular weight(Mw) of sol fraction	3917350	5151010
Molecular weight(Mn) of sol fraction	63400	91240
Mw/Mn	62	56

Interestingly, no flocculation occurred during this synthesis and this leads us to believe that the above assumption is correct. The gel content as well as the molecular weight of sol fraction is high (cf. Table 9) in the presence of stoichiometric amount of bisphenol A. This could be due to the high cross-linking occurred during chain extension. Figure 19 shows the particle size variation of the two latexes (T145-50% BPA and T-159-Full amount of BPA) with time. The increase of particle size compared to the initial particle size just after the synthesis is due to the reaction of free NCO functions with water and this confirms the reaction of NCO functions with water is faster than the catalysed reaction of bisphenol A and NCO. However bisphenol A competes with water molecules and hence the increase of particle size is controlled. It is clear that the stability of particles in the presence of full amount of bisphenol A is higher than that of 50% bisphenol A.

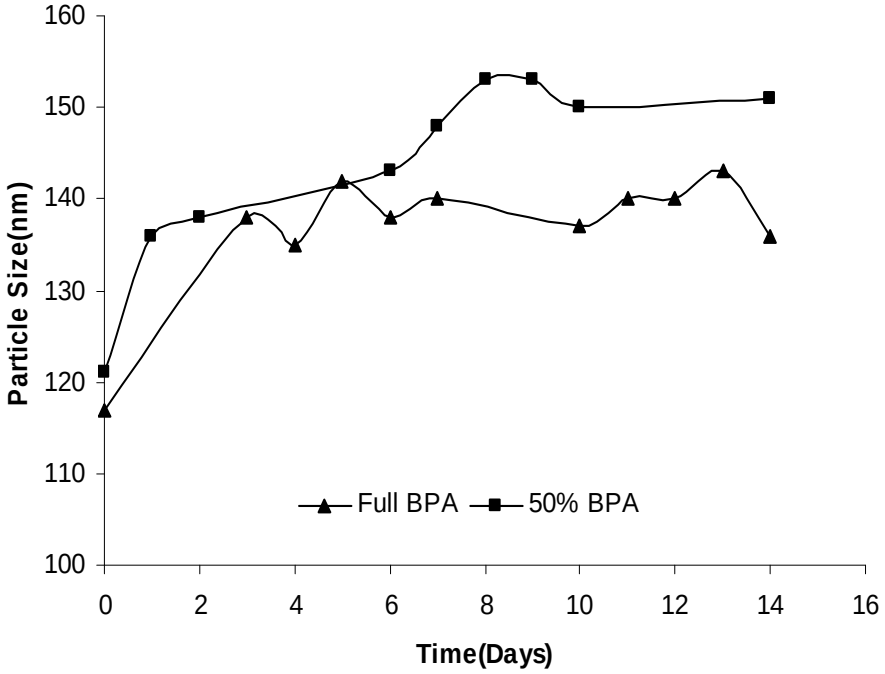

Figure 19. Variation of particle size with time

According to the tack experimental results of T159 which are not shown here, the strain of this latex is not as good as the latex of 50% bisphenol A (T145). This could be due to high cross linking of the hybrid particles. Since we have added more bisphenol A, the chain extension reaction between bisphenol A and free NCO functions may increase the cross linking strength. Recall that by increasing the CTA concentration, the gel content could be significantly lowered and thereby strain could be improved. Based on the adhesive test properties performed at high temperature by the industrial partner, it was decided to increase the degree of grafting by HEMA to 20%. In order to find out the best CTA concentration which gives better strain properties while using the full amount of bisphenol A and HEMA (20% NCO grafting), a new series of experiments was performed by varying the amount of CTA. The characteristics of the resulting latexes are summarized in Table 10. Figure 20 (a) and (b) show the monomer conversion with time and the evolutions of N_p/N_d relevant to the above experiments. The similar trend of monomer conversion and the variation of N_p/N_d observed in the previous experiments could be observed in this series of experiments also.

Table 10. Main characteristics of the hybrid miniemulsions and hybrid latexes elaborated in the presence of varying amount of CTA

Sample Identity	T 160	T 161	T 162	T 163	T164
PU (Incorez-701, %)	25	25	25	25	25
CTA (%)	0.3	0.2	0.25	0.3	0.4
NCO grafting (%)	10	20	20	20	20
Droplet size (nm)	120	121.2	118.5	121	115.1
Final particle size (nm)	143.5	119.8	118.6	123	115.4
N_p/N_d of final latex	5.13E-1	9.08E-1	8.75E-1	8.35E-1	8.7E-1
Conversion (%)	100	100	100	100	100
Solid content (%)	49.1	49.1	50	49.9	49.1
Gel content (%)	38.5	57.5	52.5	44.6	43.6

a

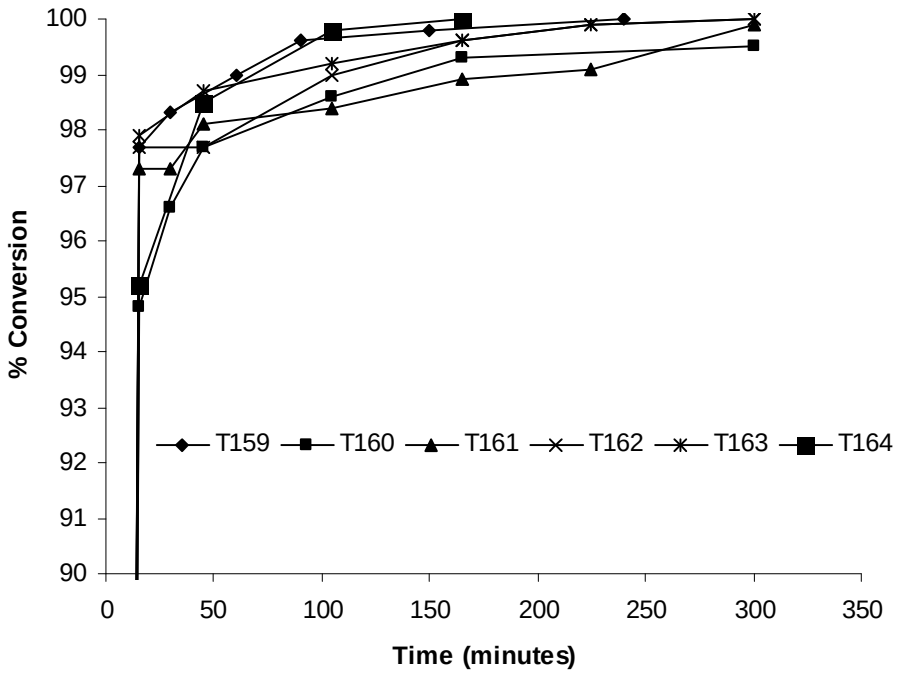

b

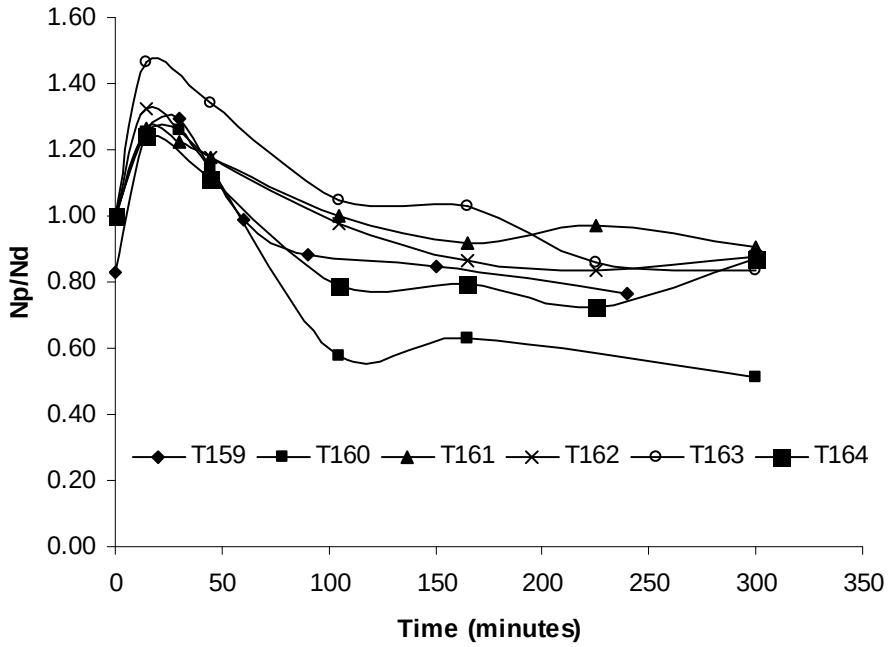

Figure 20(a). Evolution of monomer conversion for a series of miniemulsion polymerisation performed in the absence of ODA and in the presence of varying amount of CTA. (b). Evolution of N_p/N_d for the same series of miniemulsion polymerisation.

Figure 21 shows the tack experimental results for the samples from T161 to T164. As expected, with increasing CTA quantity, the deformation of hybrid latex is higher and hence the strain is higher. Figure 22 shows the tack experimental results for the samples T160 (0.3% CTA & 10%NCO grafted by HEMA) and T163 (0.3% CTA & 20% NCO grafted by HEMA). Although similar strain could be observed for both samples, the stress of T 163 is higher and this is due to the high degree of grafting by HEMA.

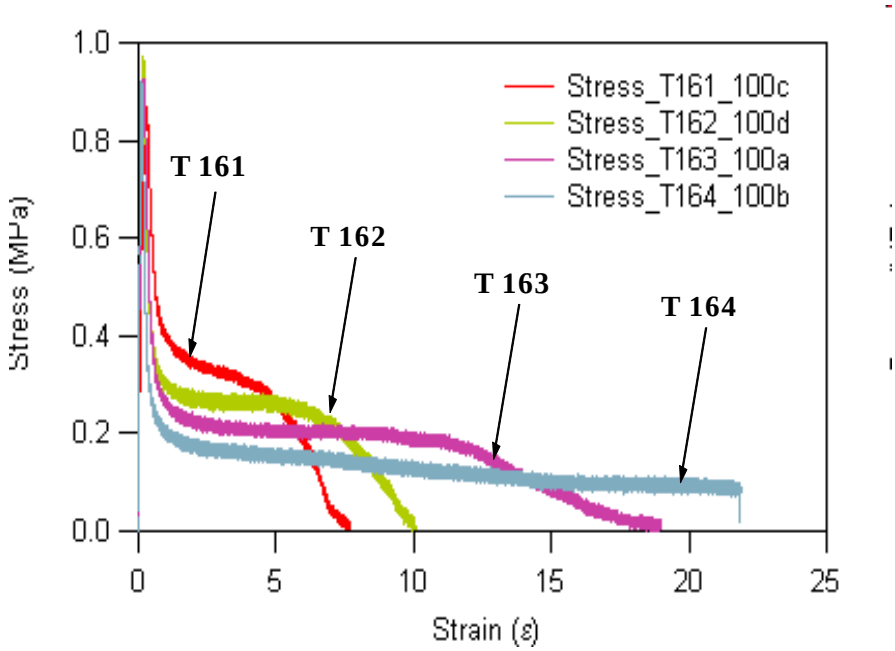

Figure 21. Stress-Strain behaviour of hybrid latexes with increasing CTA quantity

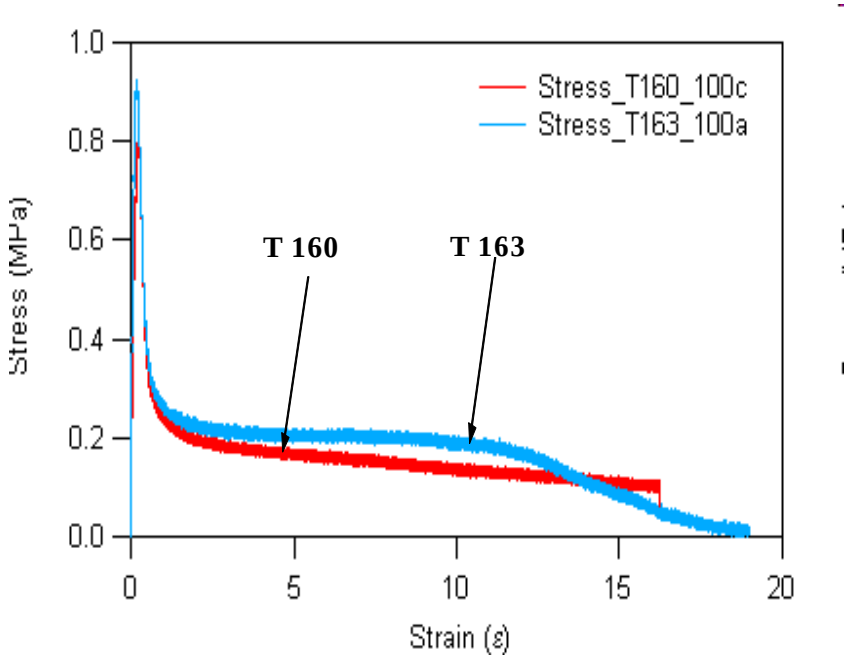

Figure 22. Stress-Strain behaviour of hybrid latexes with similar CTA quantity (0.3%) and different degree of grafting by HEMA

Figure 23 shows the tack experimental results for the samples with similar CTA amount (0.2%) and similar degree of grafting by HEMA (20%) but with different amounts of bisphenol A. In T 149, the amount of bisphenol A was 50% by the calculated amount and the amount of ODA was (5 wt% by monomer). In T161, the full amount of bisphenol A was used as per calculation in the absence of ODA. It can be seen that the sample with no ODA (T 161) is much more deformable, and with a higher adhesion energy. This could be explained by the longer chains synthesised when there is a complete reaction of NCO with OH of BPA.

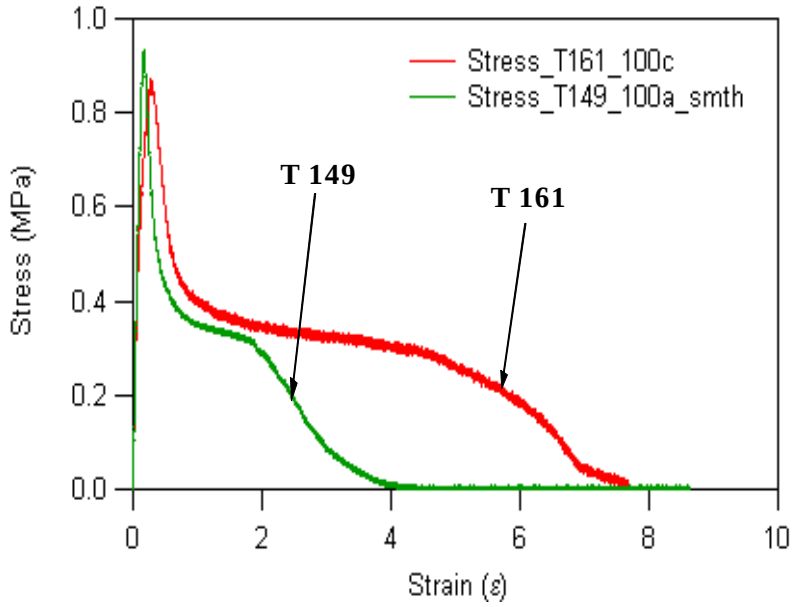

Figure 23. Stress-Strain behavior of hybrid latexes with similar CTA quantity (0.2%) and similar degree of grafting by HEMA (20%) but with different amounts of Bisphenol A

Figure 24 shows the variation of tensile strength of the samples described in Table 10. Some similar conclusions can be made with these samples. We can clearly see the effect of CTA: the more CTA, the softer the samples, with less hardening and less pronounced. This is due to less cross linking. Regarding samples with different grafting degree, the results are consistent with the tack: the more grafting (T163), the higher the stress before the softening means the tougher the sample. Figure 25 shows the tensile strength of the samples with similar CTA amount (0.2%) and similar degree of grafting by HEMA (20%) but with different amounts of bisphenol A (The similar comparison done for the tack behaviour as in Figure 23). Here we have interesting results comparing the two series with different OH/NCO ratio. The samples with OH/NCO=1 (complete

reaction of the remaining NCO with BPA) have higher deformation and less hardening. The curve also breaks for higher stresses. This is probably due to the PU chain length.

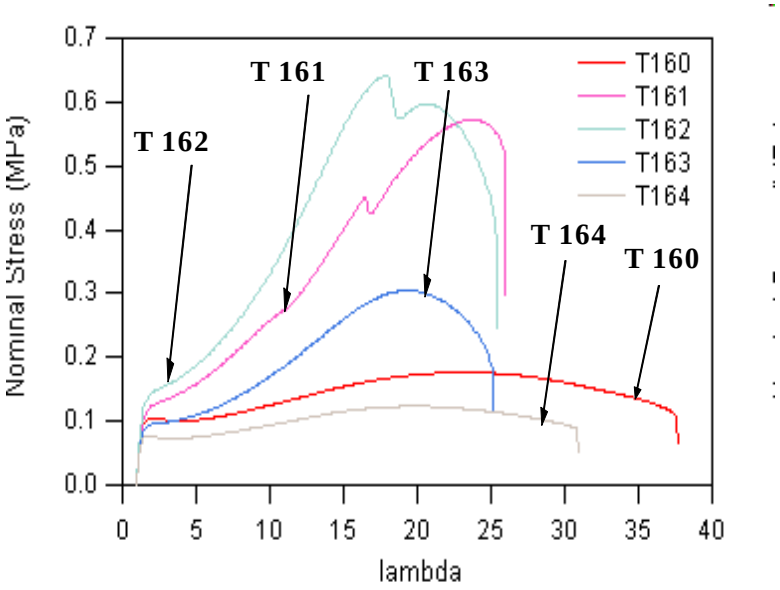

Figure 24.Variation of tensile strength of the samples described in Table 10

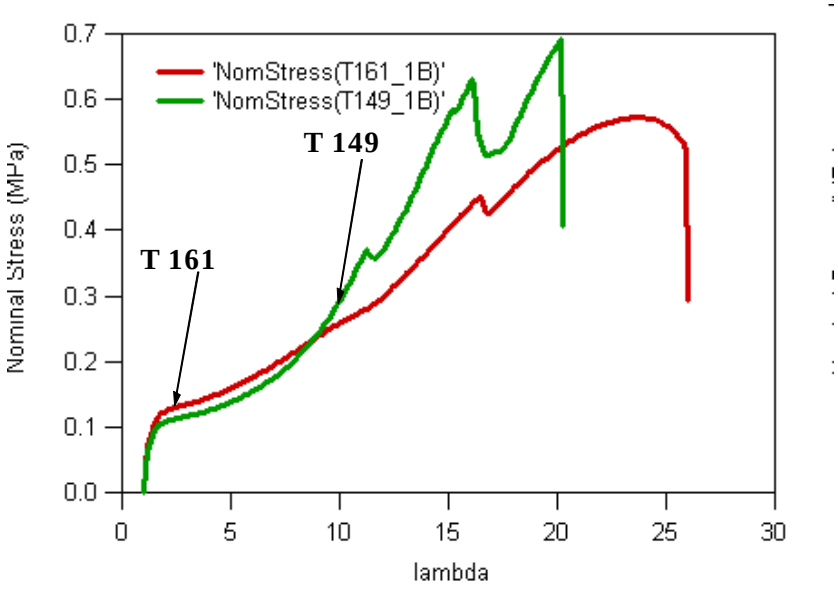

Figure 25. Tensile strength behaviour of hybrid latexes with similar CTA quantity (0.2%) and similar degree of grafting by HEMA (20%) but with different amounts of bis phenol A

4.4.2.6 Transmission Electron Microscopy (TEM) of hybrid latex

Figure 26(a), (b) and (c) show the images of hybrid latex obtained by TEM. A dark interior which occupies about 90% of the particle volume and a light exterior could be clearly observed in the TEM images. The core of particles should correspond to hydrophobic compounds (Poly BA and hydrophobic chain extended PU). The thin outer layer should correspond to hydrophilic PMMA. We have pointed out that the homogeneous nucleation occurs during the early stages of polymerisation of hybrid miniemulsions by studying the variation of N_p/N_d with monomer conversion. It was shown that the homogenous nucleation could be due to a composition drift (The early reaction of MMA in a batch miniemulsion of MMA and BA) and the ejection of monomer due to high degree of grafting and cross linking. Therefore it is reasonable to assume that the thin outer layer is mainly composed of PMMA. The small particles also could be due to homogeneous nucleation. Figure (b) & (c) also show the solid interior of particles and it is reasonable to assume that PU is in the core of particles.

a

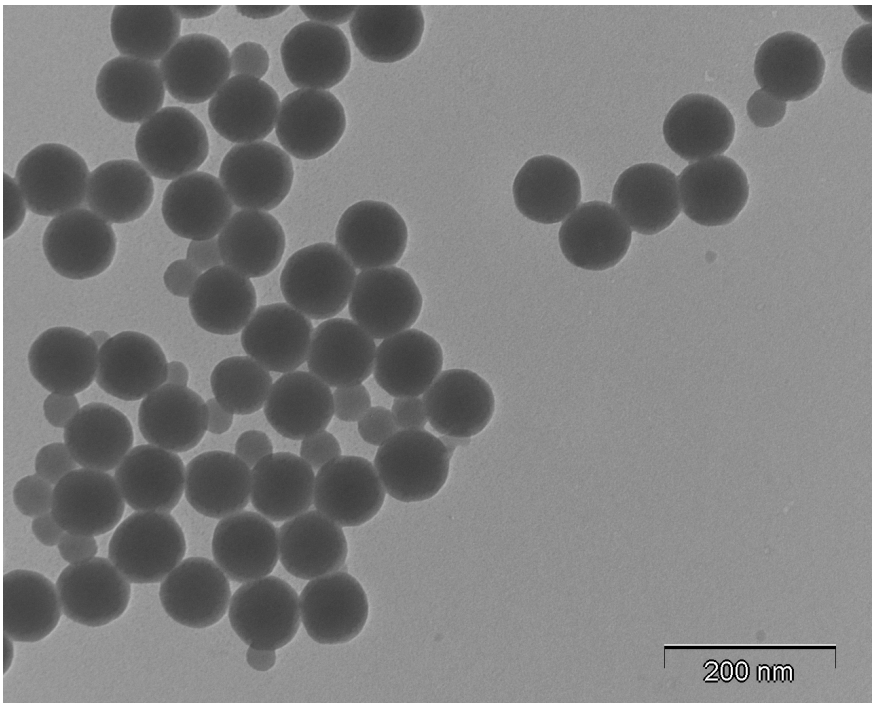

b

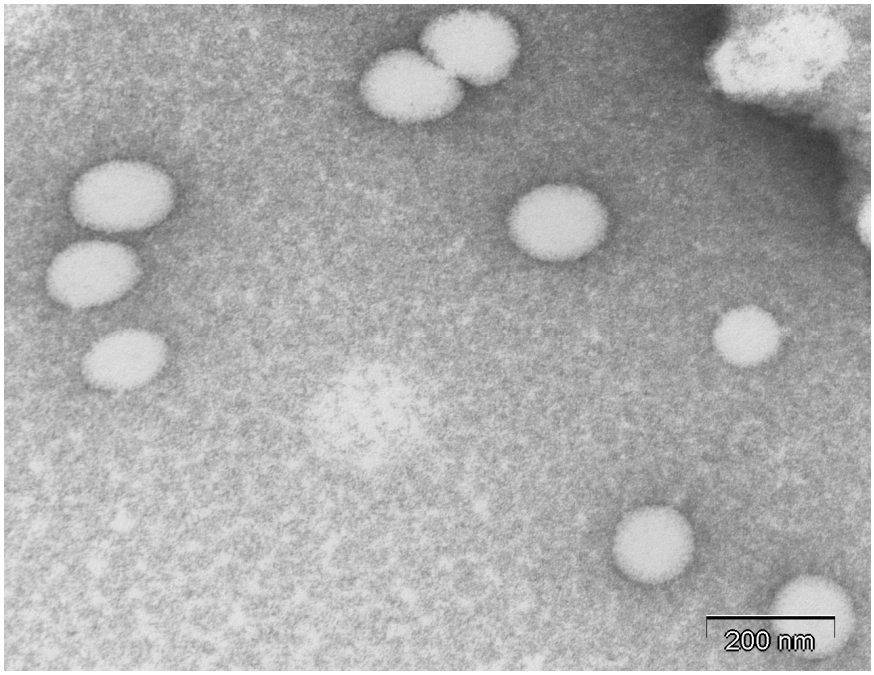

c

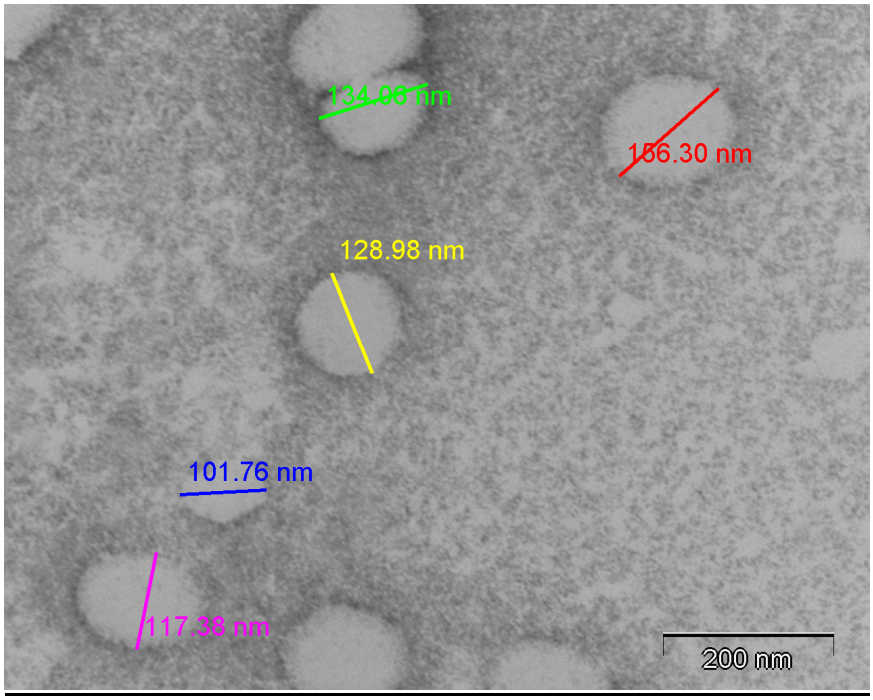

Figure 26(a). A TEM image of hybrid latex after curing the sample by UV light. (b) & (c). TEM images of hybrid latex after adding Phosphotungstic acid to the sample and cured by UV light

4.5 Industrial Application

The following samples described in Table 11 were tested for properties at industrial laboratories (Cytec).

Table 11. Description of samples sent to Cytec

Sample Id:	TSC%	%PU (wt. by monomer)	%CTA (wt. by monomer)	% Degree of NCO grafting by HEMA
T147	50	25	0.2	5
T148	50	25	0.2	15
T150	48	5	0.2	10
T151	50	15	0.2	10
T153	50	50	0.2	10

The standard FINAT industrial test methods were used for property testing. A summary of test procedures is described below.

4.5.1 Preparation of a coated sample

The objective of this test is to prepare a dry adhesive film with variable coat weight laminated between a face material and a release liner. The method can also be used to prepare a free film of adhesive between two siliconized papers.

An adhesive can be coated in transfer or direct:

- **Transfer:** the adhesive is coated on a release liner (= silicone paper) and laminated on a face material after drying.

- **Direct:** the adhesive is coated on the face material and laminated on a release liner after drying.

The direct method was used during this study and latex samples were coated directly on a polyester film (PET-23 microns thickness).

4.5.2 Coat weight

The objective of this test is to determine the amount of dry adhesive material applied to the surface of a pressure sensitive construction (e.g., label, tape), which has been prepared manually on a laboratory coater or any industrial coater. Adhesive coat weight is expressed as the weight of dry adhesive on a standard sized area of material – in grams per square meter (g/m^2). The

targeted coat weight for dry films is **25 ± 1 g/m^2**. The coat weight has indeed a significant influence on the adhesive performances of the PSA films.

4.5.3 Drying

It is recommended to dry films for 180 seconds, with a temperature, measured at film surface, of maximum 110°C.

4.5.4 Resistance to shear from a standard surface

This test method measures the ability of an adhesive to withstand static forces applied in the same plane as the labelstock. It gives an indication of the likely mode of bond failure, i.e. adhesive failure or cohesion failure.

Resistance to shear from a standard surface is defined as the time required for a standard area of pressure sensitive coated material to slide from a standard flat surface in a direction parallel to the surface.

The test strips should be taken from a representative sample of material. The strips should be 25mm wide and have a minimum length of 175mm in the machine direction. The cuts should be clean and straight. At least three strips should be taken from each material sample.

Resistance to shear from a standard surface is expressed as the average time taken for the three strips to shear from the test plate.

Failure Description Code:

CP Clear Panel - no visible stain on panel.
PS Panel Stain – discoloration of test area, but no tacky residue.
CF Cohesive Failure – the adhesive film is split during the test, leaving residue of adhesive on both the panel and the front material.
AT Adhesive Transfer – the adhesive separates cleanly from the front material, leaving adhesive film on the test panel. The approximate extent of transfer should be quoted as percentage.

4.5.5 Peel adhesion (180°C) at 300mm per minute

This test method is designed to quantify the permanence of adhesion or peelability of self-adhesive pressure sensitive materials.

Peel adhesion is defined as the force required to remove pressure sensitive coated material, which has been applied to a standard test plate under specified conditions from the plate at a specified angle and speed.

Peel adhesion (180°C) is expressed as the average result for the strips tested in Newtons per 25mm width for either 20 minutes or 24 hours application time. The latter is considered as the ultimate adhesion.

4.5.6 'Loop' tack measurement

This test method describes a means of assessing probably the most important and yet the hardest to measure property of pressure sensitive materials, the tack. The method should allow the end user to compare the "initial grab" or "application tack" of different laminates and can be extremely useful to those working with automatic labeling equipment where this property is of particular importance.

The 'loop' tack value of a pressure sensitive material is expressed as the force required to separate, at a specified speed, a loop of material (adhesive outermost) which has been brought into contact with a specified area of a standard surface.

'Loop' tack is expressed as the average value (ignoring the initial peak) and range for the five strips tested in Newtons.

If the force exceeds the strength of a paper facing material, the result quoted should be the maximum reached before the paper tears and this result should be followed by the postscript PT (paper tear).

If adhesive transfer occurs, this should be indicated by the letters AT, and the approximate extended of transfer quoted as percentage.

4.5.7 Substrate details and cleaning methods

4.5.7.1 Stainless steel:

- Grade: INOX 304 BA (thickness = 1mm).
- Cleaning procedure:
    - Wipe them clean with Acetone, then soap and finally Acetone again.
    - Dry them at 110°C for > 10 minutes
    - Always clean new plates before first use *(Then preliminary step to normal cleaning: 24h immersion in ethanol)*.
- Only use the face which is initially protected by plastic film

4.5.7.2 HDPE plates

- Grade: PE plates
- Cleaning procedure:
    - Keep the plates a short time in ethyl acetate and then wipe them clean by plastic blade
    - Dry them at room temperature for > 20 minutes
    - Always clean new plates before first use.
- Both sides of the plates can be used

The property test results of these samples as reported by Cytec are described in Table 12 and Table 13 respectively.

Table 12. Property test results

Transfer-coating*		No
Coat weight:	gsm	25 g/m²
Drying:		110°C/3min
Face:		**P ester 23µ**
Conditioning laminates:		≥ 24H @ 23°C, 50% RH

Table 13. Property test results

Coating	Units	T147	T148	T150	T151	T153
SHEAR on stainless steel 1 inch^2 /kg	min.	1680 CF	>10000	46CF	222CF	>10000
ADHESION 180°C	N/25mm					
Stainless steel 20		7.1	6.3	13.3CT	8.5(tr/start)	4.3
ADHESION 180°C	N/25mm					
Stainless steel 20		8.9(tr/start)	8(tr/start)	12CT	22.1 CT	4.9
ADHESION 180°C	N/25mm					
PE-3124H	N/25mm	6.2	5.4	11.3	18.9 CT	1.9
LOOPTACK	N/25mm					
Stainless steel	N/25mm	9.8	9.8	15.8	7.5	3.5

The synthesis of some selected samples which showed better properties was carried out at the R&D laboratories of Cytec. The results of these syntheses are presented in Table 14.

Table 14. Synthesis test results

Sample Id.	% grafting of NCO by HEMA	Total Solid Content (%)	% Conversion of Monomers	Initial Droplet Size(nm)	Final Particle Size(nm)
145	10	49.6	99.5	148.2	146.5
147	5	49.9	100	149.8	159.3
145[a]	10	48.7	97.2	172	170
148[b]	15	49.8	99.8	149.6	145.4

a. Semi-continuous addition of feed. Flow rate and reaction time should be adjusted.
b. 0.25% of chain transfer agent.

The property tests were done by Cytec and the results of these tests as reported by Cytec are described in Table 15 and
Table **16** respectively.

Table 15. Property test results

Transfer-coating*		no
Coatweight:	gsm	25 g/m²
Drying:		110°C/3min
Face:		**P ester 23µ**
Conditioning laminates:		≥ 24H @ 23°C, 50% RH

Table 16. Property test results

Coating	Units	T145	T147	145[a]	148[b]
SHEAR on stainless steel 1 inch^2 /kg	min.	9463 CF	>1252 CF	>10000	>10000
ADHESION 180°C	N/25mm				
Stainless steel 20		6.9	7.3	6.8	6.4
LOOPTACK	N/25mm				
Stainless steel	N/25mm	10.5	9.6	8.4	8.7

4.6 Conclusions

Hybrid miniemulsions with both non reactive and reactive PU could be successfully synthesised. Since desirable latex properties could not be achieved using non reactive PU, reactive PU was used in further experiments. Reactive PU was quantitatively characterised by conductimetry and the molar mass of PU was determined based on the NCO functions quantified by conductimetry. This value of molar mass (3285g) was compared with the molar mass (Mn) obtained from GPC (4338g while the mass relevant to main peak is 3720g with a polydispersity index of 1.42). The molar mass of 3285g was used for the quantification of NCO functions because this molar mass was purely based on NCO functions. After verifying the molar ratio between HEMA and NCO which gives 100% yield, miniemulsion polymerisation was carried out by changing different parameters. The amount of CTA, the degree of grafting of NCO by HEMA (hence different ratios of HEMA/bis phenol A) and different amounts of PU were studied with respect to adhesive properties. In general a good control of N_p/N_d around 1 could be obtained for all of these experiments and the complete monomer conversion could be achieved in each case. Better adhesive properties could be obtained in the combination of 0.2% CTA, 25% PU and 5 or 10% NCO grafting by HEMA.

The conditions for the use of full amount of bis phenol A was investigated and showed that under controlled hydrophobic conditions (in the absence of ODA), the calculated amount of bis phenol A could be used. The laboratory samples sent to the industrial partner (Cytec) could be successfully reproduced at the R&D laboratories of Cytec while retaining the good properties. The semi-continuous feed of monomer was also tested and showed that final properties of both batch and semi-continuous syntheses are similar.

Acknowledgement

Ms. Elise Degrandi, PhD candidate at PPMD/ESCPI, 10, rue Vauquelin, 75231, Paris Cedex-05, carried out the tack experiments under the supervision of Dr. Costantino Creton. The other property tests were carried out by **Cytec Industries, Belgium**. I thank Elise and Cytec Industries for carrying out the property tests of my samples.

4.7 References

1. Li, M.; Daniels, E. S.; Dimonie, V.; Sudol, E. D.; El-Aasser, M. S., Preparation of Polyurethane/Acrylic Hybrid Nanoparticles via a Miniemulsion Polymerisation Process. *Macromolecules* **2005,** 38, 4183-4192.

2. Gooch, J. W.; Dong, H.; Schork, F. J., Waterborne Oil-Modified Polyurethane Coatings via Hybrid Miniemulsion Polymerisation. *Journal of applied Polymer Science* **2000,** 76, 105-114.

3. Zhang, G.; Zhang, Z.; Hu, Z.; Xi, H., Seeded-emulsion polymerization of styrene with waterborne polyurethane stabilizer via 60Co gamma ray. *Colloids and Surfaces A: Physicochem. Eng. Aspects* **2005,** 264, 37-42.

4. Kukanja, D.; Golob, J.; Valant, A. Z.; Krajnc, M., The structure and Properties of Acrylic-Polyurethane Hybrid Emulsions and Comparison with Physical Blends. *Journal of Applied Polymer Science* **2000,** 78, 67-80.

5. Barrère, M.; Landfester, K., High Molecular Weight Polyurethane and Polymer Hybrid Particles in Aqueous Miniemulsion. *Macromolecules* **2003,** 36, 5119-5125.

6. Li, C. Y.; Chiu, W. Y.; Don, T. M., Preparation of Polyurethane Dispersions by Miniemulsion Polymerization. . *Journal of Polymer Science: Part A: Polymer Chemistry* **2005,** 43, 4870-4881.

7. Cheong, I. W.; Nomura, M.; Kim, J. H., Synthesis and aqueous solution behaviour of water-soluble polyurethane (IPDI-PPG-DMPA) resin. . *Macromol Chem Phys* **2000,** 201, 2221-2227.

8. Kim, B. K.; Lee, Y. M., Polyurethane ionomers from cycloaliphatic diisocyanate and polytetramethylene glycol. *J Macromol Sci Pure Appl Chem* **1992,** 29, 1207-1221.

9. Lee, J. S.; Kim, B. K., Polyurethane cationomers from polypropylene glycol and isophorone diisocyanate: emulsion characteristics and tensile properties of cast films. *Prog Org Coat* **1995,** 25, 311-318.

10. Lan, P. N.; Corneille, S.; Schacht, E.; Davies, M.; Shard, A., Biocompatibility of biodegradable and nonbiodegradable polymer-coated stents implanted in porcine peripheral arteries. *Biomaterials* **1996,** 17, 2273-2280.

11. Wang, C.; Chu, F.; Guyot, A., Mechanical Properties of Films from Hybrid Acrylic-Polyurethane Polymer Colloids. *Journal of Dispersion Science and Technology* **2006,** 27, 325-330.

12. Klein, H.-P.; Schawb, M., Aqueous polyurethane dispersions. *Polymer Paint Colour Journal* **1994,** 184, (4357), 444-6.

13. Kim, B. Y.; Lee, J. C., Modification of Waterborne Polyurethanes by Acrylate Incorporations. *Journal of applied Polymer Science* **1995,** 58, 1117-1124.

14. Benlefki, A.; Feghouli, A., The amphiphilic character of poly(acrylo-urethane) dispersions. *European Coating Journal* **1996,** 12, 926-931.

15. Kim, J. Y.; Suh, K. D., Preparation of PEG-modified urethane acrylate emulsion and its emulsion polymerization. *Colloid Polymer Science* **1996,** 274, 920-927.

16. Hirose, M.; Zhou, J.; Nagai, K., The structure and properties of acrylic-polyurethane hybrid emulsions. *Prog Org Coat* **2000,** 38, 27-34.

17. Farzi, G. A., *PhD Thesis University of Claude Bernard Lyon1* **2007**.

18. Mabille, C.; LCalderon, F.; Bibette, J.; Schmitt, V., Monodisperse fragmentation in emulsions: Mechanisms and kinetics. *Europhys. Lett.* **2003,** 61, (5), 708-714.

5. Conclusions and Perspectives

The objectives of the research project were:

- To explore a range of miniemulsification techniques in order to obtain nano sized (100nm) droplets for hybrid systems of 50% solids.

- To synthesise and characterise hybrid latexes for coating(alkyd-acrylic hybrid system) and adhesive applications (polyurethane acrylic hybrid system)

We have explored different techniques, namely sonication, homogenisation with a rotor-stator and static mixers to miniemulsify an alkyd-acrylic hybrid system of 50% solids in order to obtain an initial droplet size of 100nm. The main factor that acts against the applied mechanical energy was shown to be the dispersed phase viscosity in the presence of high alkyd resin quantity (0 – 25 wt % by monomer). As a result, the target droplet size could not be achieved for the hybrid system of 50% solids and at least 25 wt % alkyd resin when rotor-stator and static mixer were used for miniemulsification. However sonication was powerful enough to obtain at least a closer droplet size to the required value for a hybrid system of 50% solids. Therefore sonication was employed as the miniemulsification method of choice during the rest of study.

Alkyd-acrylic hybrid system

Although complete monomer conversion and one to one copy of droplets to particles (Np/Nd=0.8) could be achieved for low amount 5 wt % of alkyd, limiting monomer conversion was the main problem encountered as the alkyd weight fraction was increased. We have attempted different means of increasing the monomer conversion as discussed in the section of alkyd-acrylic hybrid systems (Chapter 3). The complex nature of limiting monomer conversion was evident upon examination of the following three factors.

1. Complete monomer conversion could be achieved via enhanced renucleation by adding a surfactant solution with KPS after the initiation of the polymerisation with AIBN for the hybrid system of 50 wt % unsaturated alkyd and 44% solids.

2. Although renucleation is enhanced by adding a similar surfactant solution with KPS, final monomer conversion could not be increased beyond 96% and 91% respectively for the

hybrid system of 25 wt % and 50 wt % unsaturated alkyd and 50% solids when the polymerisation was initiated with KPS.

3. The similar limiting monomer conversion (96%) could be observed for the hybrid system of 25 wt % saturated alkyd and 50% solids.

We have shown during our study that the interactions between alkyd and monomer are stronger than those of standard hydrophobes such as ODA and hexadecane. As a result, alkyd is highly dispersed in the organic phase. We have also shown that the observed limiting monomer conversion in the presence of 25(wt %) alkyd is due to butyl acrylate. The change of hybrid particle morphology to an alkyd rich core and acrylic rich shell after about 40-50% monomer conversion was verified by studying the evolution of N_p/N_d with monomer conversion. When all these factors are considered collectively, it can be concluded that a certain amount of monomer is trapped due to strong interactions between alkyd and monomer. This trapped monomer is not readily accessible to the growing polymer chain due to the increasing viscosity of the hybrid particles and this could be a possible reason for the observed limiting monomer conversion.

We have shown by controlling the hydrophobicity of organic phase, the broad droplet size distribution could be narrowed and hence homogeneous nucleation could be minimised. Finally we have synthesised an alkyd grafted copolymer of 50% solids and approximate particle size of 100nm. The maximum monomer conversion of this system is 96% and the ratio of N_p/N_d is 1.2. Future research on this system should be based on overcoming limiting monomer conversion without creating new particles.

PU-acrylic hybrid system

Starting with a non-reactive PU, stable hybrid miniemulsions and latexes could be achieved for the non-reactive PU- acrylic hybrid systems. Since the resulting latexes did not exhibit the desired product properties, reactive PU-acrylic systems were studied. The main reason for the failure of the non-reactive PU- acrylic system was the absence of any cross linking mechanism to incorporate PU into the copolymer. The advantage of using the reactive PU was the presence of NCO functional group which can chemically react with other compounds such as HEMA which contain an –OH functional group.

Conclusion

Since the success of using reactive PU mainly depends on the NCO functional group and the efficient chemical incorporation of it into the hybrid latex, the reactive PU was characterised qualitatively and quantitatively. The correct quantitative determination of NCO functional groups by conductimetry lead us to determine the exact amount of HEMA that completely reacted with NCO during a reaction period of overnight(12h). The importance of use of free NCO functional groups in hydrophobic chain extension by reacting with bisphenol A was emphasised and thereby the hydrophobicity and molecular weight of the reactive PU could be increased. By using free NCO functional groups in chain extension reaction, the loss of NCO functional groups via a reaction with water was also minimised. The conditions of using stoichiometric amount of bisphenol A based on free NCO groups were investigated and showed that under controlled hydrophobic conditions (in the absence of ODA), the stoichiometric amount of bisphenol A could be used. The amounts of HEMA, bisphenol A and 1-dodecylmercaptan were optimised using experiments that measured the properties of the final products. The hybrid latexes were tested for particular properties in both academic and industrial laboratories. Latex samples that met the desired specifications at the lab scale were subjected to further testing at the industrial scale. Accordingly we have successfully synthesised PU grafted acrylic hybrid latex of 50% solids with an approximate particle size of 100nm. This synthesis procedure is to be adapted on an industrial scale.

Appendix I

Appendix I: NMR spectra of pure alkyd resin and alkyd grafted copolymer

Sample A. 33mg. CDCl3, te=25.

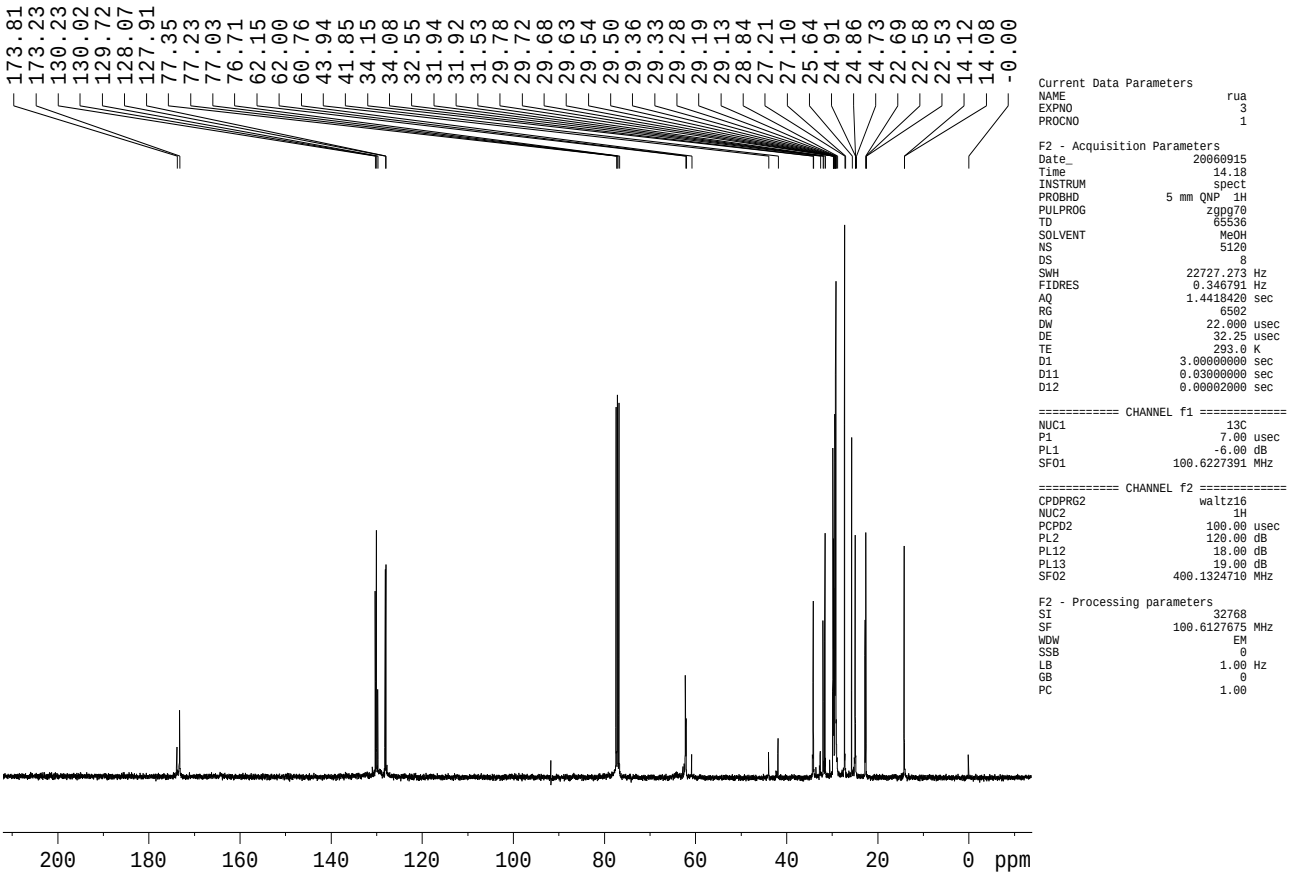

Current Data Parameters

NAME	rua
EXPNO	3
PROCNO	1

F2 - Acquisition Parameters

Date_	20060915
Time	14.18
INSTRUM	spect
PROBHD	5 mm QNP 1H
PULPROG	zgpg70
TD	65536
SOLVENT	MeOH
NS	5120
DS	8
SWH	22727.273 Hz
FIDRES	0.346791 Hz
AQ	1.4418420 sec
RG	6502
DW	22.000 usec
DE	32.25 usec
TE	293.0 K
D1	3.00000000 sec
D11	0.03000000 sec
D12	0.00002000 sec

========== CHANNEL f1 ==========

NUC1	13C
P1	7.00 usec
PL1	-6.00 dB
SFO1	100.6227391 MHz

========== CHANNEL f2 ==========

CPDPRG2	waltz16
NUC2	1H
PCPD2	100.00 usec
PL2	120.00 dB
PL12	18.00 dB
PL13	19.00 dB
SFO2	400.1324710 MHz

F2 - Processing parameters

SI	32768
SF	100.6127675 MHz
WDW	EM
SSB	0
LB	1.00 Hz
GB	0
PC	1.00

(a)

Appendix I

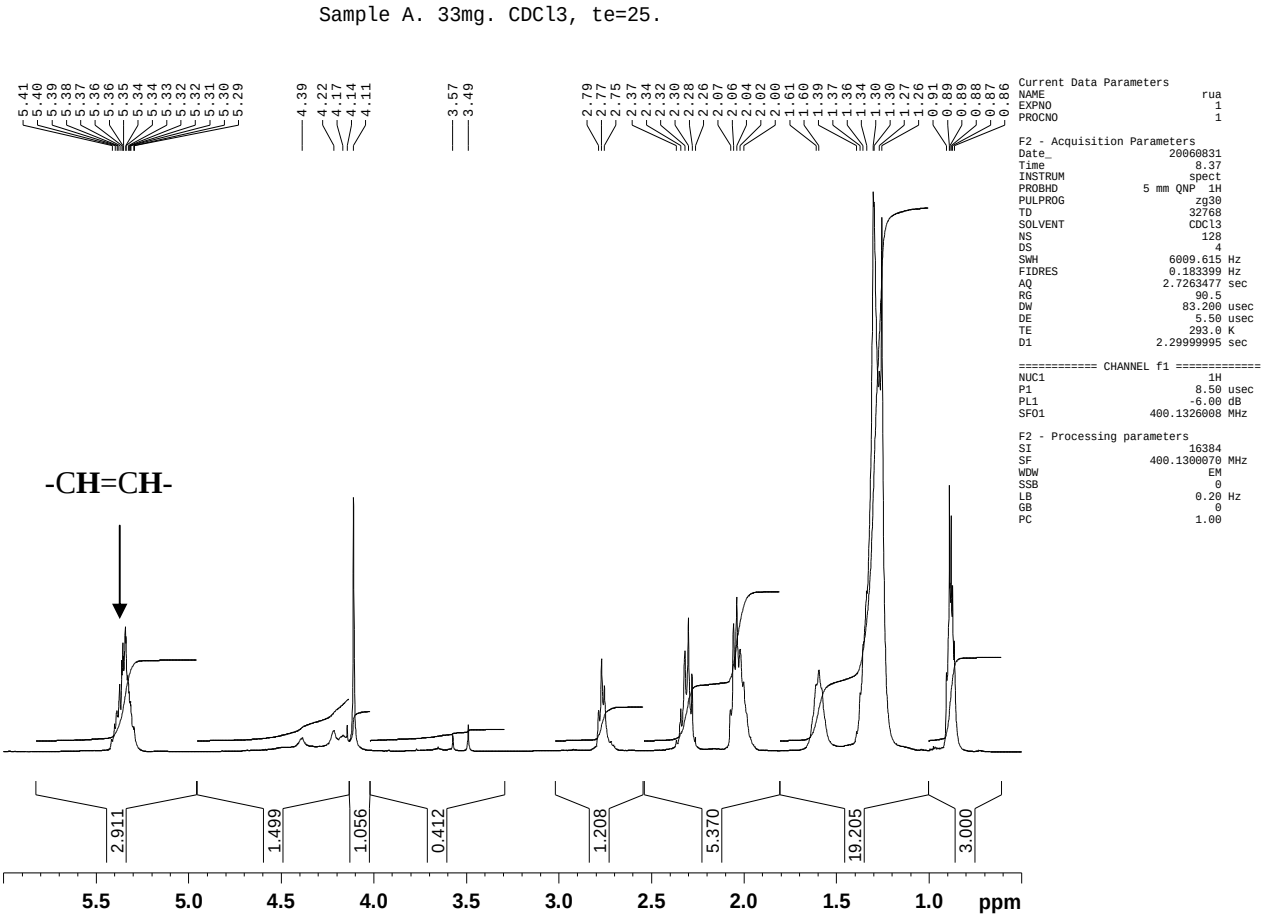

(b)

Figure 1(a). ^{1}H and ^{13}C NMR spectrum of pure alkyd Resin. (b) A selected enlarged region of ^{1}H and ^{13}C NMR spectrum of pure alkyd Resin.

Appendix I

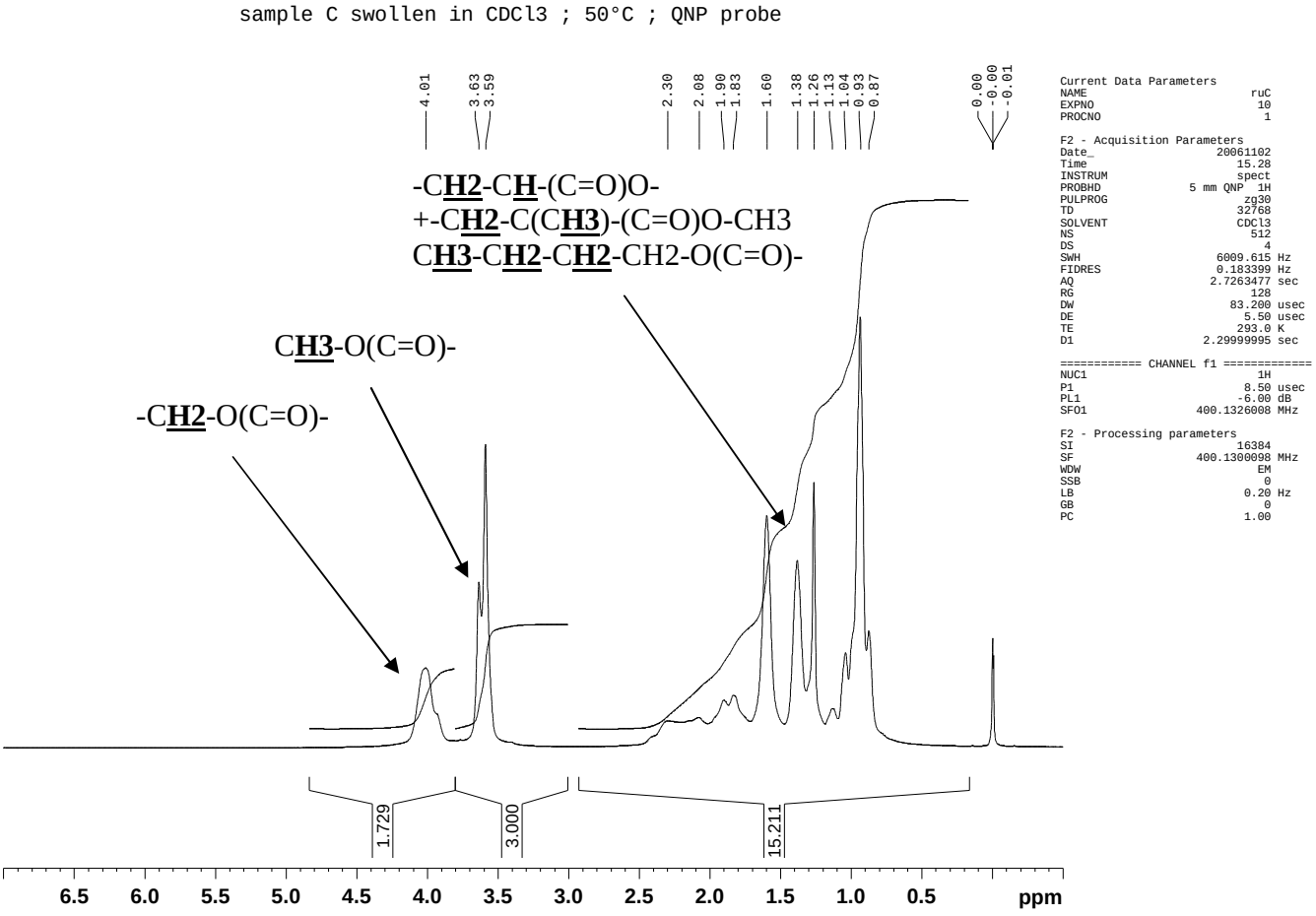

Figure 2. ^{1}H spectrum of alkyd (25%) grafted copolymer

Appendix II

Appendix II: Modifications to initiator and surfactant flow.

Table A1. Recipes for miniemulsion polymerization reactions

Run	H_2O (g)	Dowfax (g)	BA (g)	MMA (g)	AA (g)	Alkyd (g)	ODA (g)	KPS (1) (g)	KPS(2) (g)	$NaHSO_3$ (g)	TBHP (g)	SFS (g)
17[a]	133.0	4.03	45.0	45.00	0.90	25.0	9.41	0.18	-	-	0.31	0.72
18[b]	122.5	2.01	23.0	23.00	0.51	12.5	5.20	0.11	0.12	0.25	0.22	0.15
19[c]	125.5	4.02	45.0	45.00	0.90	10.1	9.41	0.17	0.12	0.25	0.22	0.16
20[d]	125.5	4.00	90.0	-	0.93	25.0	9.40	0.16	0.12	0.25	0.22	0.16
21[e]	125.5	4.04	-	90.00	0.90	25.0	9.40	0.16	0.12	0.25	0.22	0.16
22[f]	125.5	4.00	45.0	45.00	0.90	-	9.40	0.16	0.12	0.24	0.22	0.16
23[g]	127.5	4.02	45.0	45.00	0.91	25.0	9.40	0.16	0.12	-	0.22	0.16
24[h]	117.0	4.01	45.0	45.00	0.91	25.0	9.46	0.16	-	-	0.22	0.16
25[i]	122.0	4.04	45.0	45.00	0.90	25.0	9.44	0.20	-	-	-	-
26[j]	117.0	4.00	45.1	45.10	0.90	25.1	4.54	0.21	-	-	-	-

[a] In addition to SFS, EDTA (1.6g) & FeSo4 (0.48g) were coupled with TBHP and added semi continuously for 4h at 6ml/h. [b]Theoretical solid content was lowered to 35%. [c]The resin quantity was lowered to 10(% wt. by monomer). [d] Only BA and AA were used as monomers. [e] Only MMA and AA were used as monomers. [f] No resin was used. [g] 5g of MMA in 5ml of water with 0.12% KPS in 3ml of water was added semi continuously for 1h. [h] 0.14%wt LPO in 10g of Ethyl Acetate was added semi-continuously for 1h after 2h from the beginning of reaction and the redox system of TBHP was added after 3h. [i] Only one dose of KPS was added. [j] After 2h, 0.14%wt LPO in 5g of MMA was added as only one dose.

Appendix III

Appendix III: A summary of experiments carried out to increase monomer conversion

Table A2

Experiment No.	Brief Description
T 6	Percentage of resin (wt: by total monomer) 2.50. Total Solid Content (TSC) theoretical: 40.4%; TSC (actual): 40%; Monomer conversion: 100.0%. Injection of initiator at t=0h, 0.4 %(wt. by monomer) KPS (one dose) only.
T 7	Percentage of resin (wt: by total monomer) 10. TSC (theoretical): 42.0%; TSC (actual): 39.7%; Monomer conversion: 94.0%. Injection of initiator at t=0h, 0.4 %(wt: by monomer) KPS (one dose) only.
T 8	Percentage of resin (by total monomer) 20. TSC (theoretical): 43.0%; TSC (actual): 41.8%; Monomer conversion: 96.1%. Injection of initiator at t=0h, 0.4 %(wt: by monomer) KPS (one dose) & at t=2h, 0.1% KPS (one dose) only.
T 30	Percentage of resin (by total monomer) 24.1. TSC (theoretical): 47.65%; TSC (actual): 42.43%; Monomer conversion: 86.0%. Injection of initiator at t=0h, 0.2 %(wt: by monomer) KPS (one dose) & at t=2h, 0.4% KPS coupled with NaHSO3 semi continuously for 1h.
T 31	Percentage of resin (by total monomer) 24.1. TSC (theoretical): 49.5%; TSC (actual): 46.1%; Monomer conversion: 91.30%. Injection of initiator at t=0h, 0.2 %(wt: by monomer) KPS (one dose) & at t=2h, 0.12% KPS coupled with NaHSO3 semi continuously for 1h. At t=3h, 0.17 %(wt: by monomer) TBHP coupled with SFS (One dose).
T 32	Percentage of resin (by total monomer) 24.1. TSC (theoretical): 49.53%; TSC (actual): 45.9%; Monomer conversion: 90.70%. Injection of initiator at t=0h, 0.2 %(wt: by monomer) KPS (one dose) & at t=2h, 0.12% KPS coupled with NaHSO3 semi continuously for 1h. At t=3h, 0.17 %(wt: by monomer) TBHP coupled with SFS (One dose). At t=5h, another dose (As at t=3h) of redox system.
T 33	Percentage of resin (by total monomer) 24.1. TSC (theoretical): 50.4%; TSC (actual): 47.46%; Monomer conversion: 92.50%. Initiator system similar to T32. After 3h semi continuous addition of BA for 2h at 1ml/h.
T 38	Percentage of resin (by total monomer) 24.1.TSC (theoretical): 49.64%; TSC (actual): 47.26%; Monomer conversion: 94.00%. Initiator system similar to T32. Resin Vacuum distilled.

Appendix III

Table A3

Experiment No.	Brief Description
T 40	Percentage of resin (by total monomer) 24.1. TSC (theoretical): 49.65%; TSC (actual): 48.42%; Monomer conversion: 96.70%. Injection of initiator at t=0h, 0.15 %(wt: by monomer) KPS (one dose) & at t=2h, 0.12% KPS coupled with NaHSO3 semi continuously for 1h. At t=3h, 0.17 %(wt: by monomer) TBHP coupled with SFS (One dose). Resin Vacuum distilled.
T 41	Percentage of resin (by total monomer) 24.1. TSC (theoretical): 49.61%; TSC (actual): 47.00%; Monomer conversion: 93.34%. Initiator system similar to T41. Resin Vacuum distilled with the addition of Ethyl Acetate.
T 44	Percentage of resin (by total monomer) 24.1. TSC (theoretical): 50.23%; TSC (actual): 47.55%; Monomer conversion: 93.26%. Injection of initiator at t=0h, 0.15 %(wt: by monomer) KPS (one dose) & at t=2h, 0.12% KPS coupled with NaHSO3 semi continuously for 1h. Resin Vacuum distilled with the addition of Ethyl Acetate.
T 56	Percentage of resin (by total monomer) 33.6. TSC (theoretical): 49.2%; TSC (actual): 47.5%; Monomer conversion: 95.31%. Injection of initiator at t=0h, 0.15 %(wt: by monomer) KPS (one dose) & at t=2h, 0.12% KPS coupled with NaHSO3 semi continuously for 1h. At t=3h, 0.17 %(wt: by monomer) TBHP coupled with SFS (One dose). Resin Vacuum distilled without the addition of Ethyl Acetate.
T 58	Percentage of resin (by total monomer) 40. TSC (theoretical): 52.68%; TSC (actual): 48.9%; Monomer conversion: 88.72%. Injection of initiator at t=0h, 0.15 %(wt: by monomer) KPS (one dose) & at t=2h, 0.12% KPS coupled with NaHSO3 semi continuously for 1h. At t=3h, 0.17 %(wt: by monomer) TBHP coupled with SFS (One dose). Resin Vacuum distilled without the addition of Ethyl Acetate.
T 59	Percentage of resin (by total monomer) 20. TSC (theoretical): 48.8%; TSC (actual): 47.8%; Monomer conversion: 97.5%. Injection of initiator at t=0h, 0.15 %(wt: by monomer) KPS (one dose) & at t=2h, 0.12% KPS coupled with NaHSO3 semi continuously for 1h. At t=3h, 0.17 %(wt: by monomer) TBHP coupled with SFS (One dose). Resin Vacuum distilled without the addition of Ethyl Acetate.

Appendix III

Table A4

Experiment No.	Brief Description
T 61	Percentage of resin (by total monomer) 25. TSC (theoretical): 50.89%; TSC (actual): 47.57%; Monomer conversion: 91.53%. Injection of initiator at t=0h, 0.15 %(wt: by monomer) KPS (one dose) & at t=3h, 0.21 %(wt: by monomer) TBHP coupled with SFS, EDTA & FeSo4 semi continuously for 4h at 6ml/h. Resin Vacuum distilled without the addition of Ethyl Acetate.
T 63	Percentage of resin (by total monomer) 24.3. TSC (theoretical): 34.57%; TSC (actual): 33.50%; Monomer conversion: 96.14%. Injection of initiator at t=0h, 0.10 %(wt: by monomer) KPS (One dose) & at t=1.5h, 0.12% KPS coupled with NaHSO3 semi continuously for 1h. At t=3h, 0.17 %(wt: by monomer) TBHP coupled with SFS (One dose).Resin Vacuum distilled without the addition of Ethyl Acetate.
T 64	Percentage of resin (by total monomer) 10.0. TSC (theoretical): 46.74%; TSC (actual): 45.60%; Monomer conversion: 97.25%. Injection of initiator at t=0h, 0.15% (wt: by monomer) KPS (One dose) & at t=1.5h, 0.12% KPS coupled with NaHSO3 semi continuously for 1h. At t=3h, 0.17 %(wt: by monomer) TBHP coupled with SFS (One dose).Resin Vacuum distilled without the addition of Ethyl Acetate.
T68	Percentage of resin [by total monomer (BA only)] 25. TSC (theoretical): 49.86%; TSC (actual): 47.96%; Monomer conversion: 95.14%. Initiator system similar to T64. Resin Vacuum distilled without the addition of Ethyl Acetate.
T69	Percentage of resin [by total monomer (MMA only)] 25. TSC (theoretical): 51.6%; TSC (actual): 51.3%; Monomer conversion: 99.3%. Initiator system similar to T68. Resin Vacuum distilled without the addition of Ethyl Acetate.
T73	Percentage of resin (by total monomer) 0. TSC (theoretical): 44.9%; TSC (actual): 44.9%; Monomer conversion: 100%. Initiator system similar to T69.
T75	Percentage of resin [by total monomer (BA only)] 0. TSC (theoretical): 44.4%; TSC (actual): 44.4%; Monomer conversion: 100.0%. Initiator system similar to T69.

Appendix III

Table A5

Experiment No.	Brief Description
T 76	Percentage of resin (by total monomer) 25.0. TSC (theoretical): 50.41%; TSC (actual): 48.70%; Monomer conversion: 95.51%. Injection of initiator at t=0h, 0.15% (wt: by monomer) KPS (One dose) & at t=2h, 5g of MMA in 5g of water with 0.12% KPS in 3ml of water semi continuously for 1h. At t=3h, 0.17 %(wt: by monomer) TBHP coupled with SFS (One dose).Resin Vacuum distilled without the addition of Ethyl Acetate.
T 79	Percentage of resin (by total monomer) 25. TSC (theoretical): 49.2%; TSC (actual): 48.25%; Monomer conversion: 97.5%. Injection of initiator at t=0h, 0.15% (wt: by monomer) KPS (One dose) & at t=1.5h, 0.14% LPO in 10g of Ethyl Acetate semi continuously for 1h. At t=3h, 0.17 %(wt: by monomer) TBHP coupled with SFS (One dose).Resin Vacuum distilled without the addition of Ethyl Acetate.
T 82	Percentage of resin (by total monomer) 25. TSC (theoretical): 50.62%; TSC (actual): 47.4%; Monomer conversion: 91.92%. Injection of initiator at t=0h, 0.2% (wt: by monomer) KPS (One dose) only.
T 83	Percentage of resin (by total monomer) 25. TSC (theoretical): 51.66%; TSC (actual): 49.52%; Monomer conversion: 94.74%. Injection of initiator at t=0h, 0.2% (wt: by monomer) KPS (One dose) only. At t=2h, 0.14% LPO in 5g of MMA (one dose) only.

Appendix IV

Appendix IV: The variation of N_p/N_d with monomer conversion relevant to the experiments described in Tables A2 to A5.

Experiment T6 :

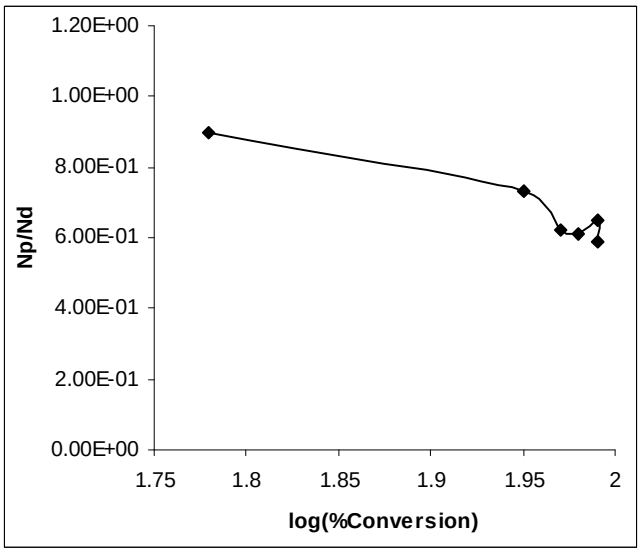

Experiment T7 :

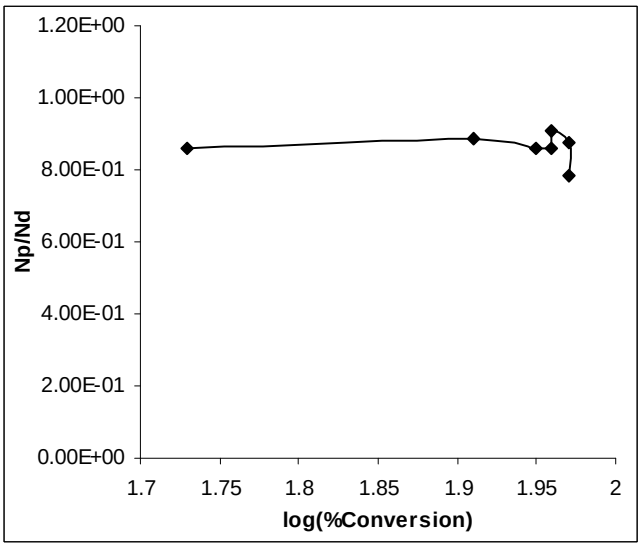

Experiment T8 :

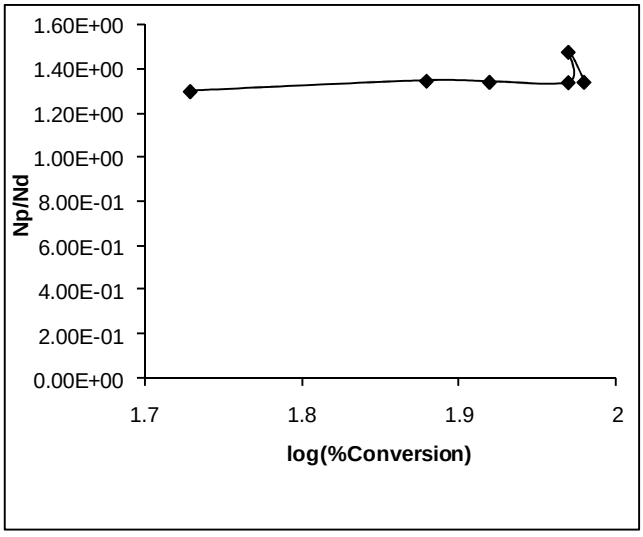

Experiment T30 :

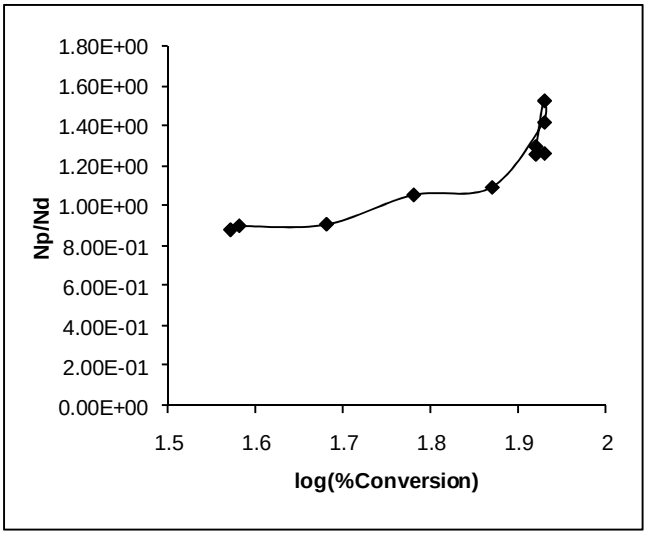

Appendix IV

Experiment T31

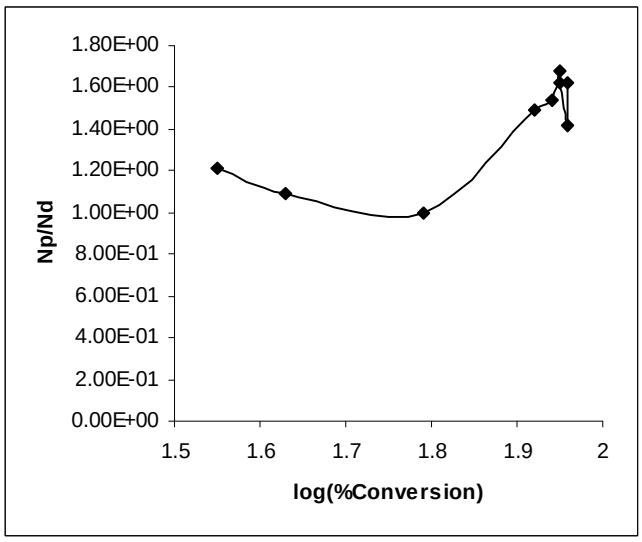

Experiment T32

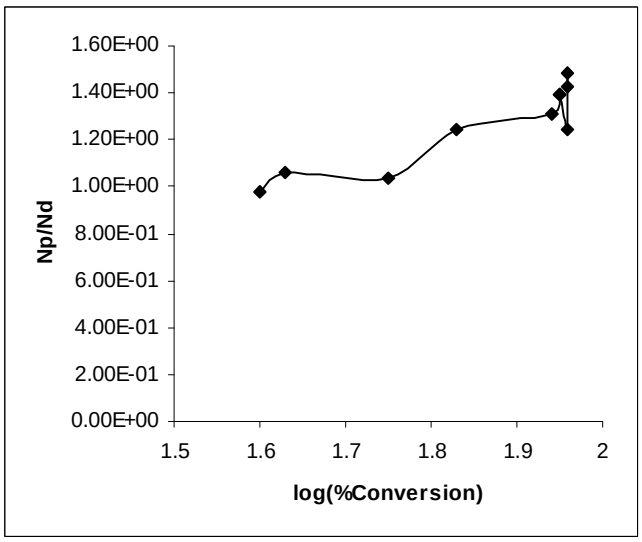

Experiment T33

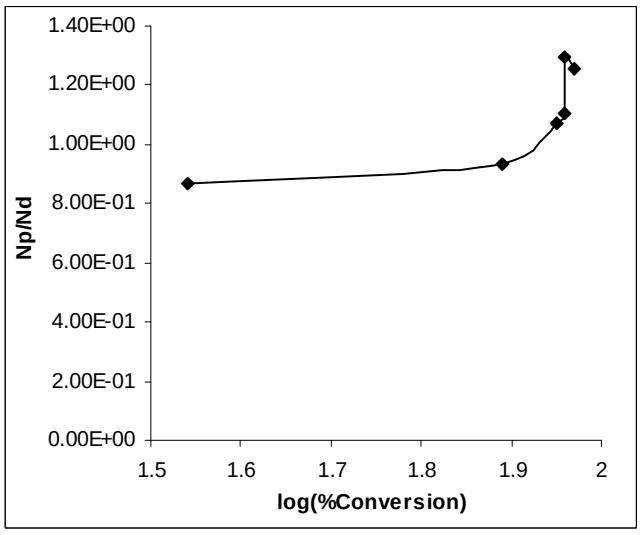

Experiment T38

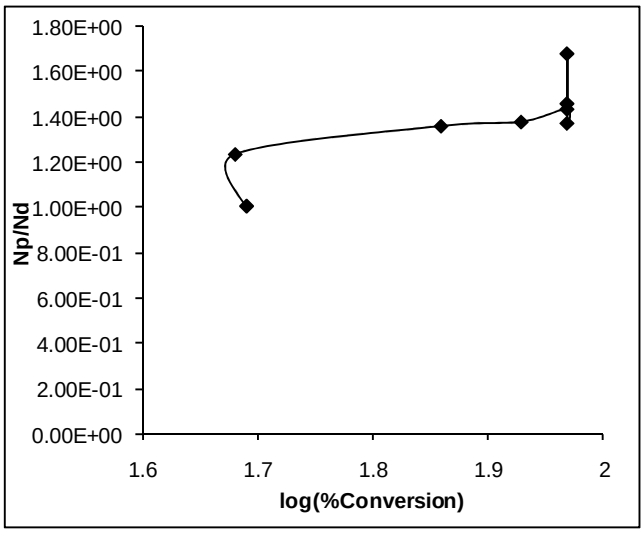

Appendix IV

Experiment T40

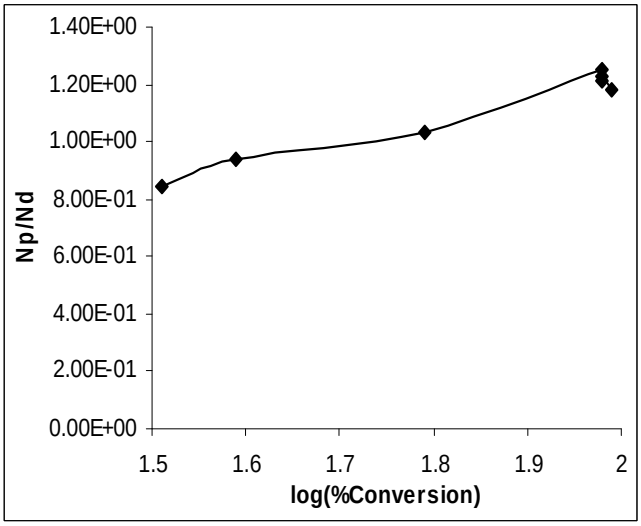

Experiment T41

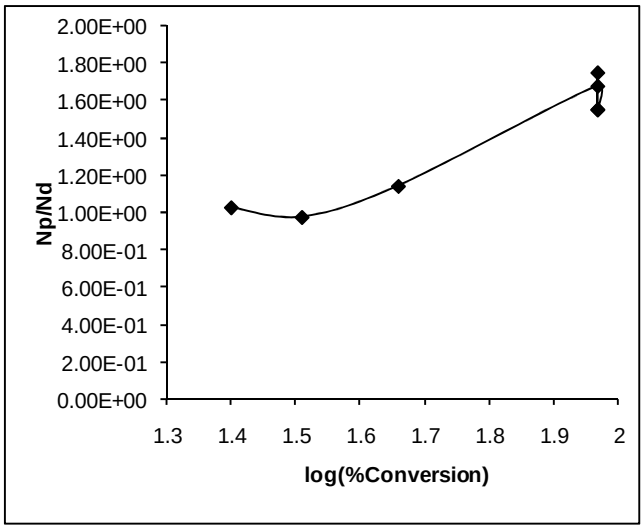

Experiment T44

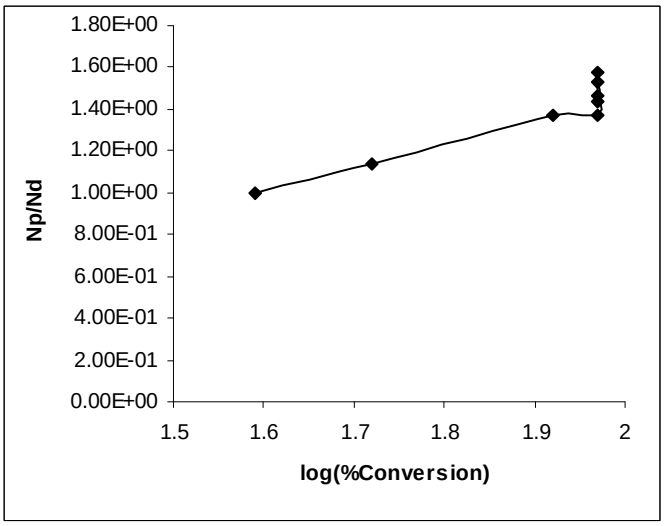

Experiment T56

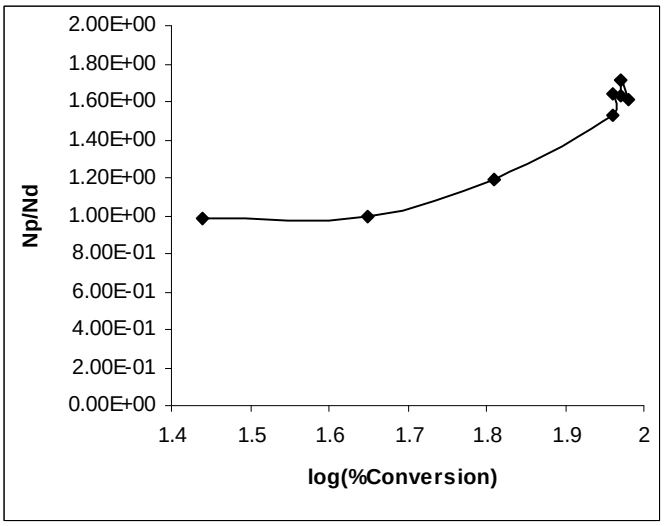

Appendix IV

Experiment T58

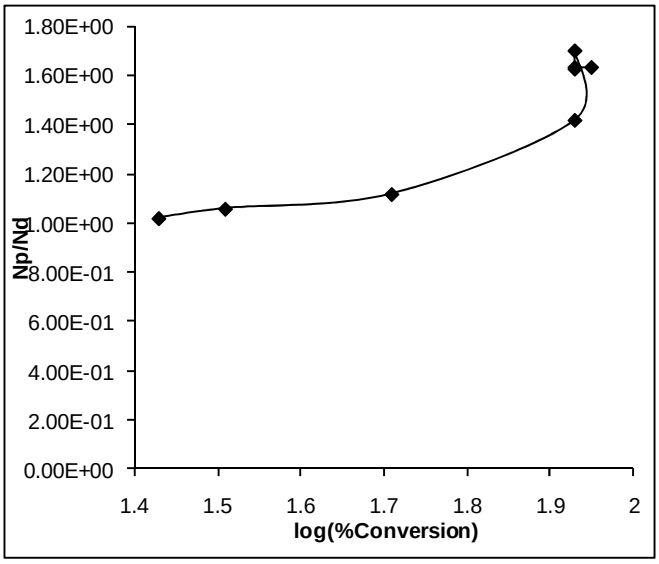

Experiment T59

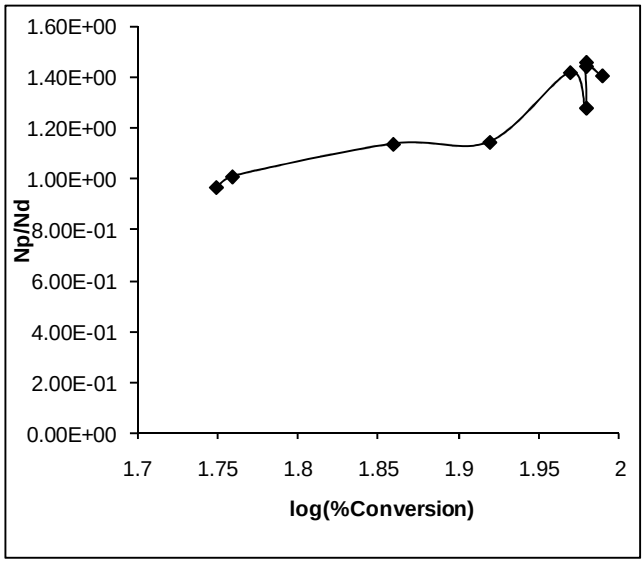

Experiment T61

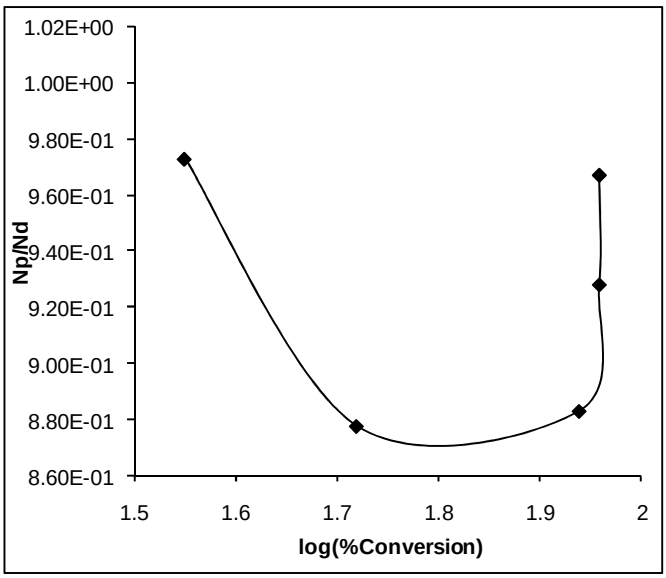

Experiment T63

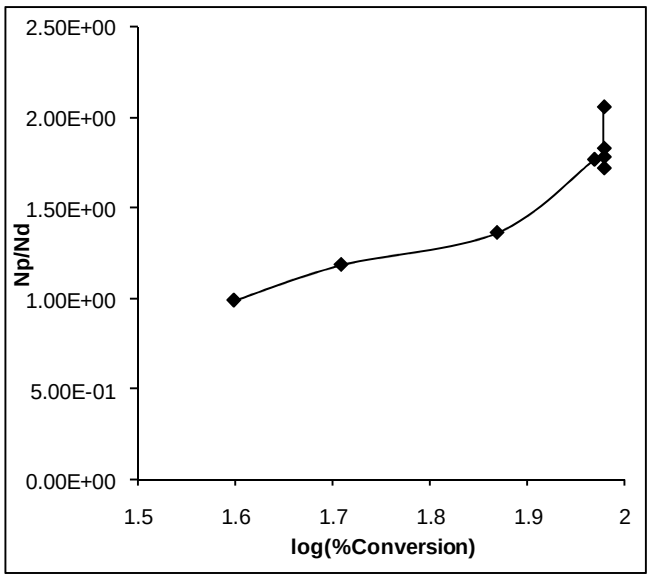

Appendix IV

Experiment T64

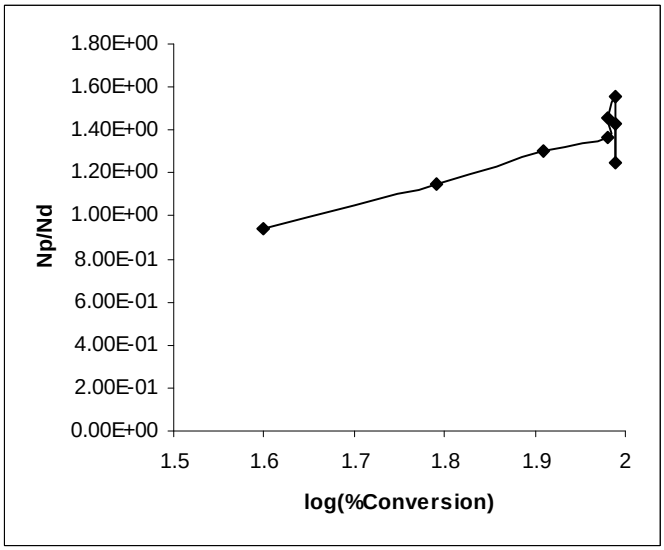

Experiment T68

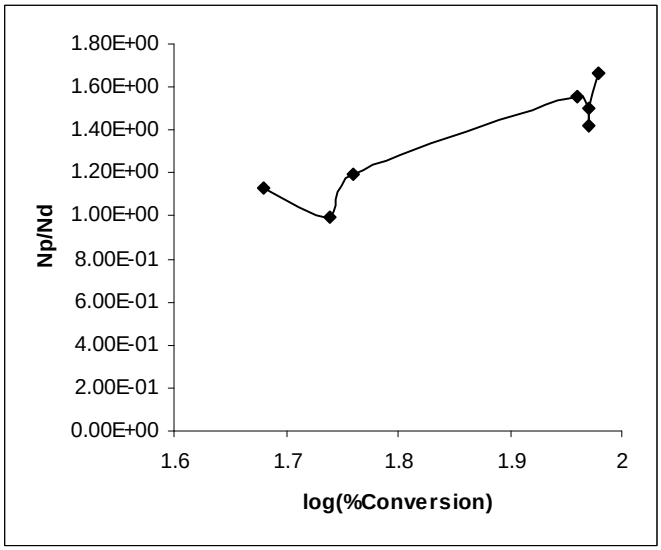

Experiment T69

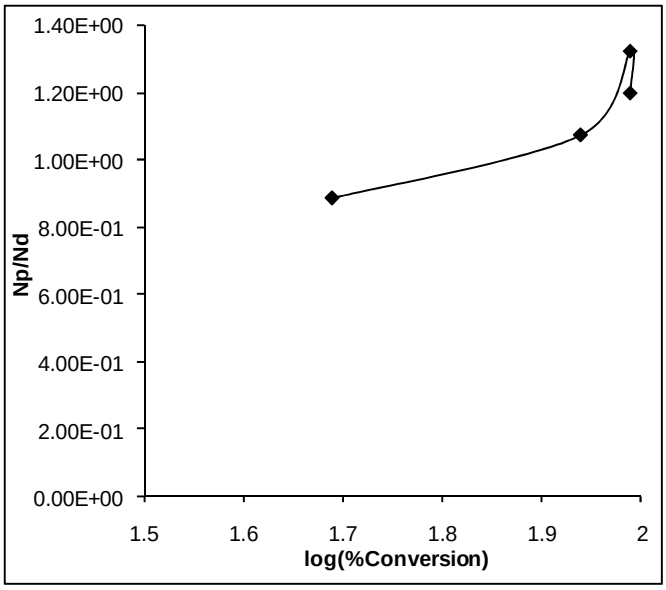

Experiment T73

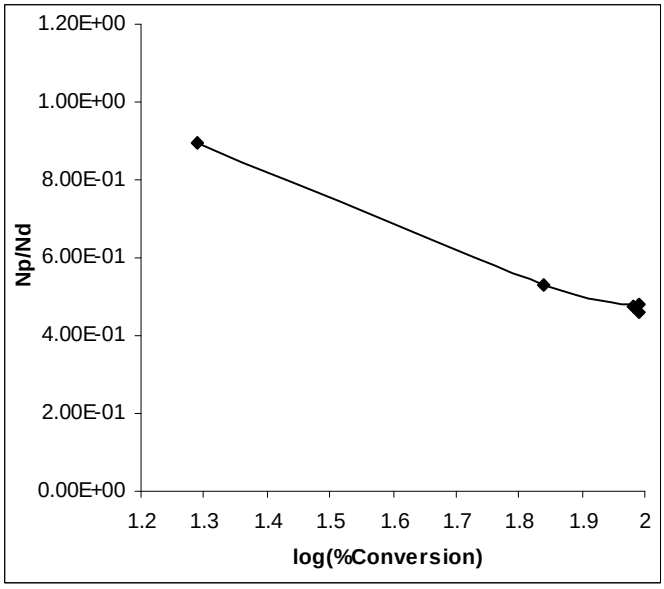

Appendix IV

Experiment T75

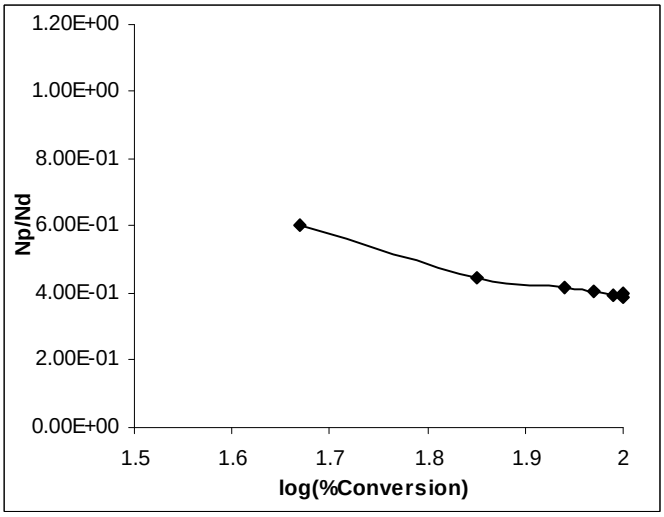

Experiment T76

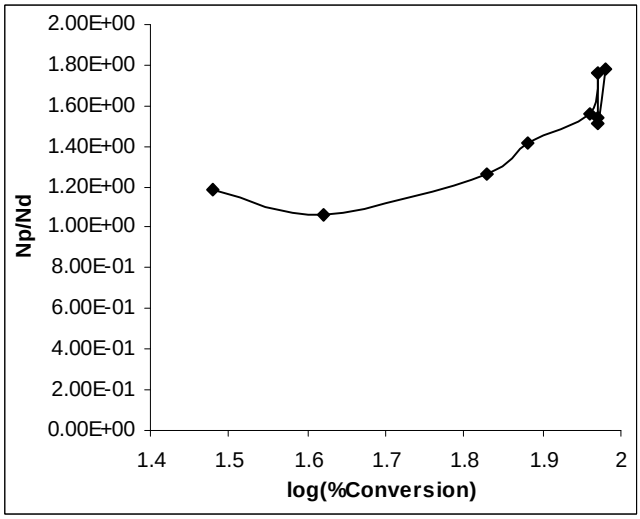

Experiment T79

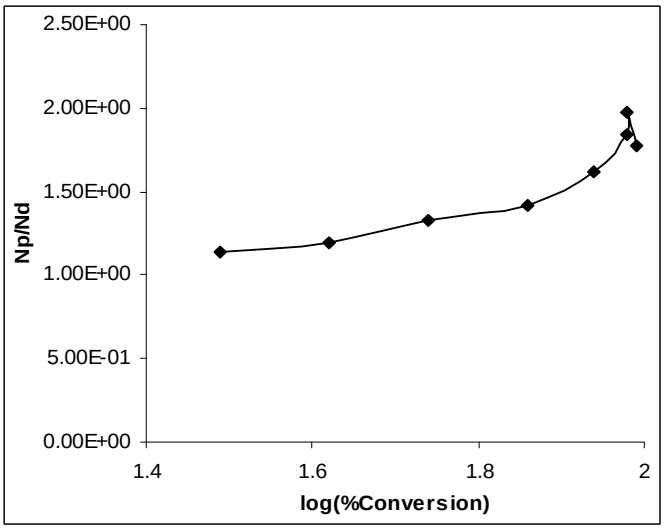

Experiment T82

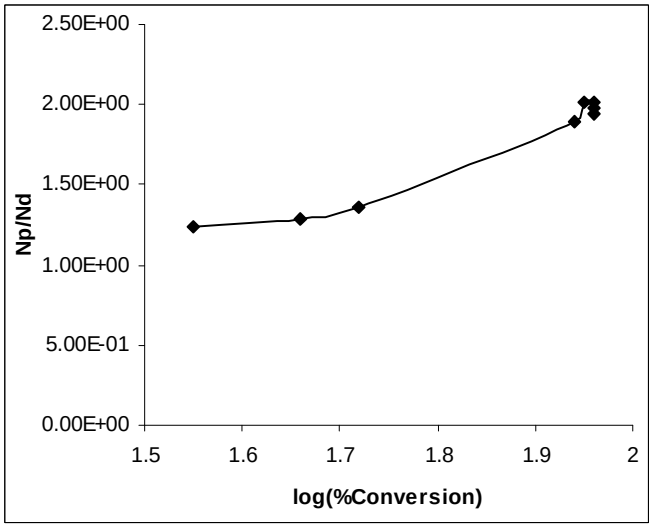

Appendix V

Appendix V: Droplet size distribution of the miniemulsions with alkyd (25%) and ODA (T-78) & without ODA and with alkyd (25%) [T-100]

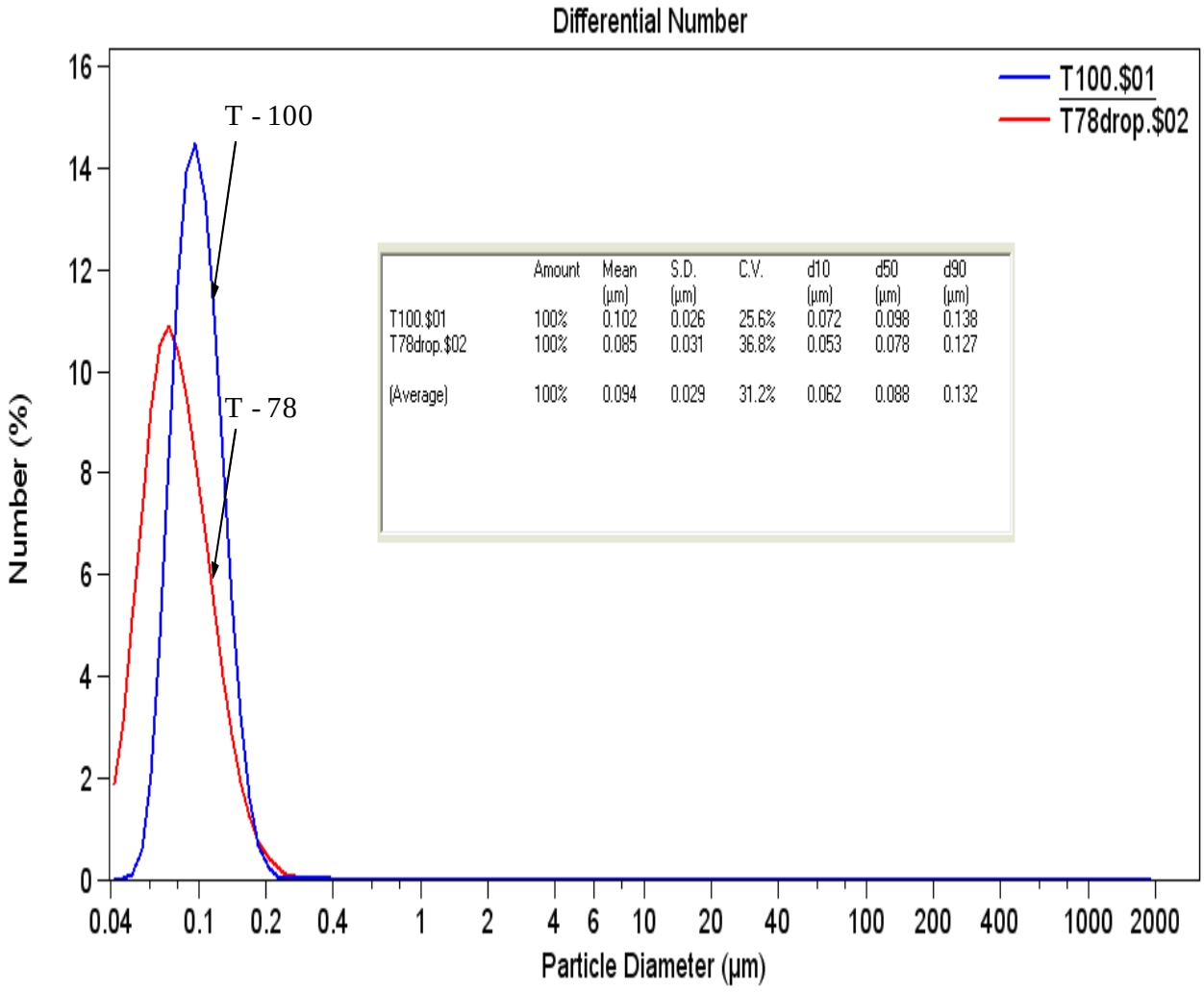

	Amount	Mean (µm)	S.D. (µm)	C.V.	d10 (µm)	d50 (µm)	d90 (µm)
T100.$01	100%	0.102	0.026	25.6%	0.072	0.098	0.138
T78drop.$02	100%	0.085	0.031	36.8%	0.053	0.078	0.127
(Average)	100%	0.094	0.029	31.2%	0.062	0.088	0.132

Figure 1.Droplet size distribution by number

Appendix V

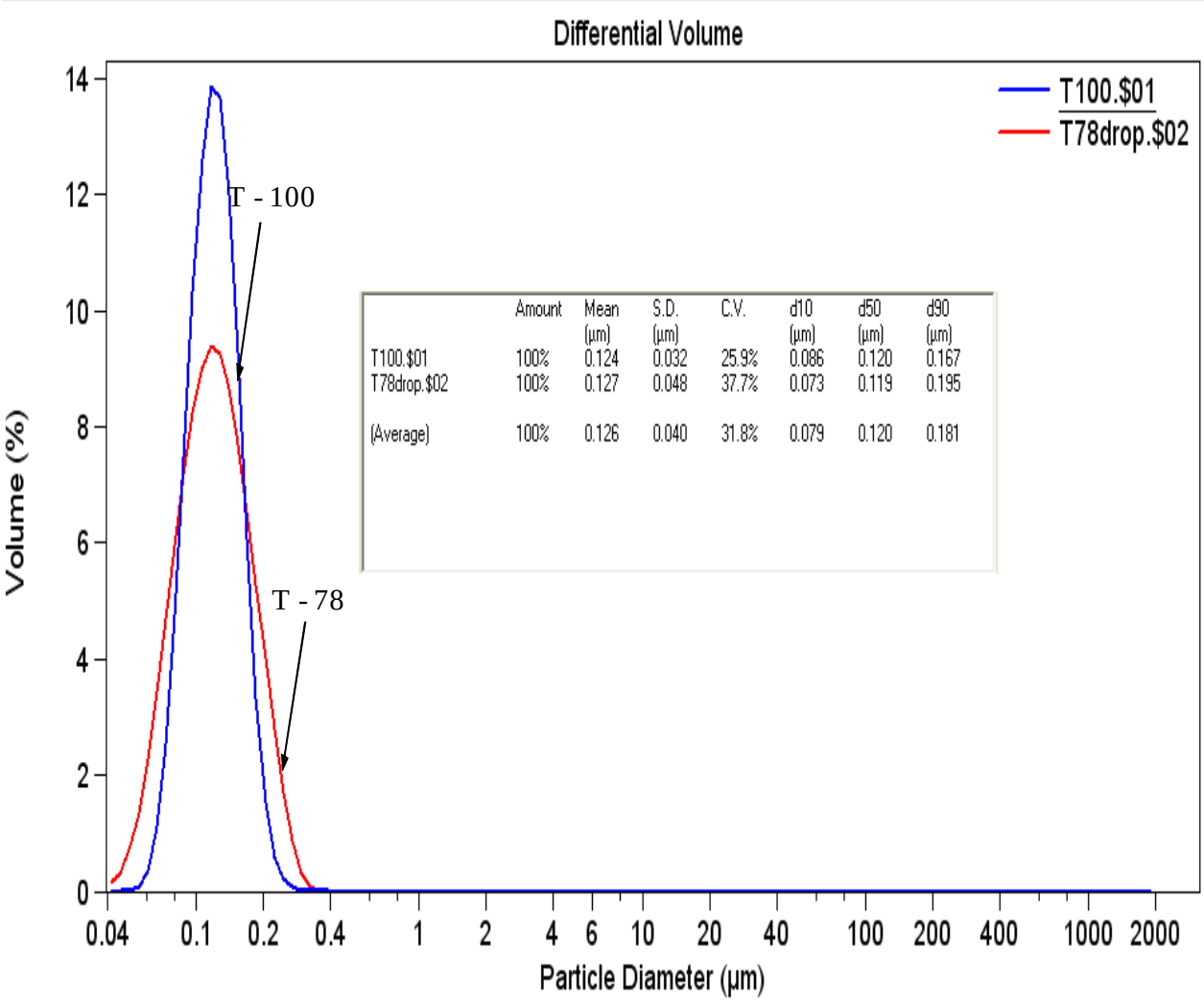

	Amount	Mean (µm)	S.D. (µm)	C.V.	d10 (µm)	d50 (µm)	d90 (µm)
T100.$01	100%	0.124	0.032	25.9%	0.086	0.120	0.167
T78drop.$02	100%	0.127	0.048	37.7%	0.073	0.119	0.195
(Average)	100%	0.126	0.040	31.8%	0.079	0.120	0.181

Figure 2. Droplet size distribution by volume

Appendix VI: The evolution of droplet and particle size distribution of the miniemulsions with alkyd (25%) and ODA (T-78)

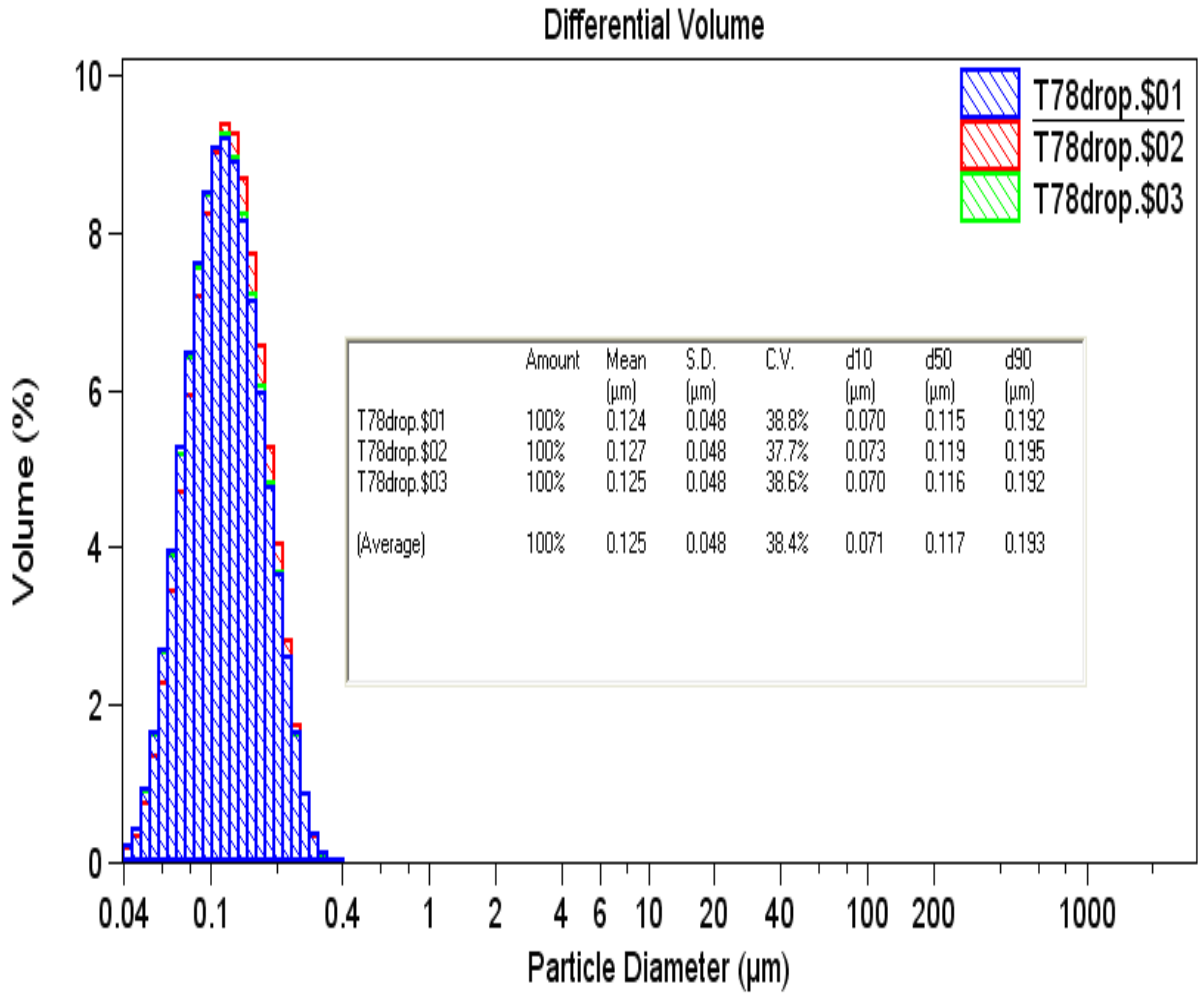

	Amount	Mean (µm)	S.D. (µm)	C.V.	d10 (µm)	d50 (µm)	d90 (µm)
T78drop.$01	100%	0.124	0.048	38.8%	0.070	0.115	0.192
T78drop.$02	100%	0.127	0.048	37.7%	0.073	0.119	0.195
T78drop.$03	100%	0.125	0.048	38.6%	0.070	0.116	0.192
(Average)	100%	0.125	0.048	38.4%	0.071	0.117	0.193

Figure 1. Droplet size distribution by volume before polymerization

Appendix VI

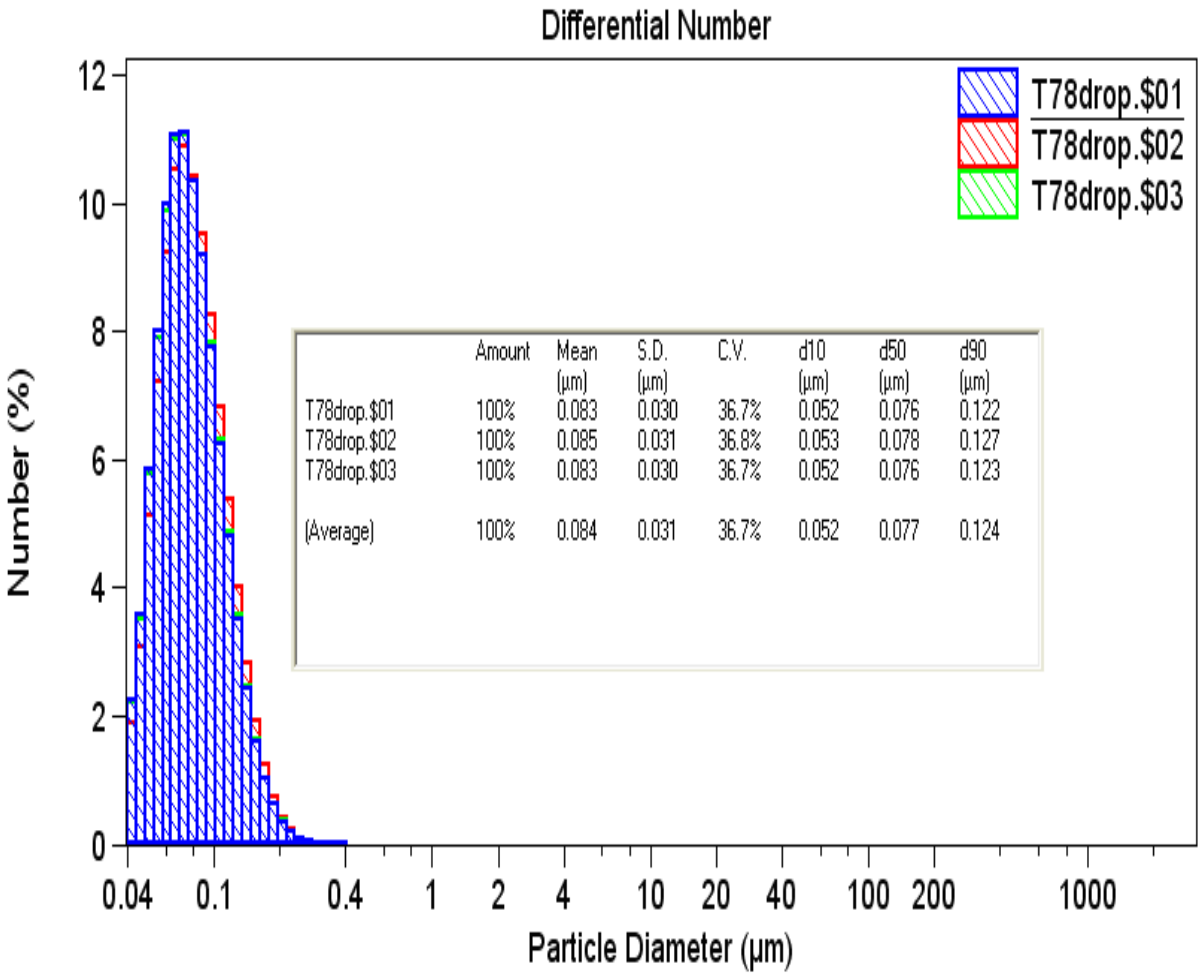

Figure 2. Droplet size distribution by number before polymerization

The following distributions refer to particle size distribution of the samples of T78 taken at different time intervals during polymerization. From p1 to p8 correspond to the samples taken at 15, 30, 60, 90, 180, 240, 300, and 360 minutes from the beginning of polymerization. It should be noticed that a considerable rearrangement of particle size distribution by number takes place. When this rearrangement is concerned it is clear that very small droplets react first and hence the fraction of very small droplet disappears gradually with polymerization.

Appendix VI

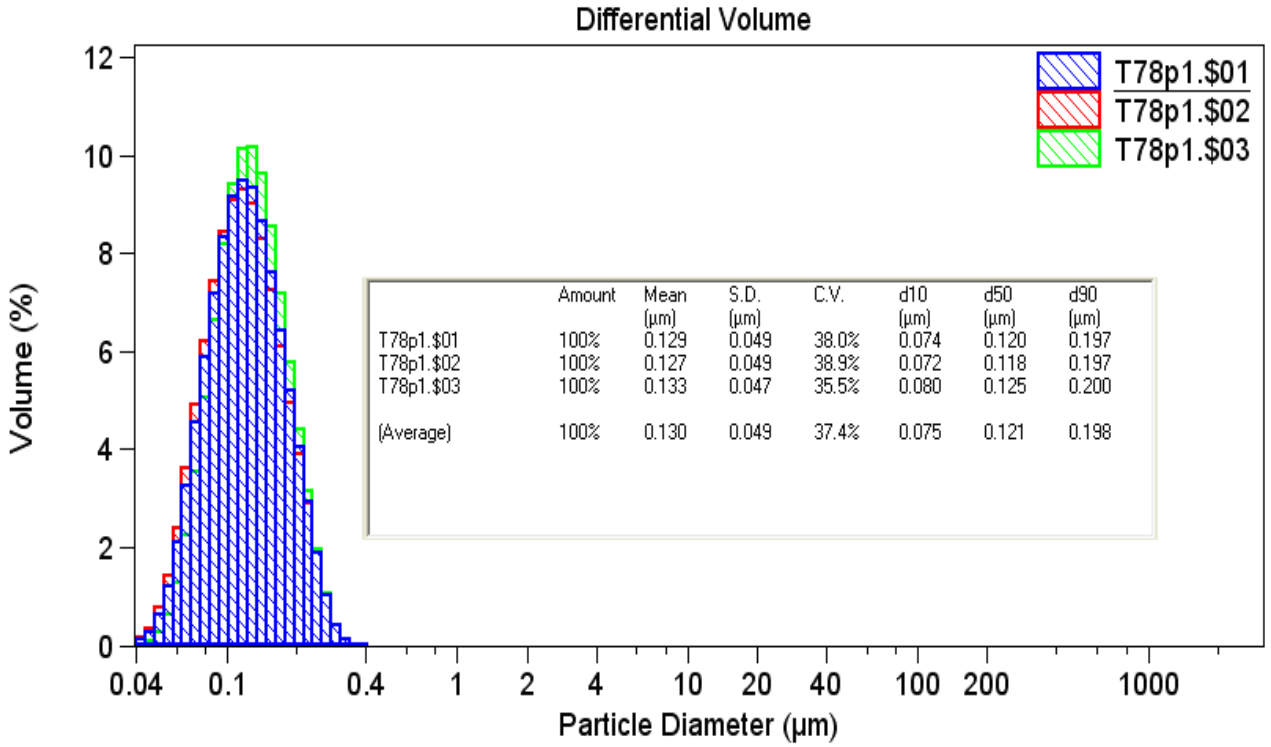

	Amount	Mean (µm)	S.D. (µm)	C.V.	d10 (µm)	d50 (µm)	d90 (µm)
T78p1.$01	100%	0.129	0.049	38.0%	0.074	0.120	0.197
T78p1.$02	100%	0.127	0.049	38.9%	0.072	0.118	0.197
T78p1.$03	100%	0.133	0.047	35.5%	0.080	0.125	0.200
(Average)	100%	0.130	0.049	37.4%	0.075	0.121	0.198

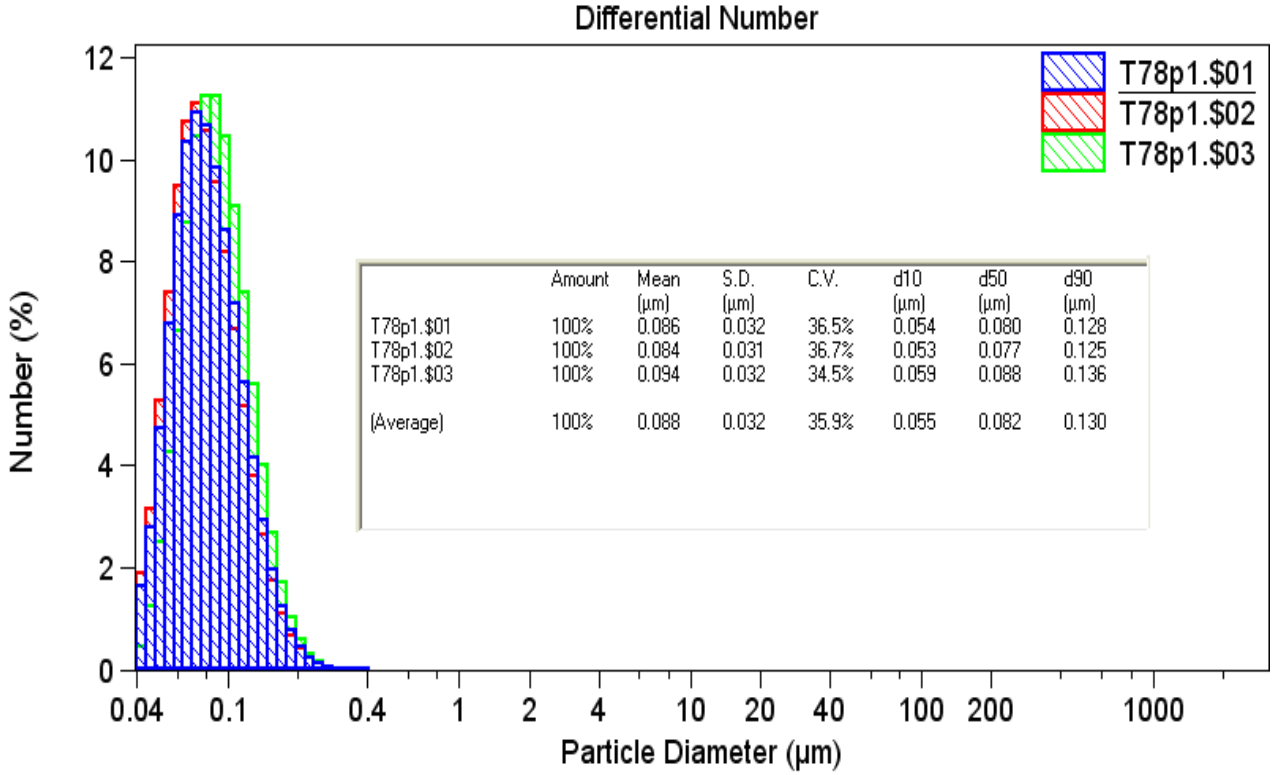

	Amount	Mean (µm)	S.D. (µm)	C.V.	d10 (µm)	d50 (µm)	d90 (µm)
T78p1.$01	100%	0.086	0.032	36.5%	0.054	0.080	0.128
T78p1.$02	100%	0.084	0.031	36.7%	0.053	0.077	0.125
T78p1.$03	100%	0.094	0.032	34.5%	0.059	0.088	0.136
(Average)	100%	0.088	0.032	35.9%	0.055	0.082	0.130

Appendix VI

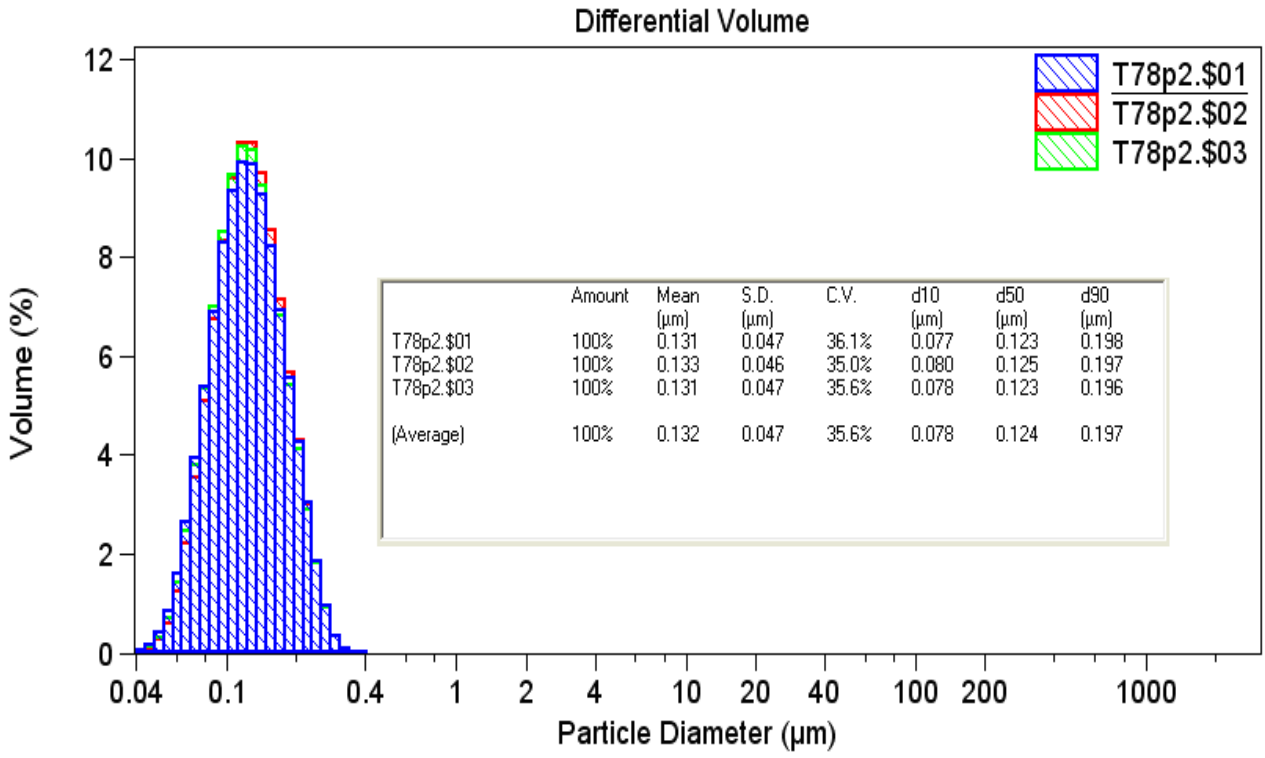

	Amount	Mean (µm)	S.D. (µm)	C.V.	d10 (µm)	d50 (µm)	d90 (µm)
T78p2.$01	100%	0.131	0.047	36.1%	0.077	0.123	0.198
T78p2.$02	100%	0.133	0.046	35.0%	0.080	0.125	0.197
T78p2.$03	100%	0.131	0.047	35.6%	0.078	0.123	0.196
(Average)	100%	0.132	0.047	35.6%	0.078	0.124	0.197

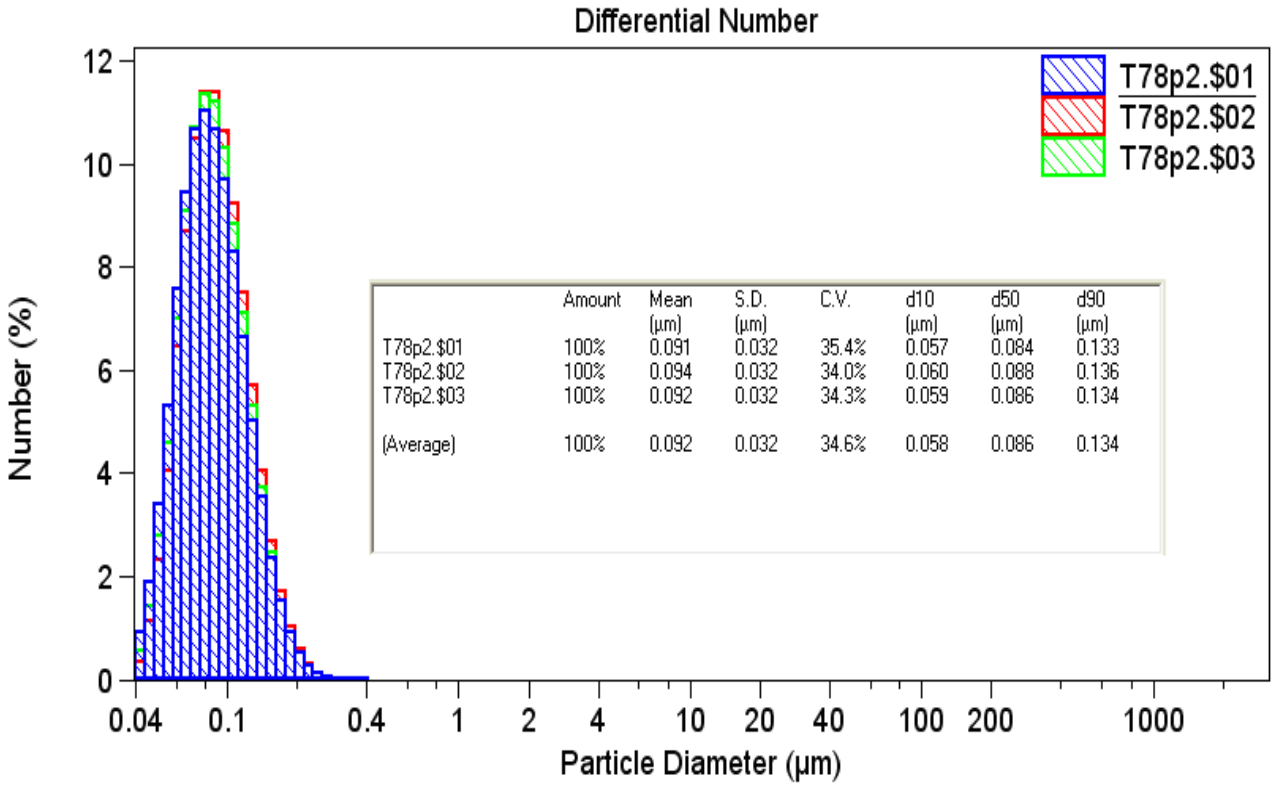

	Amount	Mean (µm)	S.D. (µm)	C.V.	d10 (µm)	d50 (µm)	d90 (µm)
T78p2.$01	100%	0.091	0.032	35.4%	0.057	0.084	0.133
T78p2.$02	100%	0.094	0.032	34.0%	0.060	0.088	0.136
T78p2.$03	100%	0.092	0.032	34.3%	0.059	0.086	0.134
(Average)	100%	0.092	0.032	34.6%	0.058	0.086	0.134

Appendix VI

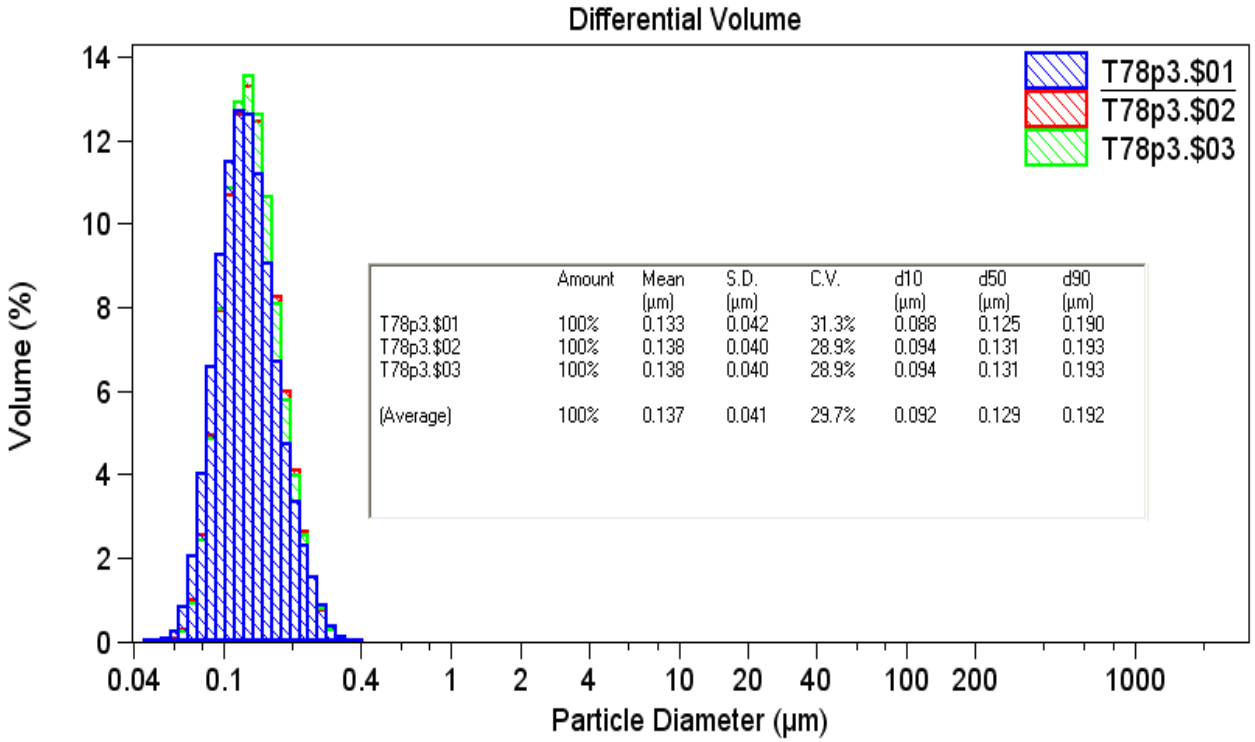

	Amount	Mean (µm)	S.D. (µm)	C.V.	d10 (µm)	d50 (µm)	d90 (µm)
T78p3.$01	100%	0.133	0.042	31.3%	0.088	0.125	0.190
T78p3.$02	100%	0.138	0.040	28.9%	0.094	0.131	0.193
T78p3.$03	100%	0.138	0.040	28.9%	0.094	0.131	0.193
(Average)	100%	0.137	0.041	29.7%	0.092	0.129	0.192

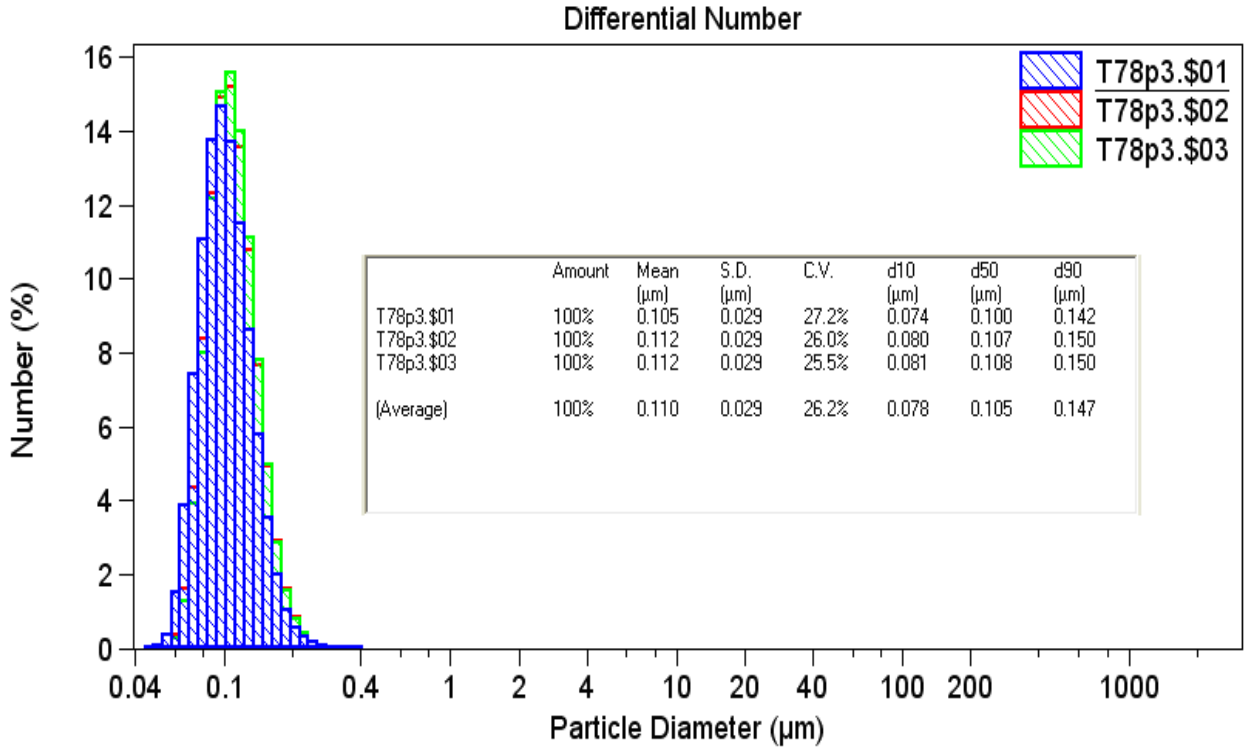

	Amount	Mean (µm)	S.D. (µm)	C.V.	d10 (µm)	d50 (µm)	d90 (µm)
T78p3.$01	100%	0.105	0.029	27.2%	0.074	0.100	0.142
T78p3.$02	100%	0.112	0.029	26.0%	0.080	0.107	0.150
T78p3.$03	100%	0.112	0.029	25.5%	0.081	0.108	0.150
(Average)	100%	0.110	0.029	26.2%	0.078	0.105	0.147

Appendix VI

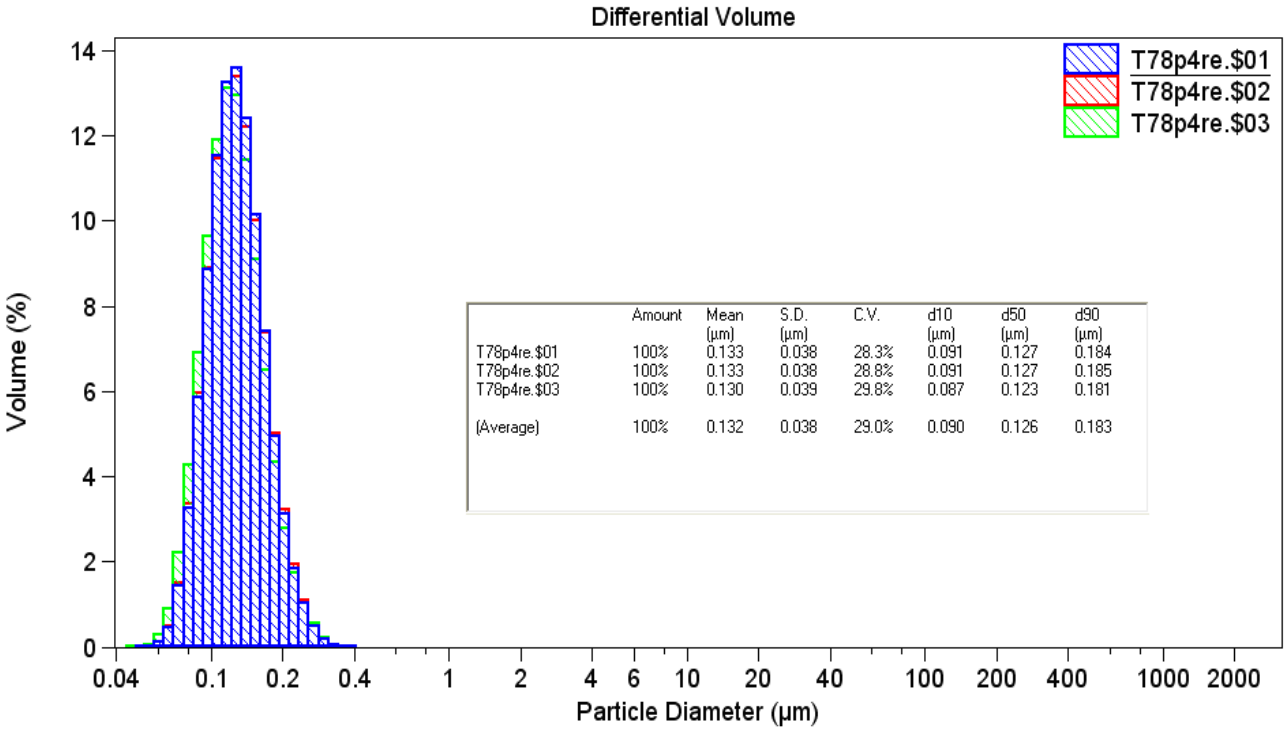

	Amount	Mean (µm)	S.D. (µm)	C.V.	d10 (µm)	d50 (µm)	d90 (µm)
T78p4re.$01	100%	0.133	0.038	28.3%	0.091	0.127	0.184
T78p4re.$02	100%	0.133	0.038	28.8%	0.091	0.127	0.185
T78p4re.$03	100%	0.130	0.039	29.8%	0.087	0.123	0.181
(Average)	100%	0.132	0.038	29.0%	0.090	0.126	0.183

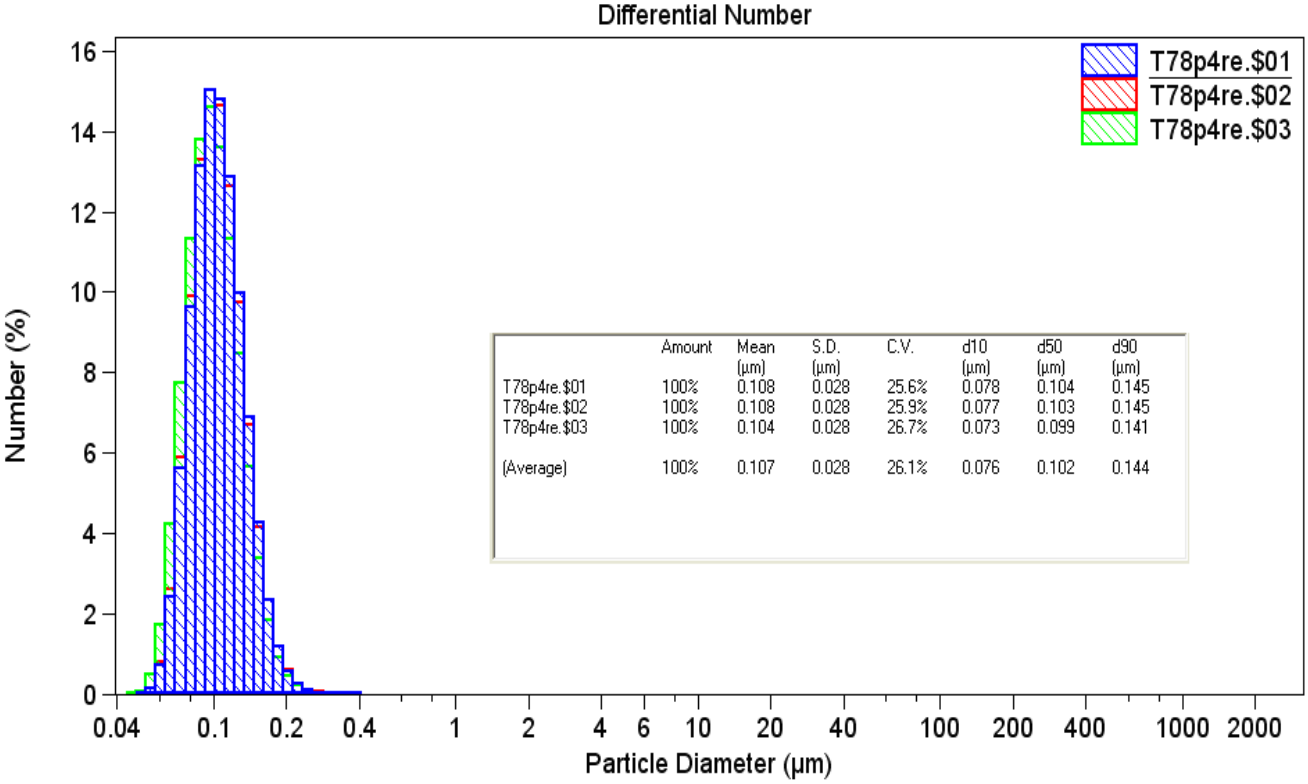

	Amount	Mean (µm)	S.D. (µm)	C.V.	d10 (µm)	d50 (µm)	d90 (µm)
T78p4re.$01	100%	0.108	0.028	25.6%	0.078	0.104	0.145
T78p4re.$02	100%	0.108	0.028	25.9%	0.077	0.103	0.145
T78p4re.$03	100%	0.104	0.028	26.7%	0.073	0.099	0.141
(Average)	100%	0.107	0.028	26.1%	0.076	0.102	0.144

Appendix VI

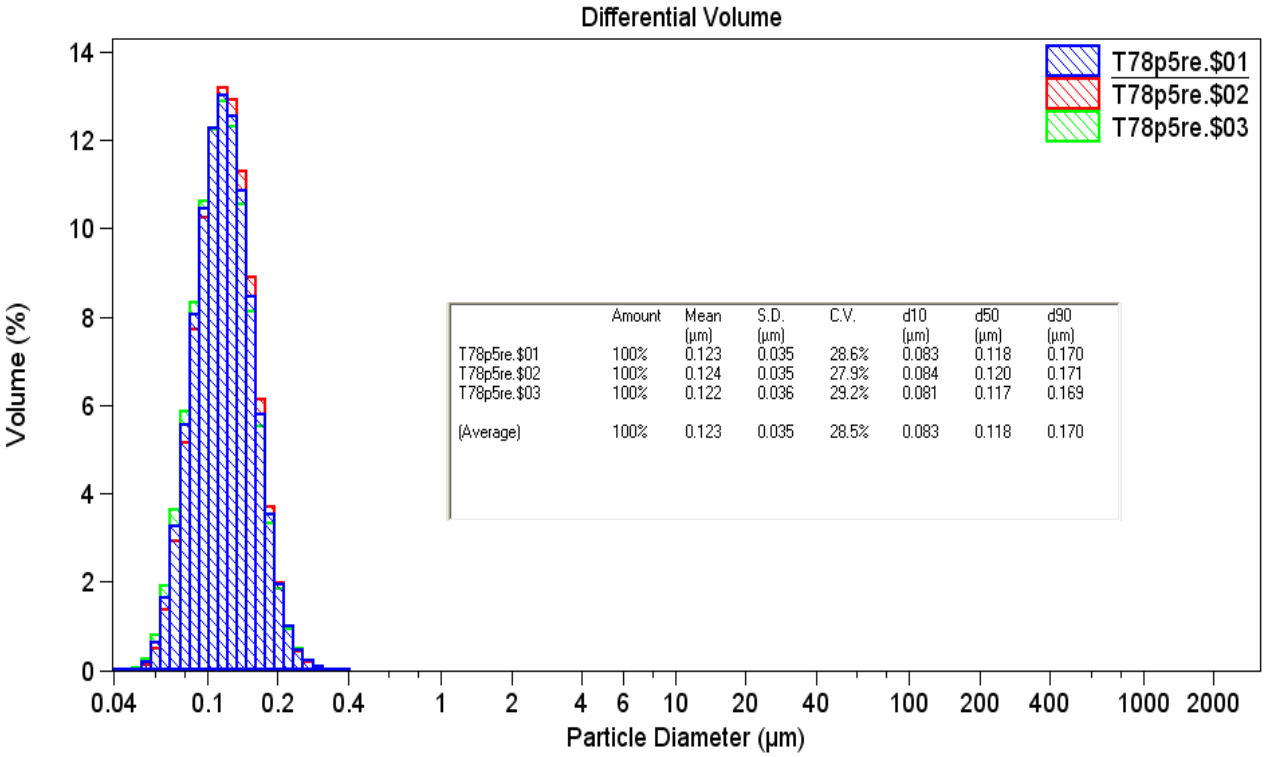

	Amount	Mean (µm)	S.D. (µm)	C.V.	d10 (µm)	d50 (µm)	d90 (µm)
T78p5re.$01	100%	0.123	0.035	28.6%	0.083	0.118	0.170
T78p5re.$02	100%	0.124	0.035	27.9%	0.084	0.120	0.171
T78p5re.$03	100%	0.122	0.036	29.2%	0.081	0.117	0.169
(Average)	100%	0.123	0.035	28.5%	0.083	0.118	0.170

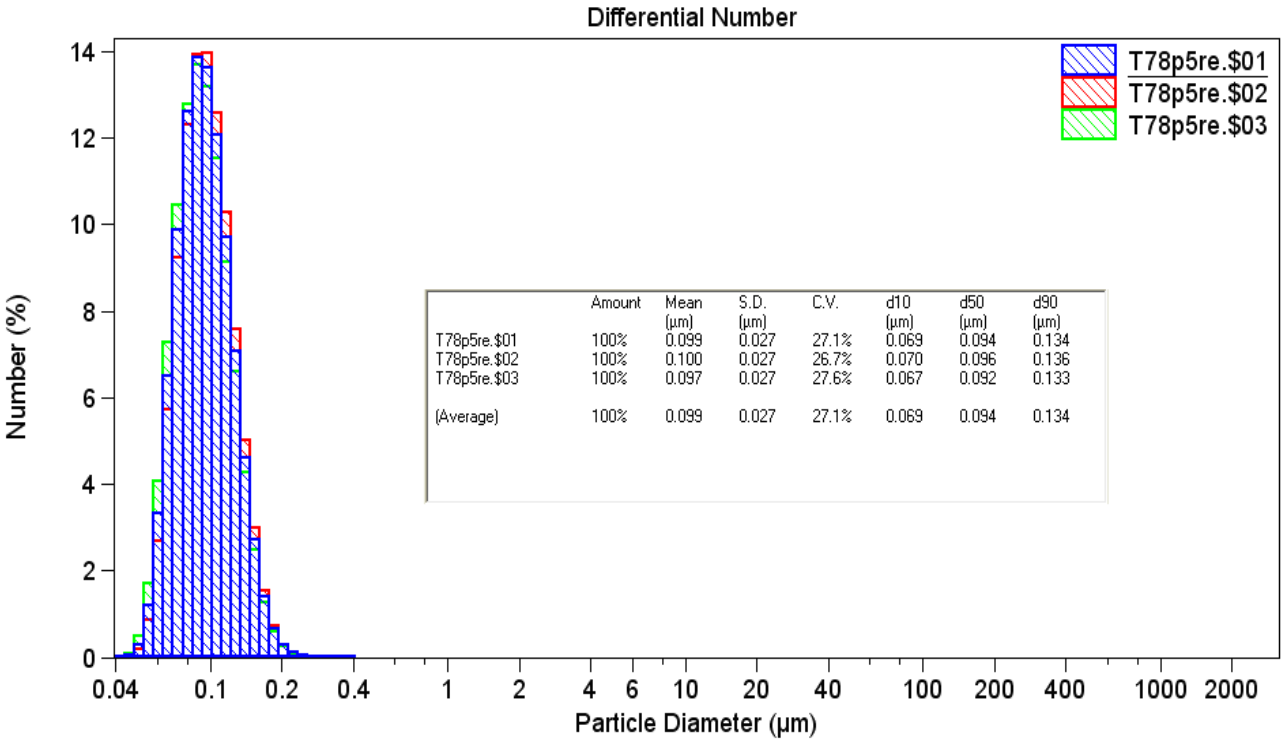

	Amount	Mean (µm)	S.D. (µm)	C.V.	d10 (µm)	d50 (µm)	d90 (µm)
T78p5re.$01	100%	0.099	0.027	27.1%	0.069	0.094	0.134
T78p5re.$02	100%	0.100	0.027	26.7%	0.070	0.096	0.136
T78p5re.$03	100%	0.097	0.027	27.6%	0.067	0.092	0.133
(Average)	100%	0.099	0.027	27.1%	0.069	0.094	0.134

Appendix VI

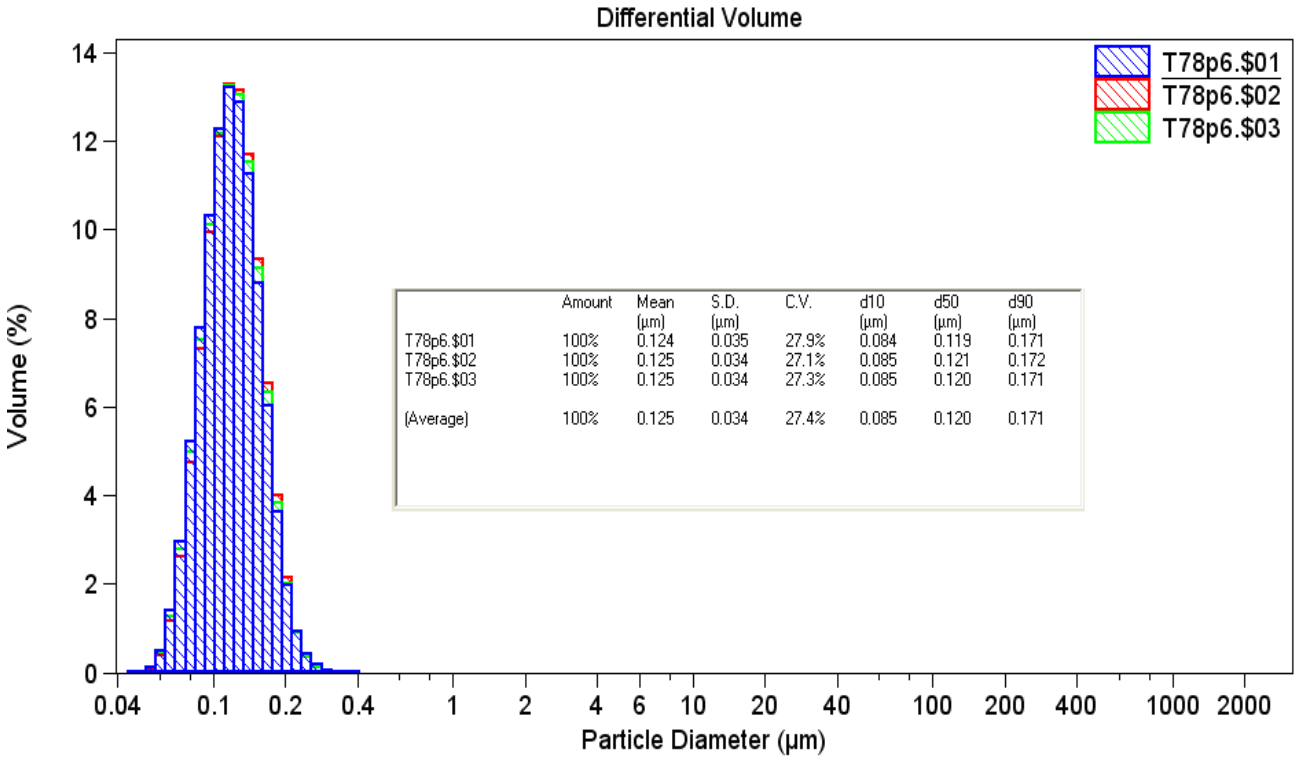

	Amount	Mean (µm)	S.D. (µm)	C.V.	d10 (µm)	d50 (µm)	d90 (µm)
T78p6.$01	100%	0.124	0.035	27.9%	0.084	0.119	0.171
T78p6.$02	100%	0.125	0.034	27.1%	0.085	0.121	0.172
T78p6.$03	100%	0.125	0.034	27.3%	0.085	0.120	0.171
(Average)	100%	0.125	0.034	27.4%	0.085	0.120	0.171

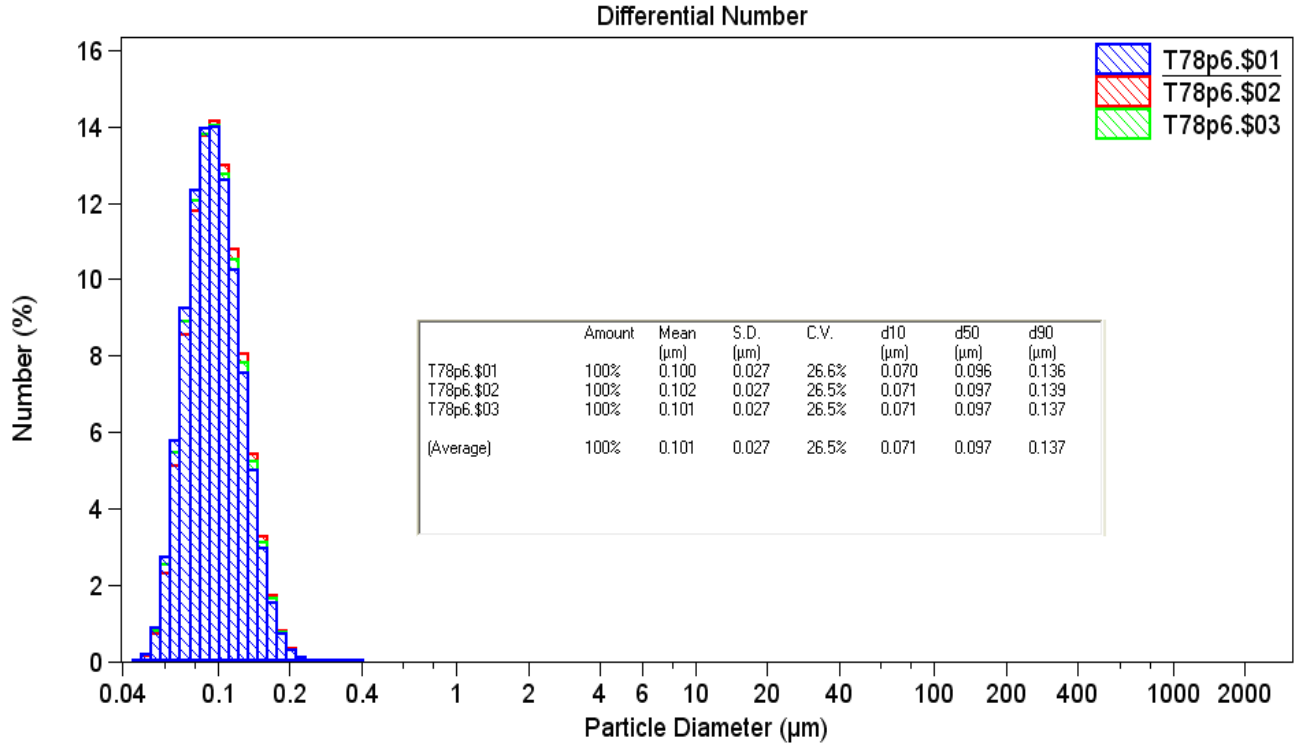

	Amount	Mean (µm)	S.D. (µm)	C.V.	d10 (µm)	d50 (µm)	d90 (µm)
T78p6.$01	100%	0.100	0.027	26.6%	0.070	0.096	0.136
T78p6.$02	100%	0.102	0.027	26.5%	0.071	0.097	0.139
T78p6.$03	100%	0.101	0.027	26.5%	0.071	0.097	0.137
(Average)	100%	0.101	0.027	26.5%	0.071	0.097	0.137

Appendix VI

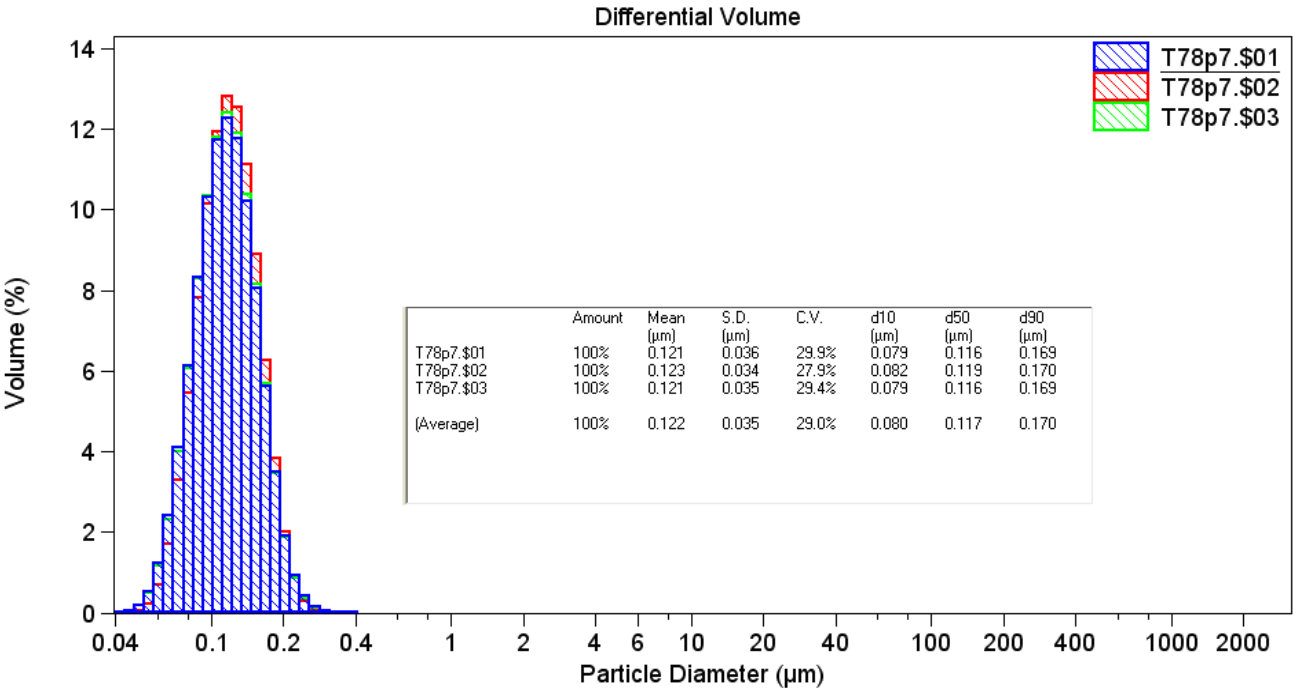

	Amount	Mean (µm)	S.D. (µm)	C.V.	d10 (µm)	d50 (µm)	d90 (µm)
T78p7.$01	100%	0.121	0.036	29.9%	0.079	0.116	0.169
T78p7.$02	100%	0.123	0.034	27.9%	0.082	0.119	0.170
T78p7.$03	100%	0.121	0.035	29.4%	0.079	0.116	0.169
(Average)	100%	0.122	0.035	29.0%	0.080	0.117	0.170

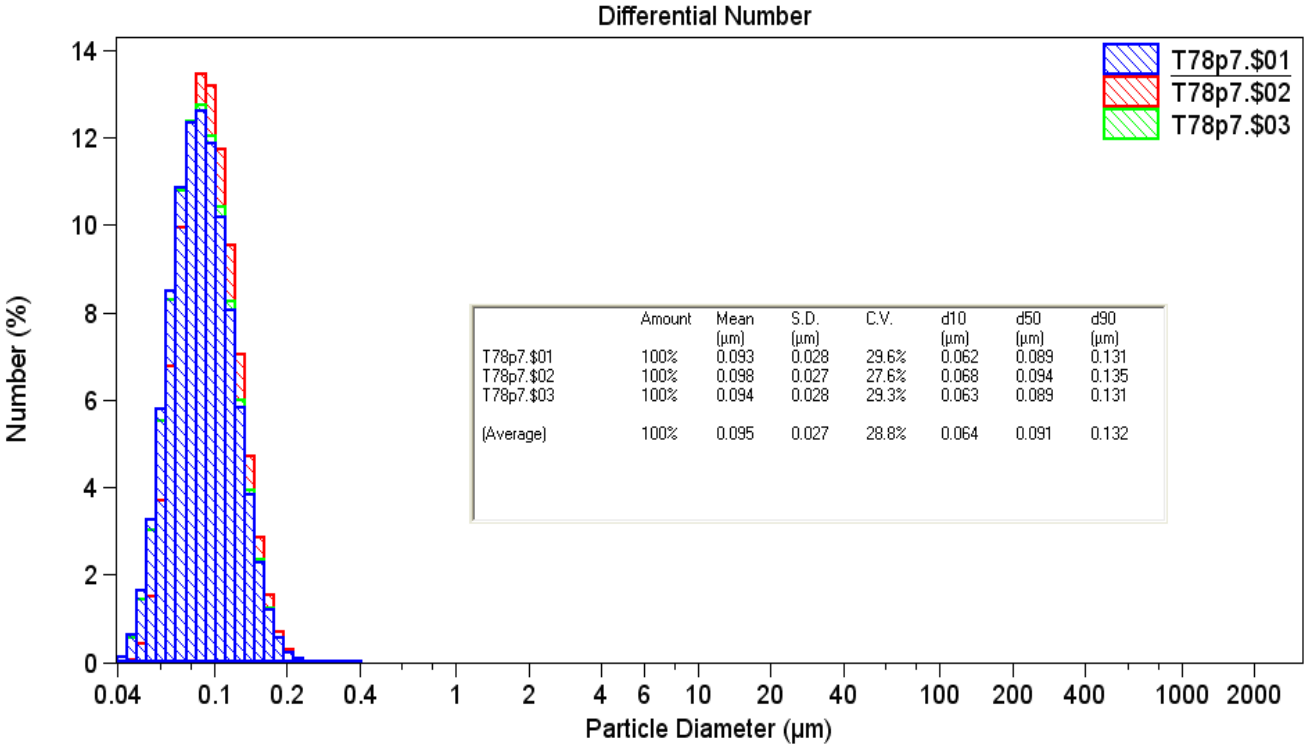

	Amount	Mean (µm)	S.D. (µm)	C.V.	d10 (µm)	d50 (µm)	d90 (µm)
T78p7.$01	100%	0.093	0.028	29.6%	0.062	0.089	0.131
T78p7.$02	100%	0.098	0.027	27.6%	0.068	0.094	0.135
T78p7.$03	100%	0.094	0.028	29.3%	0.063	0.089	0.131
(Average)	100%	0.095	0.027	28.8%	0.064	0.091	0.132

Appendix VI

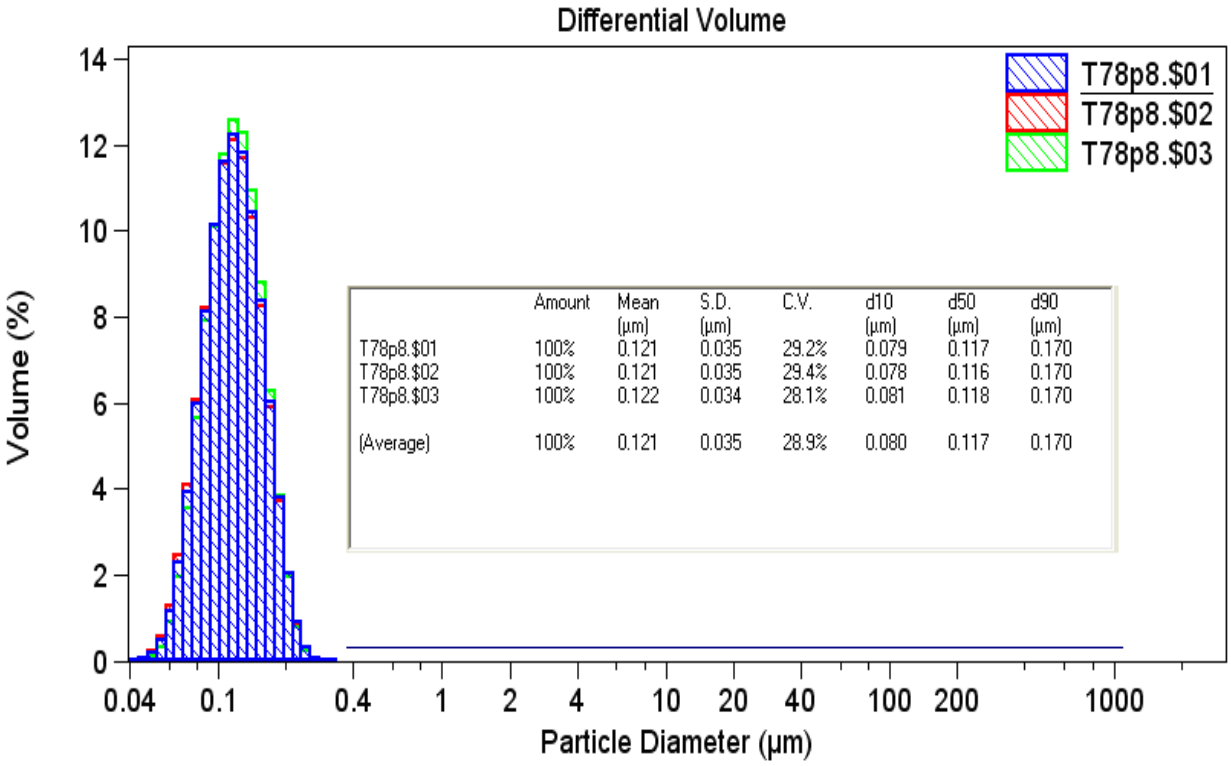

	Amount	Mean (µm)	S.D. (µm)	C.V.	d10 (µm)	d50 (µm)	d90 (µm)
T78p8.$01	100%	0.121	0.035	29.2%	0.079	0.117	0.170
T78p8.$02	100%	0.121	0.035	29.4%	0.078	0.116	0.170
T78p8.$03	100%	0.122	0.034	28.1%	0.081	0.118	0.170
(Average)	100%	0.121	0.035	28.9%	0.080	0.117	0.170

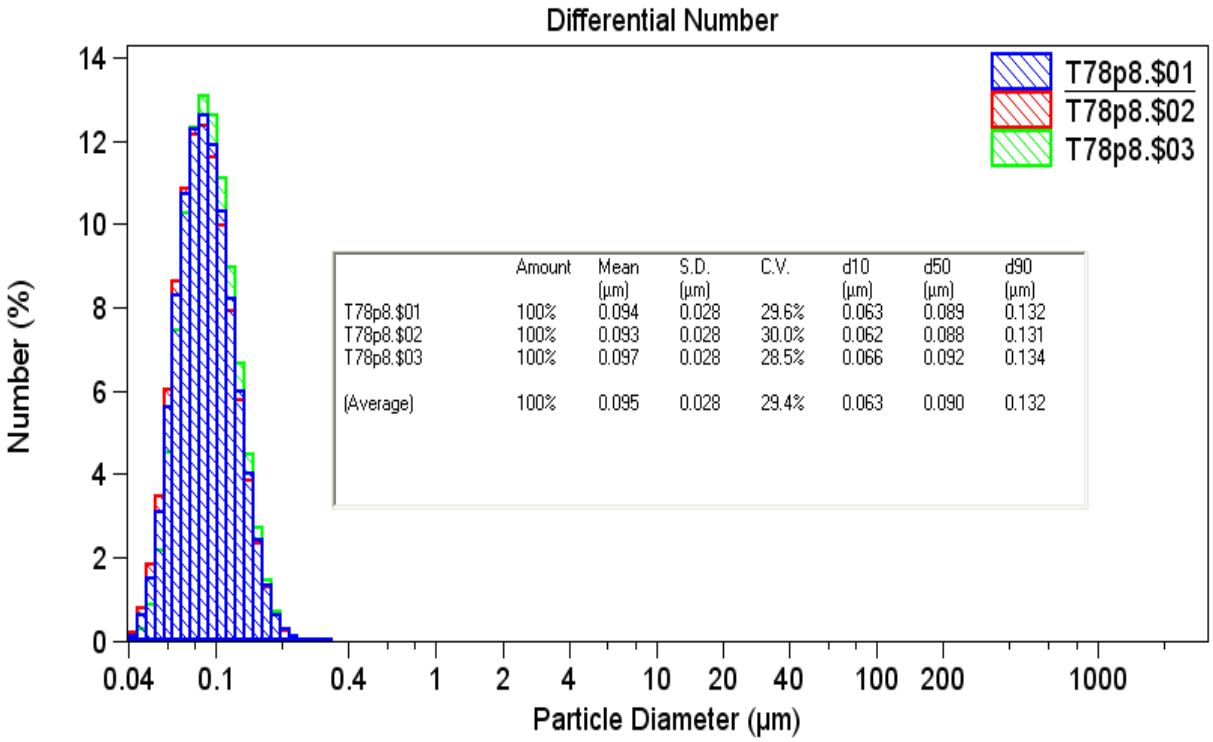

	Amount	Mean (µm)	S.D. (µm)	C.V.	d10 (µm)	d50 (µm)	d90 (µm)
T78p8.$01	100%	0.094	0.028	29.6%	0.063	0.089	0.132
T78p8.$02	100%	0.093	0.028	30.0%	0.062	0.088	0.131
T78p8.$03	100%	0.097	0.028	28.5%	0.066	0.092	0.134
(Average)	100%	0.095	0.028	29.4%	0.063	0.090	0.132

Appendix VII: The evolution of particle size distribution of the latex with alkyd (25%) only (T-100)

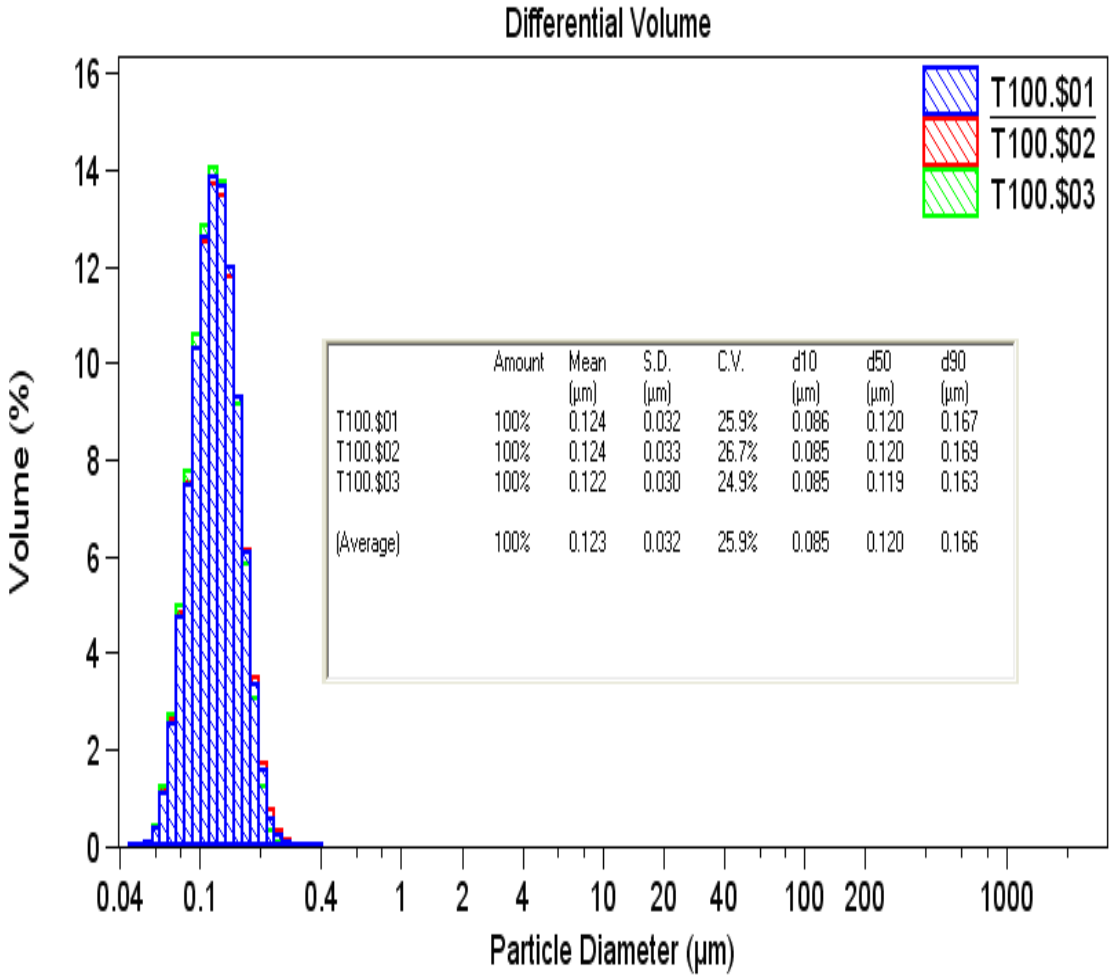

Figure 1. Particle size distribution (by volume) of the latex sample taken at the end of synthesis of T100

Appendix VII

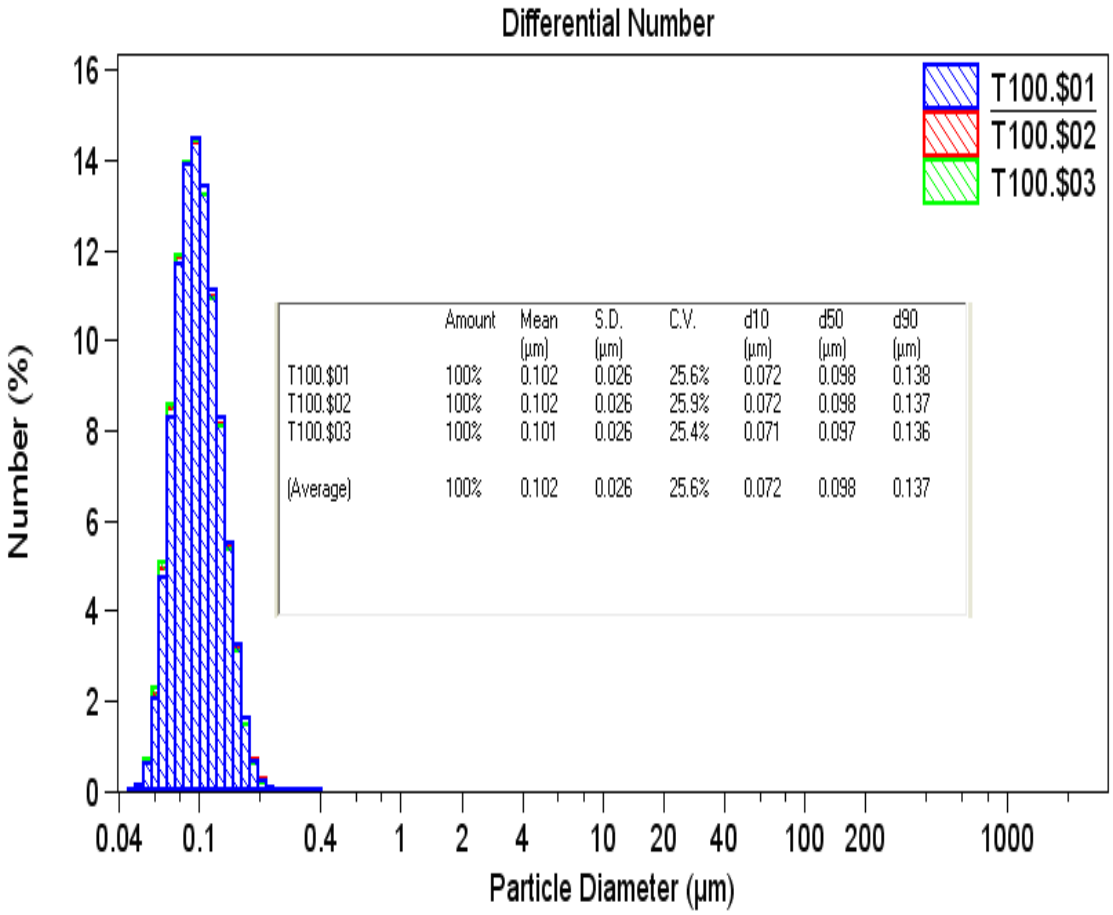

Figure 2. Particle size distribution (by number) of the latex sample taken at the end of synthesis of T100

Appendix VIII

Appendix VIII. Conductimetry titration curves relevant to the calculation of molar mass of PU

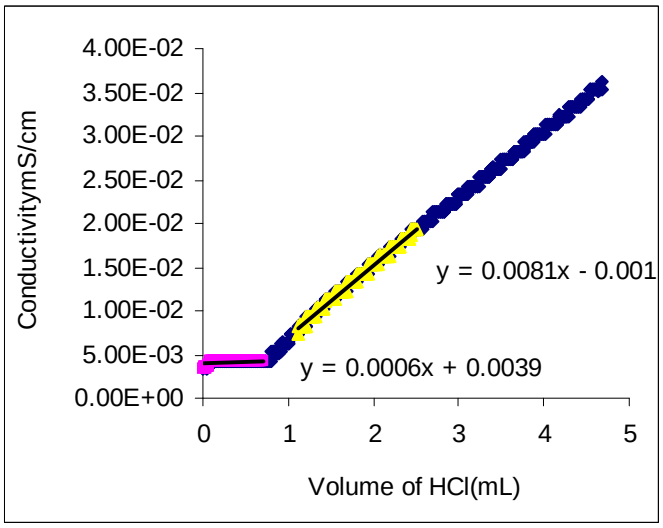

Figure 1. Conductimetric titration curve

	0.0006	0.0039	
	0.0081	-0.001	
VHcl	0.653		
			Volume
Moles of amine	68.07	*10-5	29.07
	11.71		5
Moles of amine reacted	11.055		
Moles of NCO	61.25	*10-5	par g PU

Moles of amine in 29.07mL of organic solution = $68.07*10^{-5}$

Moles of amine in 5mL of organic solution = $11.71*10^{-5}$

Moles of amine correspondent to 0.653 mL of 0.01N HCl = $6.53*10^{-6}$

Moles of amine reacted with NCO = $11.055*10^{-5}$

Moles of NCO in 5 mL of organic solution = $11.055*10^{-5}$

Moles of NCO in 1g of PU = $61.25*10^{-5}$

Appendix VIII

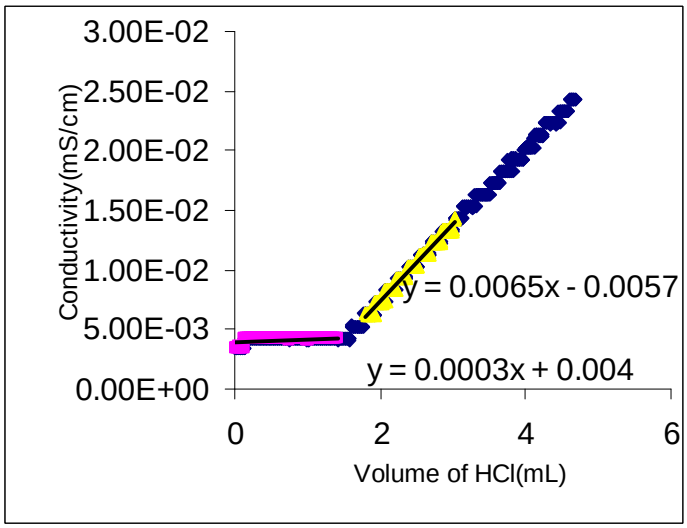

Figure 2. Conductimetric titration curve

	0.0003	0.004	
	0.0065	-0.0057	
VHcl	1.565		
			Volume
Moles of amine	68.07	*10-5	29.07
	23.30		9.95
Moles of amine reacted	21.735		
Moles of NCO	60.52	*10-5	par g PU

Moles of amine in 29.07mL of organic solution = $68.07*10^{-5}$

Moles of amine in 9.95mL of organic solution = $23.30*10^{-5}$

Moles of amine correspondent to 1.565 mL of 0.01N HCl = $1.565*10^{-5}$

Moles of amine reacted with NCO = $21.735*10^{-5}$

Moles of NCO in 9.95 mL of organic solution = $21.735*10^{-5}$

Moles of NCO in 1g of PU =$60.52*10^{-5}$

Appendix VIII

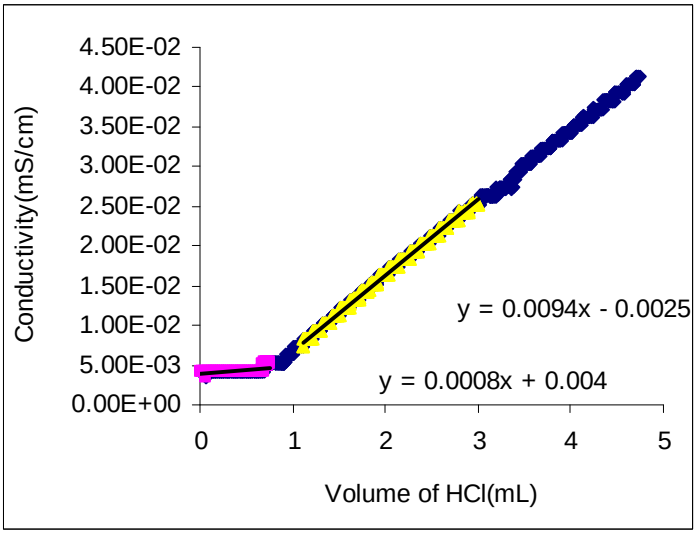

Figure 3. Conductimetric titration curve

	0.0008	0.004	
	0.0094	-0.0025	
VHcl	0.756		
			Volume
Moles of amine	68.07	*10-5	29.07
	11.73		5.01
Moles of amine reacted	10.976		
Moles of NCO	60.69	*10-5	per g PU

Moles of amine in 29.07mL of organic solution = $68.07*10^{-5}$

Moles of amine in 5.01mL of organic solution = $11.73*10^{-5}$

Moles of amine correspondent to 0.756 mL of 0.01N HCl = $7.56*10^{-6}$

Moles of amine reacted with NCO = $10.976*10^{-5}$

Moles of NCO in 5.01 mL of organic solution = $10.976*10^{-5}$

Moles of NCO in 1g of PU = $60.69*10^{-5}$

Appendix IX

Appendix IX. Conductimetry titration curves relevant to the determination of the yield of the reaction between HEMA and NCO

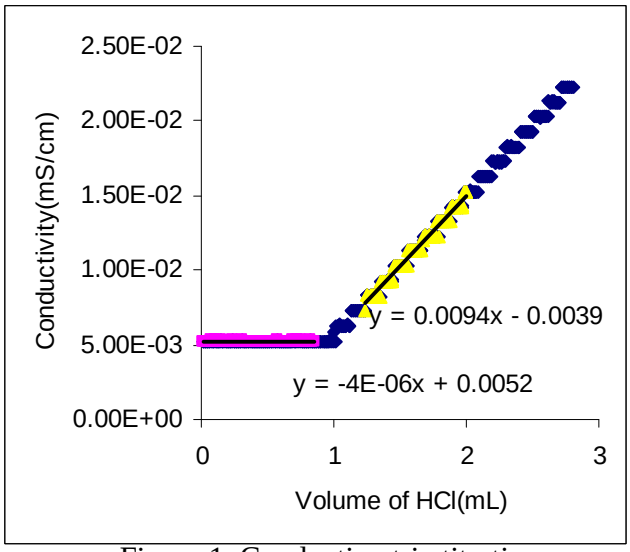

Figure 1. Conductimetric titration curve

	-4.00E-06	0.0052	
	0.0094	-0.0039	
VHcl	0.968		
			Volume
Moles of amine	58.95	*10-5	29.12
	5.08		2.51
Moles of amine reacted	4.114		
Nb NCO	44.83	*10-5	par g PU
HEMA	12.25	*10-5	par g PU
Nb NCO tot	57.08	*10-5	par g PU

Moles of amine in 29.12mL of organic solution = $58.95*10^{-5}$
Moles of amine reacted with NCO (per 1g of PU) = $44.83*10^{-5}$(Calculated based on conductivity titration)
Since we have established the number of moles of NCO per 1g of PU as $60.88*10^{-5}$, the remaining moles of NCO should be $16.05*10^{-5}$.
Total number of moles of HEMA added (per 1g of PU) = $12.25*10^{-5}$

The sum of number of moles of HEMA and free NCO calculated from the titration should be approximately equal to $60.88*10^{-5}$. In this case the sum is $57.08*10^{-5}$ moles and therefore the yield of the reaction between HEMA and NCO is 100%.

Appendix IX

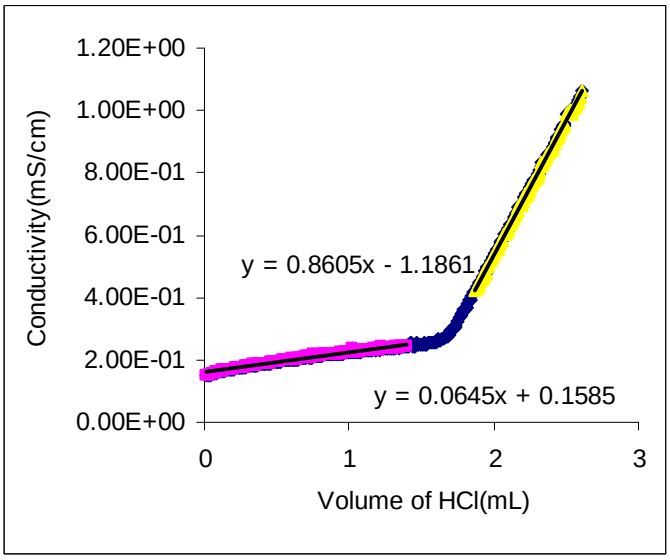

Figure 2. Conductimetric titration curve

	6.45E-02	0.1585	
	0.8605	-1.1861	
VHcl	1.689		
			Volume
Moles of amine	64.67	*10-5	29.12
	11.10		5
Moles of amine reacted	9.415		
Nb NCO	50.77	*10-5	par g PU
HEMA	26.89	*10-5	par g PU
Nb NCO tot	77.66	*10-5	par g PU

Moles of amine in 29.12mL of organic solution = $64.67*10^{-5}$

Moles of amine reacted with NCO (per 1g of PU) (Calculated based on conductivity titration) = $50.77*10^{-5}$

Therefore number of moles of NCO reacted with HEMA (per 1g of PU) = $10.11*10^{-5}$

Total number of moles of HEMA added per 1g of PU = $26.11*10^{-5}$

The yield of the reaction = 38.72%

Appendix IX

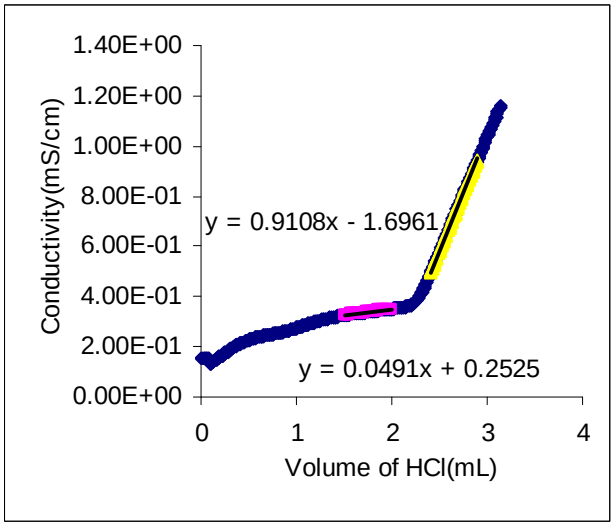

Figure 3. Conductimetric titration curve

	4.91E-02	0.2525	
	0.9108	-1.6961	
VHcl	2.261		
			Volume
Moles of amine	64.53	*10-5	29.12
	11.08		5
Moles of amine reacted	8.819		
Nb NCO	47.56	*10-5	par g PU
HEMA	49.64	*10-5	par g PU
Nb NCO tot	97.20	*10-5	par g PU

Moles of amine in 29.12mL of organic solution = $64.53*10^{-5}$

Moles of amine reacted with NCO (per 1g of PU) = $47.56*10^{-5}$
(Calculated based on conductivity titration)

Therefore, number of moles of NCO reacted with HEMA (per 1g of PU) = $13.32*10^{-5}$

Total number of moles of HEMA added per 1g of PU = $49.64*10^{-5}$

The yield of the reaction = 26.83%

Appendix X

Appendix X. Analysis of GPC data

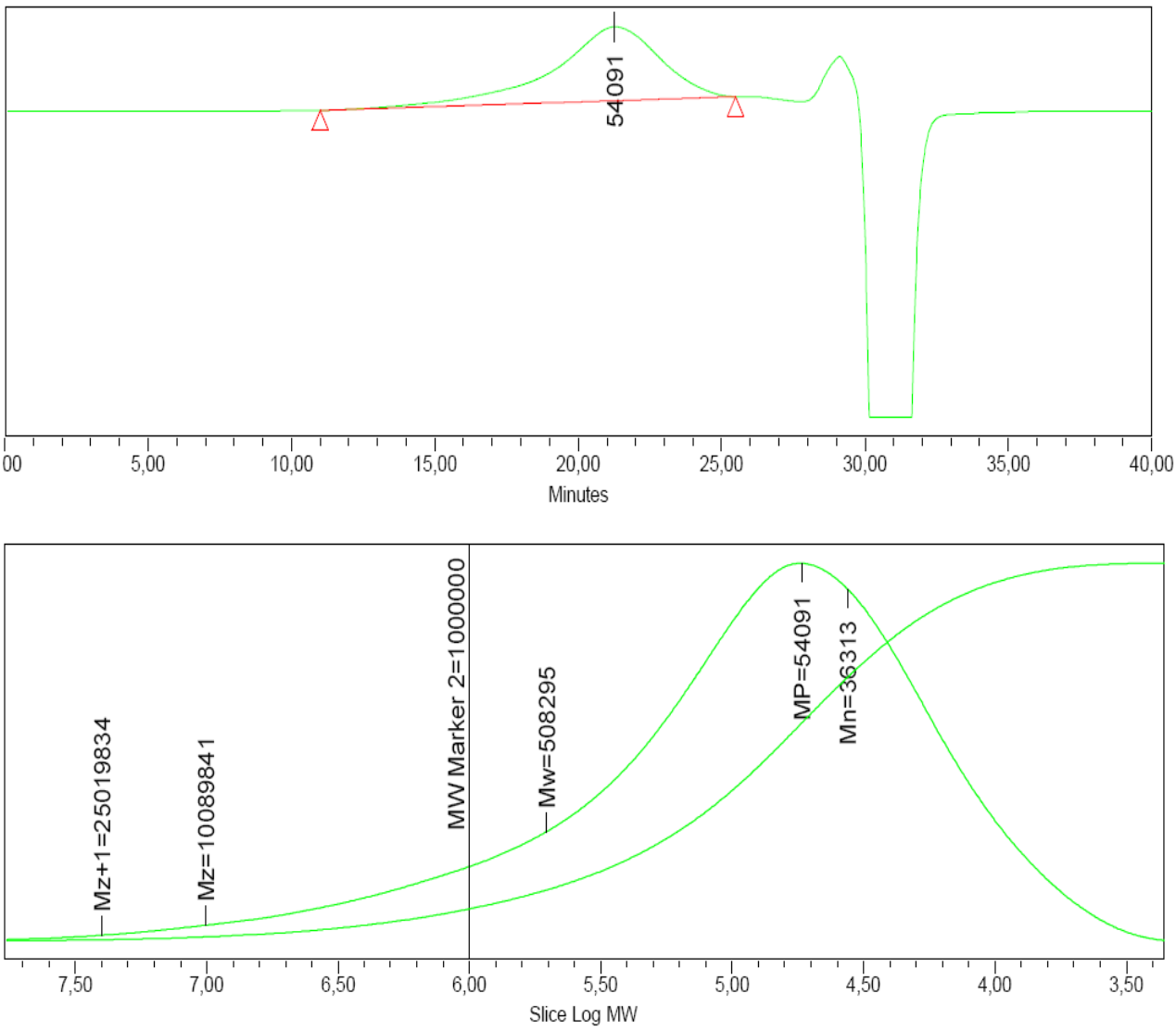

GPC of T143

Analysis of GPC of T143

	Detect	RT (min)	Mn	Mw	MP	Mz	Mz+1	Mv	IP	Area (µV*sec)	Area %
1	RI	21.3	36313	508295	54091	10089841	25019834		14.00	153738666	100.0

Appendix X

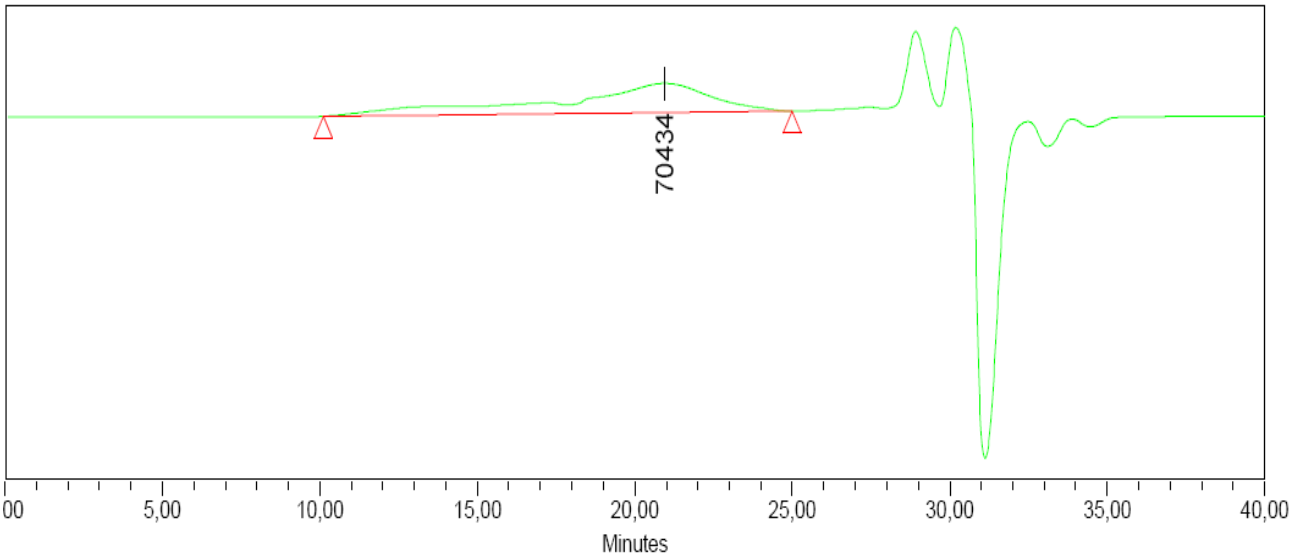

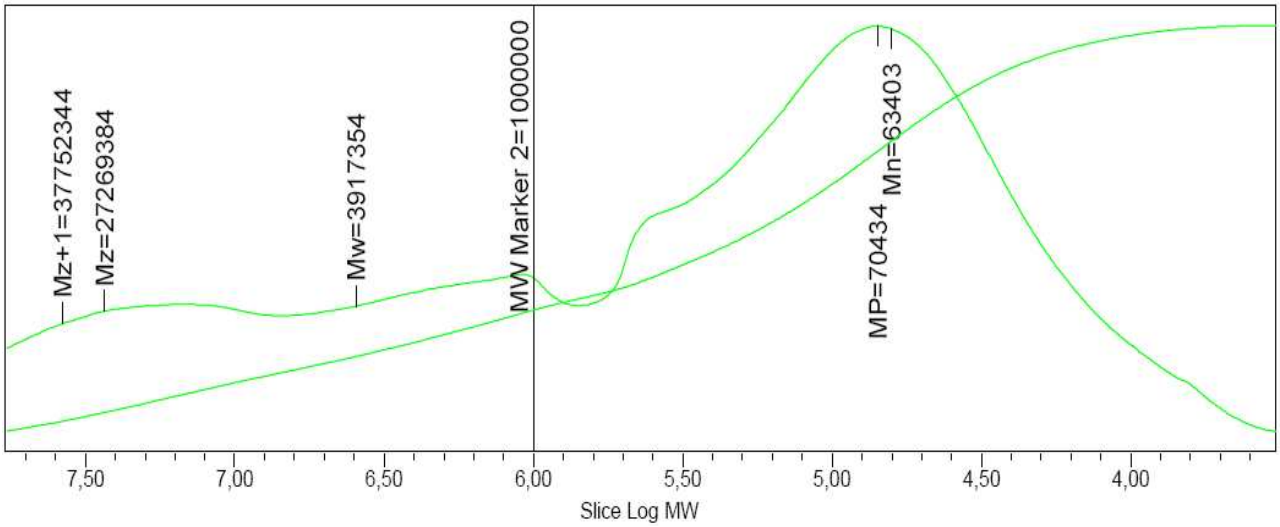

GPC of T145

Analysis of GPC of T145

	Detect	RT (min)	Mn	Mw	MP	Mz	Mz+1	Mv	IP	Area (µV*sec)	Area %
1	RI	20.9	63403	3917354	70434	27269384	37752344		61.78	36629254	100.0

Appendix X

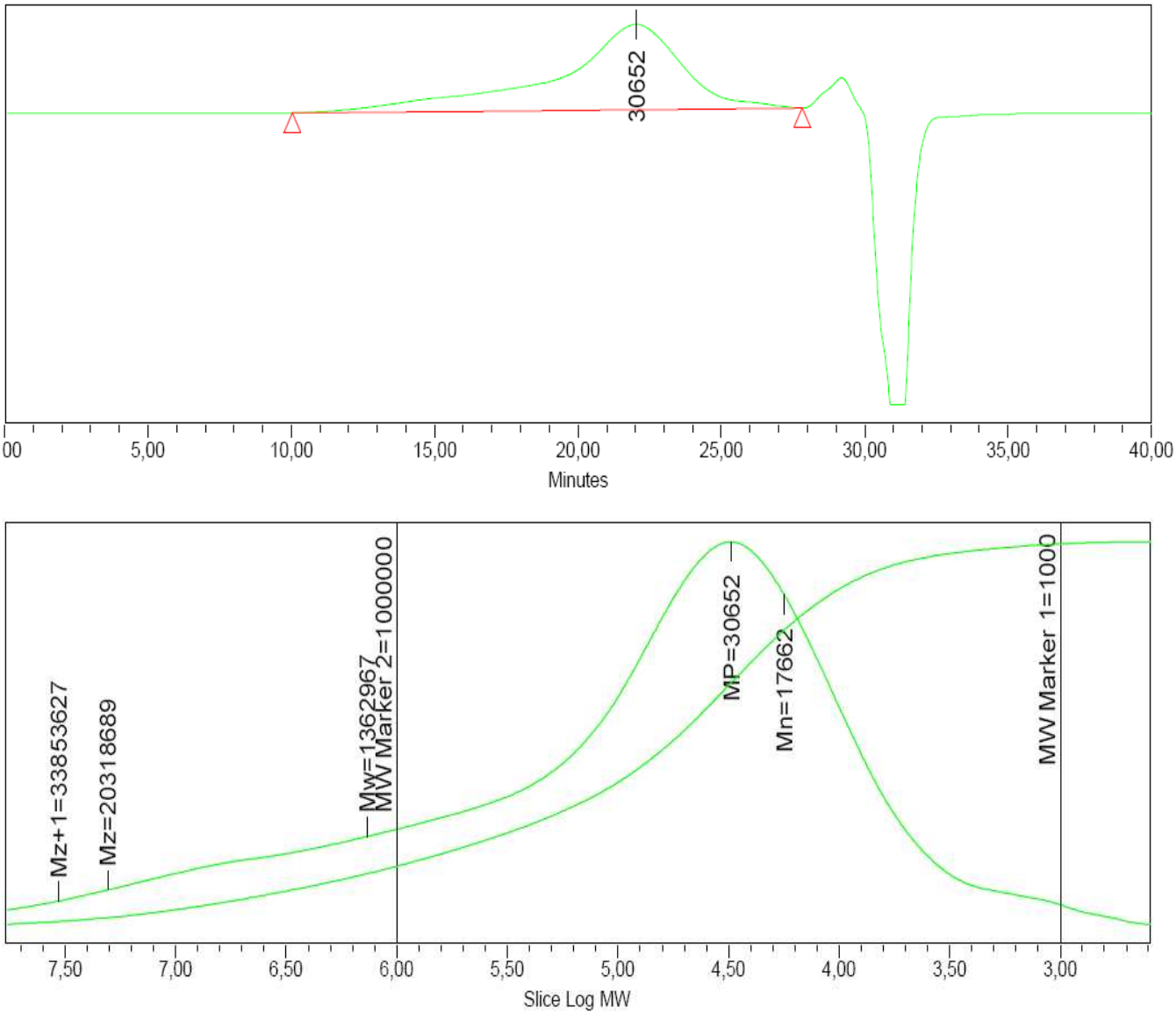

GPC of T146

Analysis of GPC of T146

	Detect	RT (min)	Mn	Mw	MP	Mz	Mz+1	Mv	IP	Area (µV*sec)	Area %
1	RI	22.0	17662	1362967	30652	20318689	33853627		77.17	221500246	100.0

Appendix X

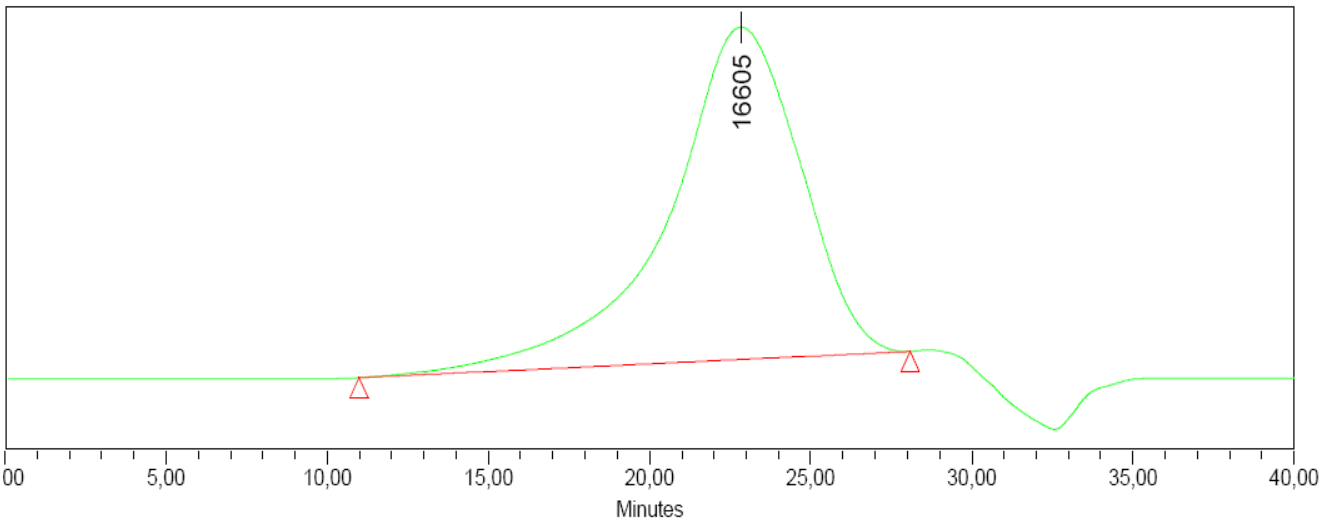

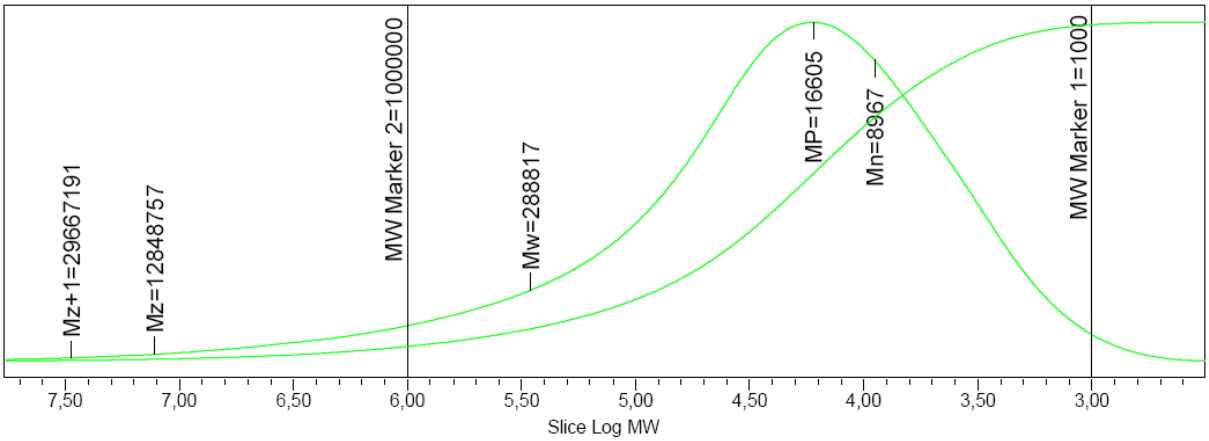

GPC of T147

Analysis of GPC of T147

	Detect	RT (min)	Mn	Mw	MP	Mz	Mz+1	Mv	IP	Area (µV*sec)	Area %
1	RI	22.8	8967	288817	16605	12848757	29667191		32.21	972026265	100.0

Appendix X

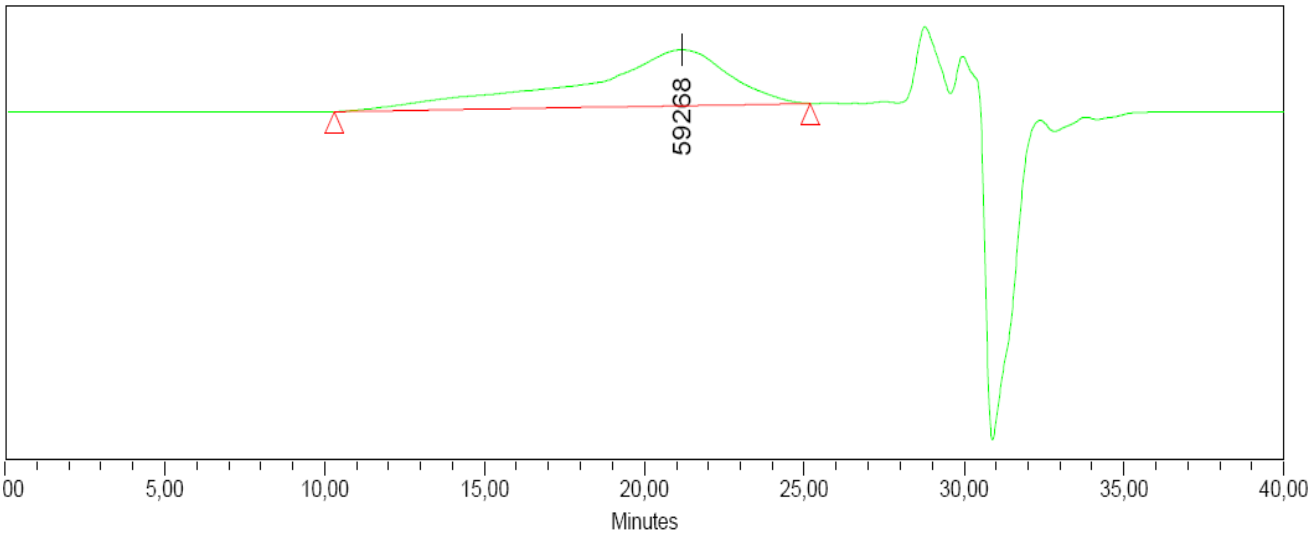

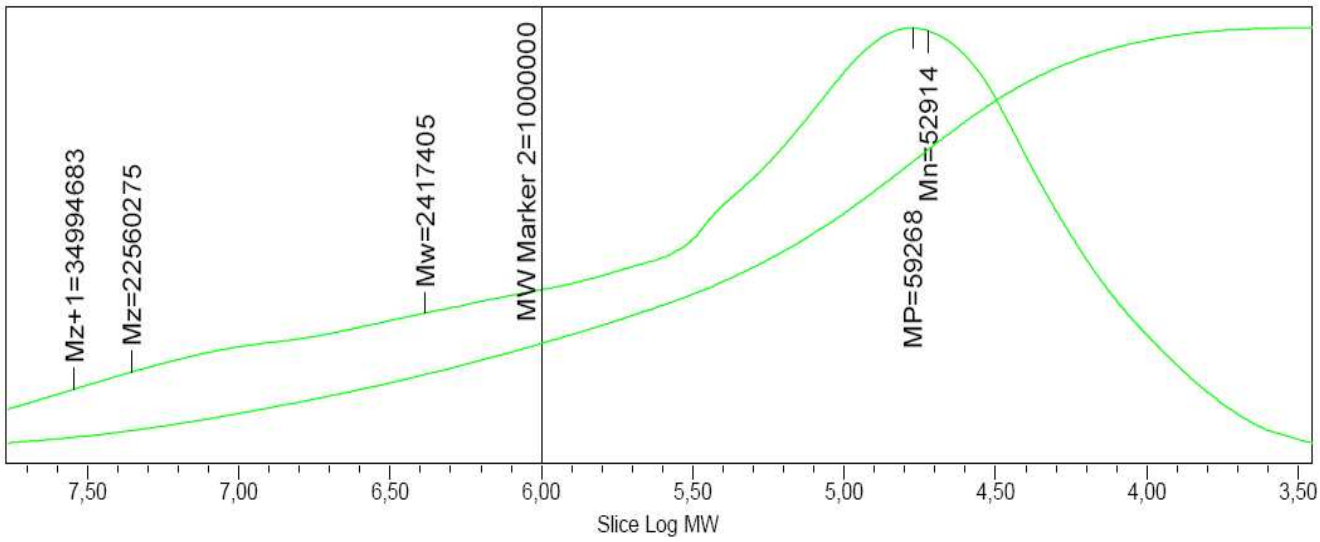

GPC of T149

Analysis of GPC of T149

	Detect	RT (min)	Mn	Mw	MP	Mz	Mz+1	Mv	IP	Area (µV*sec)	Area %
1	RI	21.2	52914	2417405	59268	22560275	34994683		45.69	60519722	100.0

Appendix X

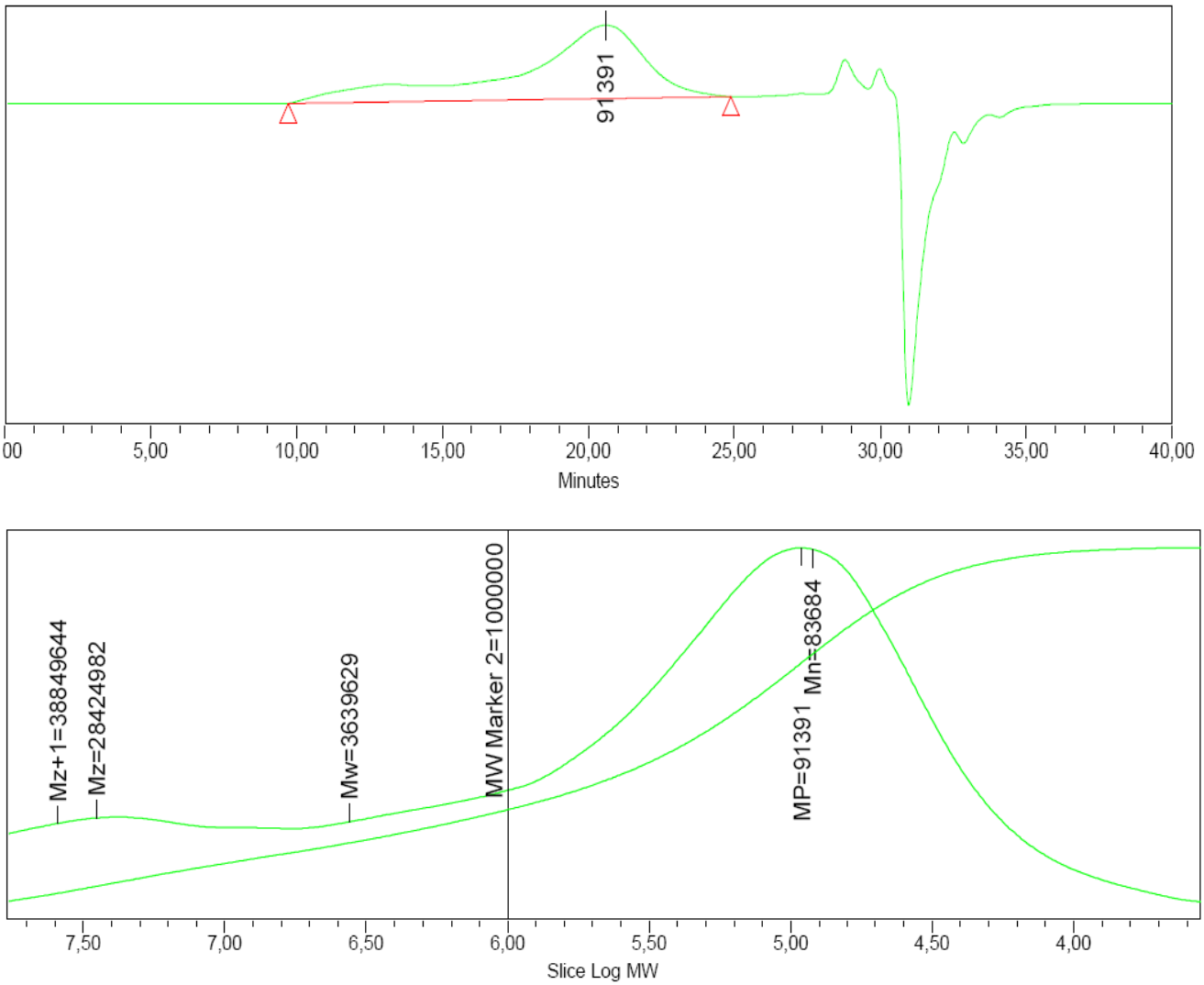

GPC of T150

Analysis of GPC of T150

	Detect	RT (min)	Mn	Mw	MP	Mz	Mz+1	Mv	IP	Area (µV*sec)	Area %
1	RI	20.6	83684	3639629	91391	28424982	38849644		43.49	56011393	100.0

Appendix X

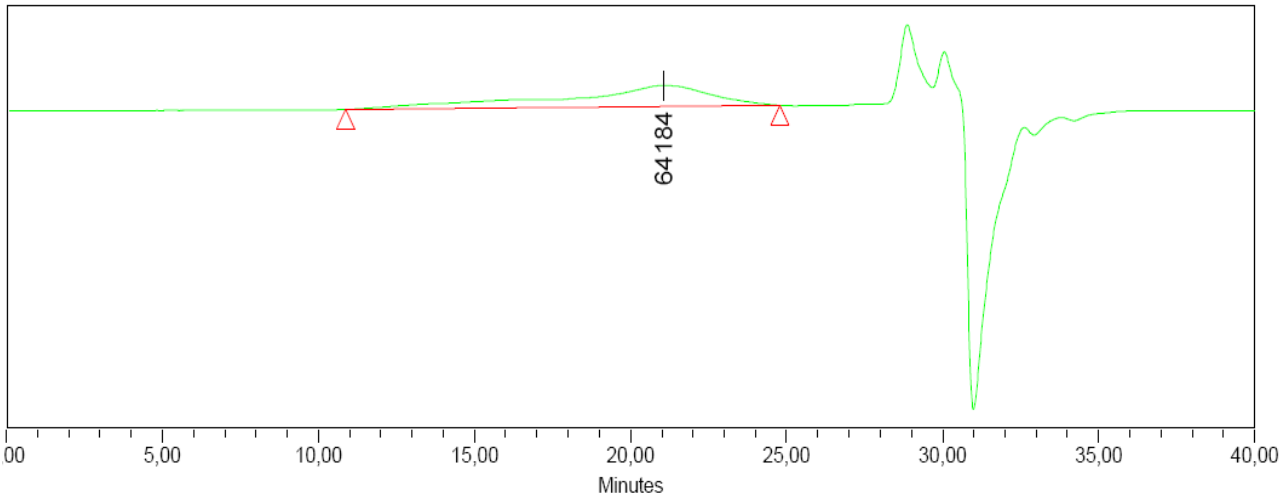

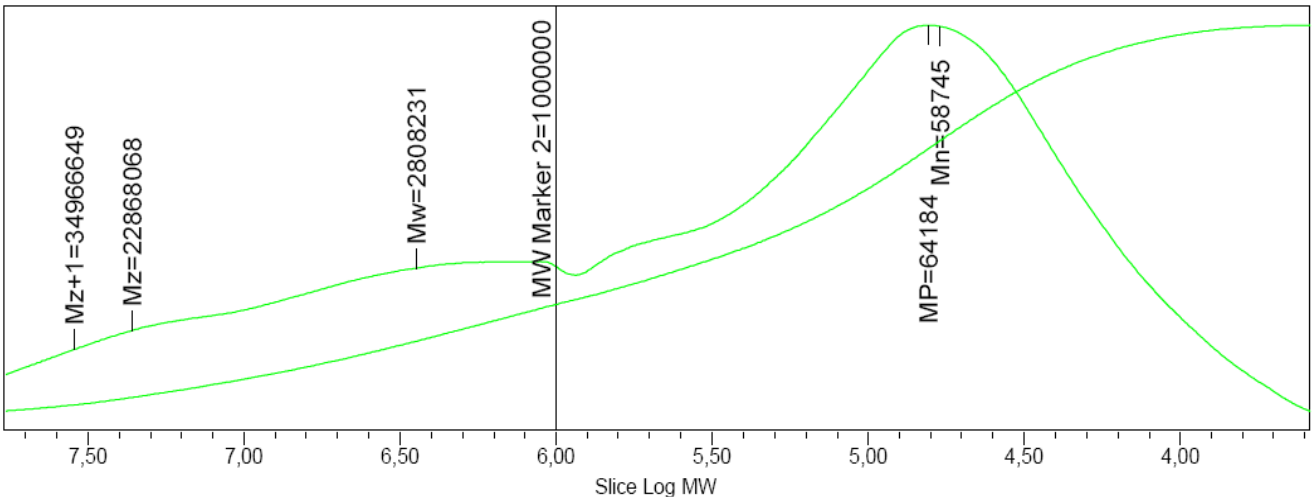

GPC of T152

Analysis of GPC of T152

	Detect	RT (min)	Mn	Mw	MP	Mz	Mz+1	Mv	IP	Area (µV*sec)	Area %
1	RI	21.1	58745	2808231	64184	22868068	34966649		47.80	24032939	100.0

Appendix X

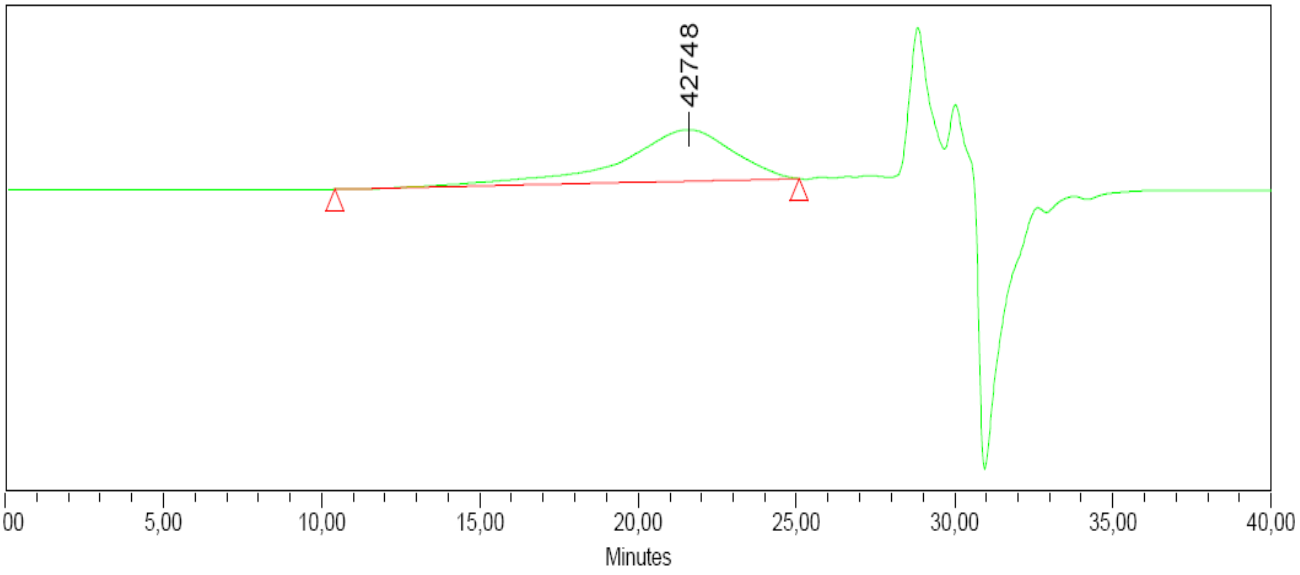

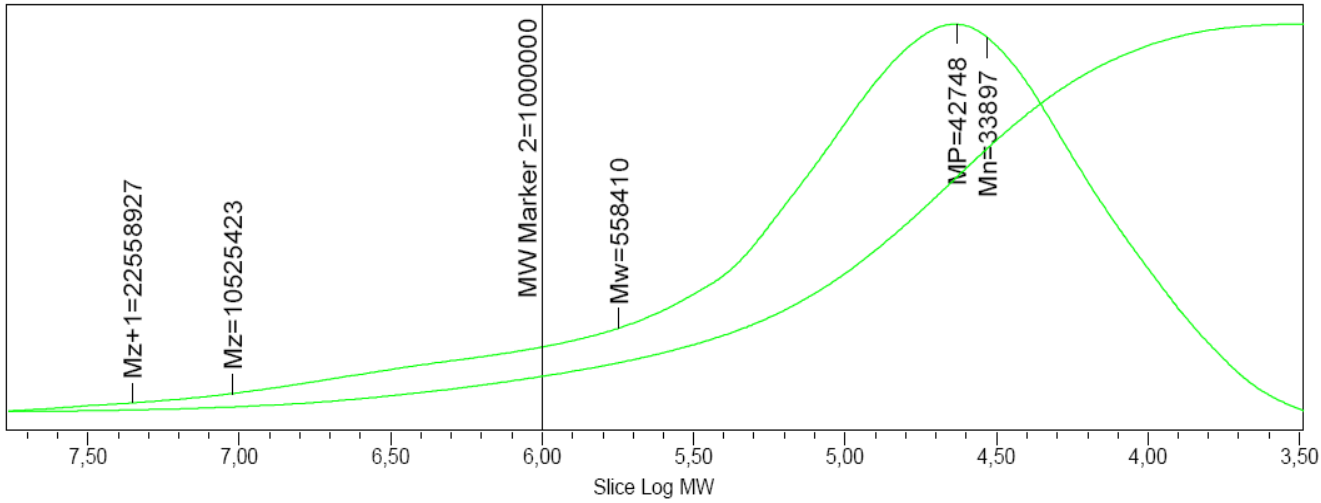

GPC of T153

Analysis of GPC of T153

	Detect	RT (min)	Mn	Mw	MP	Mz	Mz+1	Mv	IP	Area (µV*sec)	Area %
1	RI	21.6	33897	558410	42748	10525423	22558927		16.47	48944548	100.0

Appendix X

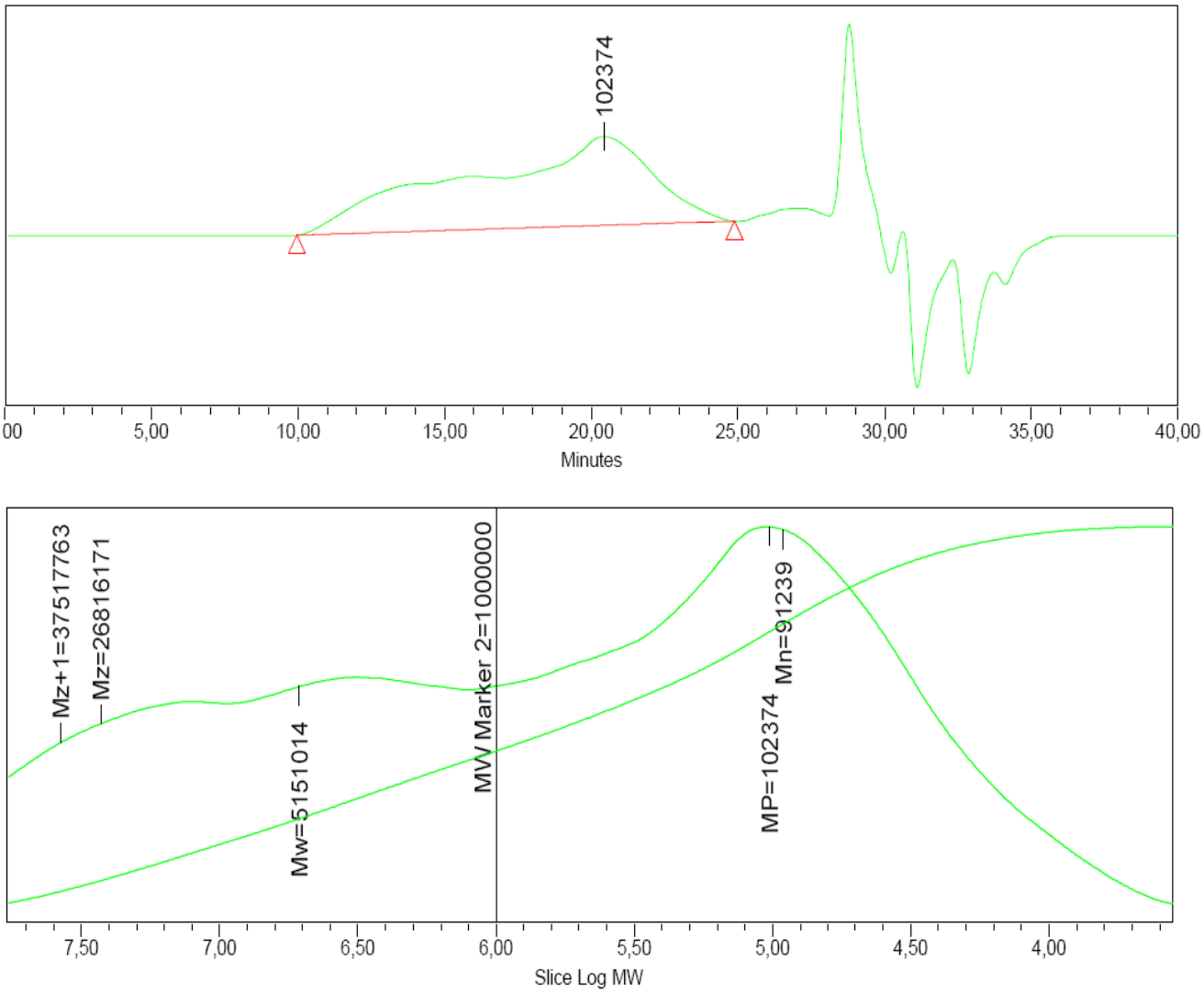

GPC of T159

Analysis of GPC of T159

	Detect	RT (min)	Mn	Mw	MP	Mz	Mz+1	Mv	IP	Area (µV*sec)	Area %
1	RI	20.4	91239	5151014	102374	26816171	37517763		56.46	29558061	100.0

Appendix XI

Appendix XI. Off-line monitoring of the polymerisation

Determination of polymer content (PC) and monomer conversions

Samples are withdrawn during the reaction and transferred into a pre-weighed aluminium dish. The sample is then weighed and placed in an oven at 100°C under vacuum in order to remove water and residual monomer. The polymer content is calculated according to the following equation:

$$PC(\%) = \left[\frac{m_{d,dried} - m_{d,empty}}{m_{d,full} - m_{d,empty}} \times 100 \right] - \left[\frac{m_{np}}{m_{latex}} \times 100 \right] \qquad \text{Equation 1}$$

Where $m_{d,dried}$ is the mass of dish with dried matter: $m_{d,,full}$ is the mass of dish with latex: $m_{d,empty}$ is the mass of empty dish: m_{np} is the mass of non polymer matter(resin, surfactant, initiator etc...): m_{latex} is the total mass of latex.

The overall or global conversion $X_{G(T)}$ and the instantaneous conversion $X_{i(t)}$ are calculated according to the Equation 2 and Equation 3 respectively.

$$X_{G(t)} = \frac{PC_{(t)} \times m_{latex(t)}}{m^{tot}_{mon(t_{final})}} / 100 \qquad \text{Equation 2}$$

Where $m_{latex(t)}$ is the mass of latex at the moment: $m^{tot}_{mon(t)}$ is the mass of total monomer added by the end of the reaction.

$$X_{i(t)} = \frac{PC_{(t)} \times m_{latex(t)}}{m^{tot}_{mon(t)}} / 100 \qquad \text{Equation 3}$$

Where $m^{tot}_{mon(t)}$ is the mass of monomer added at the moment (t).

Individual monomer conversion

Individual monomer conversion is detected by gas chromatography (GC). By comparing the surface area of GC peaks of the injected known weighed latex samples with the corresponding standards, the amount of free monomer of the injected sample can be calculated.

Appendix XI

Particle size measurement

Samples are regularly withdrawn during the polymerisation experiments. For each sample the average particle diameter is measured by Dynamic Light Scattering with a Malvern Autosizer Lo-C.

Malvern Autosizer Lo-C: DLS single angle of detection at 90°C

The Malvern Autosizer Lo-C gives us a mean diameter in intensity with a polydispersity index (PI) reflective of the width of the distribution. The manufactures consider that the particle size distribution (PSD) is monodisperse when we have PI ≤ 0.1. PI corresponds to the variance of the distribution. The intensity (i) scattered by the particles is measured as a function of time (t) according to a sampling time (τ). From this measurement the autocorrelation function G(t) is deduced as expressed in Equation 4. This function reflects the probability of a particle being at the same place at the time (t+ τ).

$$G(t) = \sum i(t).i(t+\tau) \qquad \text{Equation 4}$$

G(t) is a decreasing exponential function that can be written as in Equation 5:

$$G(t) = \sum c_i(t) \exp(-\gamma_i t) \qquad \text{Equation 5}$$

Where c_i is the intensity scattered by the particles having a size i, and where γ_i is a function of the diffusion coefficient as expressed by Equation 6.

$$\gamma_i = D_i q^2 \qquad \text{Equation 6}$$

Where D_i is the Diffusion coefficient of the particles with a size i: q is the wave vector, which depends on the refractive index of the dispersing medium, the angle of diffusion and the wavelength of the laser as shown in Equation 7.

$$q = \frac{4\pi n \sin(\alpha/2)}{\lambda} \qquad \text{Equation 7}$$

Where n is the refractive index of the dispersing medium (water): α is the angle between the laser source and the photomultiplicator (α: 90°): λ is the wavelength of the laser.

The normal logarithm of the autocorrelation function, which is a straight line that can be expressed as indicated in Equation 8, allows us to determine the mean particle diameter in intensity (Z-average nm) and the PI as can be seen in Equation 9.

$$\ln G(t) = a + bt + ct^2 \qquad \text{Equation 8}$$

Where b is the Z-average mean (nm)

Polydispersity index or variance of the distribution:

$$PI = 2c / b^2 \qquad \text{Equation 9}$$

The Stokes-Einstein relation allows us to calculate the particle diameter from the diffusion coefficient D according to the following equation:

$$d_p = \frac{K_B T}{3\pi\eta D} \qquad \text{Equation 10}$$

Where K_B is the Boltzmann constant: T is the temperature: η is the viscosity of the suspending medium (water).

Determination of number of droplets (N_D) and particles (N_P) in a miniemulsion

$$N_D = \frac{\sum\left[\frac{m_i}{\rho_m} + \frac{m_x}{\rho_x}\right]}{\frac{\pi}{6} \times D_d^3} \qquad \text{Equation 11}$$

Where m_i is the mass of monomer: ρ_m is the density of monomer: m_x is the mass of resin: ρ_x is the density of resin: π=22/7: D_d is the droplet diameter.

$$N_P = \frac{\{(\frac{m_x}{\rho_x}) + (\frac{\sum m_i}{\rho_p} \times X_{G(t)}) + [\frac{\sum m_i}{\rho_m}(1 - X_{G(t)})]\}}{\frac{\pi}{6} \times D_p^3} \qquad \text{Equation 12}$$

Where ρ_p is the density of polymer: $X_{G(T)}$ is the overall conversion: D_p is the particle diameter.

Appendix XI

Determination of surface coverage (θ) of latex

$$\theta = \frac{\frac{m_{TA}^{tot}}{M_{TA}} \times A_S \times N_A}{N_P \pi d_P^2}$$ Equation 13

Where m_{TA}^{tot} is the total active weight of anionic surfactant (Dowfax): M_{TA} is the molar mass of surfactant: A_S is the specific surface area occupied by a molecule of surfactant on a particle of the polymer of interest: N_p is particle number: d_p is particle diameter.

Critical Micellar Concentration (CMC) Determination of Dowfax 2AI and hence calculation of the specific surface area (A_S) of Dowfax 2 AI

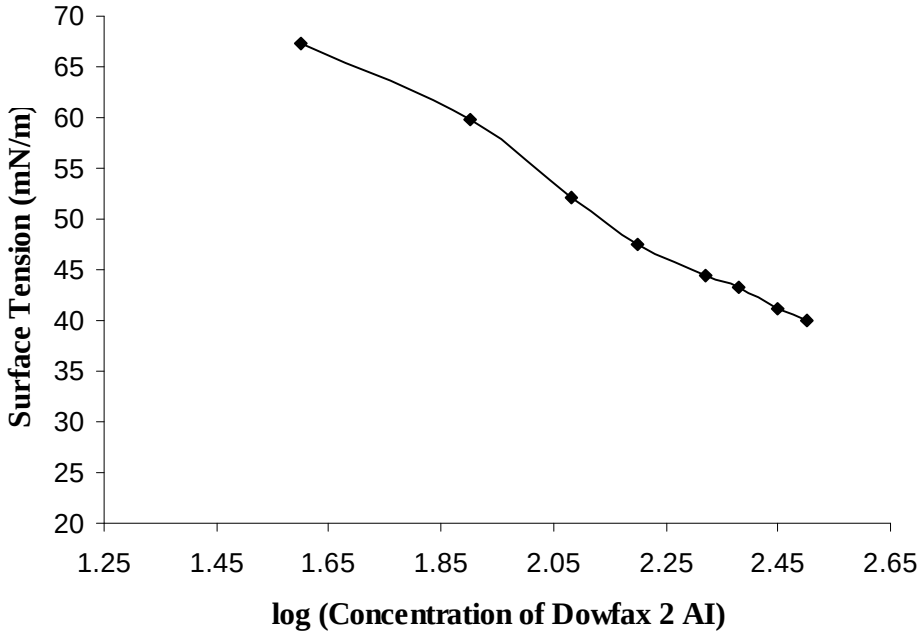

Figure 1. CMC Determination curve for Dowfax 2AI in deionized water

CMC of Dowfax 2AI in water = 0.2g/L

Appendix XI

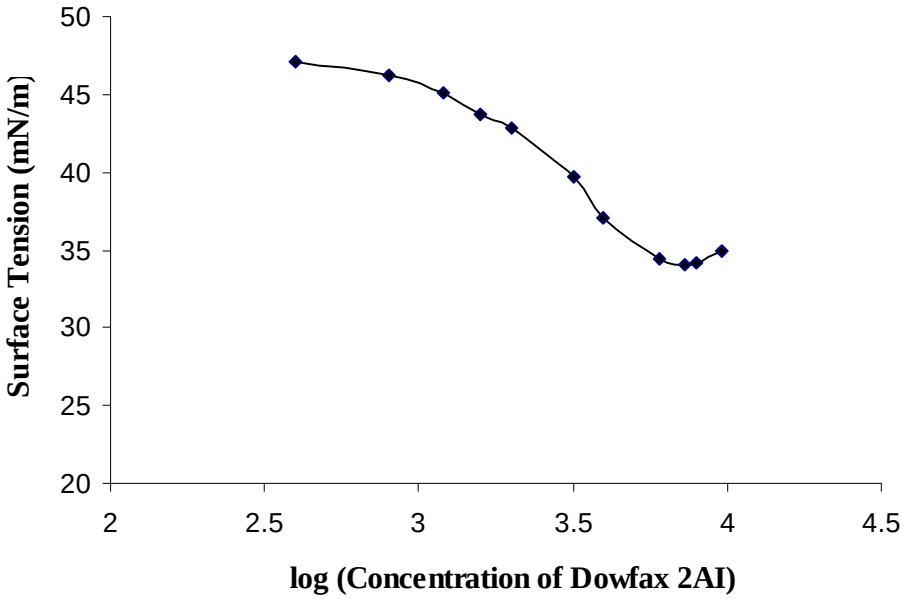

Figure 2. CMC Determination curve for Dowfax 2AI in diluted (5% solid) hybrid latex of original latex (25% alkyd: 50% solid)

CMC of Dowfax in 5% hybrid latex = 5.623g/L

CMC of Dowfax in water =0.2g/L

Concentration of Dowfax adsorbed by latex =5.423g/L

Surface area of the polymer $= N_P \times \pi \times D^2$

$$=1.32\times10^{17}\times\frac{22}{7}\times(116\times10^{-7})^2$$

Surface area of adsorbed surfactant (S_{Dowfax}) $$=\frac{Wt.Dowfax}{MWDowfax}\times A_S \times N_A$$

$$=\frac{5.423}{576}\times A_S \times 6\times10^{23}$$

$$1.32\times10^{17}\times\frac{22}{7}\times(116\times10^{-7})^2 = \frac{5.423}{576}\times A_S \times 6\times10^{23}$$

A_S = 99 Å^2

Appendix XI

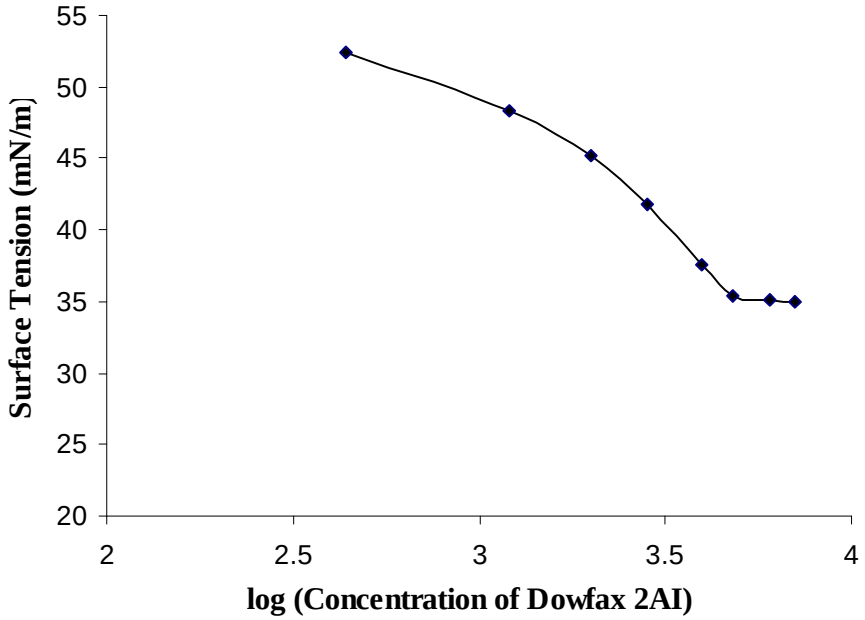

Figure 3. CMC Determination curve for Dowfax 2AI in diluted (5% solid) latex of original latex (MMA/BA/AA: 50% solid)

CMC of Dowfax in 5% hybrid latex = 4.677g/L

CMC of Dowfax in water = 0.2g/L

Concentration of Dowfax adsorbed by latex = 4.477g/L

Surface area of the polymer $= N_P \times \pi \times D^2$

$$=1.14\times10^{17}\times\frac{22}{7}\times(115\times10^{-7})^2$$

Surface area of adsorbed surfactant (S_{Dowfax}) $$=\frac{Wt.Dowfax}{MWDowfax}\times A_S \times N_A$$

$$=\frac{4.477}{576}\times A_S \times 6\times10^{23}$$

$$1.14\times10^{17}\times\frac{22}{7}\times(115\times10^{-7})^2 = \frac{4.477}{576}\times A_S \times 6\times10^{23}$$

A_S = 101 Å^2

SUMMARY

The objectives of work presented in this thesis are to understand droplet and particle formulation processes in order to make useful polymer-polymer hybrids in aqueous dispersions and use our fundamental understanding of these processes to:

1. Improve monomer conversion as much as possible.
2. Understand impact of these processes on hybrid film properties.

The need of such hybrid systems has arisen with the growing environmental concerns due to the emission of volatile organic compounds (VOCs) associated with the traditional solvent borne compounds based products. The advantage of miniemulsion polymerisation is the possibility of chemical incorporation of these highly hydrophobic compounds in an environmental friendly aqueous medium. Specific case studies of interest under commercially feasible conditions (i.e. solids content of 50wt %) were done based on two systems namely alkyd-acrylic and polyurethane-acrylic. Miniemulsification, chemical incorporation of alkyd and polyurethane to acrylic monomers, miniemulsion polymerisation and characterisation of hybrid latex were studied in detail. We have been able to successfully synthesise and characterise hybrid latex of about 100nm in particle diameter and high solids content (50wt %) to be used in coating and adhesive applications.